

EUR 4254 e

EUROPEAN ATOMIC ENERGY COMMUNITY - EURATOM

ORGEL DYNAMICS

by

**W. BALZ, C. BONA, A. DEGRESSIN, H. D'HOOF, F. LAFONTAINE
and J. NOAILLY**

1969



ORGEL Program

**Joint Nuclear Research Center
Ispra Establishment - Italy**

**ORGEL Project
and
Scientific Data Processing Center - CETIS**

EURATOM

15. 6. 1969

BIBLIOTH. - R. I.

LEGAL NOTICE

This document was prepared under the sponsorship of the Commission of the European Communities.

Neither the Commission of the European Communities, its contractors nor any person acting on their behalf :

Make any warranty or representation, express or implied, with respect to the accuracy, completeness, or usefulness of the information contained in this document, or that the use of any information, apparatus, method, or process disclosed in this document may not infringe privately owned rights; or

Assume any liability with respect to the use of, or for damages resulting from the use of any information, apparatus, method or process disclosed in this document.

This report is on sale at the addresses listed on cover page 4

at the price of FF 35.—	FB 350.—	DM 28.—	Lit. 4 370	Fl. 25.25
-------------------------	----------	---------	------------	-----------

When ordering, please quote the EUR number and the title, which are indicated on the cover of each report.

Printed by SMEETS
Brussels, April 1969

This document was reproduced on the basis of the best available copy.

EUR 4254 e

EUROPEAN ATOMIC ENERGY COMMUNITY - EURATOM

ORGEL DYNAMICS

by

W. BALZ, C. BONA, A. DECRESSIN, H. D'HOOF, F. LAFONTAINE

and **J. NOAILLY**

1969



ORGEL Program

**Joint Nuclear Research Center
Ispra Establishment - Italy**

**ORGEL Project
and
Scientific Data Processing Center - CETIS**

ABSTRACT

During the years 1966, 1967 and 1968 different studies were undertaken, in the frame of the ORGEL project, in order to investigate and to analyse the stability and the dynamic behaviour of an ORGEL type reactor coupled to a 250 MW_e power plant.

In the first part of the studies the heat exchanger attached to the reactor is a drum boiler. The model of simulating the power plant is explained.

The studies have been taken up again at the request of the industrial group participating in the "ORGEL Prototype Contest". According to their choice the heat exchanger investigated is of the Benson type.

KEYWORDS

ORGEL REACTOR
POWER PLANTS
STABILITY
REACTOR KINETICS

HEAT EXCHANGERS
BOILERS
SIMULATORS
PROGRAMMING

CONTENTS**I. INTRODUCTION**

1. First part of the studies
2. Second part of the studies

II. FIRST PART**1. The mathematical model****1.1. Introduction****1.2. The reactor simulation****1.2.1. Symbols for the reactor equations****1.2.2. The reactor neutron kinetics****1.2.3. The heat transmission in the reactor****1.3. The drum boiler simulation****1.3.1. Organic side****1.3.2. Wall equations****1.3.3. Secondary side****1.4. The control and regulating system****1.4.1. Requirements****1.4.2. Regulator equations and block diagram****1.4.3. The steady-state program****2. The analogue computation results****2.1. The instable core****2.1.1. Main characteristics of the channel****2.1.2. The reactor stability****2.1.3. Optimization of the regulator parameters****2.1.4. Ability of the regulator to control the reactor****2.1.5. Heat exchanger: steady-state checks****2.1.6. Running at 100% of the power, handling of fuel****2.1.7. Changes in power****2.1.8. Control loss and recovery****2.1.9. Scram****2.1.10. Remarks on the control system**

2.2. The stable core**2.2.1. Main characteristics of the channel****2.2.2. Temperature coefficient of the positive coolant****2.2.3. Temperature coefficient of the negative coolant****2.3. General remarks on the regulator designs****III. SECOND PART****1. The mathematic model****1.1. Introduction****1.2. Hydraulics of the loops****1.2.1. Primary loop****1.2.2. Secondary loop****1.3. Heat transfer equations in the Benson****1.3.1. Location of phase-change zones****1.3.2. Calculation of the temperature distributions****1.3.3. Set of the equations****1.4. The control and regulating system****2. Analogue computation results****2.1. Transient responses of the primary loop****2.2. Stability of the secondary loop****2.3. Heat exchanger behavior****2.3.1. Accuracy of the mathematic model****2.3.2. Steady-state performances****2.3.3. Transient responses****2.3.4. Internal dynamic variations****IV. APPENDIX**

Section A: Servo-mechanism analysis of the ORGEL reactor control system

Section B: DYNOR: a numerical program for the DYNamic simulation of an ORGEL power plant

ORGEL DYNAMICS*)I. INTRODUCTION

During the years 1966, 1967 and 1968, different studies were undertaken, in the frame of the ORGEL project, in order to investigate and to analyze the stability and the dynamic behavior of an ORGEL-250 MWe power plant. This report presents the sum of the effected work.

1. First part of the studies

The different prototypes ORGEL studied till now were characterized by a weak intrinsic stability; either they were slightly instable, or little stable. The following situations might occur:

- The stable reactor with its initial core becomes instable when its core is reaching the equilibrium, the fuel temperature coefficient being always negative and the coolant temperature coefficient always positive.
- The reactor is stable even at the equilibrium, but the coolant temperature coefficient is always positive.
- The reactor is still more stable, the two temperature coefficients being negative.

This situation led to search what might be the influence of the stability of the control-system design, and whether there was a clear advantage to choose a stable prototype, this by reducing the moderation ratio, which involves a loss of fuel burn-up and some technological difficulties in order to reduce the lattice pitch.

*) Manuscript received on 3 January 1969.

In this first part, then, the reactor stability aspect has been emphasized. After having designed a control system for the instable core, it has been searched which simplifications might be brought to this system when this core becomes stable. An analytic study has enlarged some results obtained during the analogue computation; it is reported in the Appendix of this report.

The power plant attached to the reactor has been defined from hypothesis chosen for the sake of simplicity but assuring a satisfactory run of the power plant from technological and economical points of view:

- The complex and expensive solutions (by-pass on exchangers and pumps, variable speed pumps, control valves) have been rejected; the loop is a constant primary flow loop, without by-pass and pump speed control.
- The heat exchanger is a natural circulation drum boiler.
- The control program must ensure the most stable variations:
 - . in the primary, the smallest possible temperature variations in the channel to limit stresses in the cladding and in the channel; these problems have formed the subject of distinct studies because they concern local variables;
 - . in the secondary, the smallest variations of steam conditions: the steam temperature variations limit the change of speed of the turbine charge, the maximum admissible temperature variation at the turbine is in the range of 3°C/min., pressure variations may not be superior to maximum pressure ratios of classical pumps (ratios about 1,4).

This first part presents the model of simulation of the power plant, i.e. reactor, loop and drum boiler, including the regulating system for the instable core; this regulating system will be justified when the analogue computation results will be reported. This model has completely been retaken in a digital code described in the Appendix, where all the numerical values used can be found.

2. Second part of the studies

The studies have been taken up again at the request of the industrial group participating to the "ORGEL prototype contest"; they enter in the frame of a preliminary design.

The power plant hypothesis have been deeply modified by the choice done by the industrial group of Benson-type heat exchangers equipped with primary by-passes; this has justified new studies and another design of the control system. Indeed, the transient behavior of the Benson heat exchangers is very different from the drum boiler and does not allow to extend the conclusions from one case to another. Its fast responses, because of weaker fluid quantities, and its variable behavior according to the power level (in contrast with the drum boiler, which presents a true internal stabilization because of its recirculation), are so that its dynamical behavior involves that of the whole plant.

The aspect of the plant seen from the reactor is rejected to the background; this is also due to the fact that the studies of the first part showed that the ORGEL reactor stability had not a determinant influence on the regulating system; however, as the stable reactors presented a behavior clearly more favorable in case of control loss, it had been chosen for the prototype a weak moderation ratio.

As in the first part, the power plant is foreseen for running as basic plant, and contains four identical loops. The group has decided on the following operating conditions:

Reactor side

The coolant flow is constant; the output temperature is held to its set value.

Heat exchanger side

The steam temperature and the steam pressure are held to their set value.

This second part will not present the test results of the regulating design defined by the industrial group. It will mainly share in the original developments from EURATOM, which have been necessary for the representation of the Benson heat exchanger, and set off the conditions which have to be respected if one will design an efficient control and regulating system.

II. FIRST PART

1. The mathematic model

1.1. Introduction

This paragraph resumes the mathematic model for the simulation of the dynamic behaviour of the power plant. This model was originally derived to simulate the system on an Analogue Computer, but, as presented here, is quite general and has been utilized for numerical computation as well (see Appendix).

The validity is limited to the study of power excursions ranging from 25% to 100% of full nominal power, and of disturbances which do not change the neutron flux shape or the temperature distribution shape in the reactor, since a point-model is used for all equations related to the reactor. In the heat exchanger, a finite-difference approximation of the original equations is necessary, due to the important masses and transit time involved.

The validity of these assumptions have been verified by computation.

Section 1.2. will discuss briefly the formulation of the reactor kinetics and the thermal equation in a reactor channel.

Section 1.3. gives the derivation of the equation related to the heat exchanger, which is of the natural circulation type.

Section 1.4. gives the equations and a discussion on the regulator mechanism.

The turbine is not simulated, assuming that its time constants do not influence the dynamical behavior of the power station.

1.2. The reactor simulation1.2.1. Symbols for the reactor equations

C_i	= delayed neutron precursor concentration (of species i)
$2H$	= reactor length
h	= reactor power density
K_{eff}	= effective reproduction constant
l	= neutron lifetime
n	= neutron thermal flux
p	= effective periphery for heat transfer
R	= reactor radius
r	= radial distance of a channel from core center
S	= effective cross-sectional area
T	= mean temperature
T_o	= coolant temperature outlet
T_i	= coolant temperature inlet
t_c	= local temperature of coolant
t_u	= local temperature of fuel
t	= time
U	= coolant velocity
V	= core volume
W	= channel power
z	= distance along channel measured from center
α	= heat transfer coefficient can to coolant
α_c	= temperature coefficient of coolant
α_u	= temperature coefficient of fuel
β_i	= delayed neutron fraction of species i
λ_i	= decay constant for latent nuclei of species i
μ	= heat capacity of unit reactor volume

Subscripts

c	indicates quantities applying to coolant
g	indicates quantities applying to can
o	indicates initial conditions
s	indicates value at the surface
u	indicates quantities applying to fuel

Δ is used for the difference between the actual value of a variable and its steady-state value (denoted by the subscript o) or between two steady-state values of the variable.

The reactor simulation involves two parts:

- the reactor neutron kinetics;
- the heat transmission in the reactor.

1.2.2. The reactor neutron kinetics

The kinetics equations are given for a one-point model and thus are spatially independent.

In this study, the effects of moderator temperature and Xenon poisoning are neglected because of their long time constants (about ten minutes for the moderator temperature, some hours for the Xenon poisoning) in comparison with the other effects to occur. A constant coolant flow is considered.

The neutron flux and the power distribution in the reactor satisfy the diffusion equation for one diffusion group and six groups of delayed neutrons.

$$(1.1) \quad \frac{dn(t)}{dt} = \frac{K_{\text{eff}}(t)(1-\beta)-1}{\ell} n(t) + \sum_{i=1}^6 \lambda_i C_i(t)$$

$$\text{where } \beta = \sum_{i=1}^6 \beta_i$$

$n(t) = \frac{W(t)}{K}$: K constant < 1 takes into account that all the fission power is not removed by the coolant.

$$(1.2.) \quad \frac{dC_i(t)}{dt} = \frac{K_{\text{eff}}(t) \beta_i}{\rho} n(t) - \lambda_i C_i(t)$$

The steady-state values of $K_{\text{eff}}(t)$ and $C_i(t)$ are:

$$K_{\text{eff}}^0 = 1 \text{ by definition}$$

$$C_i^0 = \frac{\beta_i n^0}{\lambda_i} \text{ from Eq. (2.2.)}$$

Assuming that the temperature coefficients are independent of the temperatures and of position in the reactor (1)

$$(1.3.) \quad K_{\text{eff}}(t) = K_{\text{eff}}^0 + \alpha_u \frac{\int^V (t_u - t_u^0) n^2 dv}{\int^V n^2 dv} + \alpha_c \frac{\int^V (t_c - t_c^0) n^2 dv}{\int^V n^2 dv}$$

dv element of volume varying in fuel and coolant temperature by amounts $\Delta t_u = (t_u - t_u^0)$ and $\Delta t_c = (t_c - t_c^0)$.

n being the thermal neutron flux at the point dv and we assume that the temperature deviations do not modify the nuclear characteristics.

If, in a certain range, we assume that the relative distribution of temperature in the reactor remains approximately constant, the temperature at a given point maintains a fixed ratio to the value at any other point; Eq. (1.3.) may be written:

$$(1.4.) \quad K_{\text{eff}}(t) = K_{\text{eff}}^0 + \alpha_u \Delta T_u^*(t) \left[\frac{\int^V \frac{\Delta t_u}{\Delta T_u^*} n^2 dv}{\int^V n^2 dv} \right] + \alpha_c \Delta T_c^*(t) \left[\frac{\int^V \frac{\Delta t_c}{\Delta T_c^*} n^2 dv}{\int^V n^2 dv} \right]$$

(1) α_u and α_c can be interpreted as averaged over the reactor so that a slight modification of nuclear characteristics by temperature can be taken into account.

where $\Delta T_u^*(t)$ and $\Delta T_c^*(t)$ are the temperature changes at any chosen point or the mean values of given temperatures which will be defined later, evaluating for the reactor the bracketed expressions which are constants independent of the temperature changes.

1.2.3. The heat transmission in the reactor

Since a one-point model is used for the kinetic equations, it is unnecessary to establish a spatio-temporal thermodynamic model dividing the reactor into axial and radial zones and that is furthermore supported by the fact that the transit time delay of the coolant through the core is very short, about half a second.

Considering the heat balance for each of the elements of the cell shown in Fig. 1.1., the equations determining the fuel cladding and coolant temperatures may be written as:

$$(1.5.) \quad \mu_u \frac{\partial T_u}{\partial t} = W - A(T_u - T_g)$$

$$(1.6.) \quad \mu_g \frac{\partial T_g}{\partial t} = A(T_u - T_g) - B(T_g - T_c)$$

$$\mu_c \frac{\partial T_c}{\partial t} = B(T_g - T_c) - \mu_c U \frac{\partial T_c}{\partial z}$$

with μ_u , μ_g , μ_c heat capacities per unit volume of fuel, cladding and coolant in the channel, and where A and B are heat transfer coefficients and the coolant flows with the velocity U in the positive z direction.

A and B are obtained from the steady-state. Eqs. (1.5.) and (1.6.) give:

$$\left| \begin{array}{l} 0 = W^0 - A(T_u^0 - T_g^0) \\ 0 = A(T_u^0 - T_g^0) - B(T_g^0 - T_c^0) \end{array} \right.$$

then:

$$A = \frac{W^0}{T_u^0 - T_g^0}, \quad B = \frac{W^0}{T_g^0 - T_c^0}$$

The term $\partial T_c / \partial z$ creates some difficulty, but, assuming that the time constant of the coolant perturbation is much longer than the transit time⁽¹⁾ of the coolant, we may write it as:

$$\frac{T_o - T_i}{2H} \quad \text{or}$$

$$\frac{T_c - T_i}{H} \quad \text{where } T_c = \frac{T_i + T_o}{2}, \quad \text{to obtain:}$$

$$(1.7.) \quad \lambda_c \frac{\partial T_c}{\partial t} = B(T_g - T_c) - C(T_c - T_i)$$

$$\text{where } C = \frac{\lambda_c U}{H} = \frac{W^0}{T_c^0 - T_i}$$

We must then rewrite the previous system of equations in terms of differences between the actual and steady-state values:

$$(1.8.) \quad \lambda_u \frac{d \Delta T_u}{dt} = \Delta W - A(\Delta T_u - \Delta T_g)$$

$$(1.9.) \quad \lambda_g \frac{d \Delta T_g}{dt} = A(\Delta T_u - \Delta T_g) - B(\Delta T_g - \Delta T_c)$$

$$(1.10.) \quad \lambda_c \frac{d \Delta T_c}{dt} = B(\Delta T_g - \Delta T_c) - C(\Delta T_c - \Delta T_i)$$

In order to obtain the real reactivity in steady-state conditions, we must evaluate the two following quantities of Eq. (1.4.):

(1) It is the same argument which allows to consider a single average uranium temperature and ignore the variations through the fuel element.

$$(1.11.) \quad \int^V \Delta t_c n^2 dv / \int^V n^2 dv \quad \text{noted} \quad \Delta T_c^*$$

$$(1.12.) \quad \int^V \Delta t_u n^2 dv / \int^V n^2 dv \quad \text{noted} \quad \Delta T_u^*$$

First, we must establish the equations giving the steady-state local temperatures of coolant and fuel.

To investigate the process of heat exchange between the fuel rods and the coolant, a dz length of one channel is considered. Writing the heat balance for each of the elements of the cell shown in Fig. 1.1. gives:

$$a) \quad h(r,z)S_u dz = \mu_c U(r)dt_c(r,z)$$

$$h(r,z) \text{ is proportional to } n(r) n(z)$$

$$U(r) \text{ is proportional to } n(r)$$

$$\text{then} \quad dt_c = a n(z) dz \quad (1.13.)$$

where a is a constant for a specified power level. Integrating the two parts of Eq. (1.13.) gives:

$$t_c(z) - T_i = a N(z)$$

$$\text{where} \quad N(z) = \int_{-H}^z n(z) dz$$

and writing in differences between two steady-state values, we get:

$$(1.14.) \quad \Delta t_c(z) - \Delta T_i = Aa N(z)$$

$$b) \quad \mu_c U(r)dt_c(z) = \alpha(r)p_g dz \left[t_g(r,z) - t_c(z) \right]$$

$t_g(r,z)$ is rather independent of r , as it was verified for ORGEL reactors when the flows in the channels are regulated to obtain the same temperature span; thus we must assume

that $\alpha(r)$ is proportional to the velocity and write with (1.13.):

$$t_g(z) - t_c(z) = bn(z) \quad (1.15.)$$

where b is a constant for a specified power level

$$c) \quad t_u^s(r,z) - t_g(z) = \beta_c \frac{h(r,z)S_u}{p_u} \quad (1.16.)$$

$$d) \quad t_u(r,z) - t_u^s(r,z) = \frac{h(r,z)S_u}{8\pi\lambda_u} \quad (1.17.)$$

Combining Eq. (1.16.) and (1.17.) gives:

$$t_u(r,z) - t_g(z) = cn(r) n(z) \quad (1.18.)$$

where c is a constant for a specified power level.

Combining Eqs. (1.15.) and (1.18.) gives:

$$(1.19.) \quad \Delta t_u(r,z) - \Delta t_c(z) = \Delta b n(z) + \Delta c n(r) n(z)$$

Let us also calculate the averaged temperatures of coolant and fuel over the channel. By definition, the averaged temperature of coolant in any channel is:

$$\Delta T_c = \frac{1}{2H} \int_{-H}^H \Delta t_c(z) dz$$

Substituting Eq. (1.14.), we get:

$$(1.20.) \quad \Delta T_c = \Delta T_i + \frac{\Delta a}{2H} \int_{-H}^H N(z) dz$$

By definition, the averaged temperature of fuel in the channel of radius r_o is:

$$\Delta T_u(r_o) = \frac{1}{2H} \int_{-H}^H \Delta t_u(r_o, z) dz$$

Substituting Eq. (1.19) gives:

$$(1.21) \quad \Delta T_u(r_o) = \Delta T_c + \frac{\Delta b}{2H} \int_{-H}^H n(z) dz + \frac{\Delta c}{2H} n(r_o) \int_{-H}^H n(z) dz$$

Let us now develop ΔT_c^* and ΔT_u^* :

$$\Delta T_c^* = \frac{\int^V \Delta t_c n^2 dv}{\int^V n^2 dv}$$

$$\Delta T_u^* = \frac{\int^V \Delta t_u n^2 dv}{\int^V n^2 dv}$$

Eqs. (1.11.) and 1.14.) give:

$$\Delta T_c^* = \frac{\int_0^R \int_{-H}^H n^2(r)n^2(z) \left[\Delta T_i + \Delta N(z) \right] r dr dz}{\int_0^R \int_{-H}^H n^2(r)n^2(z) r dr dz}$$

Separating the two space variables and substituting Eq. (1.18.) using the notation:

$$(1.22.) \quad \gamma_c = 2H \frac{\int_{-H}^H n^2(z)N(z)dz}{\int_{-H}^H n^2(z)dz} \int_{-H}^H N(z)dz$$

gives:

$$(1.23.) \quad \Delta T_c^* = \Delta T_i + \gamma_c (\Delta T_c - \Delta T_i)$$

Eqs. (1.12.) and (1.19.) give:

$$\Delta T_u^* = \frac{\int_0^R \int_{-H}^H n^2(r)n^2(z) \left[\Delta t_c(z) + \Delta b n(z) + \Delta c n(r)n(z) \right] r dr dz}{\int_0^R \int_{-H}^H n^2(r)n^2(z) r dr dz}$$

$$\Delta T_u^* = \Delta t_c + \Delta b \frac{\int_{-H}^H n^3(z)dz}{\int_{-H}^H n^2(z)dz} + \Delta c \cdot \frac{\int_0^R n^3(r)rdr}{\int_0^R n^2(r)rdr} \int_{-H}^H n^3(z)dz \Big/ \int_{-H}^H n^2(z)dz$$

From Eqs. (1.21. and 1.23.) and using the notation

$$(1.24.) \quad n(r_0) = \frac{\int_0^R n^3(r)rdr}{\int_0^R n^2(r)rdr}$$

$$(1.25.) \quad \gamma_u = 2H \frac{\int_{-H}^H n^3(z)dz}{\int_{-H}^H n^2(z)dz} \Big/ \frac{\int_{-H}^H n^2(z)dz}{\int_{-H}^H n(z)dz}$$

we obtain:

$$(1.26.) \quad \Delta T_u^* = \Delta T_i + \gamma_c (\Delta T_c - \Delta T_i) + \gamma_u [\Delta T_u(r_o) - \Delta T_c]$$

ΔT_c^* and ΔT_u^* are two temperatures linked linearly to the averaged temperatures of coolant and fuel of the channel of radius r_o defined by Eq. (1.24.) and called the representative channel.

Taking back Eq. (1.4.), we must write in dynamic conditions:

$$(1.27.) \quad K_{\text{eff}}(t) = K_{\text{eff}}^0 + \alpha_u \Delta T_u^*(t) + \alpha_c \Delta T_c^*(t)$$

where ΔT_u^* and ΔT_c^* are expressed by Eqs. (1.26.) and (1.23.) and the variations in the time of ΔT_u and ΔT_c given by the system (1.8., 1.9., 1.10.), the steady-state values corresponding to the so-called representative channel.

The complete set of thermal equations is thus constituted by Eqs. (1.27., 1.26., 1.23., 1.8., 1.9., 1.10.).

For a cosine axial neutron flux, we have $n(z) = \cos \frac{\pi}{2H} z$ and from Eqs. (1.25.) and (1.22.), we must calculate:

$$\begin{cases} \gamma_u = 4/3 \\ \gamma_c = 1 \end{cases}$$

The representative channel is obtained from the radial neutron flux distribution calculating the ratio of Eq. (1.24.). It is included between the central channel and the channel of medium power. We must then write Eq. (1.27), assuming the coolant temperature inlet to be constant:

$$(1.28.) \quad K_{\text{eff}}(t) = K_{\text{eff}}^0 + \alpha'_v \Delta T_v + \alpha'_c \Delta T_c$$

where:

$$\begin{cases} \alpha'_v = \frac{4}{3} \alpha_v \\ \alpha'_c = \alpha_c - \frac{1}{3} \alpha_v \end{cases}$$

1.3. The drum boiler simulation

The heat exchanger is a drum boiler with natural circulation. The main circuit of the power station consists of two loops.

1.3.1. Organic side

As well known, the equations describing the thermal behavior of two fluids which exchange heat through a wall constitute a partial derivative system which states that, for every elementary volume of both fluids, the mass, momentum, energy are conserved, i.e., for the mass: the net difference between the masses which go in and out from the elementary volume equates the variation in time of the mass being in the volume (fixed walls are assumed); the energy and momentum conservation laws can be expressed in an analogue way.

As a partial derivative system cannot be handled by a traditional analogue computer, such a system has been reduced to the "finite differences" in space, that is, the heat exchanger has been divided in a number of zones or "cells" of finite volume for each of which the conservation equations has been written in global form; the equations obtained are thus in terms of "mean variables".

Fig. 12 gives a scheme of the cells in which the heat exchanger has been divided, the number of cells being limited by the amount of analogue elements required.

It must be remembered that a lumped parameter model of this kind described very well the behavior of the physical system at low frequency but finds its limit at high frequency where it behaves as a low band filter, that is, the high frequency transients of the physical system will appear smoothed when studied with a finite difference model as this.

In the primary, the specific heat of the organic liquid and its density can be considered as remaining constant.

The heat transfer coefficient different values have been assumed from zone to zone (superheater, boiler, economizer), but the same value, constant in time, has been taken for the cells in the same zone as there the velocities and the heat exchanging surfaces are the same.

The behavior of the primary is described by the energy balance equations:

$$(1.29.) \quad VO_i C \rho \frac{d TOL_i}{dt} = WOL C (TOL_i - TOL_{i-1}) - HLOS S_i (TOL_i - TPA_i)$$

where:

- i is the index related to the zone, (increasing in the direction of the organic flow)
- VO_i is the zone volume
- ρ is the density
- TOL_i is the average organic temperature in cell i
- WOL is the organic mass flow
- C is the organic specific heat
- $HLOS$ is the heat transfer coefficient
- S_i is the wetted surface in the cell i

For the first zone, the variable TOL_{i-1} has to be replaced by the delayed outlet temperature of the reactor.

The approximation can be improved assuming C and ρ as constant in time but varying along the heat exchanger and taking for each cell the value corresponding to its steady-state temperature. In any case, a comparison of the steady-state temperatures computed with this model, with the steady-state temperature at the same powers computed with a digital code which takes account of the dependence of the organic liquid physical properties on the temperature, has shown that the error done in this way is reasonably low (see next section).

1.3.2. Wall equations

The wall is considered only as a thermal capacity in which a certain amount of heat can be stored and represents a time constant between the primary and the secondary side.

For each cell, the mean temperature of the mass of steel which is interested in the heat transfer is computed by writing energy conservation balance between the stored heat and the difference between the heat transferred from the primary and the heat transferred to the secondary.

No heat transmission between adjacent cells along the wall has been considered. This can be justified considering the big difference between the heat fluxes along and across the pipe walls.

The heat balance equations for the wall is:

$$(1.30.) \quad AP_i * ROP_i * CP \frac{d TPA_i}{dt} = HLOS * S_i (TOL_i - TPA_i) - \\ - HLV_i * SV_i (TPA_i - TSEC_i)$$

AP is the wall cross-section
 ROP is the density of the wall
 CP is the specific heat of the wall in cell i
 HLV is the heat transmission coefficient between wall and secondary
 SV_i is the wetted perimeter at the secondary
 TSEC_i is the average temperature at the secondary in cell i

All other symbols are as defined for Eq.

(1.29.).

To obtain a system of equations suitable for computation, equations (1.29.) and (1.30.) have to be developed,

giving to the indices values related to the physical dimensions of the heat exchanger. How this can be done is illustrated in figures 1.3., 1.4. and 1.5.

1.3.3. Secondary side

a) Economizer

What has been said for the primary side still holds true for the secondary side in the economizer, where we have one liquid phase; the only difference is that the secondary fluid mass flow rate is no more constant but varies following the power delivered to the turbine.

Note that, if the boiler free level is to be kept constant, as we assume, during transients the mass flow in the economizer will differ from the steam flow to the turbine. In our model, while the boiler free level is supposed to be constant, the difference between the mass flow in the economizer and in the superheater has been assumed to be negligible.

The mass flow rate, which is supposed to be the same in the economizer's cells, is computed as follows:

$$WREQ = \frac{POWER}{\Delta H} ,$$

where POWER is the power delivered to the turbine in Kcal/sec and ΔH the difference between the feedwater and steam enthalpy in Kcal/kg.

The cell's temperature is deduced from the energy conservation law. These are written for each cell in Fig. 1.8., where the usual schematic drawings, the list of symbols and the values of the constant coefficients are also represented.

To simulate the effect on the primary side of an eventual boiling in the economizer, a circuit has been added to prevent that the temperature of the last cell in the economizer become greater than $TSAT(p)$, the saturation temperature at the secondary pressure.

b) Natural circulation boiler

Fig. 1.9. gives a schematic drawing of the paths of the primary and secondary fluid in the boiler.

To have a detailed description of the behavior of the boiler, this should be divided into cells, and for each the conservation laws should be written (for mass, energy and momentum).

Even if the slip ratio in the riser is disregarded, and the water-steam mixture is considered as homogenous, the equations will be highly non linear and present many computational difficulties, in particular for the analogue computer.

But, for the simulation of a power station, the local behaviour of the variables in the riser is not essential, since the interest lies in a realistic estimation of the recirculation ratio WR (i.e. the ratio between the mass flow rate in the boiler and in the economizer) during the overall transients.

This ratio, which is of no importance for steady-state calculations (as the heat-transfer coefficients in the boiling region do not vary significantly with the speed of fluids), becomes significant for transients as the amount of steam generated can be different from the feedwater mass flow.

Rigorously, the recirculation ratio can be defined only for steady states, as during transients the mass flow is not constant, but determined by the local density variation:

$$\frac{\partial WR}{\partial X} = - AR \frac{\partial \rho}{\partial t}$$

where AR is the riser cross-section. Nevertheless, provided there are no local instability phenomena, as the hydraulic time constants are much shorter than the thermal ones, it is reasonable to disregard the local variations of WR along the riser and to consider the recirculation flow as being in every moment at the steady-state value corresponding to the driving force in that moment.

As, at steady-state, the sum of the friction head losses along all the boiler must equate the difference of weight of the liquids in the downcomer and in the riser, we can write:

$$WR \simeq K.(RO_{\text{downcomer}} - RO_{\text{riser}})^{\alpha} \quad (1.31.)$$

where K is an unknown coefficient depending on the geometry of the system (dimensions and head losses), and α , which has been taken equal to 0.5, is an exponent which takes account of the dependence of the head losses on the flow rate.

After a few manipulations from (1.31.), we get:

$$WR = K \cdot \sqrt{\frac{X.VS(P)}{[VL + X.VS(P)] VL}}$$

where X is the mean quality in the boiler $\left(\frac{\text{mass of steam}}{\text{total mass}}\right)$, VL the liquid specific volume and VS the steam specific volume which depends on the secondary pressure P.

The steam water mixture which fills the riser has been considered a homogeneous fluid whose temperature is always equal to the saturation temperature corresponding to the system pressure P; the riser itself has been considered as a whole (one cell) and an average quality over it has been calculated by writing the energy and mass conservation laws as shown in fig. 1.10.

In fig. 1.10., the energy conservation laws have been written in terms of mean enthalpy and mean density; we rewrite them here to show how they can be manipulated to get a form suitable to the analogue machine:

$$\text{MASS)} \quad \text{AR.LR} \frac{d\rho}{dt} = \text{WR+WREQ-WOUT} \quad (1.32.)$$

$$\text{ENERGY)} \quad \text{AR.LR} \cdot \frac{d(\rho \cdot \text{IM})}{dt} = \text{WR.ILIQ+WREQ.CLVE.TLVEC(OT)-WOUT IM} + \text{Q} \quad (1.33.)$$

where:

AR	= riser cross-section (m ²)
LR	= riser length (m)
ρ	= riser mean density (kg/m ³)
IM	= riser mean enthalpy (Kcal/kg)
ILIQ	= saturated water enthalpy (Kcal/kg)
CLVE	= water specific heat (Kcal/kg°C)
TLVEC(OT)	= water temperature at the outlet of the economizer (°C)
Q	= heat transferred from the wall (Kcal/sec)
WR	= downcomer mass flow rate (kg/sec)
WREQ	= economizer mass flow rate (kg/sec)
WR+WREQ	= mass flow rate into the riser (kg/sec)
WOUT	= mass flow rate from the riser (kg/sec)

Multiplying Eq. (1.32.) by IM and substituting it from Eq. (1.33.), we get:

$$\text{AR.LR} \cdot \rho \cdot \frac{d\text{IM}}{dt} = \text{WR.ILIQ+WREQ.CLVE.TLVEC(OT)-(WR+WREQ).IM} + \text{Q}$$

and introducing the following relations:

$$\rho = 1/\text{VSPEC}(P, X) \approx 1/[(1-X)\text{VL}+X.\text{VS}(P)] \quad \text{where } X \ll 1$$

$$\text{IM} = \text{ILIQ}(P) + \text{CLAT}(P) \cdot X$$

where:

VSPEC(P,X) is the specific volume of the mixture (m³/kg)
 VL is the specific volume of the saturated water (m³/kg)
 VS(P) is the specific volume of the saturated steam at pressure P
 P is the pressure of the system (kg/cm²)
 ILIQ(P) is the enthalpy of the saturated liquid at pressure P (Kcal/kg)
 CLAT(P) is the latent heat at pressure P (Kcal/kg)

we have:

$$\frac{AR.LR}{VL+X.VS} \cdot \frac{d ILIQ}{dt} + \frac{AR . LR}{VL+X.VS} \cdot \frac{d(CLAT.X)}{dt} =$$

$$Q + WR.ILIQ + WREQ.CLVE.TLVEC(OT) - (WR+WREQ).(ILIQ + CLAT.X) \quad (1.34.)$$

The quantities VS, CLAT and ILIQ which appear in Eq. (1.34.) are functions of P only and can be approximated with the following expressions ⁽¹⁾:

$$\begin{aligned} VS &= AVS + BVS.P \\ CLAT &= ALAT + BLAT.P \\ ILIQ &= AIL + BIL.P \end{aligned}$$

where AVS, BVS, ALAT, BLAT, AIL, BIL are constant coefficients which have been computed imposing that Eq. (1.35.) fit at the best the values of VS, CLAT and ILIQ obtained from the steam tables, for P varying from 50 to 100 kg/cm² (which is the pressure range of interest).

Figs. 1.11., 1.12., 1.13., the real values of these functions, are compared with the values given by Eq. (1.35.) ⁽²⁾. As can be seen by the maximum value of the errors

(1) For numerical computation, these could be obtained by tabulation of the steam tables or by higher order polynomials.

(2) These plots have been obtained directly by the CALCOMP plotter, using a program which computes the polynomial of order up to 20, which fits at the best a given set of points.

this fitting is quite satisfactory. By substituting the expressions (1.35.) into Eq. (1.34.), we finally have the wanted equation:

$$\begin{aligned} & \frac{AR.LR}{VL+X.VS} \cdot (BIL+BLAT.X) \frac{dP}{dt} + \frac{AR.LR}{VL+X.VS} \cdot CLAT \cdot \frac{dX}{dt} = \\ & = Q+WR (AIL+BIL.P) + WREQ.CLVE.TLVEC(OT) - \\ & (WR+WREQ).(AIL+BIL.P+X.(ALAT+BLAT.P)) \quad (1.36.) \end{aligned}$$

Note that, with respect to Eq. (1.36.), the term $\frac{dP}{dt}$ is a known quantity, its value being determined elsewhere (see c)).

The term $\frac{AR.LR}{VL+X.VS} \cdot (BIL+BLAT.X) \cdot \frac{dP}{dt}$ in Eq. (1.36.), which is null in steady state, is very important during transients, as it represents the heat which must be given to (or taken off from) the mixture in the boiler to maintain it at the saturation condition when the pressure changes (this because the amount of water involved, in this type of boilers, is very large)⁽¹⁾.

c) Upper Dome

Since we assume to have a perfect regulation of the free level in the boiler upper dome, the volume of the upper dome is to be considered constant in time. How large this volume is does not seem to have great influence on the transient behavior of the system, at least until it is not very large or very little, and the transients are not too rapid (the steady-state configuration does not depend on this parameter).

(1) The effect of this term is to prevent any quick variation in the system pressure. Suppose in fact that P has a tendency to rise, then this term will make X decrease because a part of the heat, which used to be spent into vaporization, has to be spent in rising the liquid temperature, and a decrease in X will decrease also P (see c)) and vice-versa: if P has a tendency to decrease, this term will increase X because some of the heat which was in the liquid is released.

We assume that the steam in the upper dome (which is sketched in Fig. 1.9.) could be either saturated or superheated, but never subcooled if not for a very short time. In the first case, the independent thermodynamic variables to be computed are reduced to one (in our model, we have assumed the pressure), but a new variable appears: the condensation mass flow rate; in the second case (superheated steam), this last variable is identically zero, while the independent thermodynamic variables become two (in our model, we have assumed the pressure and the steam density, the other being deduced by the state equation and the steam tables). The equations written are the mass conservation law and the energy conservation law, Fig. 1.14.

Referring to Fig. 1.14., the exact expression for the stored energy would be $V \frac{d}{dt} (R\phi \cdot i + P/J)$ ($J=427 \text{ kgm/Kcal}$), but it is very easy to see that term $V \frac{d}{dt} P/J$ is always very negligible.

Studying the steam characteristics, it turned out that the enthalpy, which is function of P and $R\phi$, can be very well approximated with an expression of the form

$$I = AI + BIPRO \cdot \frac{P}{RO} \quad (1.37.)$$

where AI and $BIPRO$ are two constants whose values were deduced by trial fitting of the above expression to the steam curves of I against P for different values of RO (Fig. 1.15.). We further assume that $ISAT$, $ILIQ$ and $ROSAT$ can be approximated as follows:

$$ISAT = AISAT + BISAT \cdot P$$

$$ILIQ = AIL + BIL \cdot P$$

$$ROSAT = AROS + BROS \cdot P$$

Where $AISAT$, $BISAT$, AIL , $AROS$ and $BROS$ are constant coefficients, the values of which have been determined imposing that the expressions (1.38.) fit at the best for $50 \leq P \leq 100 \text{ kg/cm}^2$, the corresponding functions of P , which can be deduced from the steam tables.

In Figs. 1.14., 1.16., 1.17., the real values of these functions are compared with the value computed with expressions (1.38.); as can be seen, this fitting is quite satisfactory.

By introducing the Eqs.(1.38.)and(1.37.)into the energy equation and combining it with the mass conservation (Fig. 1.10.), the energy equation can be reduced to the following form which is more suitable to the computer:

$$\begin{aligned} V \text{ BIPRO } \frac{dP}{dt} = & - \text{AI} \cdot (\text{X} \cdot (\text{WR} + \text{WREQ}) - \text{WREQ} - \text{WC}) \\ & + (\text{AISAT} + \text{BISAT} \cdot \text{P}) \cdot (\text{WR} + \text{WREQ}) \\ & - \text{WREQ} (\text{AI} + \text{BIPRO} \cdot (\text{P}/\text{RO})) \\ & - (\text{AIL} + \text{BIL} \cdot \text{P}) \cdot \text{WC} \end{aligned} \quad (1.39.)$$

Eq. (1.39.) together with the mass conservation eq.:

$$V \cdot \frac{dRO}{dt} = \text{X} (\text{WR} + \text{WREQ}) - \text{WREQ} - \text{WC} \quad (1.40.)$$

constitutes the set of equations which is to be integrated to compute RO and P in the upper dome. The only unknown left is WC which is computed as follows:

$$\text{WC} = \begin{cases} \text{K} \cdot (\text{RO} - \text{ROSAT}) & \text{RO} > \text{ROSAT} \\ 0 & \text{RO} \leq \text{ROSAT} \end{cases} \quad (1.41.)$$

The value of K must be chosen high enough to prevent RO to become greater than ROSAT for a long time, (how it happens can be understood replacing Eq. (1.41.) into (1.40.)); this is equivalent to assume that, as soon as the steam in the upper dome reaches the saturation conditions, the condensation prevents it from going deeply into the subcooled region, which seems reasonable as one regards a practical system.

Note that Eq. (1.39.) still represents fairly well the energy conservation law also when the steam in the upper

dome is at the saturation condition; in fact, in this case, for what has been said, $RO \approx ROSAT$ and Eq. (1.37) still gives an acceptable approximation of the steam enthalpy, as it can be seen in Fig. 1.18., where:

$$AI + BIPRO \cdot \frac{P}{ROSAT(P)}$$

is compared with $ISAT(P)$.

In practice, it seems that, at the frequencies of the transients which have practical interest, the steam in the upper dome is very near to the saturation condition being always a little superheated, and this is the reason why the system is not affected by the value of K .

d) Superheater

It has been supposed to make a negligible error assuming to have the same mass flow rate of steam along the whole superheater; this is true in steady state, while in transient, according to the mass conservation law, there are local variations due to the steam density variations in time:

$$\frac{\partial W}{\partial x} = - \Lambda \frac{\partial \rho}{\partial t} .$$

It was nevertheless verified that, for cases of practical interest, the maximum flow variation in the cell due to density variation remains below 1% of the total flow.

The mass conservation law is thus reduced to the trivial form $W(i) = WREQ$, where $W(i)$ is the mass flow rate in the i^{th} cell and $WREQ$ the mass flow rate into the turbine.

The energy conservation law is reported in Fig. 1.18., with the usual schemes and list of symbols. For the steam density in the different cells, we have assumed the steady-state value at full power.

1. Fig. 1.19., the values of the steam density in the different cells and at different powers have been plotted; from this figure, one could have the impression that the error committed in neglecting the density variations due to pressure and temperature variations is not too small.

In reality, looking at the equations, it is clear that the only effect of an error over RO is to modify the time constant between the temperature of the wall and the temperature of the steam, and the effect on the primary side is still attenuated by the time constant between the organic temperature and the wall temperature.

Two transients done, assuming for RO values ten times greater and ten times smaller than the real ones, have shown no appreciable variations in the system behavior. This is due to the fact that, being always very near to the steady conditions, the error over RO is highly attenuated by the very little value of $\frac{dH(i)}{dt}$ (see Fig. 1.18.).

The energy conservation law has been written assuming, as thermodynamic independent variables, the pressure P and the steam enthalpy $H(i)$. For the pressure, we assume that it is the same as in the upper dome (we neglect the pressure losses due to friction and acceleration). The error we do in this way affects the calculation of the temperature of the steam in the cell and can be estimated at approximately 0.5°C , as can be deduced from Fig. 1.20., assuming that the pressure losses over each cell can be evaluated to 0.5 kg/cm^2 .

The steam temperature which appears on the right hand side of the energy conservation law (Fig. 1.18.) has been considered a dependent variable whose value is deduced from the steam enthalpy I and pressure P with the following approximate formula:

$$T(^{\circ}\text{C}) = 1.3333 I + 1.0337 P - 686.64 \quad (1.42.)$$

where I must be expressed in Kcal/kg and P in Kg/cm^2 .

In Fig. 1.20., the values of the steam temperature against the steam enthalpy for different pressures have been plotted together with the values corresponding to Eq. (1.42.).

As it can be seen, the approximation is good, or at least comparable with the precision one can reach in computing the heat transfer coefficients, provided one remains in the region from 50 to 100 kg/cm² for the pressure, and between 25% and 110% of nominal power.

1.4. The control and regulation system

1.4.1. Requirements

The automatic control and regulation system must stabilize the reactor which is instable with respect to temperature coefficients, and adjust its power level to the power demand according to a certain steady-state program.

1.4.2. Regulator equations and block diagram

Experiments on the analogue computer have shown that the regulation mechanism must be driven by an error term which should be a combination of two variables: the neutron power and the average temperature of the organic coolant:

$$\xi = - R_1 \left[\frac{n - n_o}{n_o} - \frac{PW - PW_o}{PW_o} \right] - R_2 \frac{T_{av} - T_{avo}}{T_{avo}} \quad (1.43.)$$

where:

ξ is the actuating error
 n is the neutronic power
 PW is the power demand at the turbine
 T_{av} is the average temperature of the coolant

T_{av} = (temperature primary at the inlet of the heat exchanger + temperature primary at the outlet of the heat exchanger)/2

Note that T_{av} represents the average temperature only under steady-state conditions

R_1 and R_2 are arbitrary gains to be optimized

n_o, PW_o, T_{avo} are the values of N, PW, T_{av} at the nominal power of the reactor; they can be functions of the power

The terms $\frac{n-n_o}{n_o}$ and $\frac{PW-PW_o}{PW_o}$ allow to compare

the extracted power of the reactor to the power supplied to the turbine and to adjust one to the other. The power demand PW is the product ($WREQ \cdot \Delta H$) where $WREQ$ is the steam flow and ΔH the enthalpy span from the superheating steam temperature to the economizer water input temperature (which is assumed to be constant according to the reactor power). The power demand PW is changed by acting the steam throttle at the turbine input, which is identical to modifying the steam flow, but in a manner to verify the previous equality.

The term in n compensates the fast variations of the power, which are impossible to correct with temperature signals due to the important time delays (time delay in transferring the heat from fuel to coolant: about 3 sec. and transport delay time to the mixing main collector: about 10 sec.).

The term in T_{av} corrects any variation of the average temperature; by definition, this is a low-frequency action and has little effect on the stability of the system, but influences greatly the variation of the thermodynamical quantities of the heat exchanger.

To the error term must be added a pressure term defined as $-R_3 \frac{p-p_o}{p_o}$ and intended to improve the pressure transient; this term presents a particular interest when p_o is a constant according to the power (for a constant pressure

regulation program). T_{avo} and p_o are two thermodynamical parameters connected so that the pressure term acts in the opposite direction of the term in T_{av} ; therefore, its weight must be limited. This situation derives from the fact that a regulation program for a multiple-loop system is necessarily a compromise between contradictory requirements.

The control-rod mechanism is represented by the following transfer function:

$$\frac{p}{\xi} = \frac{R_4/S + R_5}{1 + \tau S} \quad (1.44.)$$

where:

- p is the reactivity introduced by the control mechanism
- S is the differential operator $\frac{d}{dt}$ (Laplace operator)
- τ is the time constant due to the inertia of the mechanism
- R_4 and R_5 are arbitrary gains to be optimized

Thus, the position of the control rod is changed in proportion to any error created by a power demand change or by an internal system transient. An on-off type control rod is inadequate, the reactor by itself being inherently instable; the presence of a dead zone in that discontinuous type system causes the control system to be in continuous oscillation.

The regulation is linear only within limits imposed by technology, which must be taken into account:

- the speed of the control rod has a sharp maximum limitation:

$$\frac{dp}{dt} \leq \text{max. speed of rods}$$

- the end-of-run limitations of the control rods must be considered as well:

$$p \leq \text{max. available reactivity}$$

$$p \geq \text{min. reactivity}$$

The law of variation of reactivity versus rod displacement is assumed to be linear for the computation, as it was verified on the computer that (within the limits mentioned above) any alternative (section of a sine function) does not change significantly the behavior of the control loop.

A separate mean to set the equilibrium point at any desired value between these limits must be available.

It must be remembered that, if a reactivity disturbance greater than the above value occurs for any significant length of time, the regulator loses its ability to control the reactor.

The block diagram for the whole power plant control is reported on Fig. 1.21. The detail of the regulator is given in Fig. b. and Fig. c., which represent two possible servo mechanisms being mathematically equivalent. In Fig. b., the actuating error is integrated through an electronic integrator; its output and the error signal itself drive the control mechanism which acts here as a position servo. In Fig. c., the error signal and its derivative (damping term) drive a bar mechanism which is a rate servo.

Eliminating ϵ between the relations (1.43.) and (1.44.), it appears that the proportional and integral terms are affected to the variables n , T_{av} and, eventually, p . Generally, the proportional terms are the stabilizing terms (the terms which improve the transients); the integral terms are the reset terms (refer to analogue and analytic results).

The regulator will be optimized with respect to the following parameters: R_1, R_2, R_3, R_4, R_5 , and the speed and reactivity limits of control rods. The criteria for optimality are:

- a) Minimum overshoot of all variables in transient response, in particular with respect to reactivity disturbances.
- b) Minimum time for passing from one steady state to another when the power demand is varied.
- c) Minimum time to return to steady state after any disturbance.

1.4.3. The steady-state program

In Fig. 1.21., a regulation program sets the sum of the reference terms of the Eq. (1.43.): n_o and PW_o are constants, while T_{avo} and p_o may vary according to a certain predetermined law (steady-state program) as a function of PW ; it will be recalled that T_{avo} and p_o naturally will always remain thermodynamically connected. One of the possible steady-state programs of the power plant is reported in Fig. 1.22. (program 1):

- From 100% to 75% of the power, the average temperature of the coolant remains constant; the steam pressure rises from 53,5 kg/cm² to 67 kg/cm². This range of power is considered to be the normal working zone of the plant.
- From 75% to 25% of the power, the steam pressure is maintained constant; the average organic temperature decreases from 308°C to 289°C.

The inlet and outlet temperatures of the coolant are represented on Fig. 1.22. in the same way as the steam inlet temperature at the turbine. Let us remember that the assumed steam cycle taken into account for the dynamics calculations is without reheating.

Experimentation made on computer has shown that many alternatives, all stables, are possible; in each case, the regulation can be driven by T_{av} ($R_3 = 0$), assuming a variable reference T_{avo} which depends on the power demand as in Fig. 1.22.; an additional term in $p - p_o$ ($R_3 = 0$) where p depends on the power demand as in Fig. 1.22. always improves the regulator performance.

The regulator reference is setting to the predetermined law (as a function of the power demand signal) by a program (see Fig. 1.21a) which could be a set of relays, comparators and constant gain amplifiers wired in a permanent arrangement or, for more flexibility, a small on-line computer (digital or analogue).

Other static programs studied are reported in Fig. 1.23. The numerical differences between the two programs 1 are explained by the fact that the dynamical studies have been executed on two prototype variants where the coolant organic span is, either 124°C (Fig. 1.22.), or 104°C (Fig. 1.23.); in this last case, the steam pressure rises from 60 to 74 kg/cm² when the power decreases from 100% to 75%. The results of the study are modified in no way.

2. The analogue computation results

2.1. The instable core

2.1.1. Main characteristics of the channel

Bundle	19 rods
Fuel cross-section	31 cm ²
Coolant cross-section	22 cm ²
Moderator area/coolant area ratio	15,6
Length channel	400 cm
Fuel rod radius	1,45 cm
Cladding wall thickness	0,88 mm
Finning ratio	1,9
Thermal resistance between fuel & cladding	1,5°C/w/cm ²
Maximum integral of conductivity	100 w/cm
Average velocity in the central channel	10 m/sec
Axial form factor	0,68
Radial form factor	0,85
Disadvantaged thermal flux factor	0,85

Characteristics of the "representative" channel (the power of which being 0,89 the power of the central channel) at nominal power

Removed power	4,65 MW
Input temperature	266°C
Output temperature	370°C
Average cladding temperature T_G	376°C
Average fuel temperature T_u	672,5°C

Temperature coefficients of the initial core:

- Fuel temperature coefficient:	$\alpha_u = - 1,5 \text{ pcm/}^\circ\text{C}$
- Coolant temperature coefficient:	$\alpha_c = - 0,25 \text{ pcm/}^\circ\text{C}$

Temperature coefficients of the equilibrium core:

- Fuel temperature coefficient:	$\alpha_u = - 0,45 \text{ pcm/}^\circ\text{C}$
- Coolant temperature coefficient:	$\alpha_c = + 5,6 \text{ pcm/}^\circ\text{C}$

Transport delays of coolant from reactor to heat exchanger:	12 and 13 sec.
---	----------------

2.1.2. The reactor stability

The prototype stability situations have been studied in the parametric plane ($+\alpha_{\text{coolant}}$, $-\alpha_{\text{fuel}}$), examining the open loop transient response of the reactor to an initial positive step disturbance of 50 pcm. If the second derivative of neutron power versus time is negative, after a time of 100 sec. longer than the longest time constant, the reactor is considered to be stable.

The results are reported in Fig. 1.24. for the two cases of a thermal resistance of 1.5°C/w/cm² and 0.5°C/w/cm² (the two curves are identical).

One can see that the irradiated reactor is unstable. Thus the prototype requires an automatic external control and regulating system.

2.1.3. Optimization of the regulator parameters

After experimentation, the following numerical values have been retained (if no speed limitation on control rod):

$$\begin{array}{ll}
 R_1 & = 1 \\
 R_2 & = 1 \\
 R_4 & = 10^{-2} = 10 \text{ pcm/\% variation} \\
 R_5 & = 5 \cdot 10^{-2} = 50 \text{ pcm/\% variation} \\
 \tau_{\text{inertia}} & \leq 2 \text{ sec}
 \end{array}$$

The regulator inertia $\tau_{\text{inertia}} = 2 \text{ sec.}$ was used for computation as a worst case value.

Fig. 1.25. gives the stability domain of the control mechanism versus the gains R_4 and R_5 , in the linear region of its transfer function (i.e. for disturbances which do not reach the reactivity speed and amplitude limitation). In the region to the left, the mechanism is stable and gives a damped response to a step input. In the central region, the mechanism is stable but gives a periodical response (overshot) to a step disturbance. In the right region, the loop is unstable.

The working point of the controller should be selected in the first region (damped). In fact, in order to avoid overshoots in the non-linear region, systematic experimental investigation has shown that the working point of the mechanism should be about a decade to the left of the critical damping line as, for example, point 16 if the insertion speed of reactivity is limited to 10 pcm/sec.

Fig. 1.26. and 1.27. give the response of the system in case of a step disturbance of 50 pcm considered as a worst case for a small accident (like the drop of a cluster in the channel during the fuel handling), not requiring a scram.

The two figures give the neutron power response and the control rod reactivity (position and speed):

- Fig. 1.26. for a speed limitation of the control rods of 10 pcm/sec (equivalent to 10 cm/sec) and a rod inertia time constant of 2 sec.
- Fig. 1.27. for an unlimited speed of the control rods.

During these transients, the temperatures do not change significantly.

2.1.4. Ability of the regulator to control the reactor

The regulator optimized for values of temperature coefficients corresponding to the irradiated reactor, it is interesting to investigate up to which extreme limits the regulator is capable to keep the reactor under control. The quantities which affect significantly these limits are:

- The amplitude of the reactivity disturbance (linked to the end-of-run limitations of the control rods)⁽¹⁾.
- The maximum speed allowable for the control rods.
- The temperature coefficients⁽²⁾.

The limits of efficiency of the system control are reported in Fig. 1.28. in the (α_{coolant} , α_{fuel}) plane for the following values of the control system bounds:

-
- (1) It is obvious that, if a reactivity disturbance greater than the end-of-run values occurs for any significant length of time, the regulator loses the ability to control the reactor.
- (2) The temperature coefficients associated with the fuel and the organic coolant are not easy to obtain, and there are always some doubts on their accuracy. This fact justifies this parametric study.

- Maximum rods speed: 15 cm/sec (e.g. 15 pcm/sec)
- Rod reactivity span from + 200 pcm to - 300 pcm with two sets of four rods: the negative reactivity end-of-run of the normal first set (-50 pcm) commands the release of the second group of rods (-250 pcm) (see Fig. 1.29.).
- The time constant of rods was taken = 1 sec. for this investigation.

Curves 1 and 2 give the limit above which a reactivity step disturbance of 100 and 50 pcm cannot be compensated by the regulator; curves 3 and 4 give the same limit for a step disturbance in the reactor inlet temperature of 10°C and 5°C respectively.

It turned out that the speed would be sufficient to control the system up to very high values of α_c , if the amount of reactivity supplied by the regulator is adequate. Beyond the limits of curves 1 to 4, the regulator loses its ability to control the reactor for the described disturbance.

2.1.5. Heat exchangers: accuracy of the dynamic computations - Steady-state checks

The steady-state results have been obtained for 100% and 75% of full power, as the equilibrium values of the dynamic equations. The steady-state temperature distribution for the heat exchanger is reported in Fig. 1.30. for 100% power, and Fig. 1.31. for 75% power. These results have been compared with those of a purely static digital computation (using thus a different mathematical representation. The agreement (within some degrees centigrades) between the results of the two computations represent a reliable validity (and accuracy) check for the complete analogue simulation.

2.1.6. Running at 100% of the power, handling of the fuel

The inserted reactivity law which simulates loading and unloading of a fuel element is given in curves 1L and 1U of Fig. 1.32. In these functions, horizontal segments have been abridged significantly to reduce computer time, as this does not affect the conclusions.

The curves 2U and 2L give the neutron power transient response, on a developed amplitude scale. It can be seen that the power level is virtually unaffected by the operation.

The curves 3U and 3L give the control rod position, which can be seen to compensate almost exactly (with negligible time lag) the introduced reactivity. During this transient, the temperature does not vary.

2.1.7. Changes in power

We cannot give all experiments achieved on the analogue computer; we will restrict ourselves to the essential:

- a) Regulation program 1: constant temperature/
constant pressure
Changes in power from 100% to 75%

During this transient, the power demand to the turbine is varied from 100 to 75% and then it is kept constant; the rate of variation is 5% per minute.

Figs. 1.33., 1.34. and 1.35 show the evolution of the reactor and secondary variables.

The coolant temperature and the average cladding temperature reported are the same as those of the central channel; this is not the case for the average fuel temperature: in transient state, that one of the central channel differs from that one of the so-called representative channel by a higher amplitude; it will be determined knowing that, in steady state, the span ($T_u - T_G$) is proportional to the channel power.

However, the two most significant variations on the reactor side during all dynamical attempts are the driving variables, i.e. the neutron power and the input coolant temperature (for a constant coolant flow) which can be taken as input data for a spatial-temporal code in order to particularly determine the local variations of the cladding and fuel temperatures.

Changes in power from 100% to 25%

Without pressure feedback:

The rate of variation is 5% per minute.

Fig. 1.36. shows the average organic temperature (T_{av}) evolution and Fig. 1.37. the pressure transient; it can be seen that, even through the rate of change relatively slow, the pressure overshoot is far from being negligible.

The rate of variation is 0,5% per minute.

This transient can be considered as a sequence of equilibrium states. Fig. 1.38. gives the evolution of T_{av} , and Fig. 1.39. gives the evolution of pressure, both versus time. Fig. 1.40. and 1.41. show the T_{av} and pressure variation law versus the power demand; it can be easily observed that, on the analogue computer (and, very likely in reality), it is very difficult to maintain the pressure rigorously constant. This situation is due to the fact that there is no direct action of a pressure measurement on the regulator ($R_3=0$). A definite improvement on this situation can be obtained by introducing a term in R_3 .

With pressure feedback:

The rate of variation is 5% per minute.

Same regulation program with additional pressure feedback; R_3 is set to 0,5% and a pressure term in $\frac{p - p_0}{p_0}$ is added to error ξ ; p_0 is not a constant but follows the law expressed in Fig. 1.23., curve 1.

In Fig. 1.42., curve 1 gives the pressure transient without pressure feedback; curve 2 gives the same transient with the pressure feedback introduced in the regulator. The benefit of the pressure regulation clearly appears from the comparison between these two curves.

The rate of variation is 0,5% per minute.

Fig. 1.43. gives the pressure transient for a very slow power variation which can be considered as a sequence of steady states; comparing this curve with the one of Fig. 1.41., it can be seen that the pressure fluctuations are significantly reduced. The variation of T_{av} for the same case is given in Fig. 1.44.; it shows that the penalty in variation of the average temperature is quite acceptable.

A detailed investigation is given in Fig. 1.45. and 1.46. In these figures, the recorded variables are expressed as function of power and not of time, in order to facilitate comparison.

Curve 1 gives the evolution for $R_3=0$ and a rate of change of power of 5% per minute; in curve 2, $R_3=0,5$ with the same rate of change; in curve 3, $R_3=0,5$ and power varies of 10% per minute. Fig. 1.45. gives the steam pressure; Fig. 1.46. gives the average temperature of organic, the organic temperature at the primary inlet, the superheating temperature.

do not undergo significant variation. It will be noted that, in the case of a step change of 50 pcm, the power reaches 110% in 14 sec., which is about the transport delay of coolant from the reactor outlet to the boiler inlet.

2.1.9. Scram

The scram is simulated by the instantaneous insertion of a negative reactivity in the neighborhood of 8,000 pcm; the neutron power then decreases from 100% to a level equal to 5%, which represents the effect of photo neutrons (see Figs. 1.62 to 1.65); in the same time, in order to obtain equality between the produced power and the extracted power, the signal which has ordered the insertion of the scrambling rods closes the steam throttle of the turbine inlet, so that the product $PW = WREQ \cdot \Delta H$ ($WREQ$: steam flow, ΔH enthalpy span) follows the variation of the supplied power; the boiler being at a fixed level, the water flow at the economizer input follows the variation of $WREQ$, then, it decreases abruptly while the boiler, because of the transport delay of the coolant from reactor inlet and heat exchanger, receives always hot liquid corresponding to the 100% power level; these two facts explain both the abrupt rise of the average coolant temperature on the heat exchanger side and of the steam temperature, then of the steam pressure. After 12 sec., the cold coolant front comes to the heat exchanger: all the heat exchanger temperatures decrease, likewise the pressure; finally, after some oscillations, all the variables go to their steady state, which corresponds to a power level and a water flow reduced to 5% and to a water input temperature which has remained unchanged (190°C).

In order to reduce the pressure overshoot, it is necessary to make the decrease of the water flow smaller, i.e. to delay the closing of the steam throttle. Figs. 1.66. to 1.68. show this effect: the closing throttle is affected with inertia, the time constant of this inertia being variable, 20 and 30 sec.; it will be noted that the steady state is

2.1.8. Control loss and recovery

The following case of control loss has been studied:

- The reactor stabilized at the nominal power loses suddenly its control (the control rod is blocked) and, at the same time, is subjected to a step change in reactivity of 10 or 50 pcm.
- The control system recovers the reactor when its power reaches 130%.

Figs. 1.58., 1.59., 1.60. and 1.61 show the variation in the time of the neutron power, average coolant temperature on the reactor side, average cladding and fuel temperatures.

The temperature variations are larger in the case of a step change of 10 pcm as, the integrate power being larger, the energy exchanges are more important.

The event of control loss with simultaneous insertion of a step change in reactivity of 50 pcm is highly unlikely; it presumes indeed two accidents in the same time:

- the rupture of the control system;
- the fall in the channel of a bundle during the fuel handling (fuel handling and coolant flow being in the same direction).

A more realistic event would be to consider a control loss simultaneously with the introduction of a bundle at a normal velocity (10 cm/sec), which corresponds to a step change in reactivity of 50 pcm in 25 sec. in the worse case.

During these control losses and recoveries, the variables on the boiler side and the input reactor temperature

Rate of power level variation from 100 to 75% in 5 min.		Coolant temperatures			Cladding temp.	Fuel temp.	Super-heating temp.	Steam pressure
		Input	Average	Output				
Constant average temperature program	g	+ 2,5	- 1	<u>- 3</u>	+ 4,5	- 16,5	- 2,5	+ 3
	a	+ 12	- 2,5	- 14,5	- 5	- 83	- 10	<u>+ 16</u>
Constant steam pressure program (with pressure term)	g	<u>+ 2,5</u>	- 2,5	<u>- 5</u>	- 11,5	- 19	- 3,25	<u>+ 5,75</u>
	a	+ 1,5 - 1	- 13	- 26	- 56	- 97	- 16	<u>+ 3,5</u>
Program optimized for turbine	g	- 5	- 5	<u>- 8</u>	- 8,25	- 22,5	- 7	- 7,5
	a	+ 1,5 - 13	- 30	- 44	- 46	- 115	- 28	+ 2,5 <u>- 20</u>

The amplitudes are in °C or kg/cm²; the gradients in °C/min. or kg/cm²/min.

b) Regulation program 2: constant pressure
Changes in power from 100 to 75%

The rate of variation is 5% per minute. In Figs. 1.47., 1.48., 1.49. and 1.50 are reported the variations of the characteristic parameters.

Changes in power from 100 to 25%

The rate of variation is 5% per minute. Fig. 1.51. and 1.52. give the T_{av} and pressure transient with a parametric variation of R_3 . It can be seen that, because of the long time delays, gains of $R_3 > 0,5$ lead to excessive overshoots, thus $R_3 = 0,5$ has been retained as optimum. This has been verified by more exhaustive computation with fastest transients. All these curves are not reported for the sake of brevity.

c) Other programs

It has been verified that many alternatives, all stable, are possible; in particular, the pressure term can be introduced into other regulation programs, and computer investigation has shown its usefulness. The following table gives the maximum amplitude and gradients of the characteristic variables on the reactor side and on the heat exchanger side for the three following regulation programs:

- the constant-average temperature program;
- the constant-steam pressure program;
- an optimized program for the conditions of the turbine inlet (for which the variations of the steam temperature at the turbine inlet are smallest; the turbine efficiency is a maximum; the steam moisture at the turbine outlet has the lowest possible value.

The steady state of this program is given with accuracy in Figs. 1.53., 1.54. and 1.55, where are also reported the corresponding variables of the two previous programs. The variation of some variables in transient state is given in Figs. 1.56. and 1.57.

reached much slower. The large negative gradient of the steam temperature is essentially due to the sudden decrease of the coolant temperature at the reactor outlet after the step change of power. It might be reduced by changing the coolant flow or by using a coolant by-pass, which was not possible to simulate in the model used.

2.1.10. Remarks on the control system

The validity of the control system has been verified by complementary experiments.

A possible simplification of this control design is to set $R_{1/2}$ equal to zero (see the relations (1.43.) and (1.44.)), on condition that, in the error term, the neutron power and the average temperature are present together. The average temperature being an integral variable of the power, it will indeed be verified that are rightly present a stabilizing proportional term to the power and an integral term of this power through the medium of the mean temperature which is the reset term. If in the reactor occurs an overpower in respect to that absorbed in the heat exchanger, the average temperature rises, which causes the regulator to decrease the power level.

The control system has been verified to be stable; the analogue computation shows however that the transients are a little less good (see Figs. 1.69. to 1.71). Besides, a defect in the measurement device of the average temperature would lead to a more serious accident; indeed, nothing will offer opposition to a shift of the power supplied by the reactor (whereas the integral term of the neutron power will continue to oppose in the other case). It will also be noted that, for this control design, it is necessary to use a position servo to move the control bar, what is generally not the case for the proportional type of control systems (see Fig. 1.21.). On the other hand, taking always $R_{1/2}$ equal to zero, but substituting now the average temperature term by a integral term of the steam pressure:

$$\xi = -R_1 \left[\frac{n - n_0}{n_0} - \frac{PW - PW_0}{PW_0} \right] + R_2 \int \frac{p - p_0}{p_0} dt$$

we obtain a control design which is not able to control the reactor, the steam pressure being not a representative variable of the power.

2.2. The stable core

The interest of the study is to examine whether the stable reactor can use a simplified control system design.

2.2.1. Main characteristics of the channel

Bundle	18 rods
Fuel cross-section	50 cm ²
Coolant cross-section	31 cm ²
Moderator area/coolant area ratio	9 or 7
Channel length	400 cm
Fuel rod radius	0,915 cm
Cladding wall thickness	0,915 mm
Finning ratio	1,75
Thermal resistance between fuel and cladding	0,5 °C/w/cm ²
Maximum integral of conductivity	80 w/cm
Average velocity in the central channel	10 m/sec.
Axial form factor	0,69
Radial form factor	0,86
Disadvantaged thermal flux factor	0,91

Characteristics of the so-called representative channel (assimilated with the mean channel) at its nominal power

Removed power	4,0 MW
Input temperature	293°C
Output temperature	365°C
Average cladding temperature	365°C
Average fuel temperature	500°C

Temperature coefficients for the equilibrium core

First case: $\alpha_v = 1,07 \text{ pcm}/^\circ\text{C}$
 $\alpha_c = + 1,83 \text{ pcm}/^\circ\text{C}$

Second case: $\alpha_v = - 1,5 \text{ pcm}/^\circ\text{C}$
 $\alpha_c = - 1 \text{ pcm}/^\circ\text{C}$

Time constants of the coolant circulation unchanged

2.2.2. Positive coolant temperature coefficienta) On-off system

The simplest control system is an on-off control system where the position of the control rods is changed at a fixed velocity when the error signal exceeds a predetermined value (which thus defines a dead zone). The error signal is always formed at a neutron power-term and an average temperature-term.

This control design is actually able to control the reactor, but with a smaller accuracy and chiefly a rather weak safe margin in respect to the instability field.

The parametric study of the transients (see Figs. 1.72. to 1.76.) gives an optimum for:

Dead zone:	$\pm 1\%$
Inertia time constant:	from 0,5 to 1 sec.
Velocity of the bar:	5 pcm/sec.

A dead zone of $\pm 0,25\%$ or a bar velocity of 15 pcm/sec. lead to the instability, whereas a lower bar velocity (1 pcm/sec.) or a larger dead zone lead to a transient behavior which gives too large excursions to the thermodynamical variables of the heat exchanger.

In case of power change, the regulator follows the imposed program by a step curve (and not by a continuous curve) (see Figs. 1.77. to 1.80.).

The circuit of the dead zone must be temporized to prevent a too frequent sollicitation by the reactor noise (see Fig. 1.81. where is reported the relay running).

In conclusion, the discontinuous-type regulator presents a stable running zone, but its suitability and its safe margin with respect to the instability lead to dissuade its practical use (on this subject, refer to pages 185-193 of

Ref. 1 .

b) Proportional-type system, but with error signal related to a thermal measurement of the power

The error signal is thus

$$\xi = - R_1 \left[\frac{(T_{out} - T_{in}) - \Delta T_o}{\Delta T_o} - \frac{PW - PW_o}{PW_o} \right] - R_2 \frac{\frac{T_{out} + T_{in}}{2} - T_{AVo}}{T_{AVo}}$$

where ΔT_o is the enthalpy span along the channel in steady state, and T_{in} and T_{out} are the input and output temperatures of the reactor.

This relation can be developed as follows:

$$- \xi = K_1 T_{out} + K_2 T_{in} - Ref 1$$

where K_1 , K_2 are numerical constants and Ref. 1 a reference which depends upon R_1 , R_2 , PW , PW_o and the eventual laws of variation which would be affected to T_{av} .

This control design is stable only for very weak gain values (see Figs. 1.82. and 1.83.). On the other hand, all parameters remain very critical with respect to the

instability, which would cause its realization to be difficult in practical conditions.

The optimum parameters are:

$$\left| \begin{array}{l} R_1 = R_2 = 1 \\ R_5 = 1.10^{-3} \\ R_4 = 0,2.10^{-3} \end{array} \right.$$

c) Conclusions

It is practically necessary, in this case, to use the same control design as in the previous studied unstable case. In these conditions, the transient behavior is practically identical with the unstable case; the optimum values of the calculated parameters for the unstable case remain valid. However, the stable case presents a behavior highly favorable in the event of control-loss. It must also be noted that the reactor, though being intrinsically stable according to the usual definition, is unstable when attached to the heat exchanger because of the return of hotter coolant flow due to a perturbation (then a positive reactivity is sufficient to cause instability of the overall loop). This effect appears well in Fig. 1.85.: after about 40 sec., which is the whole coolant transport delay, the temperature rises more rapidly. A mean to evacuate the excess of energy in order to stabilize the reactor is a steam discharge into the atmosphere (see Figs. 1.84. to 1.88.); another solution would be to increase the secondary flow.

The stable reactor also allows a more important safe margin with respect to the zone where it is not possible to control the reactor, as it can be seen on Fig. 1.28.

2.2.3. Negative coolant temperature coefficient

a) On-off control system

The on-off control design with error signal related to the neutron power and the average temperature runs with a greater safe margin than in the case 2.2.2.a). The optimum parameters are here (see Fig. 1.89.):

Dead zone: $\pm 1\%$
 Inertia time constant: from 0,5 to 1 sec.
 Velocity of the bar: 10 pcm/sec.

The system is unstable for a velocity of 30 pcm/sec. and a dead zone of $\pm 0,25\%$.

b) On-off control system but with error signal related to the thermal measurement of the power

This control design runs (wrong) only for very low velocities; its practical use seems to be rejected because its parameters are very critical (see Figs. 1.90. to 1.92.).

c) Proportional-type control design but with error signal related to the thermal measurement of the power

This control design runs with a superior safe margin than in the case 2.2.2.b) (see Fig. 1.93.). The optimum parameters are:

$$\left| \begin{array}{l} R_1 = R_2 = 1 \\ R_5 = 2,5 \cdot 10^{-3} \\ R_4 = 0,5 \cdot 10^{-3} \end{array} \right.$$

The gain values are larger than in the previous case.

d) Conclusions

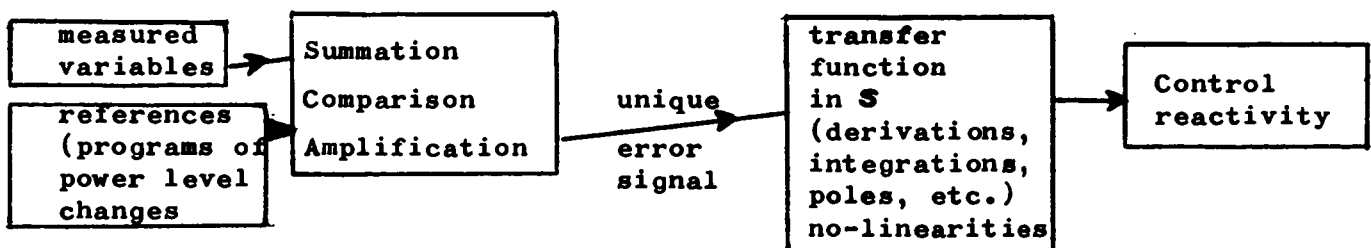
Here, the reactor presents a more intrinsic stability than in the previous case (the two temperature coefficients are negative), which allows to consider the use of regulators described in 2.2.3.a) and 2.2.3.c), also knowing that lower operating velocities must be envisaged. On the other hand, the case 2.2.3.b) is to reject.

However, the control design described in 1.4. remains the one which gives the better performances in transient and the more important safe margin for a variation of the parameters towards the field of unstable gains.

The performances, in the event of control-loss, are evidently more favorable than in the previous case. It will however be noted that, because of the negative coolant temperature coefficient, the steam discharge to a pre-fixed value causes a new steady state of the neutron power to set up at a superior level than the nominal one (Fig. 1.94.). Indeed, without steam discharge after the transient, the power would find again its initial value of 100% ($PW = 100\% = WREQ \cdot \Delta H$)..

2.3. General remarks on the regulator designs

In the regulator design as described in 1.4., the error term is independent of the transfer function of the control mechanism. Thus, the operations depending on time (integration, derivation) are effected separately on certain variables composing the error signal and not on others. The possible variants of the regulator are all described by the general following diagram:



This gives the following advantages:

- simpler design;
- possibility to fit easily the regulator with different programs of power level changes, fixing thus various laws of variation of the temperatures, steam pressure, etc.;
- reduction of the effects due to the cut of one input in certain limits.

It will still be noted that the particular formulation used in 1.4. allows still some freedom of choice in the technological realization; as it has been seen, the regulator can be realized (see Fig. 1.21.):

- by a proportional-type amplifier, a forwards-phase compensation network (derivative), and a rate servo (i.e. with tachometer feedback), excluding every integrative network in the electronic part;
- or by a proportional and integral-type circuit connected to a position servo (i.e. with potentiometer feedback).

For the regulator described in 2.1.10., a position servo is necessary.

The following table summarized the conclusions of the studies in the different cases:

	Unstable case $u = - 0.45$ $c = + 5.6$	Stable case 1 $u = - 1.07$ $c = + 1.83$	Stable case 2 $u = - 1.5$ $c = - 1$
Power coefficient* pcm/%	+ 0,55	- 2,2	- 4,3
1) Proportional-type regulator, neutron power signal and average temperature signal (pressure term in option)	yes	yes	yes
2) Proportional-type regulator, only temperature signal	no	insufficient performances	yes
3) On-off-type regulator, neutron power and temperature signals	no	insufficient performances	yes
4) On-off-type regulator, only temperature signal	no	no	insuff. perform.
5) Proportional-type regulator, pressure and/or integral pressure signals	no	no	no

Examining this table leads to envisage for the stable case 2 a regulator with the advantages of designs 1 and 2.

* Calculated from analytic relations

The configuration is:

- proportional-type servo;
- neutron power signal;
- thermal power signal;
- average temperature signal;

the reactor being able to be controlled in case of lack, by accident, of one of the error signal components.

The error signal is thus defined:

$$\xi = - R_1 \frac{(T_{out} - T_{in}) - \Delta T_o}{\Delta T_o} - R_2 \frac{\frac{T_{out} + T_{in}}{2} - T_{AVo}}{T_{AVo}} -$$

$$- K \frac{n - n_o}{n_o} + (K + R_1) \frac{PW - PW_o}{PW_o}$$

where ΔT_o , T_{AVo} , n_o are the enthalpy span along the channel, the average temperature and the neutron power in steady state, T_{in} and T_{out} the input and output temperatures of the reactor.

This expression can be developed as follows:

$$- \xi = (+ k_1 T_{out} + k_2 T_{in} - \text{Ref 1}) + (k_3 n - \text{Ref 2})$$

where k_1 , k_2 , k_3 are numerical coefficients and Ref 1 and Ref 2 are references depending on R_1 , R_2 , K , PW and PW_o , and on the eventual laws of variation which would be affected to T_{AV} .

By doing so, it can be verified on the analogue computer that, if one of the two terms between brackets is removed, the regulator is always able to control the reactor (Figs. 1.95. to 1.98.).

The analogue investigation gives the following optimum parameters:

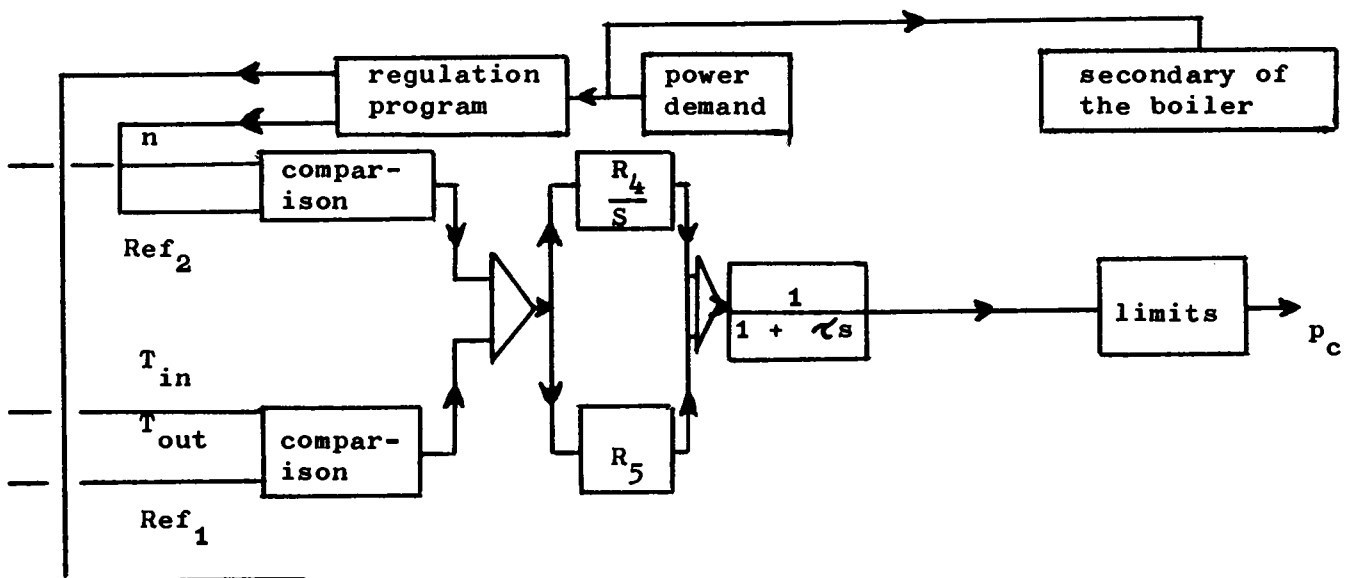
$$\begin{aligned}
 R_1 &= 1 \\
 R_2 &= 1 \\
 R_4 &= 0.5 \cdot 10^{-3} \\
 R_5 &= 2.5 \cdot 10^{-3} \\
 K &= 0.5
 \end{aligned}$$

- servo-mechanism inertia time constant 0.5 ... 1 sec.
- velocity limit of the control bars 15 pcm/sec.
- delay in the measure of the temperatures 4 sec.

Fig. 1.95. gives the behavior of such a regulator for a step change in reactivity of 50 pcm in the case of a normal running, and in the other cases of running with one of the two measurement circuits cut.

Figs. 1.96. to 1.98. give the behavior and the operating of power change if one of the two measurement circuits is cut during the running.

The control design is the following:



III. SECOND PART

1. The mathematical model

1.1. Introduction

In this second part, the model of reactor simulation has been taken again. However, as the representation of the whole plant appeared too heavy and led to minimize the number of operational amplifiers involved, all the groups of delayed neutrons have been lumped into a single group. This simple approximation is sufficient. Only one loop has been represented. It has been necessary to simulate the primary hydraulics because of the heat-exchanger by-pass and the secondary hydraulics because the pressure regulation by the water flow is not instantaneous; it will be recalled that, for a Benson heat exchanger in contrast with the drum boiler, the primary temperature and the steam pressure are not controlled independently because of the fitting of the economizer and boiler surfaces according to the power level.

The used Benson model is given afterwards; its original formulation has involved the reduction of differential equations to partial derivatives and variable limits into a system of ordinary time derivatives.

Only the main characteristics of the general control and regulating system defined by the industrial group will be reported.

2. Hydraulics of the loops

1.2.1. Primary loop

Fig. 2.1. gives a schematic drawing of the hydraulic loop; the power station of the prototype is composed of four identical loops, of which only one is represented.

Every loop includes a by-pass, the primary of the Benson heat exchanger and the primary of the reheater. The location of the pump circulation and the regulation values must be noted. The numbers of the loops reported in Fig. 2.1. correspond to the indexes of the equations expressing that the sum of the pressure losses is equal to zero in every loop:

$$(2.1.) \sum_{o} \frac{l_i}{A_i} \frac{dF_o}{dt} + \sum_{1} \frac{l_i}{A_i} \frac{dF_1}{dt} + \sum_{3} \frac{l_i}{A_i} \frac{dF_2}{dt} - \Delta p - k_o F_o^2 - k_1 F_1^2 - k_3 F_3^2$$

$$(2.2.) \sum_{o} \frac{l_i}{A_i} \frac{dF_o}{dt} + \sum_{1} \frac{l_i}{A_i} \frac{dF_1}{dt} + \sum_{2} \frac{l_i}{A_i} \frac{dF_2}{dt} + \sum_{3} \frac{l_i}{A_i} \frac{dF_4}{dt} - \Delta p - k_o F_o^2 - k_1 F_1^2 - k_2 F_2^2 - k_4 F_4^2$$

$$(2.3.) \sum_{o} \frac{l_i}{A_i} \frac{dF_o}{dt} + \sum_{1} \frac{l_i}{A_i} \frac{dF_1}{dt} + \sum_{2} \frac{l_i}{A_i} \frac{dF_2}{dt} + \sum_{5} \frac{l_i}{A_i} \frac{dF_5}{dt} - \Delta p - k_o F_o^2 - k_1 F_1^2 - k_2 F_2^2 - k_5 F_5^2$$

where F_i is the flow in kg/sec.

Δp is the heat pump pressure in kg/m²

$$\sum_i \frac{l_i}{A_i}$$

is the sum of the ratios between the length and the cross-area of the pipe sections into which the circuits of Fig. (2.1.) can be divided

$$k_i F_i^2$$

are the pressure losses attached to these pipe sections

The system (2.1.), (2.2.), (2.3.) must be completed by the equations of flow conservation:

$$(2.4.) \quad F_o = F_1 + 3 \cdot F_1^*$$

$$(2.5.) \quad F_2 = F_1 - F_3$$

$$(2.6.) \quad F_5 = F_2 - F_4$$

where F_1^* is the flow of the other not represented loops, running in parallel.

In order to introduce the system (2.1.) to (2.6.) on the computer, it is necessary to write it in a transformed form which does not contain derivatives in the second

part of the equation. Therefore, auxiliary variables will be defined, representing in fact the inertia strengths along the three loops:

$$(2.7.) \quad V_1 = \alpha_0 F_0 + \alpha_1 F_1 + \alpha_3 F_3$$

$$(2.8.) \quad V_2 = \alpha_0 F_0 + \alpha_1 F_1 + \alpha_2 F_2 + \alpha_4 F_4$$

$$(2.9.) \quad V_3 = \alpha_0 F_0 + \alpha_1 F_1 + \alpha_2 F_2 + \alpha_5 F_4$$

$$\text{where } \alpha_i = \sum \frac{l_i}{A_i}$$

Substituting gives:

$$(2.10.) \quad \frac{dV_1}{dt} = \Delta_p - k_0 F_0^2 - k_1 F_1^2 - k_3 F_3^2$$

$$(2.11.) \quad \frac{dV_2}{dt} = \Delta_p - k_0 F_0^2 - k_1 F_1^2 - k_2 F_2^2 - k_4 F_4^2$$

$$(2.12.) \quad \frac{dV_3}{dt} = \Delta_p - k_0 F_0^2 - k_1 F_1^2 - k_2 F_2^2 - k_5 F_5^2$$

$$(2.13.) \quad F_1 = \frac{\alpha_3 \alpha_4 V_3 + (\alpha_2 \alpha_4 + \alpha_2 \alpha_5 + \alpha_4 \alpha_5) \cdot V_1 + \alpha_3 \alpha_5 \cdot V_2}{(\alpha_4 + \alpha_5)(\alpha_1 \alpha_3 + \alpha_1 \alpha_2 + \alpha_2 \alpha_3) + \alpha_4 \alpha_5 (\alpha_1 + \alpha_3)}$$

$$(2.14.) \quad F_2 = \frac{(\alpha_1 + \alpha_3) F_1 - V_1}{3}$$

$$(2.15.) \quad F_5 = \frac{\alpha_4 / \alpha_3 (\alpha_1 + \alpha_3) \cdot F_1 - \alpha_4 / \alpha_3 V_1 - V_2 - V_3}{\alpha_4 + \alpha_5}$$

$$(2.16.) \quad F_3 = F_1 - F_2$$

$$(2.17.) \quad F_4 = F_2 - F_5$$

The Eqs. (2.10.) to (2.17.) are those actually represented on the computer, and analogue investigation has shown that the corresponding computation circuits are stable and give

about the same results as those obtained in numerically integrating the equations.

The pressure losses in the pipes being proportional to the squares of the flows, the k_i coefficients are constants (in newtons/m²)/(kg/sec.).

For the valves, the coefficients are variable and of the form:

$$k = \frac{\ell}{A(y)^2}$$

where ℓ is a constant
 A is a characteristic function of the valve
 y is the opening in percentage

Fig. 2.2. gives the A functions used in computation.

If the operating range of the valve is limited, for example from 20% to 100%, Fig. 2.2. can be approximated by the following expression:

$$A(y) = a_1 + a_2 y^2 + a_3 y^4$$

which allows to use the parabolic function generators of the analogue computer. (For Fig. 2.2., $a_1 = 4.36 \times 10^{-2}$, $a_2 = 2.961 \times 10^{-1}$, $a_3 = 6.54 \times 10^{-2}$; the corresponding points are reported on the figure). The pump characteristics are given in Fig. 2.3.

The temperature transfer functions of the pipes will be considered as pure time delays using a 5th order Padé's approximation to realize the delay operator.

1.2.2. Secondary loop

Fig. 2.4. is a schematic drawing of the secondary loop, where a common collector gathers the flows of the heat exchangers before distributing them towards the turbine. The feed pump is assumed to maintain the pressure independent of the value of the flows. For every heat exchanger, there is a regulation valve of the water flow. In the following, an unique heat exchanger will be represented, the others being assumed to be in the same conditions, then FD_{201} must be put equal to FD_{101} .

The flow entering into FD_{101} is deduced by the usual momentum equation:

$$\frac{Z}{A} \cdot \frac{dFD_{101}}{dt} = PD_{001} - PD_{002} - (16 KD_{001} + KD_{001} + \frac{Z}{A(YD_{101})}) FD_{101}^2$$

The pressures and the temperatures in the collector are deduced by a mass and energy balance:

$$(2.19.) \quad V_{COLL} \cdot \frac{d(RO_{002})}{dt} = 3 \cdot FD_{202} + FD_{102} - FD_{002}$$

$$(2.20.) \quad V_{COLL} \cdot \frac{d(RO_{002} \cdot ID_{002})}{dt} = 3 FD_{202} \left[EVSAT + CPS (TD_{202} - TSAT) \right] \\ + FD_{102} \left[EVSAT + CPS (TD_{102} - TSAT) \right] - FD_{002} IR_{002} \\ - y_e \cdot \frac{GECO}{AS} - y_B \cdot \frac{GEVA}{AS}$$

taking

$$(2.21.) \quad ID_{002} = AIPRO + BIPRO \cdot \left(\frac{PD_{002}}{RO_{002}} \right)$$

$$(2.22.) \quad TD_{002} = ATI \cdot (ID_{002}) + BTP \cdot (PD_{002}) + CT$$

where	VCOLL	is the collector volume
	RD_{002}	is the density of the steam in the collector
	PD_{002}	is the pressure of the steam in the collector
	ID_{002}	is the enthalpy of the steam in the collector
	TD_{002}	is the temperature of the steam in the collector
	FD_{002}	is the flow of the steam from the collector to the turbine
	GECO and GEVA	represent the mass for unit of length for the economizer and the evaporator
	Y_e and Y_B	represent the heights of the economizer and the evaporator
	AS	is the secondary cross-section of the boiler

Expressions (2.21.) and (2.22.) are linearizations of the steam characteristics, the precision of which can be judged by looking at Figs. 1.15. and 1.20.; the approximation (2.21.) has also been introduced into (2.20.). The mass flow and temperature of the steam exiting from the heat exchanger (FD_{102} , TD_{102}) are output variables from the "Benson heat exchanger block"; FD_{202} and TD_{202} can be assumed equal to FD_{102} and TD_{102} as the four loops are working in the same conditions.

The flow into the turbine is calculated by:

$$(2.23.) \quad FD_{002} = W_t PD_{002}$$

where W_t is proportional to the power demand; it is also possible to calculate the power delivered to the turbine by:

$$(2.24.) \quad W_{el} = (\Delta H_{ech} + \Delta H_{resurch} / \beta) FD_{002} \eta$$

where ΔH_{ech} and $\Delta H_{resurch}$ are the enthalpy spans on the secondary heat exchangers and reheaters

β the part of flow entering into the reheater

η the efficiency of the turbo-alternator group

1.3. Heat transfer equations in the Benson

1.3.1. Location of the phase-change zones

The primary and secondary fluids flow in opposite directions along a wall; the primary fluid (organic coolant) remains always liquid along its path, whereas the secondary fluid is changed from liquid state to wet steam and dry steam; the secondary circuit having a continuous structure, it results that the limits between the different thermodynamical states are variable in position. In the boiling zone, the same velocity will be assumed to the two phases.

The height of the economizer, of the evaporator and of the superheater is calculated from overall balances.

For any cross-element of the heat exchanger, the mass and energy balances give both for the primary and for the secondary:

$$(2.25.) \quad \frac{d}{dt} \int_{y_1}^{y_2} A \rho H dy = F_{in} H_{in} - F_{out} H_{out} + \int_{y_1}^{y_2} \alpha (T_p - T) dy$$

$$(2.26.) \quad \frac{d}{dt} \int_{y_1}^{y_2} \rho A dy = \rho_{in} F_{in} - \rho_{out} F_{out}$$

where

A	is the cross-section for flow of fluid
ρ	is the density (kg/m ³)
H	is the fluid enthalpy (kcal/kg)
F	is a mass flow (kg/sec.)
α	is the heat transfer coefficient per unit length (kcal/°C/m)
dy	is the height element
y	is the height coordinate
T	is the temperature

The indexes "in" and "out" refer to the entering and leaving fluid, and "p" to the wall.

Applying the relations (2.25.) and (2.26.) to the entire height of the economizer, the limit conditions are:

- the flow of input;
- the enthalpy of input;
- the enthalpy of saturation deduced from the pressure.

Assuming that the enthalpy distribution is changed along the heat exchanger according to a known law, Eqs. (2.25.) and (2.26.) allow to calculate the height of the economizer (y_e) and the exit flow (F_{out}). The following hypothesis must be introduced in order to resolve these equations for the economizer:

- the density is constant;
- the enthalpy is varied linearly according to the temperature:

$$H = H_o + C_p T$$

where C_p is the specific heat

- the temperature distribution is linear:

$$T = T_{in} + (T_{sat} - T_{in}) \frac{y}{y_e}$$

where T_{sat} is the saturation temperature.

The whole height of the economizer will be divided into NE cells, in order to quantify it according to the y axis. In these conditions, applying (2.25.) and (2.26.) to the secondary and on the whole economizer gives:

$$(2.27.) \rho A C_p \frac{d}{dt} (y_e \cdot T) = C_p F_{in} T_{in} - C_p F_{out} \cdot T_{sat} + \alpha \sum_1^{NE} (T_{p_i} - T_i) \cdot y_e / NE$$

$$(2.28.) \rho A \frac{d}{dt} y_e = (F_{in} - F_{out})$$

Then, after separating the variables and taking into account that $T = \frac{T_{in} + T_{sat}}{2}$:

$$(2.29.) \rho_{AC}^p \frac{T_{in} + T_{sat}}{2} \frac{dy_e}{dt} = - \frac{\rho_{AC}^p y_e}{2} \left(\frac{dT_{in}}{dt} + \frac{dT_{sat}}{dt} \right) +$$

$$+ C_p F_{in} T_{in} - C_p F_{out} T_{out} + \sum_1^{NE} (T_{p_i} - T_i) y_e / NE$$

$$(2.30.) F_{out} = F_{in} - \rho_A \frac{dy_e}{dt}$$

$$(2.31.) T_i = T_{in} + (T_{sat} - T_{in}) \frac{y_e}{NE} \cdot i$$

where T_i is the average temperature of the cell indexed i . It must be noted that, if the pressure is constant, or is little varied, the term in $\frac{dT_{sat}}{dt}$ must be neglected in (2.29.).

Likewise, in most cases the variations of the input temperature will be very slow and the term in $\frac{dT_{in}}{dt}$ will also be neglected.

In the same manner, the evaporator will be quantified in NB sections, where the hypothesis are:

- linear distribution of the enthalpy

$$H = ELSAT + (EVSAT - ELSAT) \frac{y}{y_a}$$

$$T = TSAT$$

where

$$l = l(H) = \frac{1}{v' + (v'' - v') \frac{y}{y_B}}$$

$$l' = \frac{1}{y_B H} \int_0^{y_B} l H dy$$

$$l'' = \frac{1}{y_B} \int_0^{y_B} l dy$$

$v' = \frac{1}{\rho'}$
 $v'' = \frac{1}{\rho''}$

$\bar{H} = \frac{EVSAT + ELSAT}{2}$

= specific volume of the saturated liquid

= specific volume of the saturated steam

Using Eqs. (2.25.) and (2.26.) still valid in the case of the evaporator, it results:

$$(2.32.) \quad A \rho \bar{H} \cdot \frac{dy_B}{dt} = \rho' F_{in}^{ELSAT} - \rho'' F_{out}^{EVSAT} + \sum_1^{NB} \alpha_i (T_{p_i} - T_{sat}) \frac{y_B}{NB}$$

$$(2.33.) \quad F_{out} = F_{in} - A \rho \frac{dy_B}{dt}$$

For these equations, the limit conditions are given by the output values of the economizer equations.

By integrating Eqs. (2.29.) and (2.33.), it is possible to determinate the heights of the economizer and evaporator in transient state; of course, the height of the superheater is deduced by difference.

1.3.2. Calculation of the temperature distributions

In order to obtain a rather accurate representation of the heat exchanger transient behavior, every zone previously determined has been subdivided into sections. This is not a quantification of the space variable, the zones being variable in the time, but it is a subdivision relative to these zones. This will define sections of finite differences with variable dimensions and locations.

Relations (2.25.) and (2.26.) remain valid for each of these sections. If the quantification is small enough (which must be determined by numerical computation), the output temperature T_i of the section i can be assimilated to its average temperature. For the same reason, the density and the specific heat C_p can be considered as constant in the interior of a section, which allows to take them outside the derivation operator.

The relations (2.25.) and (2.26.) become, for an indexed section i :

$$(2.34.) \quad \Delta y C_p \rho A \frac{dT_i}{dt} = C_p F_i (T_{i-1} - T_i) + \alpha \cdot \Delta T \cdot \Delta y$$

$$(2.35.) \quad F_i = F_{i-1} - A \rho \frac{dy}{dt}$$

where ΔT is the difference in temperature between the fluid and the wall and where Δy is the height of the section.

Eqs. (2.34.) and (2.35.) are used to represent the primary of the heat exchanger, in the same way as the secondary of the superheater. These equations are also available to represent the wall, when $\alpha \Delta T$ includes the algebraic sum of the exchanged heat amounts on both sides of the wall.

As the location of the sections is variable with respect to the heat exchanger, it is possible to take this movement into account by use of a fictive flow of the wall represented exactly as the real flows. In this case, Eq. (2.25.) will be completely defined if a fictive flow equal to zero at one of the ends of the heat exchanger is given as limit condition.

The equation of the wall will be the following:

$$y C_p \rho A \frac{dT_i}{dt} = F_{i-1} C_p \rho (T_{i-1} - T_i) + \alpha_p (T_p - T)_i \cdot y - \alpha_s (T - T_s)_i \cdot y$$

$$F_i = F_{i-1} - A \rho \frac{dy}{dt}$$

In the following, we will find the complete set of the equations, as applied to the computer:

1.3.3. Set of the equations

a) Calculation of the heights

$$\text{ECO) } \frac{1}{2} \text{ ROSE.AS.CSE.} (TSAT - TSIN) \frac{dYE}{dt} =$$

$$\text{CSE.FSIN.} (TSAT - TSIN) - \sum_1^{NE} i \text{ ALFAE} (TP(i) - TS(i)) \frac{YE}{NE}$$

$$\text{EVA) } \frac{1}{2} \text{ ROSB.AS.} (EVSAT - ELSAT) \frac{dYB}{dt} =$$

$$\text{FSE.} (EVSAT - ELSAT) - \sum_{NE+1}^{NE+NB} i \text{ ALFAB}(i) (TP(i) - TSAT) \frac{YB}{NB}$$

$$\text{SUP) } YS = LTPT - YE - YB$$

b) Calculation of the flowsSecondary

$$\text{ECO) } FSE = FSIN - ROSE.AS \cdot \frac{dYE}{dt}$$

$$\text{EVA) } FSB = FSE - ROSB2.AS \cdot \frac{dYB}{dt}$$

$$\text{SUP) } FS(i) = FS(i-1) - \frac{ROSS.AS}{NS} \cdot \frac{dYS}{dt}$$

$$i = NE+NB+1, NE+NB+NS$$

$$FS(o) = FSB$$

Wall

$$\text{ECO) } FP(i) = FP(i+1) - \frac{RDP.AP}{NE} \cdot \frac{dYE}{dt} \quad i = 1, NE$$

$$\text{EVA) } FP(i) = FP(i+1) - \frac{ROP.AP}{NB} \cdot \frac{dYB}{dt} \quad i = NE+1, NE+NB$$

$$\text{SUP) } FP(i) = FP(i+1) - \frac{ROP.AP}{NS} \cdot \frac{dYS}{dt} \quad i = NE+NB+1, NE+NB+NS$$

$$FP(NE+NB+NS+1) = 0$$

Primary

$$\text{ECO) } FOL(i) = FOL(i+1) - \frac{ROOL.AOL}{NE} \cdot \frac{dYE}{dt} \quad i = 1, NE$$

$$\text{EVA) } FOL(i) = FOL(i+1) - \frac{ROOL.AOL}{NB} \cdot \frac{dYB}{dt} \quad i = NE+1, NE+NB$$

$$\text{SUP) } FOL(i) = FOL(i+1) - \frac{ROOL.AOL}{NS} \cdot \frac{dYS}{dt} \quad i = NE+NB+1, NE+NB+NS$$

$$FOL(NE+NB+NS+1) = FOLIN$$

c) Calculation of the temperaturesPrimary

$$\begin{aligned} \text{ECO) } \quad \text{COL.ROOL.AOL. } \frac{dTOL(i)}{dt} &= \\ &= \text{COL.FOL}(i+1) \cdot (\text{TOL}(i+1) - \text{TOL}(i)) / \text{YE} + \text{ALFP} \cdot (\text{TOL}(i) - \text{TP}(i)) \end{aligned}$$

$$i = 1, \text{ NE}$$

$$\begin{aligned} \text{EVA) } \quad \text{COL.ROOL.AOL. } \frac{dTOL(i)}{dt} &= \\ &= \text{COL.FOL}(i+1) \cdot (\text{TOL}(i+1) - \text{TOL}(i)) / \text{YB} + \text{ALFP} \cdot (\text{TOL}(i) - \text{TP}(i)) \end{aligned}$$

$$i = \text{NE}+1, \text{ NE}+\text{NB}$$

$$\begin{aligned} \text{SUP) } \quad \text{COL.ROOL.AOL. } \frac{dTOL(i)}{dt} &= \\ &= \text{COL.FOL}(i+1) \cdot (\text{TOL}(i+1) - \text{TOL}(i)) / \text{YS} + \text{ALFP} \cdot (\text{TOL}(i) - \text{TP}(i)) \end{aligned}$$

$$i = \text{NE}+\text{NB}+1, \text{ NE}+\text{NB}+\text{NS}$$

$$\text{TOL}(\text{NE}+\text{NB}+\text{NS}+1) = \text{TOLIN}$$

Wall

$$\begin{aligned} \text{ECO) } \quad \text{CP.AP.ROP. } \frac{dTP(i)}{dt} &= \\ &= \text{CP.FP}(i+1) \cdot (\text{TP}(i+1) - \text{TP}(i)) / \text{YE} + \text{ALFP} \cdot (\text{TOL}(i) - \text{TP}(i)) - \\ &- \text{ALFSE} \cdot (\text{TP}(i) - \text{TS}(i)) \end{aligned}$$

$$i = 1, \text{ NE}$$

$$\begin{aligned} \text{EVA)} \quad \text{CP.AP.ROP.} \quad \frac{dTP(i)}{dt} = \\ \text{CP.FP}(i+1) \cdot (TP(i+1) - TP(i)) / YB (+ \text{ALFP}(TOL(i)) - TP(i)) - \\ - \text{ALFSB}(i) (TP(i) - TSAT) \end{aligned}$$

$$i = NE+1, NE+NB$$

$$\begin{aligned} \text{SUP)} \quad \text{CP.AP.ROP.} \quad \frac{dTP(i)}{dt} = \\ = \text{CP.FP}(i+1) \cdot (TP(i+1) - TP(i)) / YS + \text{ALFP} \cdot (TOL(i) - TP(i)) - \\ - \text{ALFSS}(TP(i) - TS(i)) \end{aligned}$$

$$i = NE+NB+1, NE+NB+NS+1$$

Secondary

$$\text{ECO)} \quad TS(i) = TSIN + (TSAT - TSIN) \frac{2 \cdot i - 1}{2 \cdot NE}$$

$$\text{EVA)} \quad TSI = TSAT$$

$$\begin{aligned} \text{SUP)} \quad \text{CSS.AS.ROSS.} \quad \frac{dTS(i)}{dt} = \text{CSS.FS}(i-1) \cdot (TS(i) - TS(i-1)) / YS + \\ + \text{ALFSS} \cdot (TP(i) - TS(i)) \end{aligned}$$

SYMBOLS

AOL, AL, AP	Area of heat transfer surface of the primary, of the wall and of the secondary, (m ²).
COL, CP, VSE, CSS	Specific heat of the primary, of the wall and of the secondary on economizer and superheater sides (kcal/kg °C).
ROOL, ROP, ROSE, ROSS	Average densities of the primary, of the wall and of the secondary on economizer and superheater sides (kg/m ³).
ROSB	Density of the secondary on the evaporator side (kg/m ³).
ROSB1 =	$\frac{2}{EVSAT+ELSAT} \int_0^1 ROSB.HSB dx$
ROSB2 =	ROSB dx =
ROSB =	$1/(v' + (v'' - v') \cdot x)$ kg/m ³
HSB	Enthalpy of the evaporator on secondary side (kcal/kg) = ELSA + (EVSAT - ELSAT)x
ELSAT, EVSAT	Specific heats of the liquid and of the saturated steam (kcal/kg)
v', v''	Specific volumes of the liquid and of the saturated steam (m ³ /kg)
TSAT	Temperature of saturation (°C)
YE, YB, YS	Heights of the economizer, evaporator and superheater (m)
NE, NB, NS	Number of sections for the quantification of the economizer, of the evaporator and of the superheater
LTOT	Total height of the heat exchanger (m) = YE + YB + YS
ALFAE, ALFAB(i), ALFAS	Heat transfer coefficient between wall and secondary for the economizer, the evaporator and the superheater (kcal/sec m ² °C)
ALFP	Heat transfer coefficient between wall and primary (kcal/sec m ² °C)
FSIN, FOLIN	Flows to the secondary and primary inlets (kg/sec)
FSE, FSB, FS(i)	Exit flows of the economizer, of the evaporator and of the superheater (kg/sec)
FOL(i)	Organic flow (kg/sec)
FP(i)	Fictive flow of the wall (kg/sec)
TSIN, TOLIN	Temperature at the secondary and primary inlets (°C)
TOL(i), TP(i), TS(i)	Organic, wall and secondary temperatures (°C)

1.4. The control and regulating system

We will restrict ourselves to give the general principles.

The control and regulating scheme is already given in Fig. 2.5., where the reheater has been removed by simplification. The general regulation scheme is reproduced in Fig. 7., where, by simplification, the reheater has been omitted.

The regulation must hold to the set values:

- the neutron power
- the power to the turbine
- the reactor output temperature
- the steam output temperature
- the steam pressure
- the coolant flow in the reactor

Moreover, the control system must allow the power level changes from the low powers (10 ... 25%) to the nominal power of the power station. The power station must be stable at any power level.

The mathematical simulation of the components of the control system presents no difficulties and will not be retaken here.

The representation of the effect of the valves on the hydraulic loop has been given in 1.2. The transient response of a valve is the same as the one due to a one pole transfer function, but it is necessary to represent also on the computer the velocity limit of their operating mechanism.

The control rods are made of neutron-absorptive gas; with respect to mechanical control rods, their inertia is very weak.

In the regulator, proportional and integral terms are necessary; the analogue computation has showed that the

addition of a derivative term does not improve the control-rod performances.

2. ANALOGUE COMPUTATION RESULTS

2.1. Transient responses of the primary loop

Because of the non-linearities of the primary loop, it is necessary to check the static characteristics before designing a regulating system.

Fig. (2.6.) gives the flow variations as function of heat exchanger throttle opening Y_2 , for a constant value of by-pass-valve opening.

Fig. (2.7.) shows the range of Y_2 variation (heat exchanger valve) when it is necessary to maintain the flow F_1 constant (the indexes refer to Fig. 2.1.). The different values of F_1 are reported as parameters. This figure shows that, for the large flows ($F_1 \geq 1400$ kg/sec.), the efficiency of the regulation becomes unreliable because of the neighborhood of the limits for valves motion travel stoppages, and that it is not possible for the flow regulation (which maintains constant F_1) to run with the by-pass valve too near to its stoppage. It will also be noted that the effect of the regulation valve is the same as the one due to a variable gain in the regulation loop.

According to the present data (June, 1968) of the 250-MWe prototype, it is necessary to set up a flow F_2 (primary heat exchangers and reheaters) equal to 1340 kg/sec. for a temperature span of about 50°C. In these conditions, in order to obtain a good running of the F_1 regulation, it is necessary to hold the set value of F_1 at least at 1400 kg/sec. (which has been confirmed on the computer). Then, in Fig. (2.7.), it must be shown that are necessary a heat exchanger valve opening of about 90% and a by-pass valve opening of about 45%.

Fig. (2.8.) shows that F_2 must be modulated (i.e. that the regulation of the temperature or of the steam pressure can operate) for different values of F_1 , maintained constant by a regulation. This curve shows clearly that the regulations cannot run with a too weak value of F_1 , which justifies afterwards the value of 1400 kg/sec. obtained from the prototype data.

Fig. (2.9.) shows that it is possible to modulate the reheater flow F_5 in the same conditions.

All the previous considerations show clearly that the choice of the set points of the regulating system is not indifferent, but it is practically imposed by the static characteristics of the hydraulic loop.

In the following are summarized the set points determined on the computer:

Reactor flow (for one loop):	$F_1 = 1425$ kg/sec.
By-pass flow:	$F_3 = 85$ kg/sec.
Primary heat exchangers flow:	$F_2 = 1340$ kg/sec.
Benson flow:	$F_4 = 1150$ kg/sec.
Reheaters flow:	$F_5 = 190$ kg/sec.

The pressure loss coefficients being imposed, these values allow to determine the pressure which is necessary to the pump and the pressure losses of the loop reported in the following table:

Head pressure:	21 kg/cm ²
Pressure loss in the reactor:	16.2 kg/cm ²
Pressure loss in pipes:	1.0 kg/cm ²
Pressure loss in the by-pass:	3.8 kg/cm ²
Pressure loss in the primary heat exchanger:	1.3 kg/cm ²
Pressure loss in the heat exchanger valve:	2.1 kg/cm ²
Pressure loss in the heat exchanger pipes:	0.4 kg/cm ²

2.2. Stability of the secondary loop

On the secondary hydraulic loop (see Fig. 2.4.), the steam flow FD_2 is imposed by the power demand, whereas the input water flow FD_1 is determined by the pressure at the feed pump and by the position of the secondary regulation valve. At the equilibrium, the feed water flow must be equal to the steam flow, but, for a certain frequency (of about 0,5 Hz), the phase angle is 180° between these flows and, in these conditions, instabilities can arise.

Fig. 2.10. gives a recording which shows how the instabilities settle. The recording is done in the following conditions:

At the partial opening of the feed valve (50%), the pressure at the pump is 86 kg/cm², whereas the steam pressure at the collector is 70 kg/cm², which gives an overall pressure loss on the loop of 16 kg/cm². There is no regulating system operating on the secondary. Under these conditions, the loop is stable, as can be shown in the figure. Then the feed valve opening is stepped, which involves the pressure losses in the loop to decrease. At a certain moment, the oscillation arises (it goes to a limit cycle) (the last right-hand part of the figure has an expanded scale in time, which allows to examine the phase relations).

We conclude that, first, sufficient pressure losses must be introduced into the loop in order to stabilize it and, secondly, any designed regulating system must suppress the oscillations involved.

2.3. Heat exchanger behavior

2.3.1. Accuracy of the mathematical model

The dynamic behavior of the heat exchanger involves that one of the whole power station; the accuracy of the heat exchanger simulation on the computer is capital. We have seen that this representation is based on the quantification of the three zones of the heat exchanger. The question then arises: into how many sections must be subdivided each zone? The problem can only be carried out experimentally, by examining the asymptotic convergency of the results as function of the increase of the sections number.

Fig. (2.11.) shows how converge the steady state values of temperatures and dimensions of the heat exchanger zones as function of the number of the sections by zone. Finally, the chosen subdivision is a compromise between the accuracy and the bounds of the computer. In this case, have been used:

- 1 section for the economizer
- 4 sections for the evaporator
- 2 sections for the superheater.

The results referring to this subdivision are reported to the right-hand side of Fig. (2.11.).

2.3.2. Steady-state performances.

As for the hydraulic behavior, it is necessary to take the thermal steady-state equilibriums into account, in order to set up the set points of the regulating system, which must maintain the steam characteristics (pressure, temperature) constant at different power levels.

The power level is changed by varying the secondary flow. On the primary side, several regulating programs are

possible as a principle:

- a) constant input temperature and variable flow (using a by-pass);
- b) constant flow and variable input temperature (case without by-pass);
- c) variable temperature and flow (using a by-pass).

For the case c), an infinity of solutions is possible. For the same power conditions, the options a), b) and c) lead to significative differences in the temperature distributions and then in the location of the heat exchanger phase changes. The search of a determined shape of temperature distribution will be able to be a criteria of choice between the solutions a), b) and c) in order to change the power level.

Figs. (2.12.) to (2.17.) give the state of the heat exchanger in various cases, for the base data of the prototype, for a steam temperature of 345°C and a steam pressure of 67 kg/cm².

Fig. (2.12.) gives the heat exchanger subdivision in case a). It can be shown that, for the low power levels, the evaporator fills nearly all the heat exchanger, whereas the economizer and the superheater become very small. Thus, a little variation of the primary flow involves a large variation of the steam temperature, which must cause the regulating system to be instable (at 25% of the power, a variation of 2.8°C on the steam temperature involves a variation of 1 kg/sec. on the primary flow, which is to compare with 0.033°C for 1 kg/sec. at 100% of the power). This fact makes difficult the regulation at the power levels inferior to 70% ... 50%.

Fig. (2.13.) gives the variation of the flow and of the output primary temperature for the same case a), as function of the power level.

Fig. (2.14.) gives the subdivision of the heat exchanger for case b) (no by-pass): at the low power levels, the evaporator diminishes, whereas the superheater increases. Variations on the primary will have a less important influence with respect to the previous case.

Fig. (2.15.) shows the variations of the coolant input and output temperatures in case b). This figure shows that, in case of regulation without by-pass, it is not possible to hold the reactor output temperature constant as function of the power level. The set point of this temperature must vary necessarily according to Fig. (2.15.), which involves a decrease of about 8°C for a variation of the power level from 100% to 25%. It can be seen that, at the low power levels, the heat exchanger pinch-point decreases (whereas it was constant in case a)).

Examining Figs. (2.12.) and (2.14.), it appears that it is possible to find an intermediate scheme (case c)) which allows to maintain about constant the height of the heat exchanger zones (Fig.(2.16.)) (and also the temperature distributions), this by varying the primary flow and the coolant input temperature as reported in Fig. (2.17.). This solution requires the use of a by-pass, but eliminates the defect of scheme a), which we have pointed out previously; it allows to find easier the conditions for a regulating system being stable at the low powers.

Figs. (2.12.), (2.14.) and (2.16.) would deserve a careful examination by the builder of the heat exchanger, who would have to indicate what configuration gives the better operating conditions at part loads.

2.3.3. Transient responses of the heat exchanger

The variation of the heat exchanger transient behavior as function of the power level determines essentially the performances of the regulating system (or even determines the possibility or not to regulate).

Now, we have seen in the previous chapter that the power can be varied by modifying either the primary flow or the primary input temperature, or both. As for the static cases, the transient behavior is very different and we will examine each one of these cases. It will be recalled that the output steam characteristics must be maintained independent of the power level.

The input variables of the heat exchanger are the temperature and the flow. The output variables which are of interest (because they must be regulated) are the steam output temperature and the steam pressure. As the steam pressure mainly depends on the characteristics of the secondary loop, the responses of the steam temperature to the input variables in step function will be of interest. Besides, these computations would allow to derive the heat exchanger transfer functions.

Fig. (2.18.) shows the response of the steam temperature as a result of a step-like variation of the input coolant temperature at 100% of the power level. (In this attempt, as in the next one, are reported the responses, either for a positive or for a negative variation in step function).

Figs. (2.19.) and (2.20.) give the same attempt for 75% and 50%, the power being varied according to case a) (by-pass, constant input coolant temperature). It can be shown that the transfer function is substantially modified in amplitude and phase; furthermore, the dissymmetry of the responses as a result of the positive and negative variations in step function increases. We can conclude that the running of a control system according to scheme a) will be difficult, which has been actually pointed out on the computer. In other words, according to the regulation, it is not recommended to maintain the reactor output temperature constant when the power level of the plant is varied. It will be noted that this conclusion, based on transient considerations, strengthens the one of the previous chapter which was set up on static considerations.

Fig. (2.21.) gives the response of the output temperature as a result of a step-like variation of the input flow.

Figs. (2.22.) and (2.23.) give the same attempt at 75% and 50% of the power level, always for scheme a). The comparison of the three figures between themselves involves the same conclusions (for the response to a variation of flow in step function) which we had expressed for the response to a variation

temperature in step function: i.e., the variation of the transfer function is such that the regulation will be always difficult to stabilize at the low powers. Incidentally, the examination of the six last figures shows also that an approach of stability based on a transfer function representation (i.e. on a linearization of the problem) cannot give sure results.

Figs. (2.24.) and (2.25.) give the response of the steam temperature as a result of a step-like variation of the input coolant temperature, at 75% and 50% of the power level and for scheme b) (constant flow, no by-pass). It is important to note how these curves differ from those of Figs. (2.19.) and (2.20.). Here, the amplitude and phase characteristics change little with the power level and this scheme allows immediately to consider a regulator being stable at any power. This regulator might however follow the set points as indicated in chapter 2.3.2. (steady-state performances).

Fig. (2.26.) shows the response to a variation in step function of the flow, for scheme c), at 75%, 50% and 25% of the nominal power (case where the input flow and the input temperature are both varied in order to maintain the location of the phases water-steam constant in the heat exchanger secondary). This gain in amplitude decreases at the low powers, which would made stable but unefficient a regulation of the steam temperature by regulating the primary flow. In this case, the power station might be better regulated by simply holding the primary heat exchanger flow as function of the operating power of the plant (the by-pass ensuring always the regulation of the flow in the reactor) and regulating the steam temperature by means of the fixed output reactor temperature.

2.3.4. Internal transient variations

Independently of the study of the heat exchanger as a control element, the mathematical model can yield information on the transient behavior of the internal heat exchanger variables. We will not extend ourselves over this point of view, but, for illustrative purposes, we give the following figures; these

attempts are less accurate than the previous ones; indeed, they have been set up by taking a quantification of two sections by cell into account (see (Fig.2.11.)); all refer to the case of the nominal power.

Fig. (2.27.) gives the variations as result of a positive step in input secondary temperature.

Fig. (2.28.) gives the responses to a positive step in input primary organic temperature.

Fig. (2.29.) gives the responses to a positive step in feed water flow.

Fig. (2.30.) gives the responses to a positive step in primary organic flow.

2.3. Conclusions

In this study of the heat exchanger transient behavior, it has been searched to set up the basis knowledge being necessary to design a regulating system. As usual, in this kind of study, the control engineer can choose between several arrangements for the control devices and points of measurement and each one of them, well studied, involves a suitable design. The study of the regulation must - above all - be founded on a complete investigation of the steady state operating at all power levels. Without this, it would be possible to choose criteria incompatible between themselves.

The simulation also yields information which can be useful to the design engineer or the builder, like the distribution of the pressures along the hydraulic loop or the repartition of the water-steam phases in the heat exchanger.

If several control designs, also suitable for the control engineer, are balanced, the features reported previously will allow to fix a choice based on technological considerations (thermal stresses, charges, etc...).

Another, more general, conclusion is that the dynamic study of a power plant similar to the one studied here must rest on an accurate mathematical heat exchanger representation both for the heat transfers and for the hydraulic behavior. For the reactor, a on-point model is sufficient.

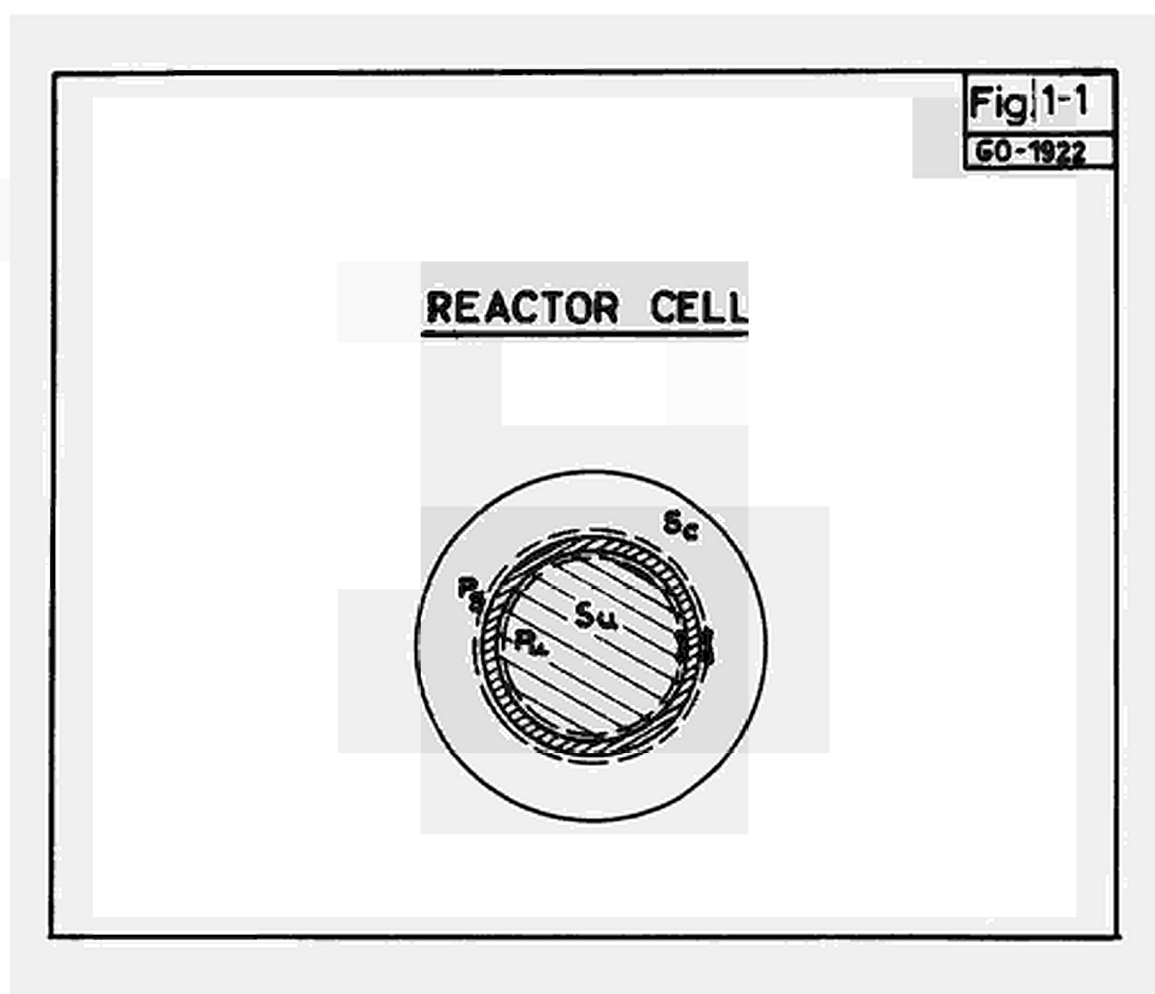
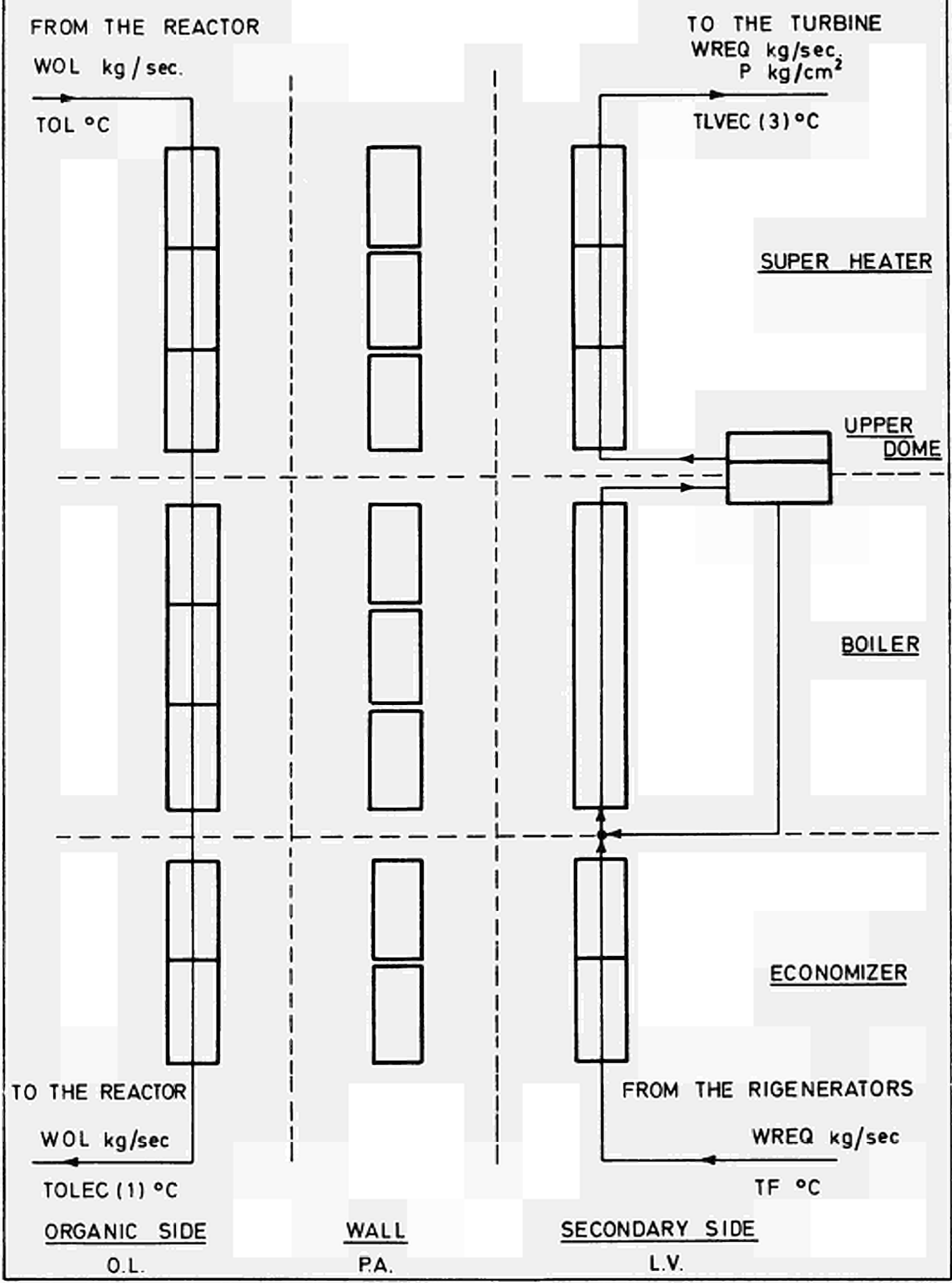


Fig. 1-2
60-1804

SCHEME OF THE CELLS INTO WHICH THE
HEAT EXCHANGER HAS BEEN DIVIDED



ENERGY TRANSPORTED IN
BY THE O.L. INCOMING

FROM THE REACTOR

WOL (kg/sec.)
TOL °C

SUPERHEATER L.O.

STORED ENERGY

$$ALOS \cdot LSUR \cdot CLOS \cdot ROLOS \cdot \frac{dTOLSU^{(3)}}{dt}$$



ENERGY TRANSPORTED OUT FROM 3
INTO 2 BY O.L.

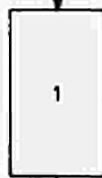
$$WOL \cdot CLOS \cdot TOLSU^{(3)}$$

$$ALOS \cdot LSUR \cdot CLOS \cdot ROLOS \cdot \frac{dTOLSU^{(2)}}{dt}$$



$$WOL \cdot CLOS \cdot TOLSU^{(2)}$$

$$ALOS \cdot LSUR \cdot CLOS \cdot ROLOS \cdot \frac{dTOLSU^{(1)}}{dt}$$



$$WOL \cdot CLOS \cdot TOLSU^{(1)}$$

TO THE BOILER

ENERGY CONSERVATION LAW

$$ALOS \cdot LSUR \cdot CLOS \cdot ROLOS \cdot \frac{dTOLSU^{(3)}}{dt} = WOL \cdot CLOS \cdot (TOL - TOLSU^{(3)}) - HLOS \cdot PLOS \cdot LSUR \cdot (TOLSU^{(3)} - TPASU^{(3)})$$

$$ALOS \cdot LSUR \cdot CLOS \cdot ROLOS \cdot \frac{dTOLSU^{(2)}}{dt} = WOL \cdot CLOS \cdot (TOLSU^{(3)} - TOLSU^{(2)}) - HLOS \cdot PLOS \cdot LSUR \cdot (TOLSU^{(2)} - TPASU^{(2)})$$

$$ALOS \cdot LSUR \cdot CLOS \cdot ROLOS \cdot \frac{dTOLSU^{(1)}}{dt} = WOL \cdot CLOS \cdot (TOLSU^{(2)} - TOLSU^{(1)}) - HLOS \cdot PLOS \cdot LSUR \cdot (TOLSU^{(1)} - TPASU^{(1)})$$

SYMBOLS

TOL O.L. INLET TEMP. °C .

TOLSU⁽ⁱ⁾ O.L. TEMP. IN THE ith CELL °C

TPASU⁽ⁱ⁾ WALL TEMP. IN THE ith CELL °C

WOL = O.L. MASS FLOW kg/sec

CLOS = O.L. SPECIFIC HEAT kcal/kg

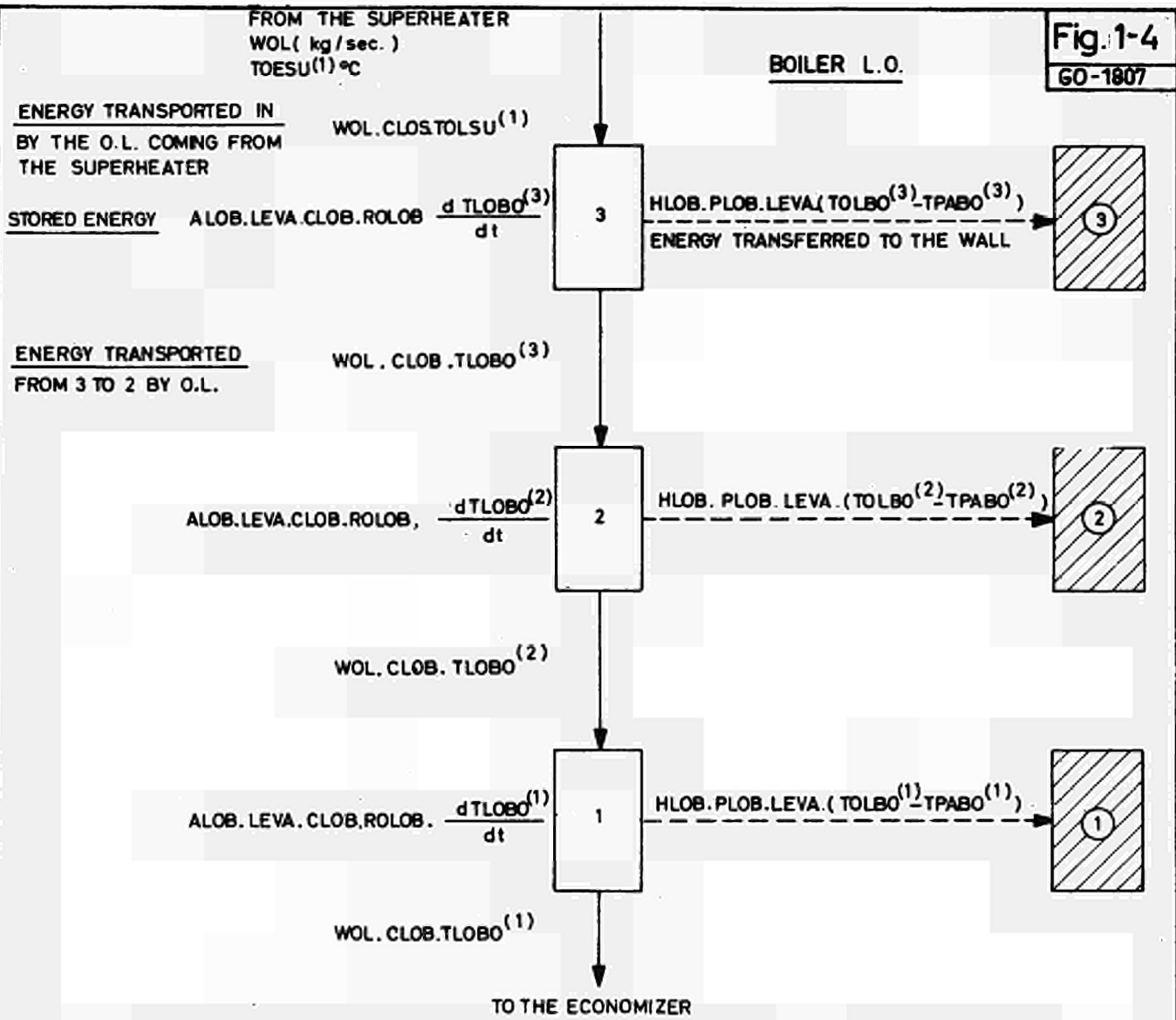
ROLOS = O.L. DENSITY kg/m³

HLOS = HEAT TRANSFER COEFF. kcal/m²sec °C

ALOS = CELL CROSS SECTION m²

LSUR = CELL LENGTH m

PLOS = CELL WETTED PERIMETER L.O. m



ENERGY CONSERVATION LAW

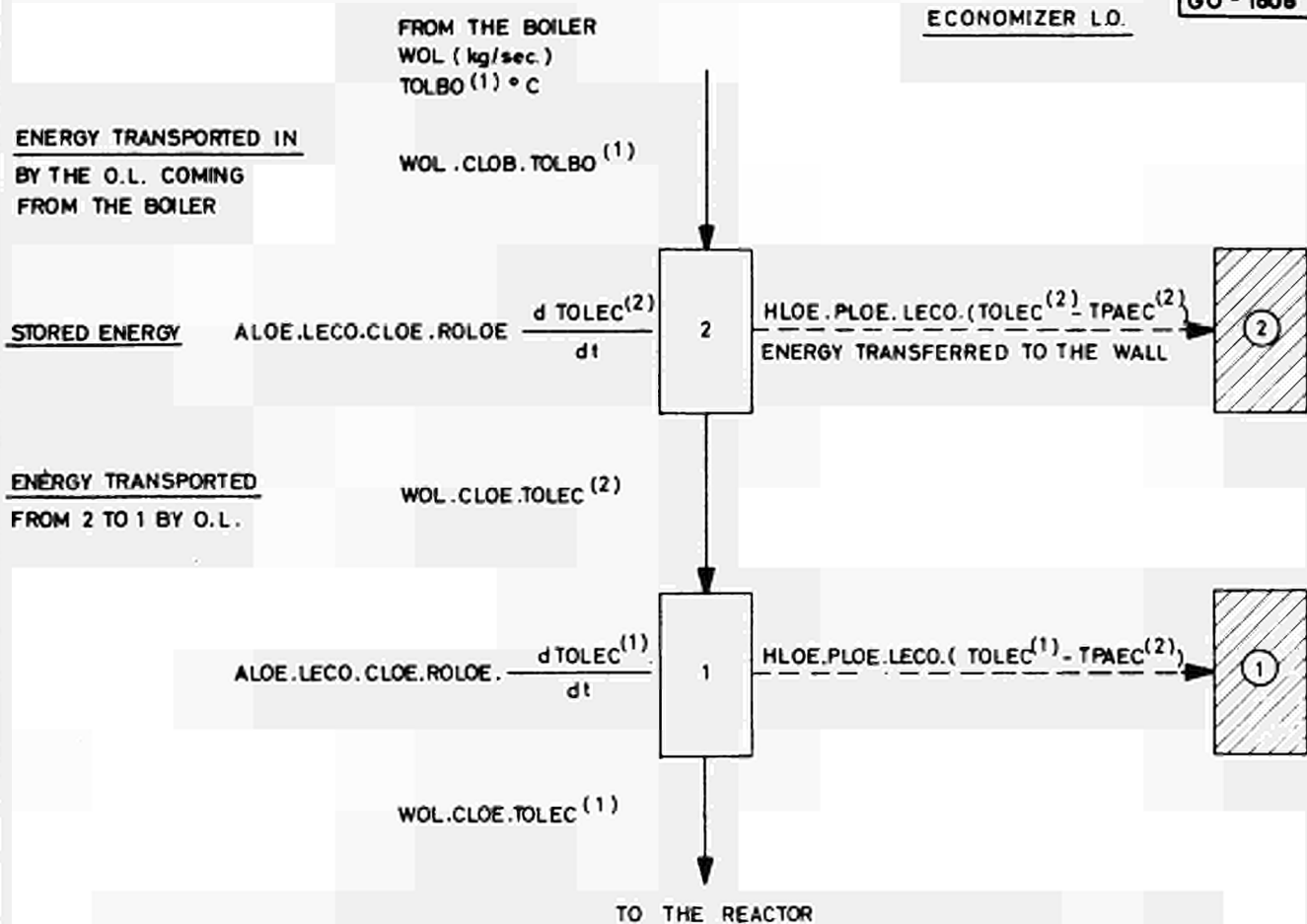
$$ALOB.LEVA.CLOB.ROLOB \cdot \frac{dTOLBO^{(3)}}{dt} = WOL \cdot (CLOS.TOLSU^{(1)} - CLOB.TLOBO^{(3)}) - HLOB.PLOB.LEVA \cdot (TOLBO^{(3)} - TPABO^{(3)})$$

$$ALOB.LEVA.CLOB.ROLOB \cdot \frac{dTOLBO^{(2)}}{dt} = WOL.CLOB \cdot (TLOBO^{(3)} - TLOBO^{(2)}) - HLOB.PLOB.LEVA \cdot (TOLBO^{(2)} - TPABO^{(2)})$$

$$ALOB.LEVA.CLOB.ROLOB \cdot \frac{dTOLBO^{(1)}}{dt} = WOL.CLOB \cdot (TLOBO^{(2)} - TLOBO^{(1)}) - HLOB.PLOB.LEVA \cdot (TOLBO^{(1)} - TPABO^{(1)})$$

SYMBOLS

- TOLSU⁽¹⁾ O.L. INLET TEMPERATURE °C
 TOLBO⁽ⁱ⁾ O.L. TEMP. IN THE ith CELL °C
 TPABO⁽ⁱ⁾ WALL TEMP IN THE ith CELL °C
- WOL = O.L. MASS FLOW kg/sec
 CLOB = O.L. SPECIFIC HEAT kcal/kg °C
 ROLOB = O.L. DENSITY kg/m³
 HLOB = HEAT TRANSFERT COEFF kcal/m² sec °C
- ALOB = CELL CROSS SECTION m²
 LEVA = CELL LENGHT m
 PLOB = CELL WETTED PERIMETER L.O. m



ENERGY CONSERVATION LAW

$$\text{ALOE} \cdot \text{LECO} \cdot \text{CLOE} \cdot \text{ROLOE} \cdot \frac{d \text{TOLEC}^{(2)}}{dt} = \text{WOL} \cdot (\text{CLOB} \cdot \text{TOLBO}^{(1)} - \text{CLOE} \cdot \text{TOLEC}^{(2)}) - \text{HLOE} \cdot \text{PLOE} \cdot \text{LECO} \cdot (\text{TOLEC}^{(2)} - \text{TPAEC}^{(2)})$$

$$\text{ALOE} \cdot \text{LECO} \cdot \text{CLOE} \cdot \text{ROLOE} \cdot \frac{d \text{TOLEC}^{(1)}}{dt} = \text{WOL} \cdot \text{CLOE} \cdot (\text{TOLEC}^{(2)} - \text{TOLEC}^{(1)}) - \text{HLOE} \cdot \text{PLOE} \cdot \text{LECO} \cdot (\text{TOLEC}^{(1)} - \text{TPAEC}^{(1)})$$

SYMBOLS

TOLBO⁽¹⁾ O.L. INLET TEMP °C

TOLEC⁽ⁱ⁾ O.L. TEMP. IN THE ⁱth CELL

TPAEC⁽ⁱ⁾ WALL TEMP. IN THE ⁱth CELL

WOL = O.L. MASS FLOW kg/sec

CLOE = O.L. SPECIFIC HEAT kcal/kg °C

ROLOE = O.L. DENSITY kg/m³

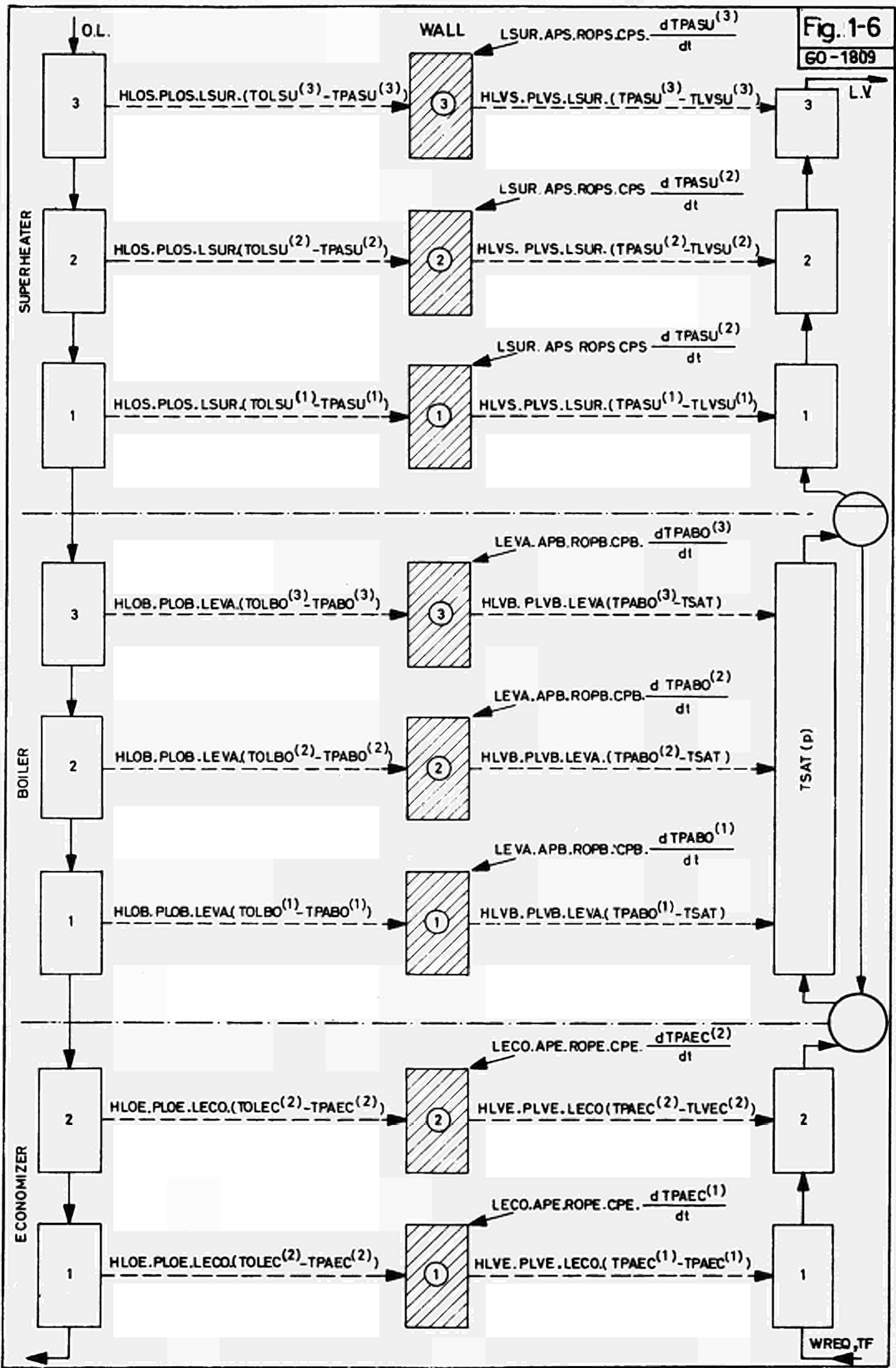
HLOE = HEAT TRANSFER COEFF kcal/m² sec °C

ALOE = CELL CROSS SECTION m²

LECO = CELL LENGTH m

PLOE = CELL WETTED PERIMETER L.O. m

Fig. 1-6
60-1809



SUPERHEATER

Fig. 1-7

60-1810

$$APS \cdot ROPS \cdot LPS \cdot \frac{d TPASU(i)}{dt} = HLOS \cdot PLOS \cdot (TOLSU(i) - TPASU(i)) - HLVS \cdot PLVS \cdot (TPASU(i) - TLVSU(i))$$

i = 1,2,3

BOILER

$$APB \cdot ROPB \cdot CPB \cdot \frac{d TPABO(i)}{dt} = HLOB \cdot PLOB \cdot (TOLBO(i) - TPABO(i)) - HLVB \cdot PLVB \cdot (TPABO(i) - TSAT(p))$$

i = 1,2,3

ECONOMIZER

$$APE \cdot ROPE \cdot CPE \cdot \frac{d TPAEC(i)}{dt} = HLOE \cdot PLOE \cdot (TOLEC(i) - TPAEC(i)) - HLVE \cdot PLVE \cdot (TPAEC(i) - TLVEC(i))$$

i = 1,2

SYMBOLS

TPASU(i) = WALL TEMP IN THE ith CELL OF THE SUPERHEATER °C

TPABO(i) = WALL TEMP IN THE ith CELL OF THE BOILER °C

TPAEC(i) = WALL TEMP IN THE ith CELL OF THE ECONOMIZER °C

TLVSU(i) = STEAM TEMP IN THE ith CELL OF THE SUPERHEATER °C

TSAT (p) = SATURATION TEMPERATURE AT PRESSURE P °C

TLVEC (i) = WATER TEMP. IN THE ith CELL OF THE ECONOMIZER °C

TOLSU(i) = O.L. TEMP. IN THE ith CELL OF THE SUPERHEATER °C

TOLBO (i) = O.L. TEMP. IN THE ith CELL OF THE BOILER °C

TOLEC (i) = O.L. TEMP. IN THE ith CELL OF THE ECONOMIZER °C

APS = WALL CROSS SECTION IN THE SUPERHEATER ROPS = ROPB = ROPE = WALL DENSITY kg/m³

APB = WALL CROSS SECTION IN THE BOILER

APE = WALL CROSS SECTION IN THE ECONOMIZER CPS = CPB = CPE = WALL SPECIFIC HEAT KCAL/kg°C

PLOS = WETTED PERIMETER IN THE SUPERHEATER, PRIMARY SIDE m

PLVS = WETTED PERIMETER IN THE SUPERHEATER, SECONDARY SIDE m

PLOB = WETTED PERIMETER IN THE BOILER, PRIMARY SIDE m

PLVB = WETTED PERIMETER IN THE BOILER, SECONDARY SIDE m

PLVE = WETTED PERIMETER IN THE ECONOMIZER, PRIMARY SIDE m

PLVE = WETTED PERIMETER IN THE ECONOMIZER, SECONDARY SIDE m

HLOS = HEAT TRANSF. COEFF. BETWEEN THE O.L. AND THE WALL IN THE SUPERHEATER KCAL/m²sec °C

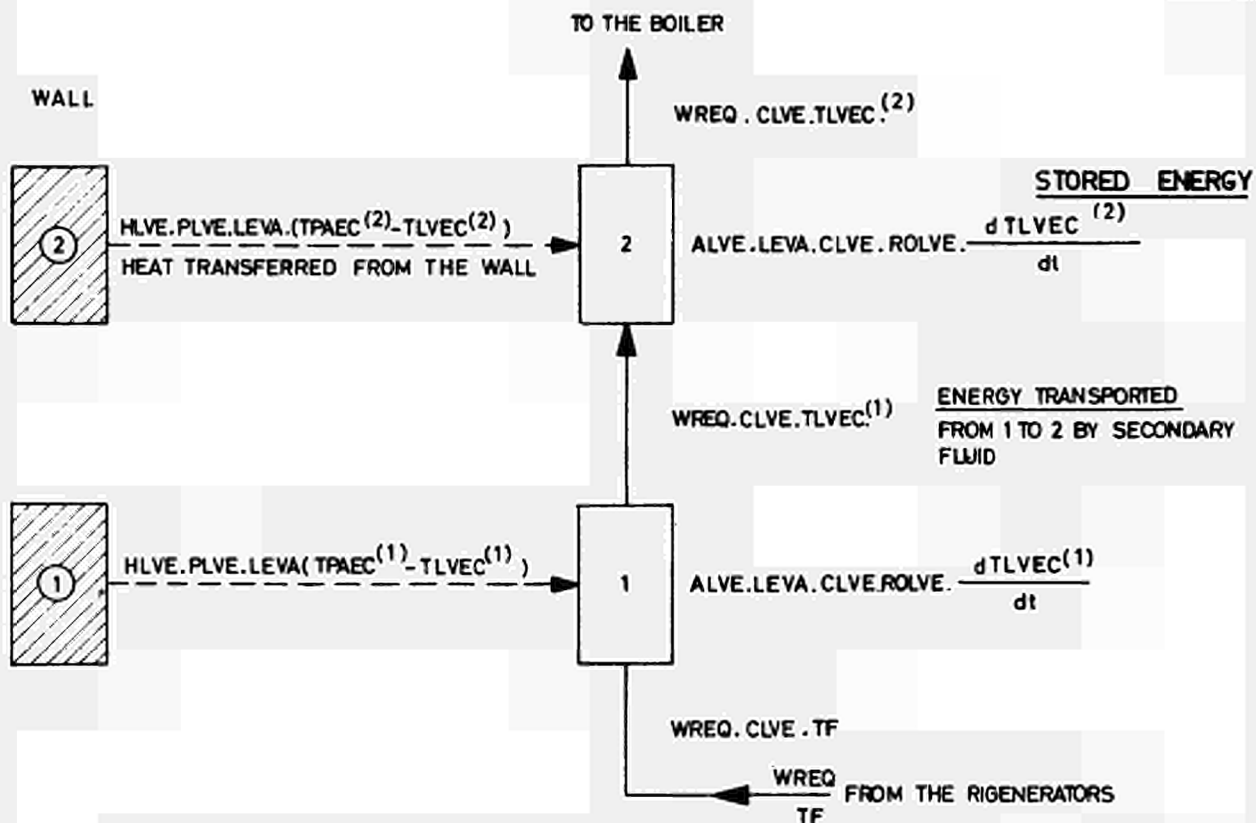
HLVS = " " " " THE WALL AND THE SECONDARY IN THE SUPERHEATER "

HLOB = " " " " THE O.L. AND THE WALL IN THE BOILER "

HLVB = " " " " THE WALL AND THE SECONDARY IN THE BOILER "

HLOE = " " " " THE O.L. AND THE WALL IN THE ECONOMIZER "

HLVE = " " " " THE WALL AND THE SECONDARY IN THE ECONOMIZER "

ENERGY CONSERVATION LAW

$$ALVE \cdot LEVA \cdot CLVE \cdot ROLVE \cdot \frac{dTLVEC^{(2)}}{dt} = WREQ \cdot CLVE \cdot (TLVEC^{(1)} - TLVEC^{(2)}) + HLVE \cdot PLVE \cdot LEVA \cdot (TPAEC^{(2)} - TPAEC^{(1)})$$

$$ALVE \cdot LEVA \cdot CLVE \cdot ROLVE \cdot \frac{dTLVEC^{(1)}}{dt} = WREQ \cdot CLVE \cdot (TF - TLVEC^{(1)}) + HLVE \cdot PLVE \cdot LEVA \cdot (TPAEC^{(2)} - TPAEC^{(1)})$$

SYMBOLS

TF FEED WATER TEMPERATURE °C

TLVEC⁽ⁱ⁾ WATER TEMPERATURE OF THE ith CELLTPAEC⁽ⁱ⁾ WALL TEMPERATURE OF THE ith CELL

WREQ WATER MASS FLOW RATE kg/sec.

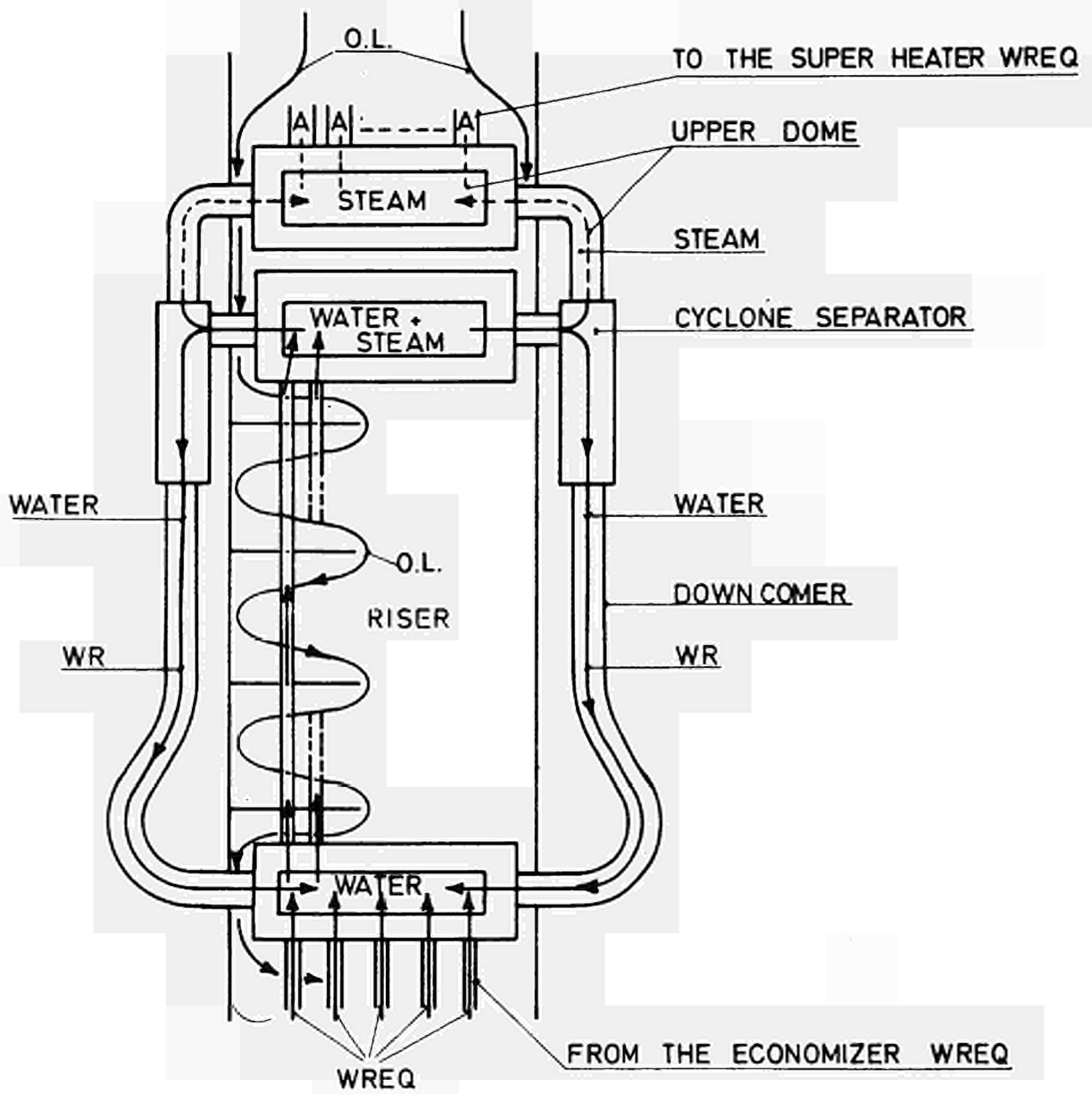
CLVE = kcal/kg °C WATER SPECIFIC HEAT

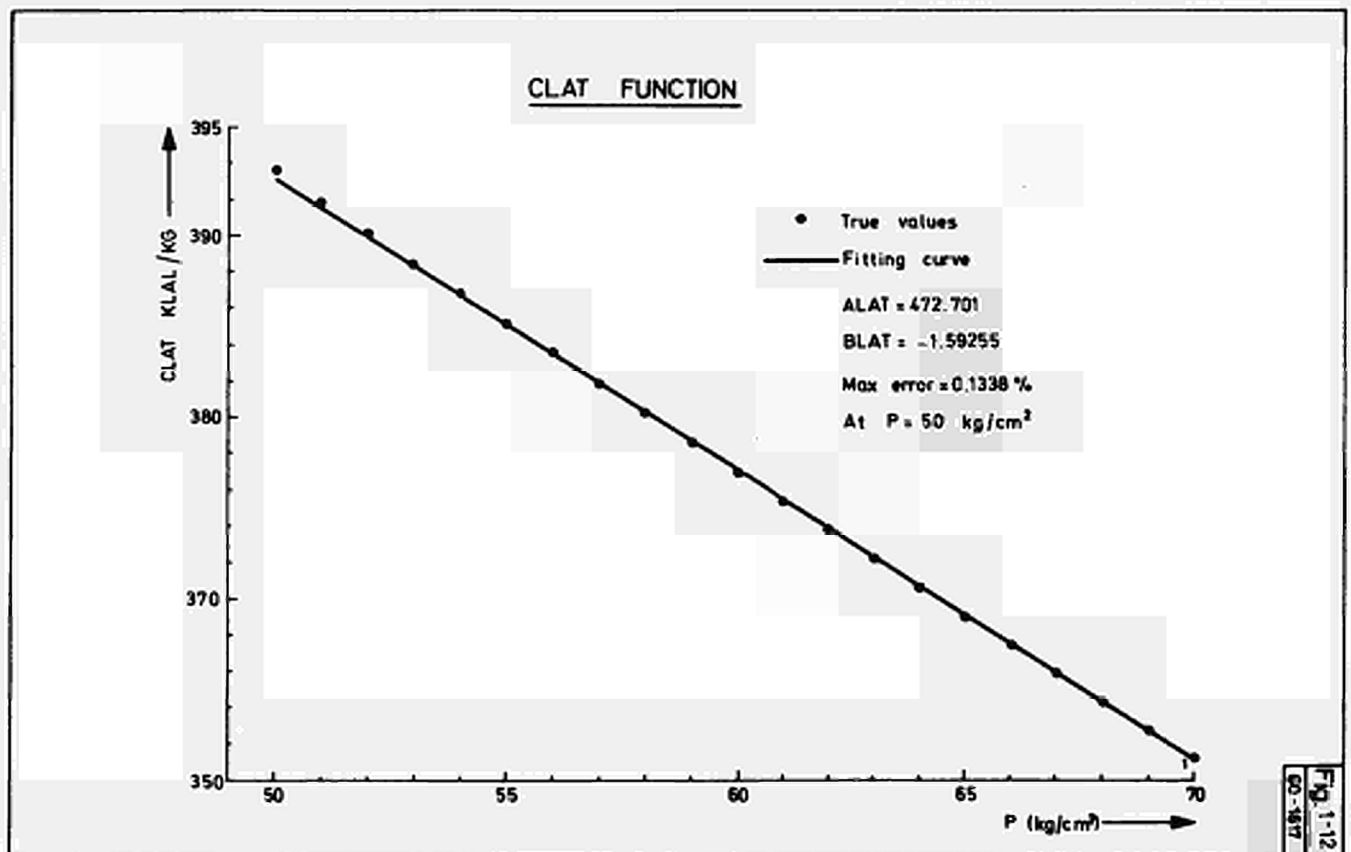
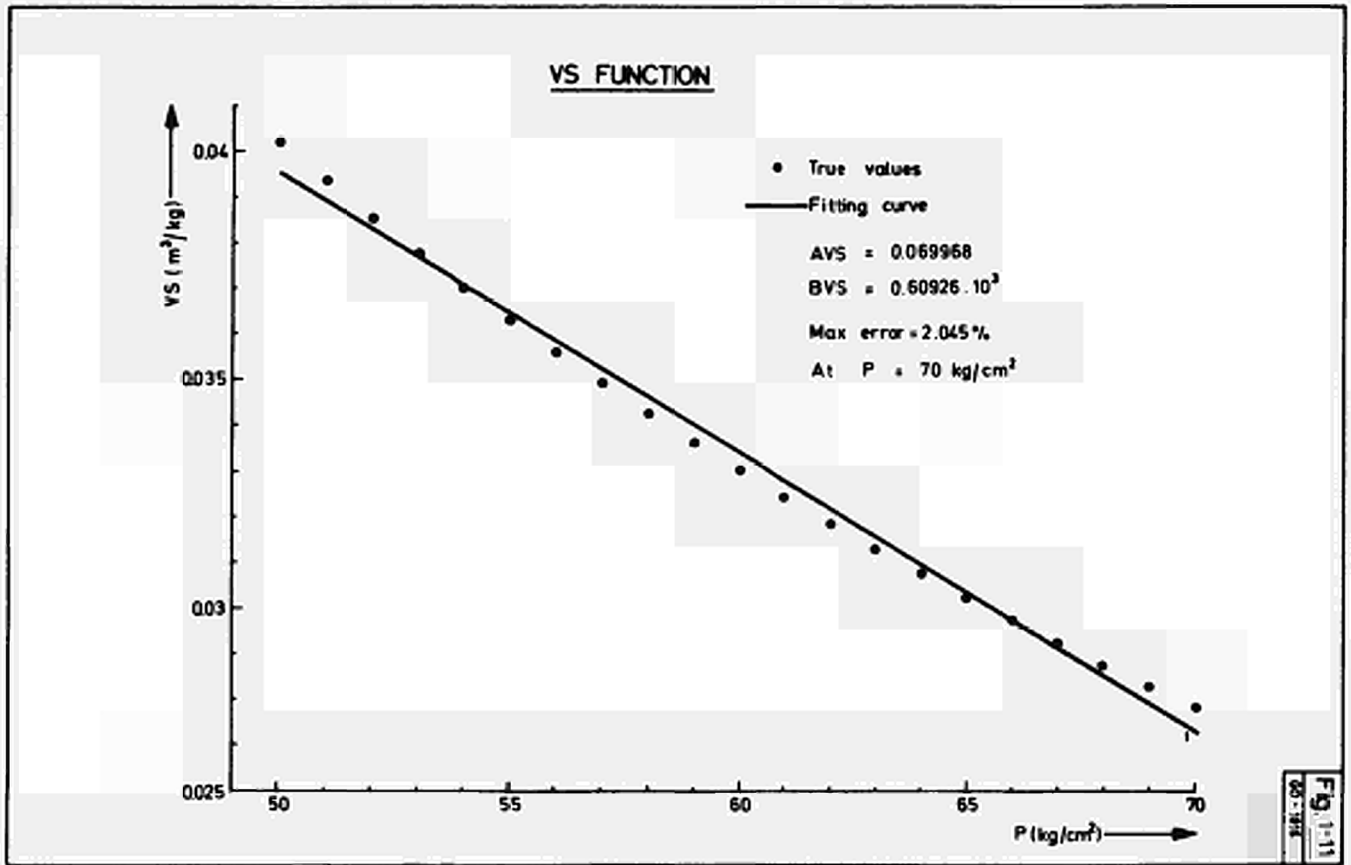
ROLVE = kg/m³ WATER DENSITYHLVE = kcal/m²sec °C HEAT TRANSF. COEFF.ALVE = m² CELL CROSS SECTION

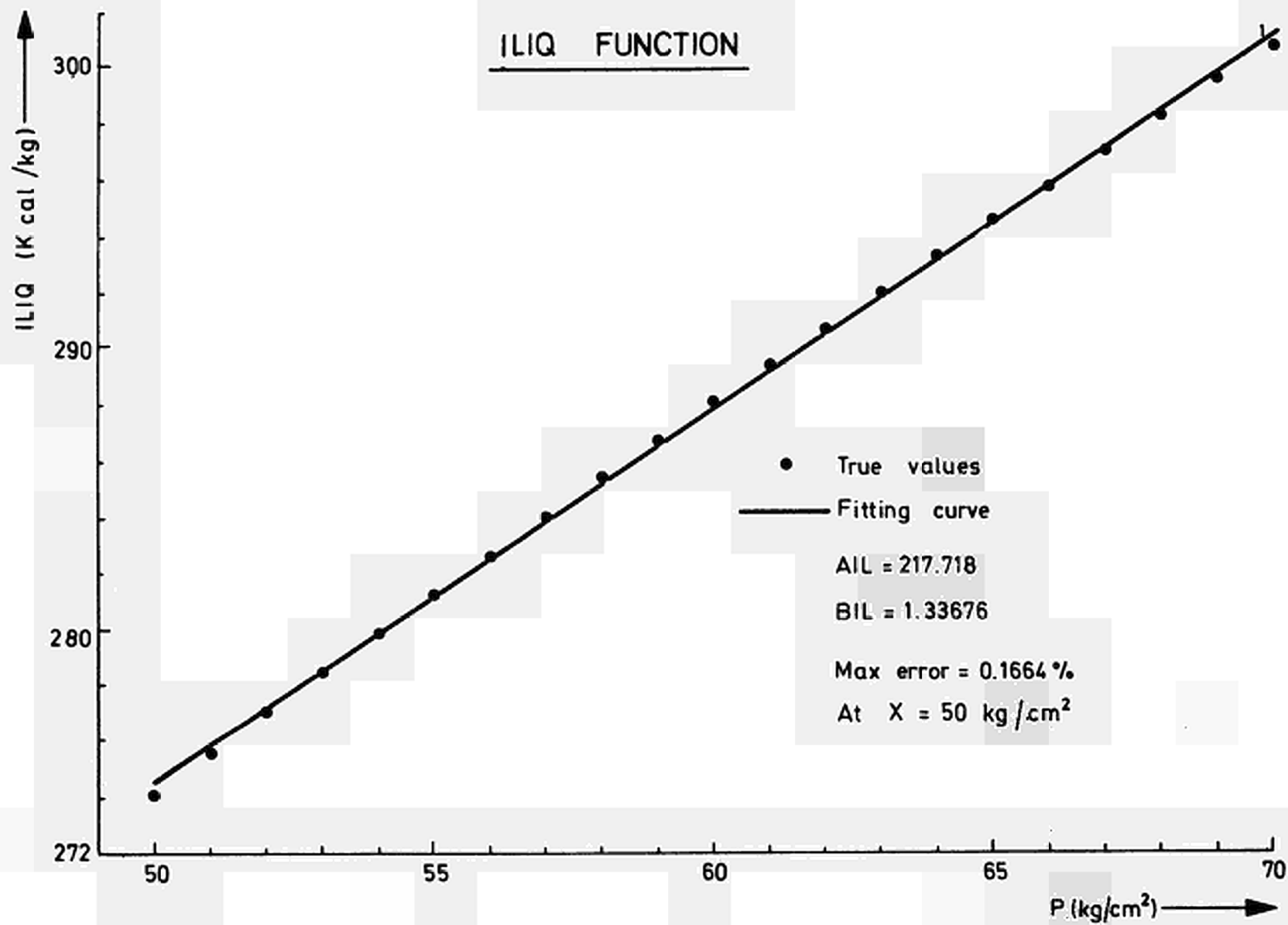
LEVA = m CELL LENGTH

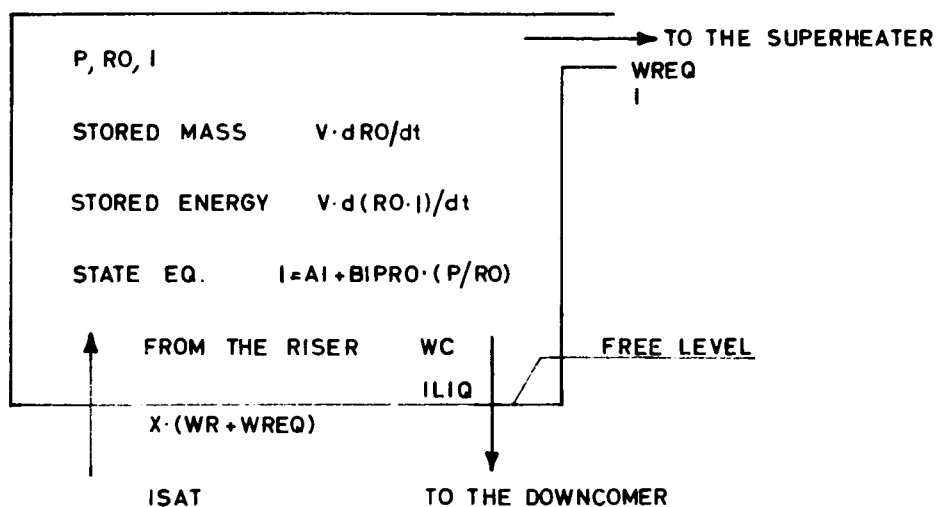
PLVE = m CELL WETTED PERIMETER

PRIMARY AND SECONDARY FLOW PATHS IN THE BOILER









MASS CONSERVATION LAW

$$V \cdot \frac{dRO}{dt} = X \cdot (WR + WREQ) - WREQ - WC$$

ENERGY CONSERVATION LAW

$$V \cdot \frac{d(RO \cdot I)}{dt} = X \cdot (WR + WREQ) \cdot ISAT - WREQ \cdot I - WC \cdot ILIQ$$

STATE EQUATION

$$I = AI + BIPRO \cdot (P/RO)$$

CONDENSATION LAW

$$WC = \begin{cases} K \cdot (RO - ROSAT) & \text{FOR } RO > ROSAT \\ 0 & \text{FOR } RO \leq ROSAT \end{cases}$$

SYMBOLS

V = 1 m ³	UPPER DOME VOLUME
P (kg/cm ²)	UPPER DOME PRESSURE
RO (kg/m ³)	DENSITY OF THE STEAM IN THE UPPER DOME
ROSAT (kg/m ³)	DENSITY OF SATURATED STEAM AT P
I (KCAL/kg)	ENTHALPY OF THE STEAM IN THE UPPER DOME
ISAT (KCAL/kg)	ENTHALPY OF SATURATED STEAM AT P
ILIQ (KCAL/kg)	ENTHALPY OF SATURATED WATER AT P
WC (kg/sec)	CONDENSATION MASS FLOW RATE
AI =	460.456
BIPRO =	103.25

STEAM ENTHALPY V.S. PRESSURE AT CONSTANT DENSITY

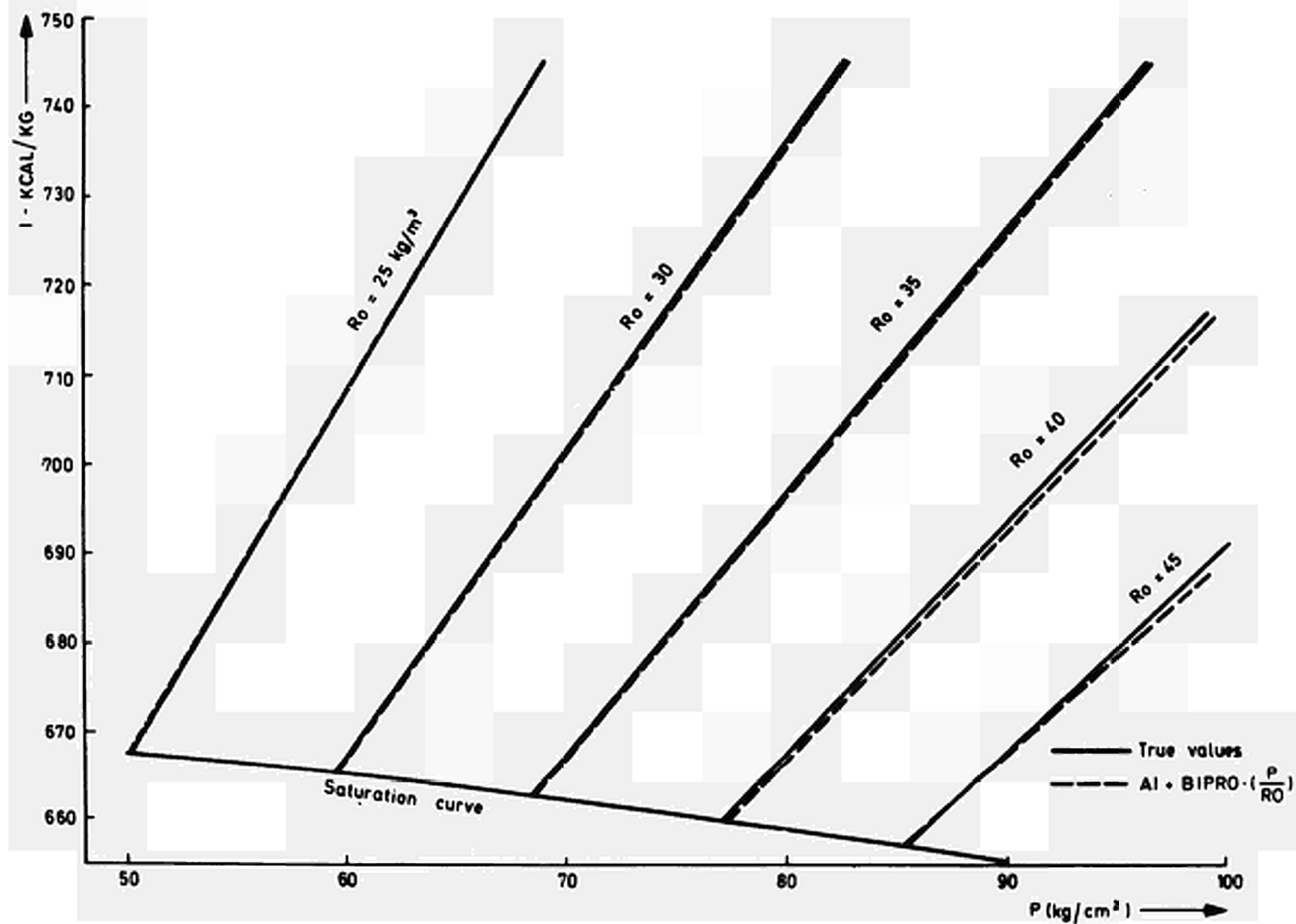
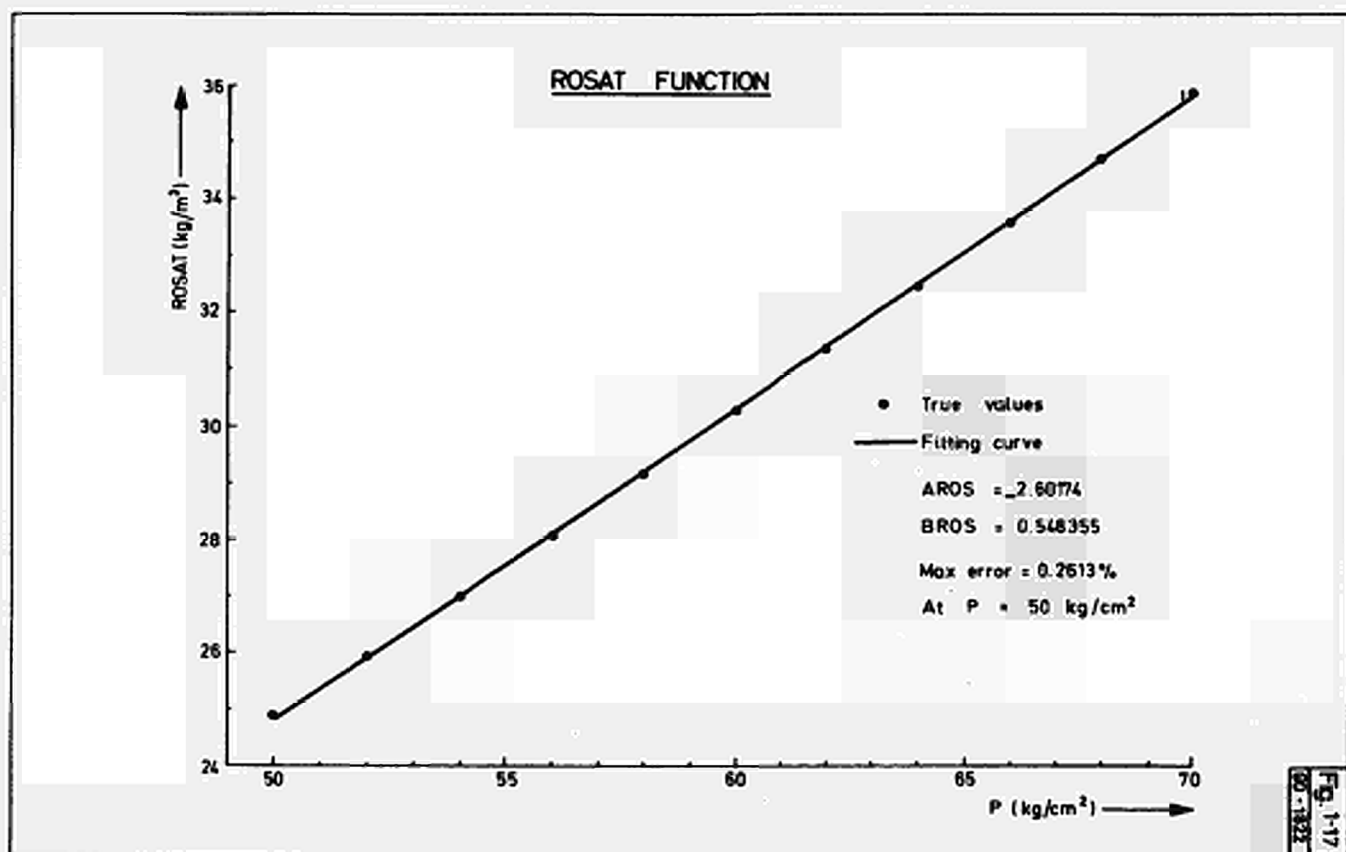
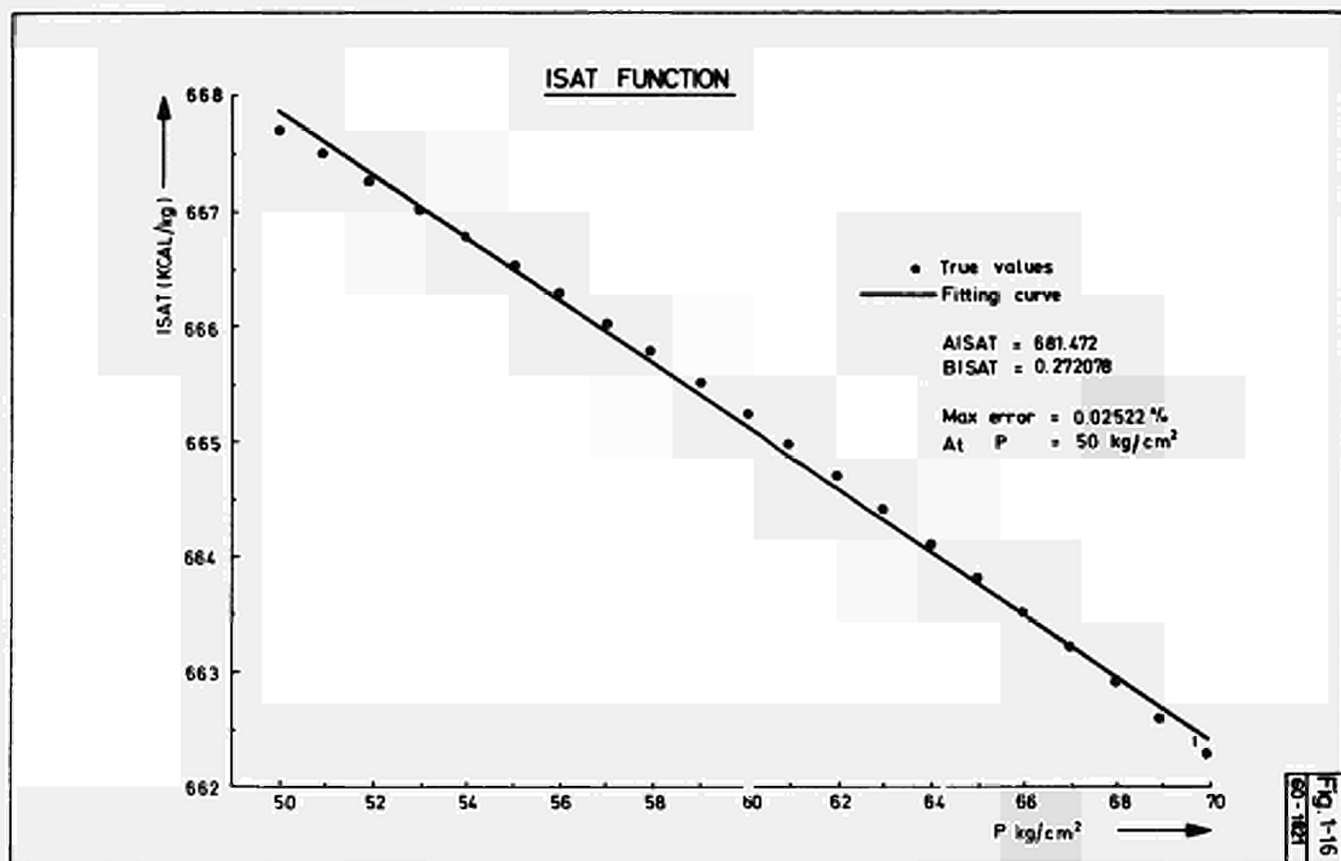
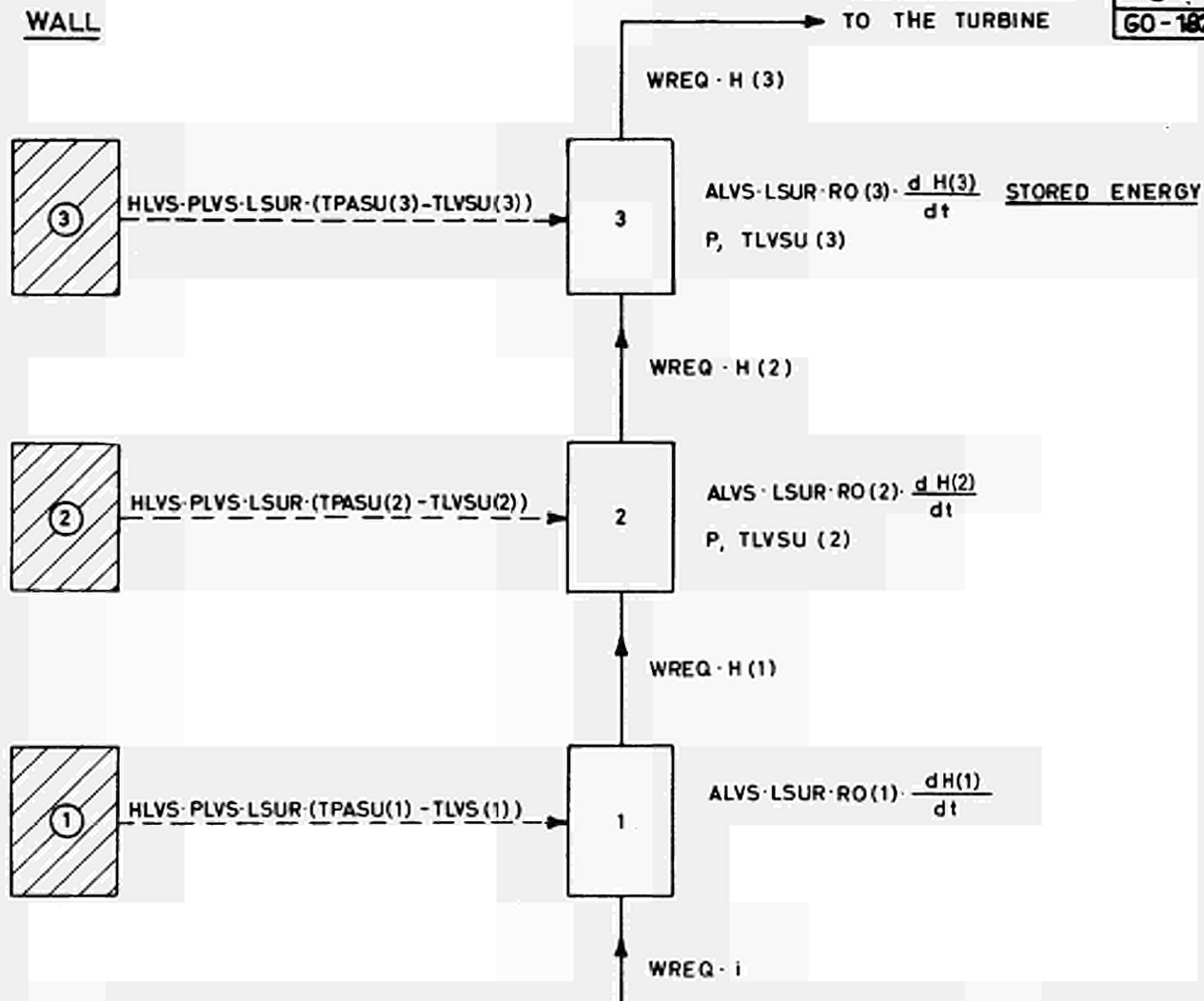


Fig. 1-15
GO-1820



**ENERGY CONSERVATION LAW**

$$ALVS \cdot LSUR \cdot RO (1) \cdot \frac{d H(1)}{dt} = WREQ \cdot (i - H(1)) + HLVS \cdot PLVS \cdot LSUR \cdot (TPASU (1) - TLVSU (1))$$

$$ALVS \cdot LSUR \cdot RO (2) \cdot \frac{d H(2)}{dt} = WREQ \cdot (H(1) - H(2)) + HLVS \cdot PLVS \cdot LSUR \cdot (TPASU (2) - TLVSU (2))$$

$$ALVS \cdot LSUR \cdot RO (3) \cdot \frac{d H(3)}{dt} = WREQ \cdot (H(2) - H(3)) + HLVS \cdot PLVS \cdot LSUR \cdot (TPASU (3) - TLVSU (3))$$

$$\text{STEAM TEMPERATURE : } TLVSU (i) = 1.3333 H(i) (\text{kcal/kg}) + 1.0937 \cdot P (\text{kg/cm}^2) - 686.64$$

SYMBOLS

TPASU (i) WALL TEMP. IN THE i^{th} CALL °C

TLVSU (i) STEAM TEMP. IN THE i^{th} CALL °C

H (i) STEAM ENTHALPY IN THE i^{th} CALL KCAL/kg.

i ENTHALPY OF THE STEAM IN THE UPPER DOME KCAL/kg

P SYSTEM PRESSURE kg/cm²

RO (1) = STEAM DENSITY IN CELL 1 kg/m³

RO (2) = STEAM DENSITY IN CELL 2 kg/m³

RO (3) = STEAM DENSITY IN CELL 3 kg/m³

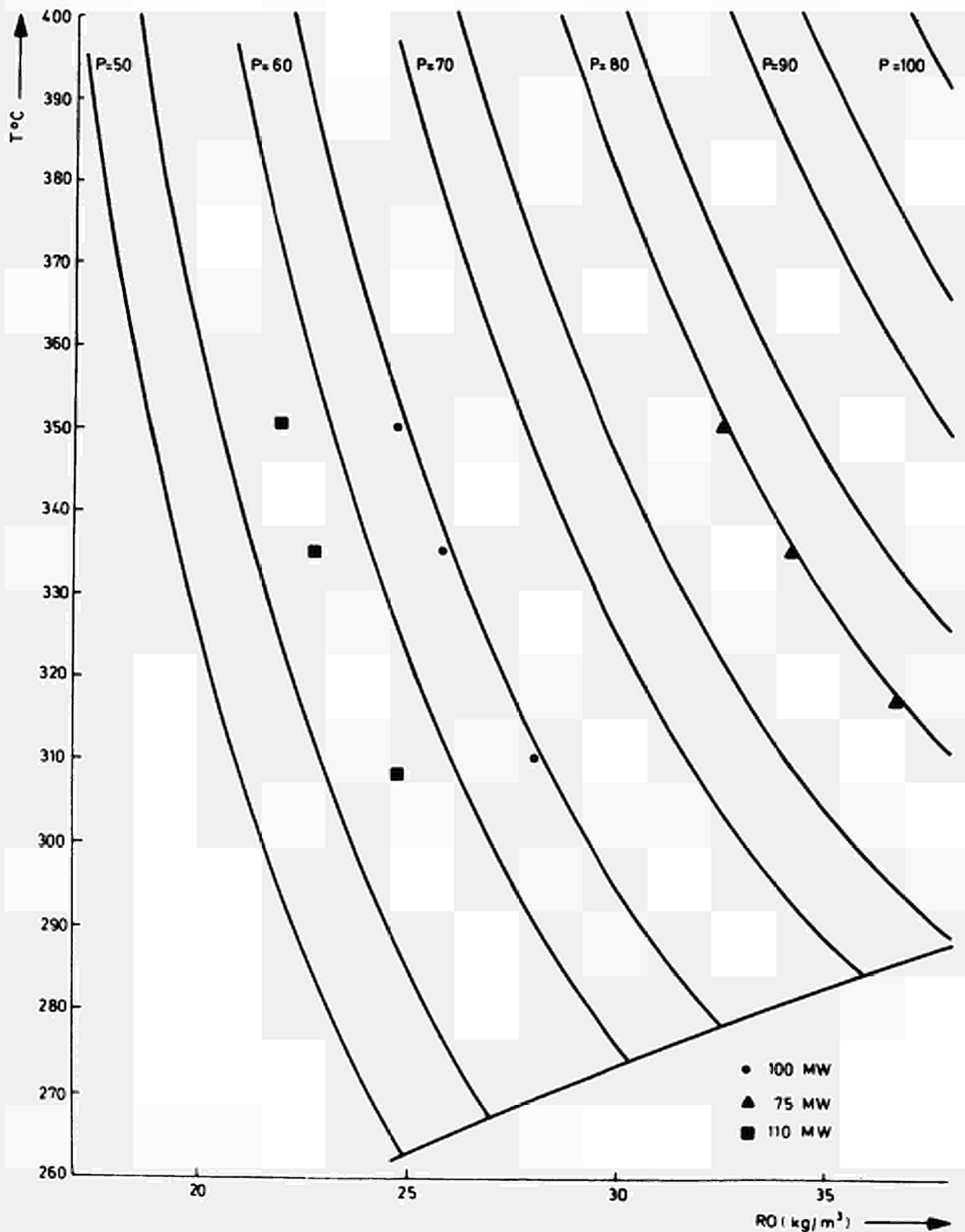
ALVS = CELL CROSS SECTION m²

LSUR = CELL LENGTH m

PLVS = CELL WETTED PERIMETER m

HLVS = HEAT TRANSF. COEFF. KCAL/m²sec °C

STEAM TEMPERATURE VS DENSITY AT DIFFERENT PRESSURES



STEAM TEMP. VS. ENTHALPY AT DIFFERENT PRESSURES. ----- $T = 1.3333 i + 1.0937 P - 686.64$

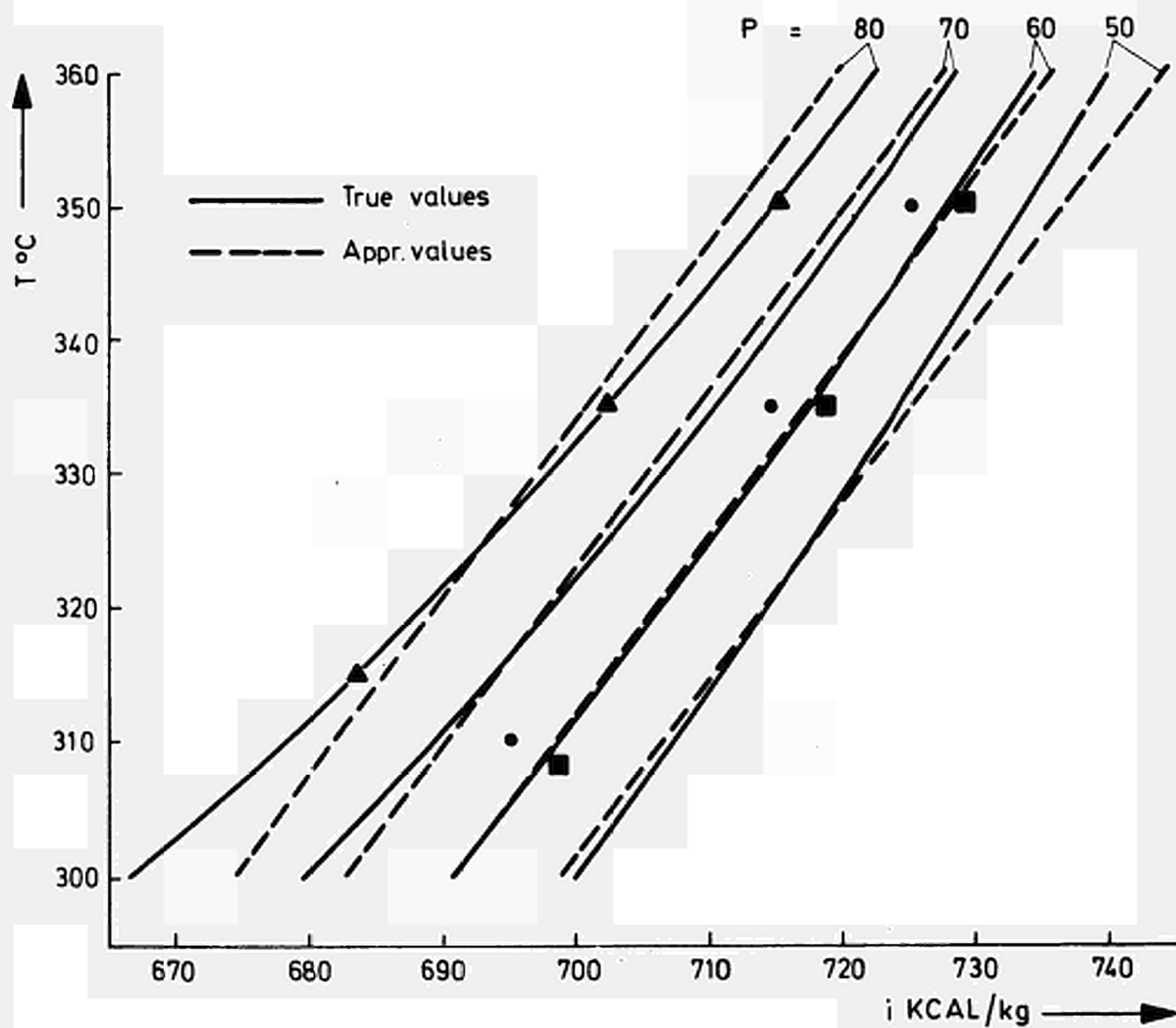


Fig. a

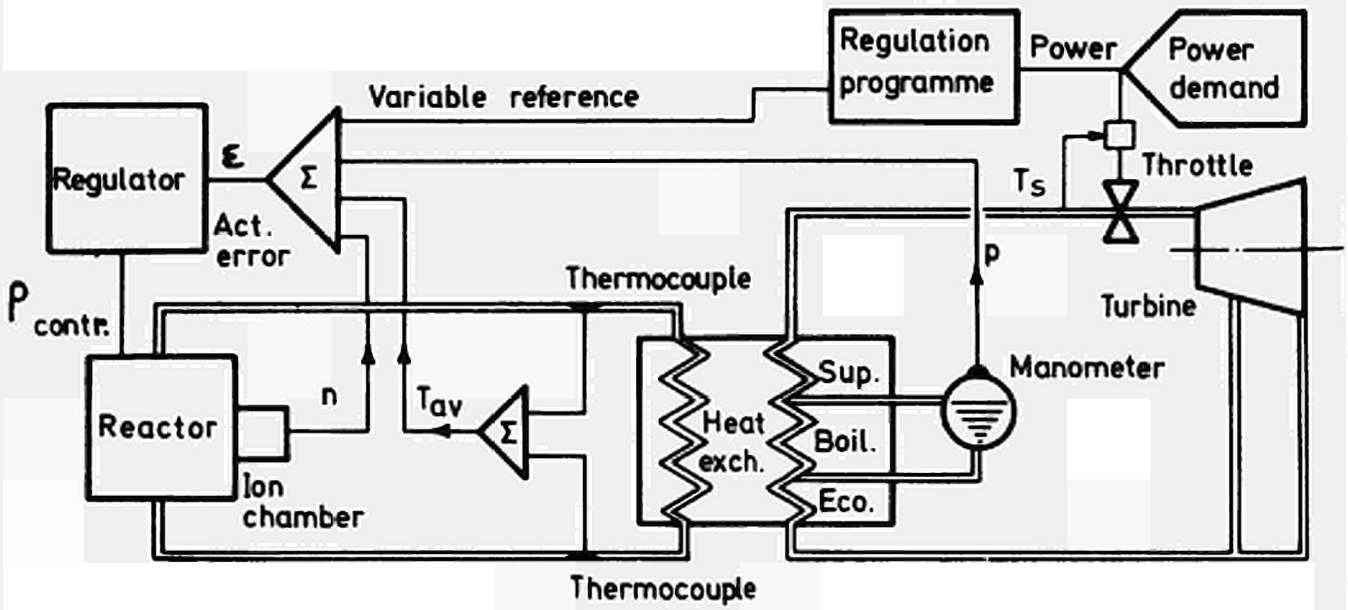


Fig. b

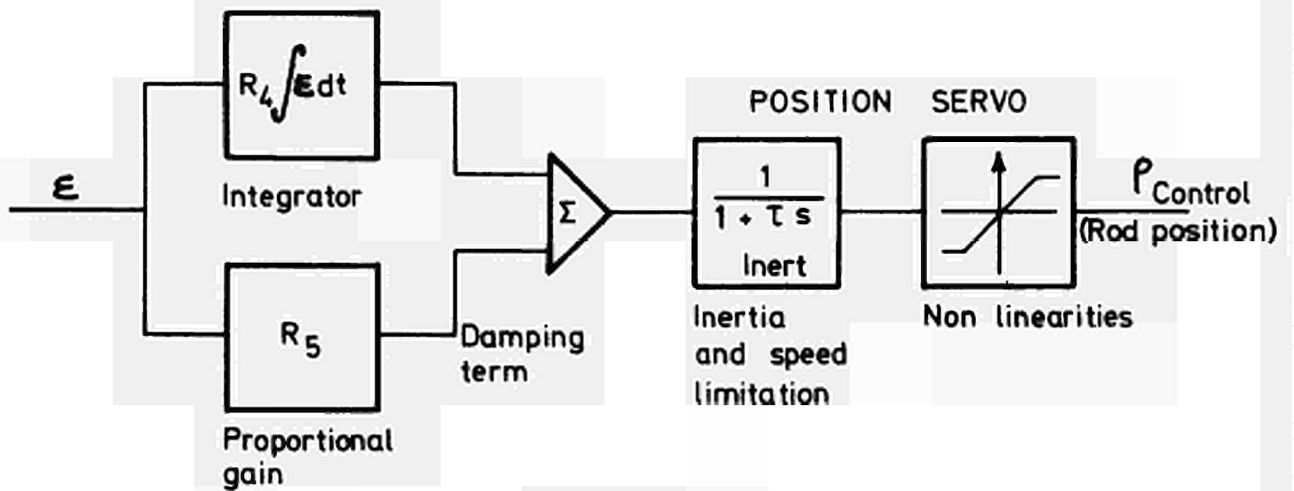
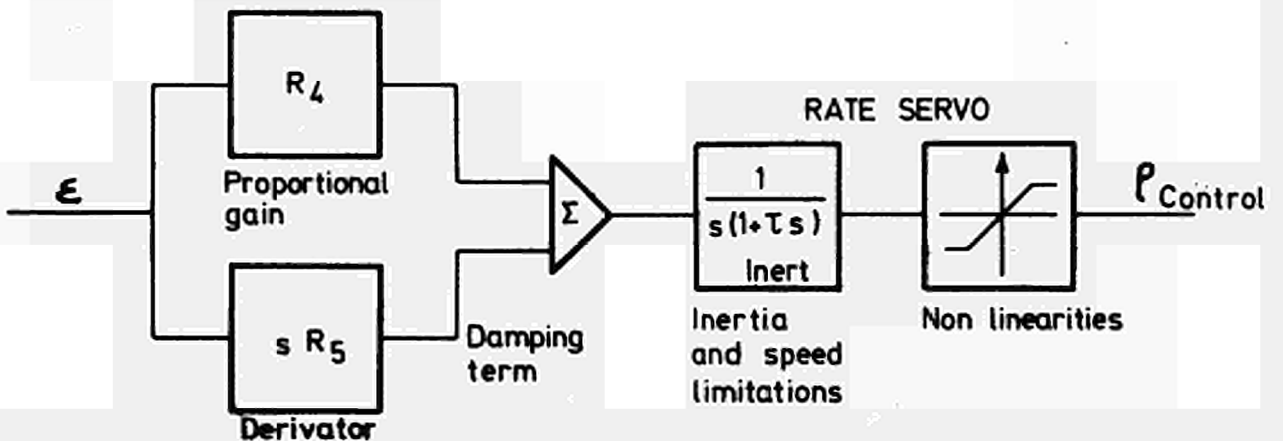


Fig. c



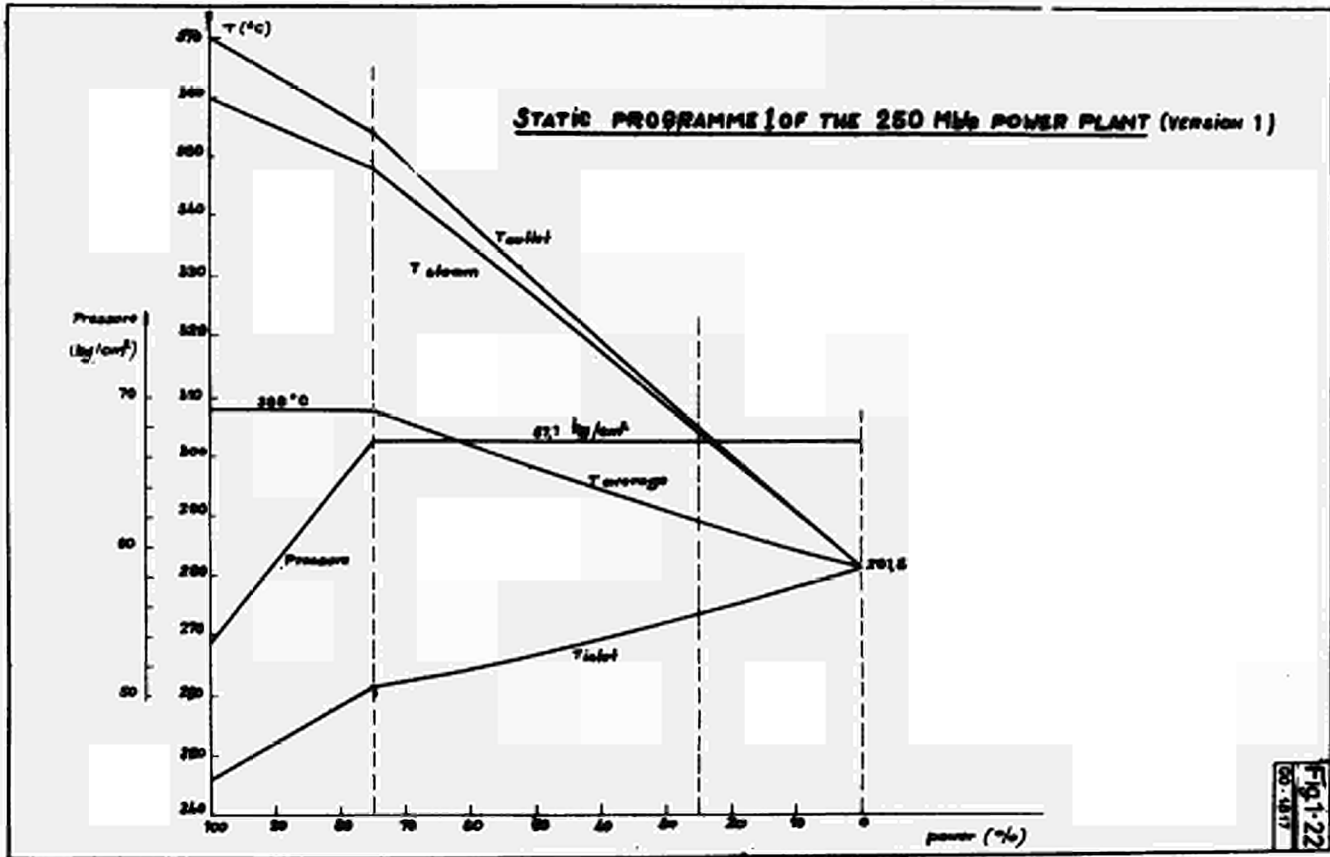


Fig 1-22
OO 1817

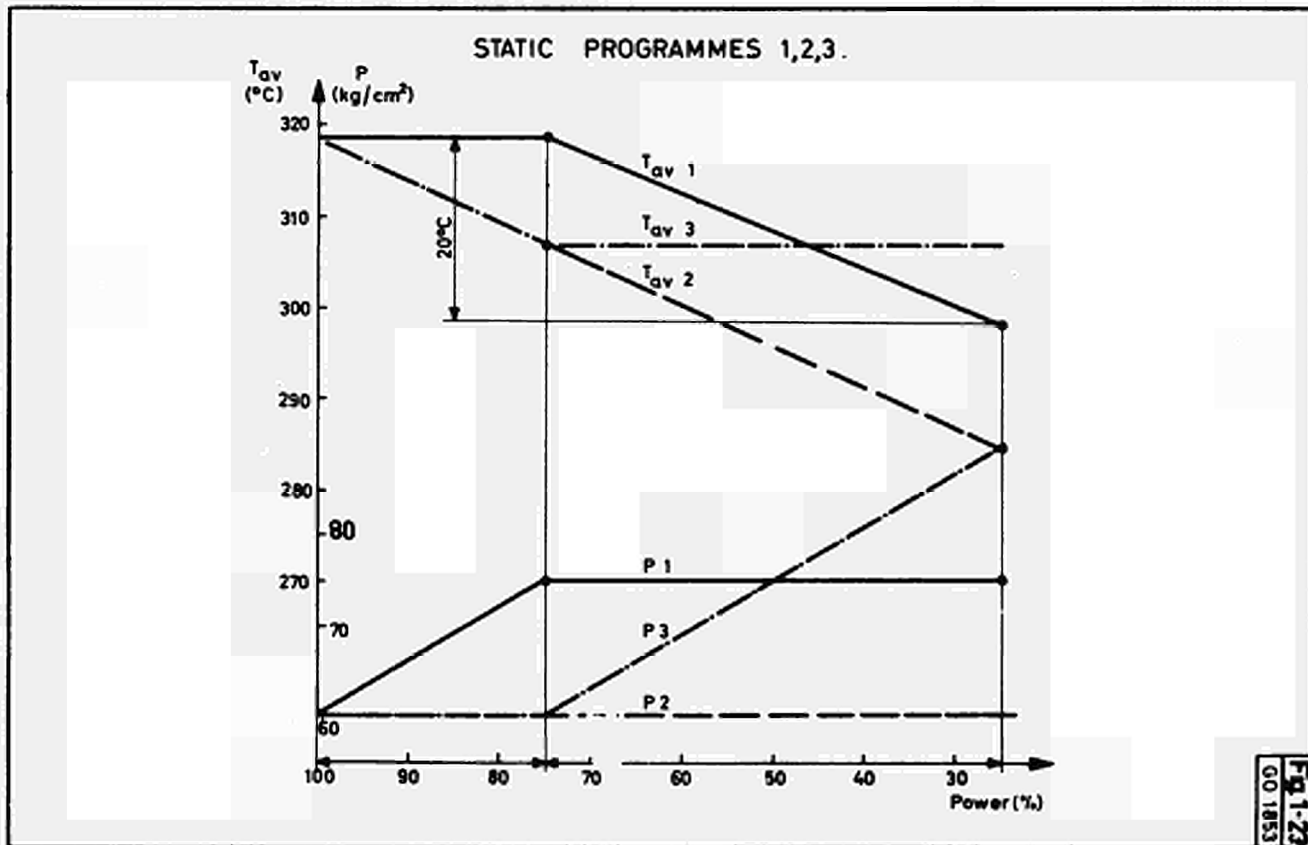
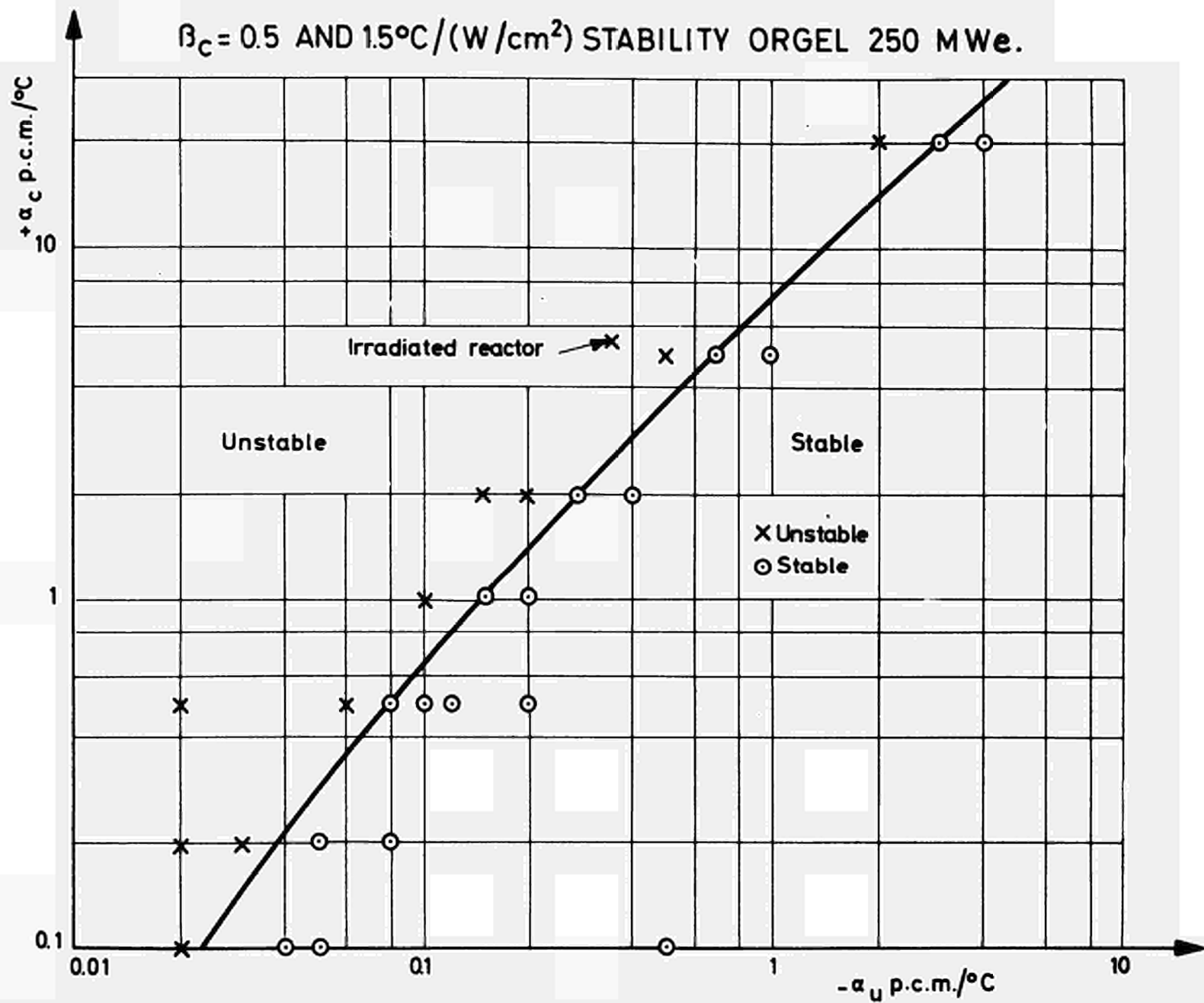


Fig 1-23
OO 1853

$\beta_c = 0.5$ AND $1.5^\circ\text{C}/(\text{W}/\text{cm}^2)$ STABILITY ORGEL 250 MWe.



STABILITY DOMAIN OF THE CONTROL MECHANISM

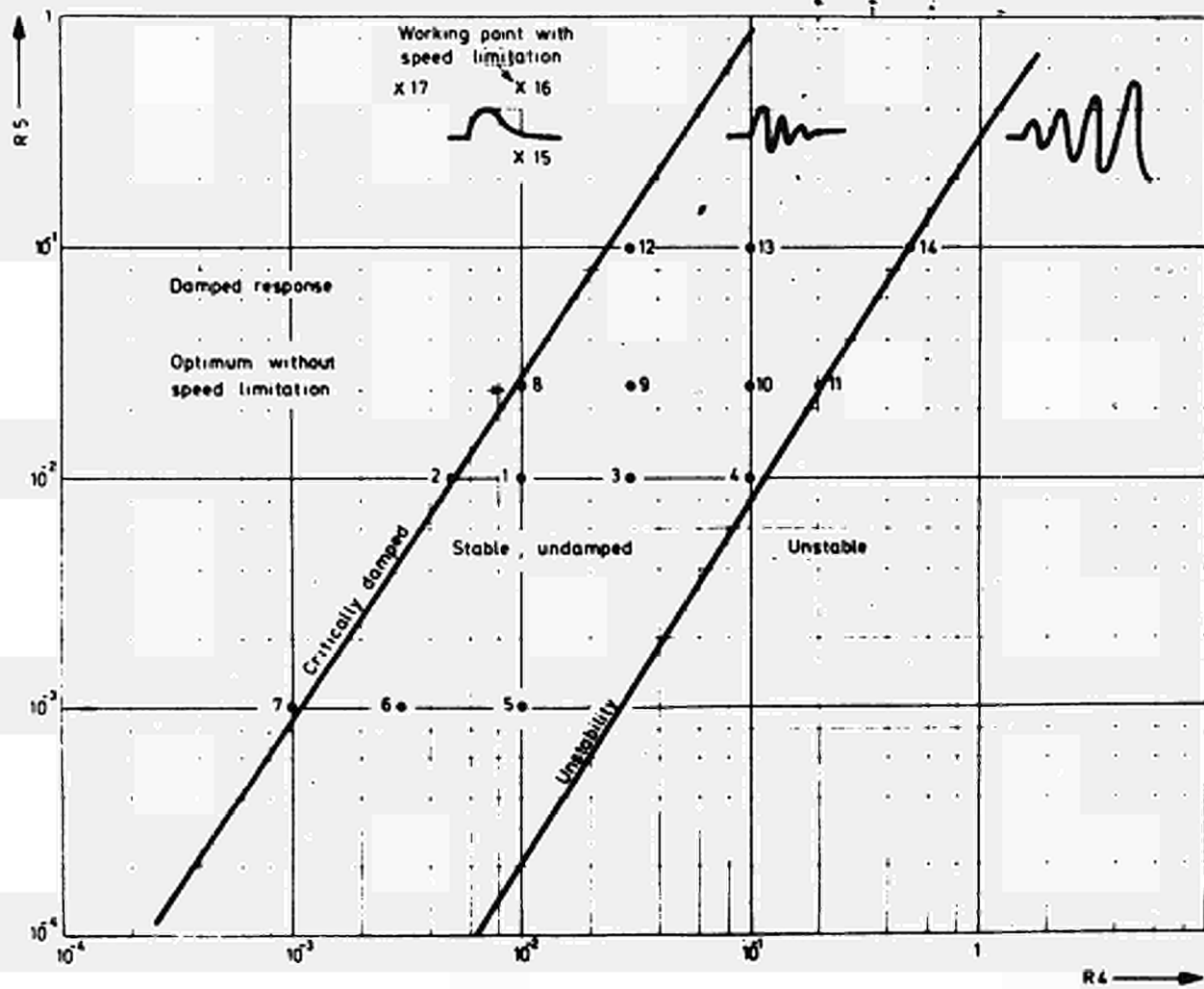


Fig. 1-25
GO. 16.18

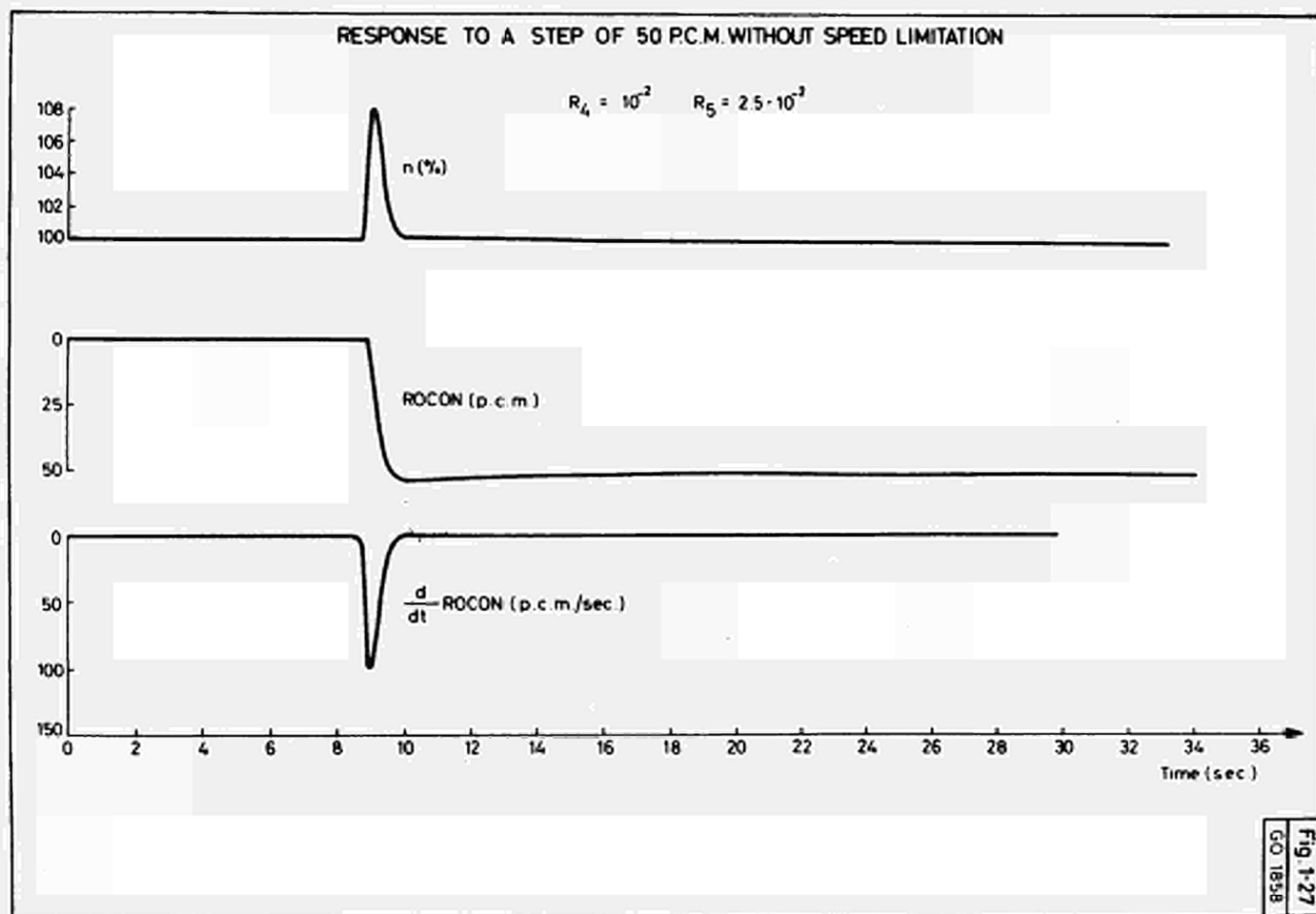
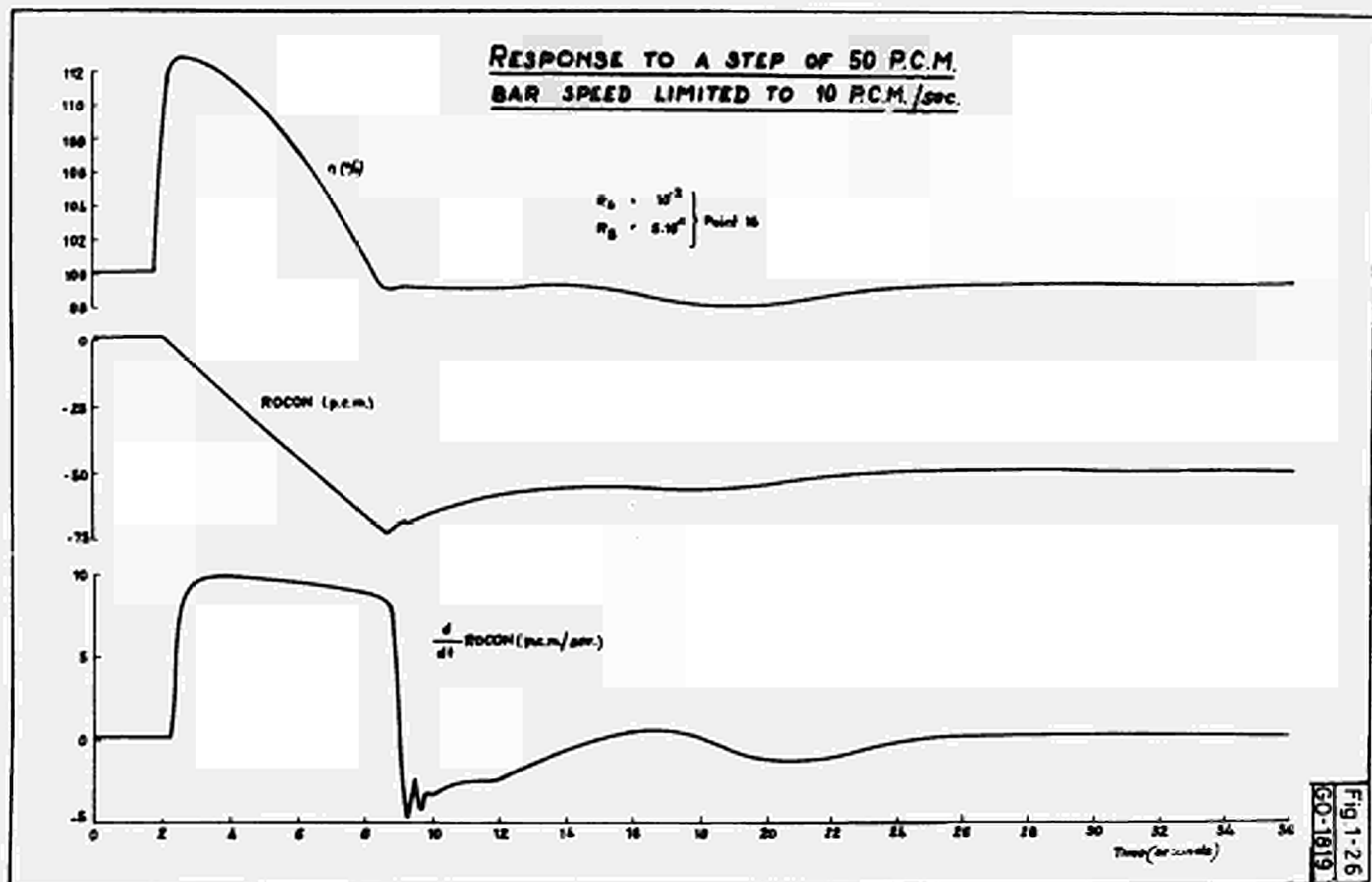


Fig.1-28
GO-1820

LIMITS OF EFFICIENCY OF THE SYSTEM CONTROL

- Rod reactivity span : +200 p.c.m. , -300 p.c.m.
 Maximum rod speed : 15 cm./sec.
 Time constant of rods : 1 sec.
1. 100 p.c.m. step disturbance
 2. 50 p.c.m. step disturbance
 3. 10 °C step disturbance
 4. 5 °C step disturbance

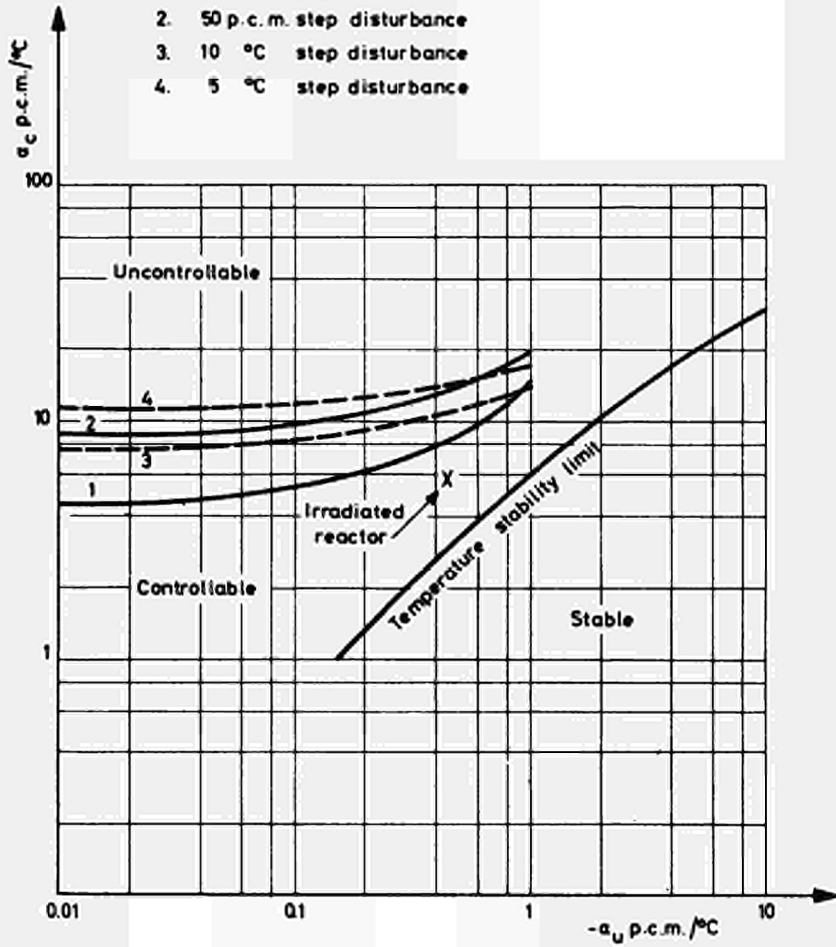
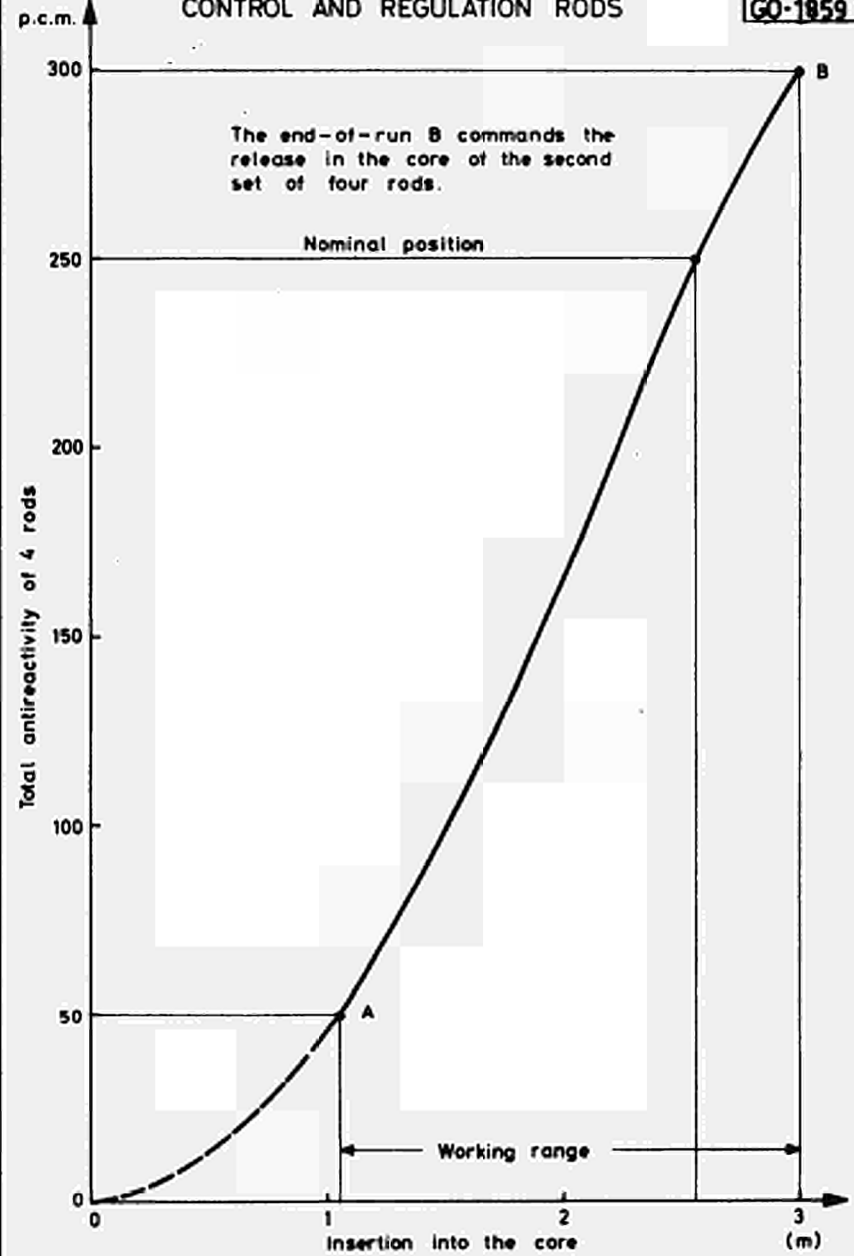
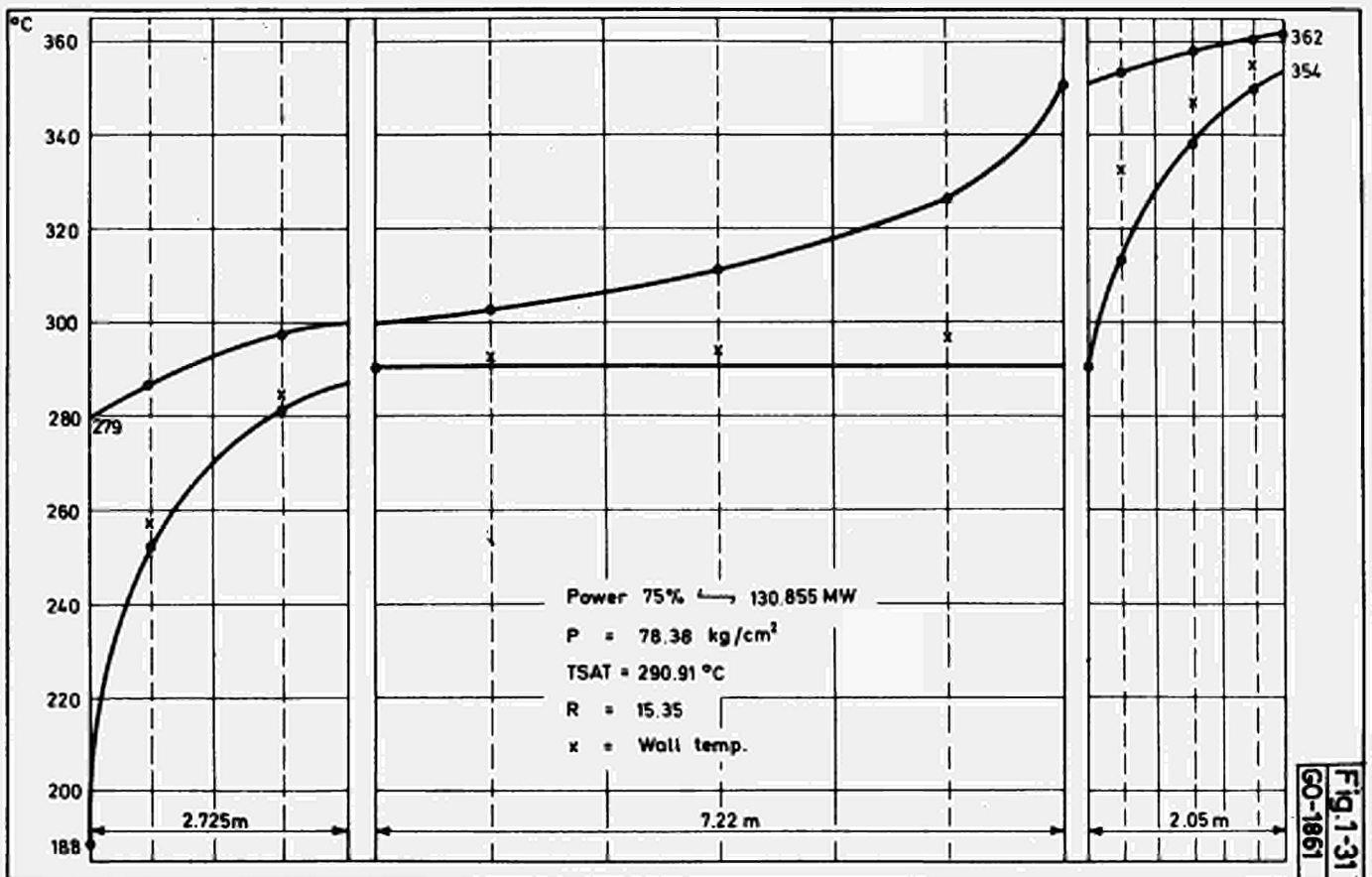
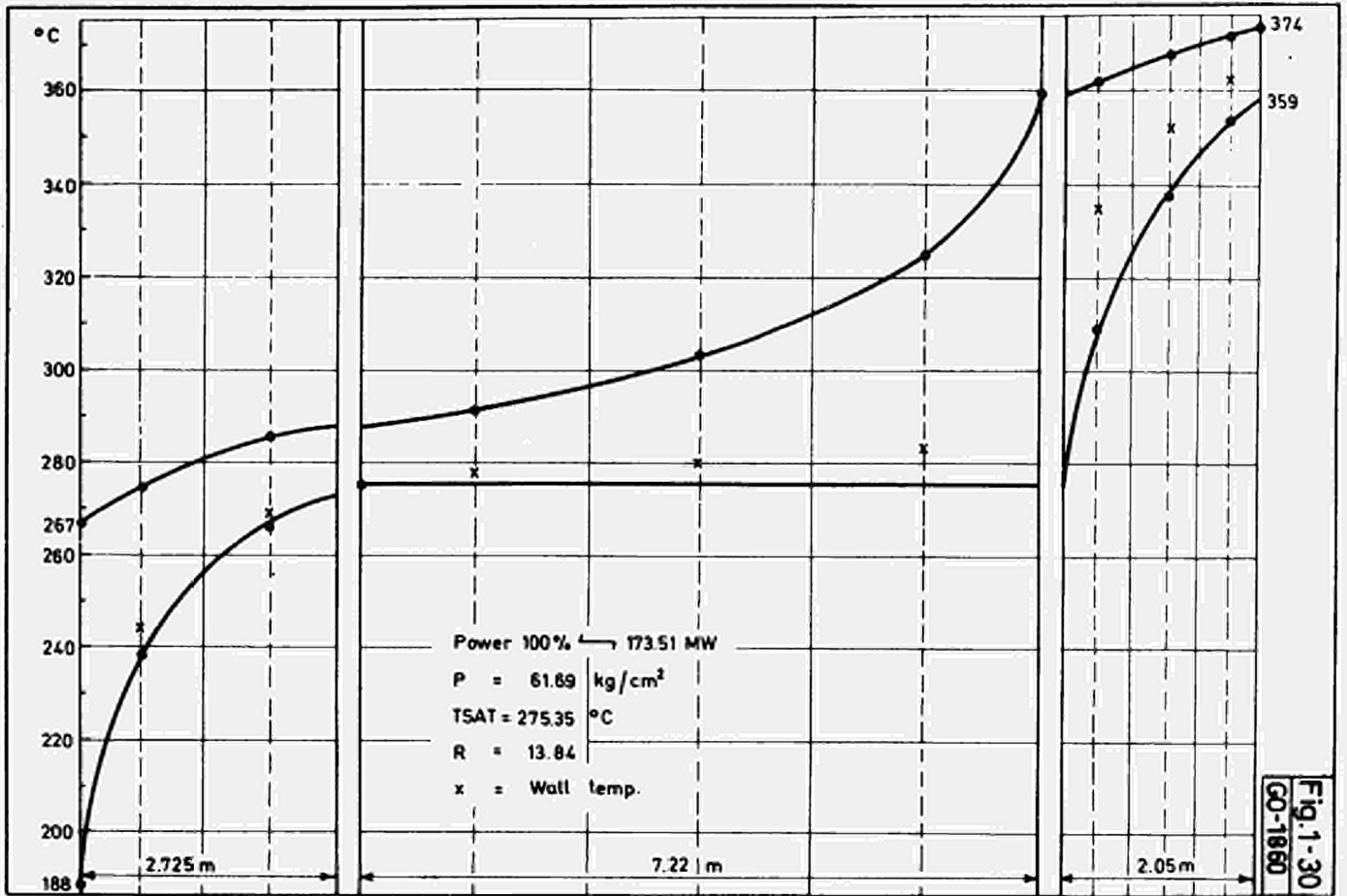


Fig.1-29
GO-1859

CONTROL AND REGULATION RODS





UNLOADING AND LOADING OF A CENTRAL FUEL ELEMENT
THE BAR SPEED IS LIMITED TO 10 P.C.M./SEC.

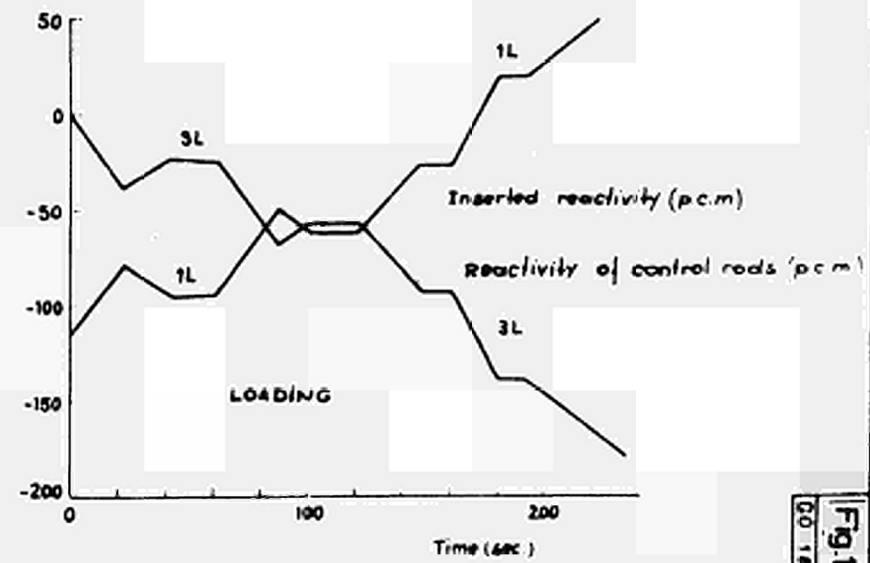
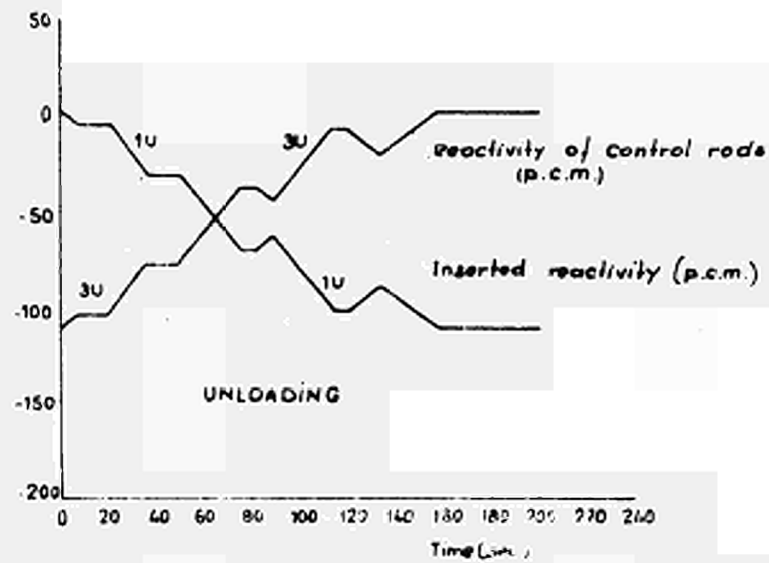
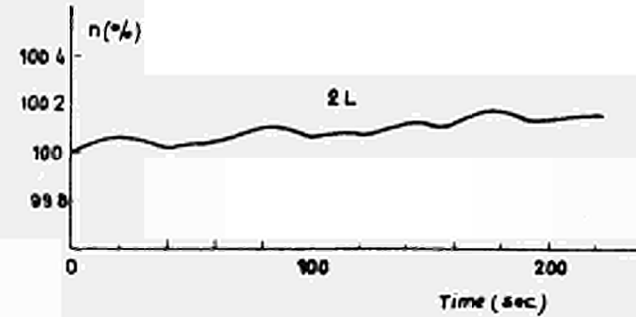
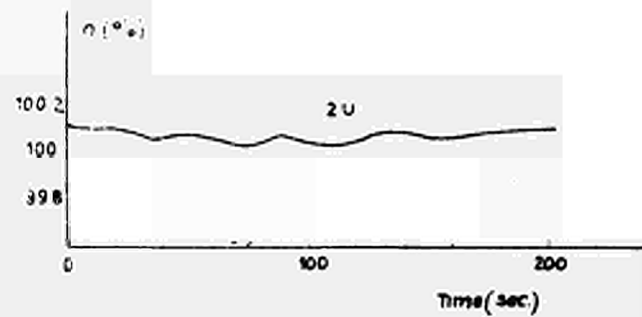


Fig. 1-32
00 1821

VARIATION OF POWER 100 - 75, 5% PER MINUTE (PROGRAMME 1)

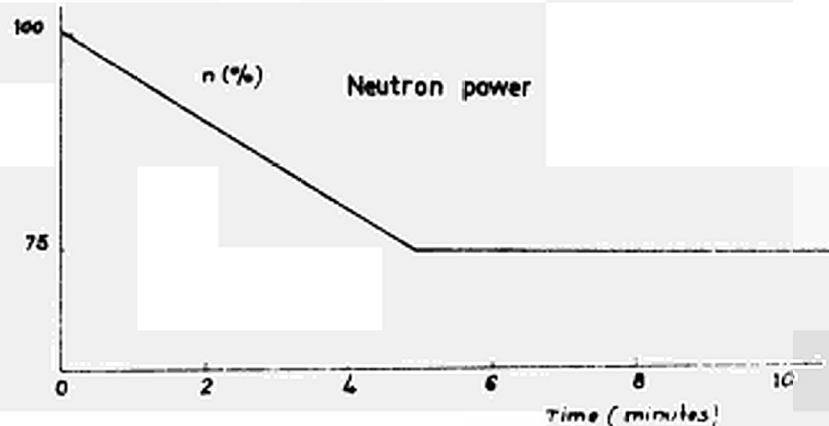
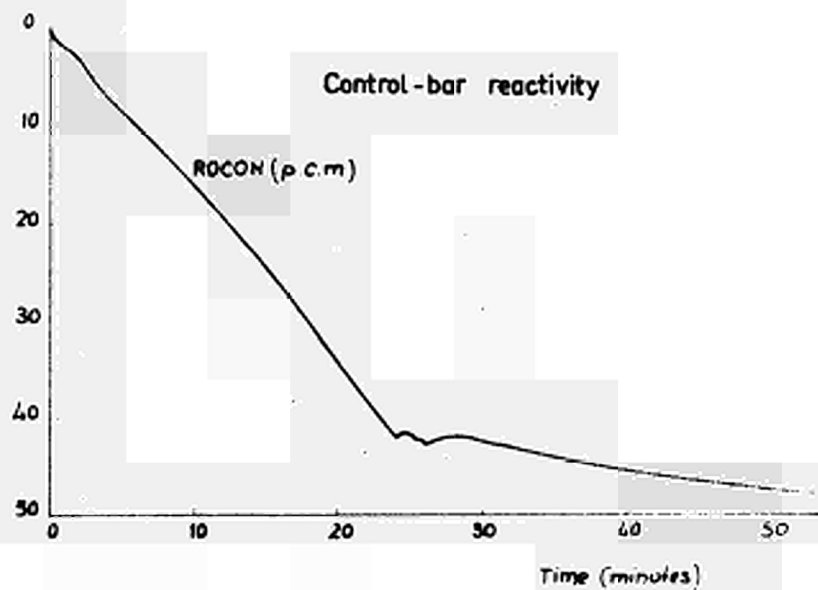
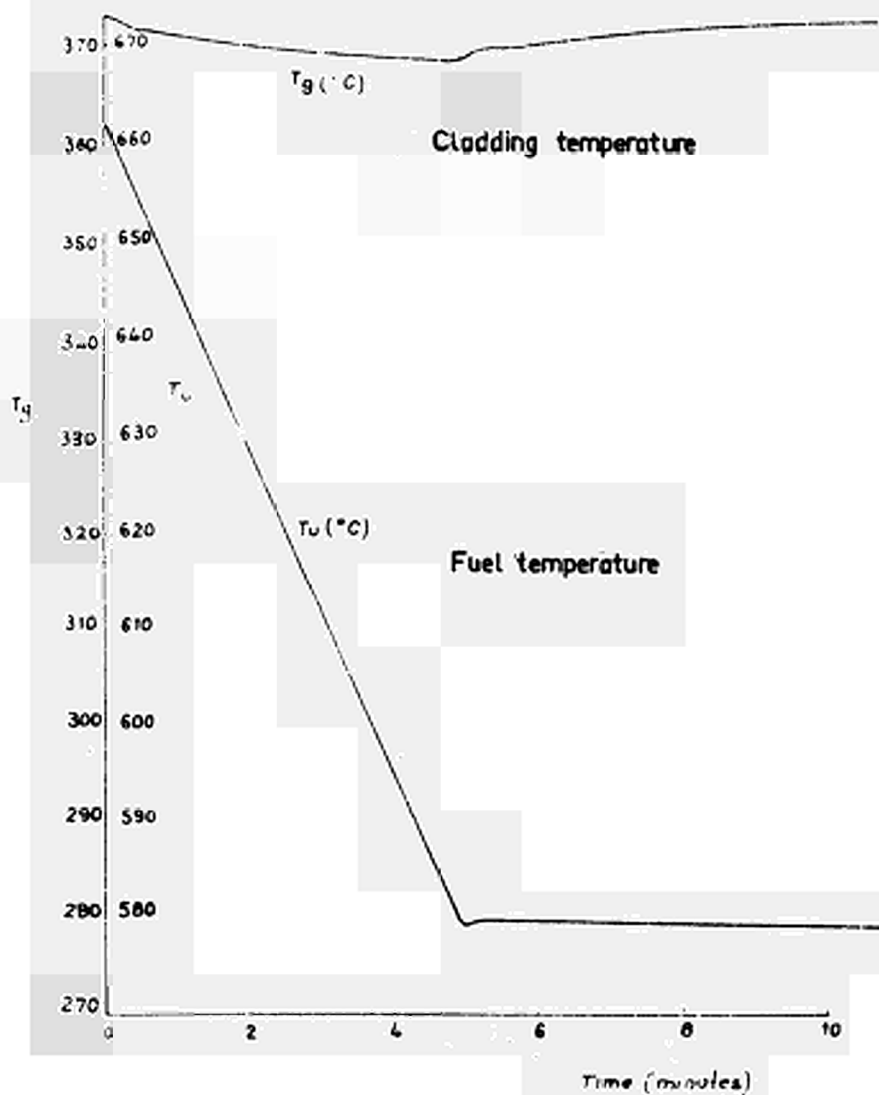


Fig. 1-33
GD-1822

Fig.1-34
GO-1823

VARIATION OF POWER FROM 100% TO 75% : 5% PER MINUTE
(PROGRAMME 1)

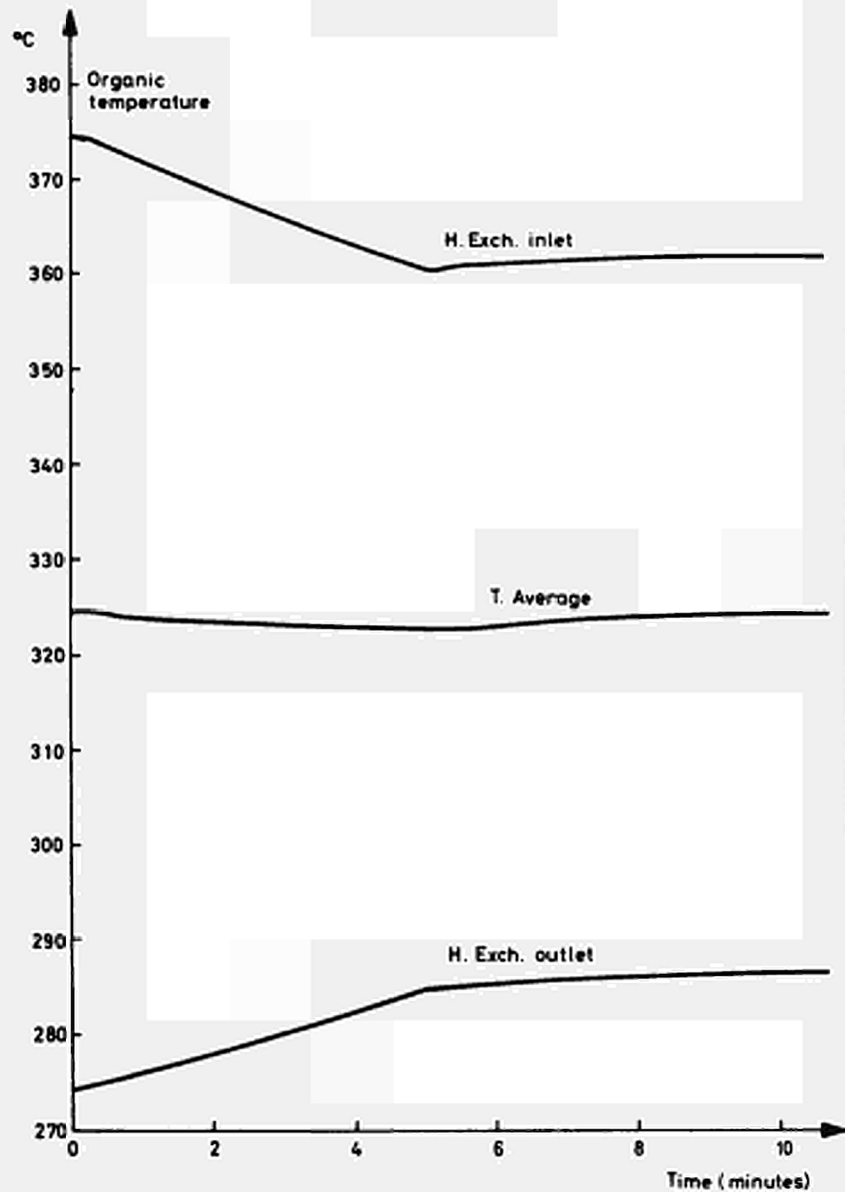
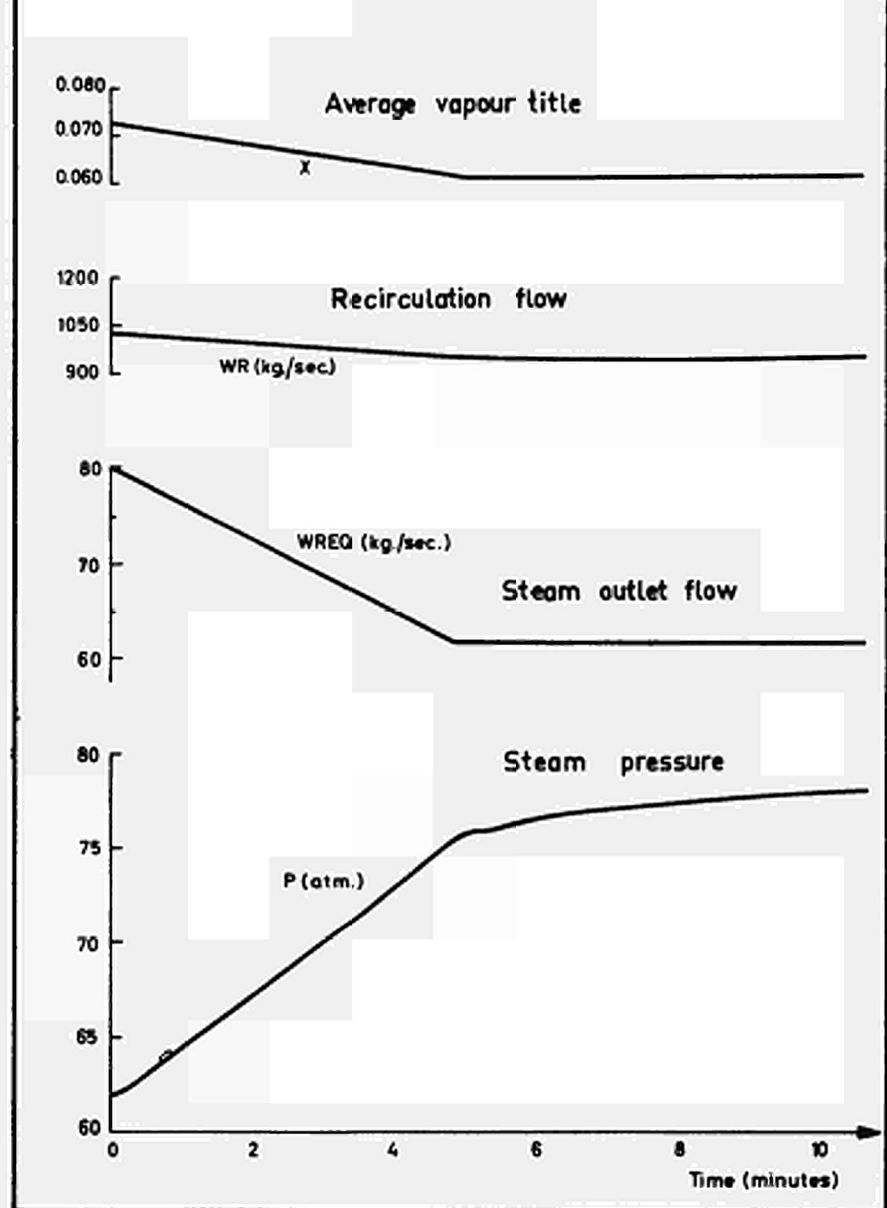


Fig.1-35
GO-1824

VARIATION OF POWER FROM 100% TO 75% : 5% PER MINUTE
(PROGRAMME 1)



**VARIATION OF POWER FROM 100% TO 25%
(PROGRAMME 1)**

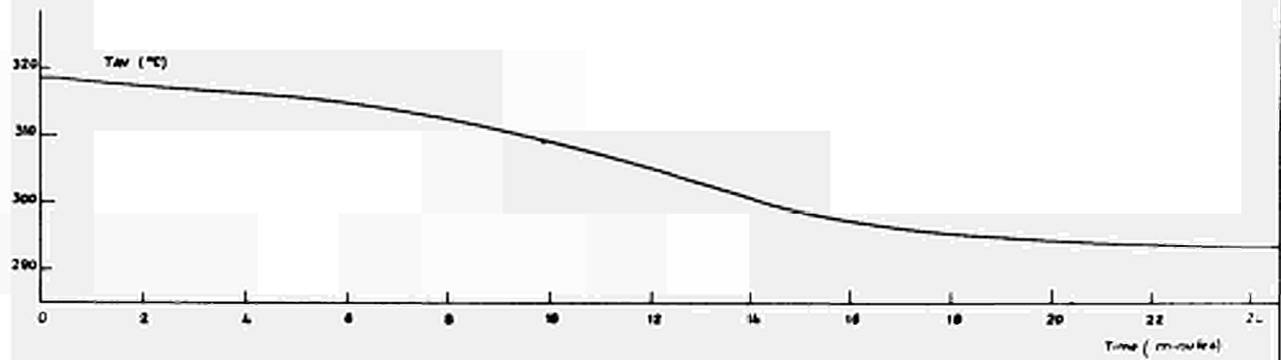


Fig. 1-36
GO-1825

**VARIATION OF POWER FROM 100% TO 25% - 5% PER MINUTE
(PROGRAMME 1)**

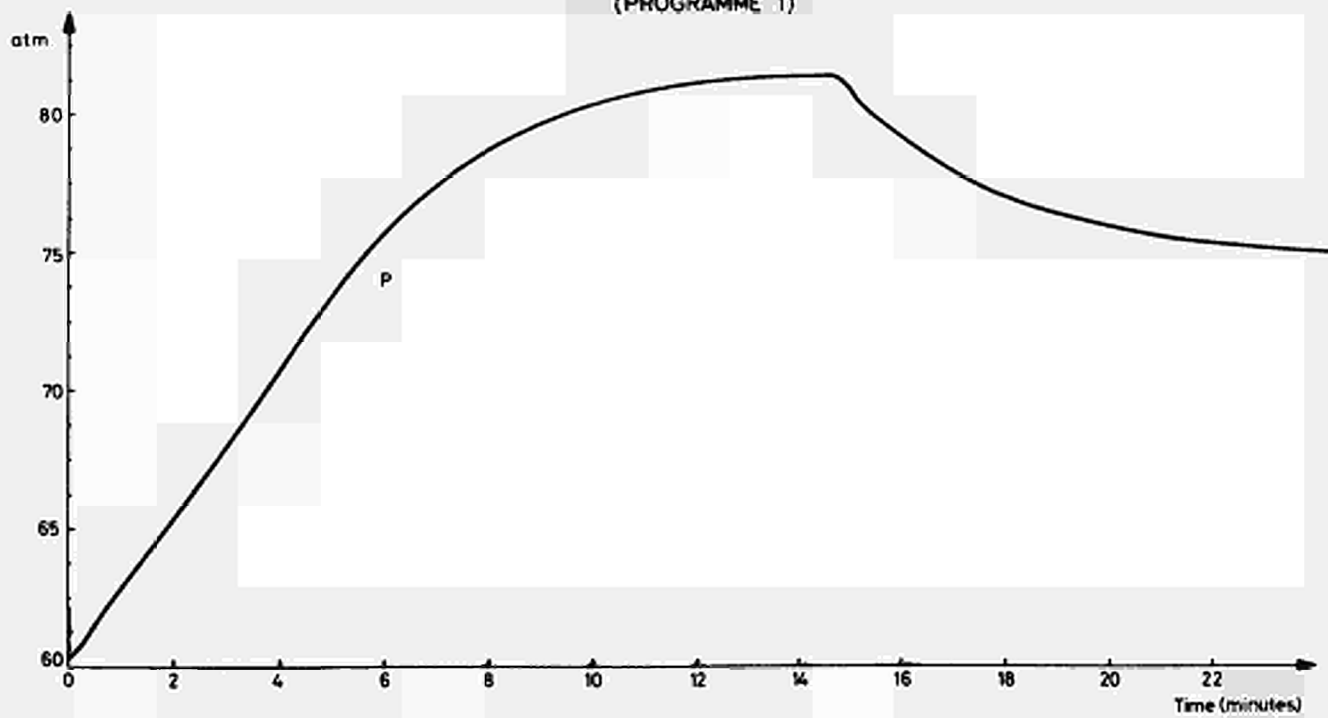
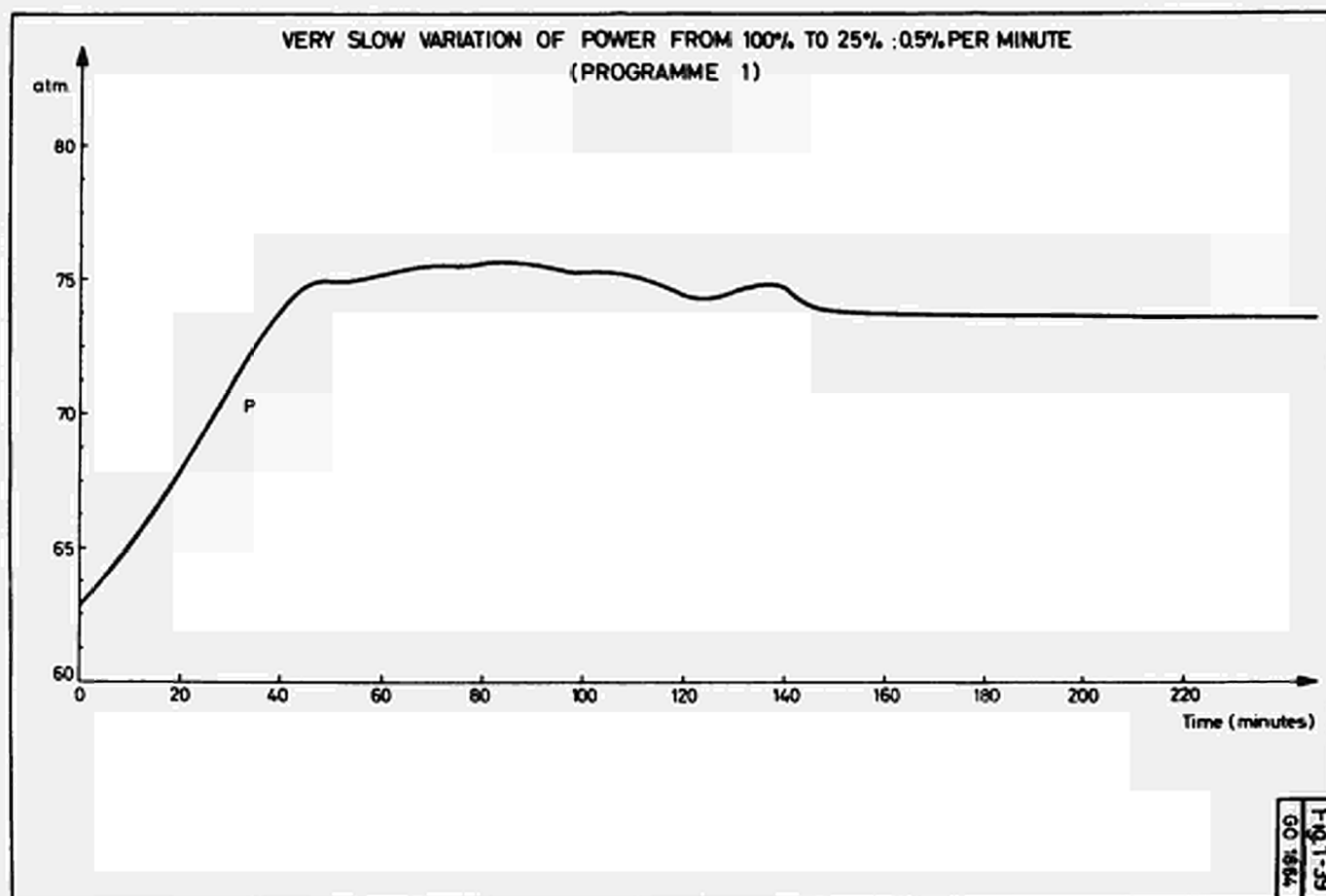
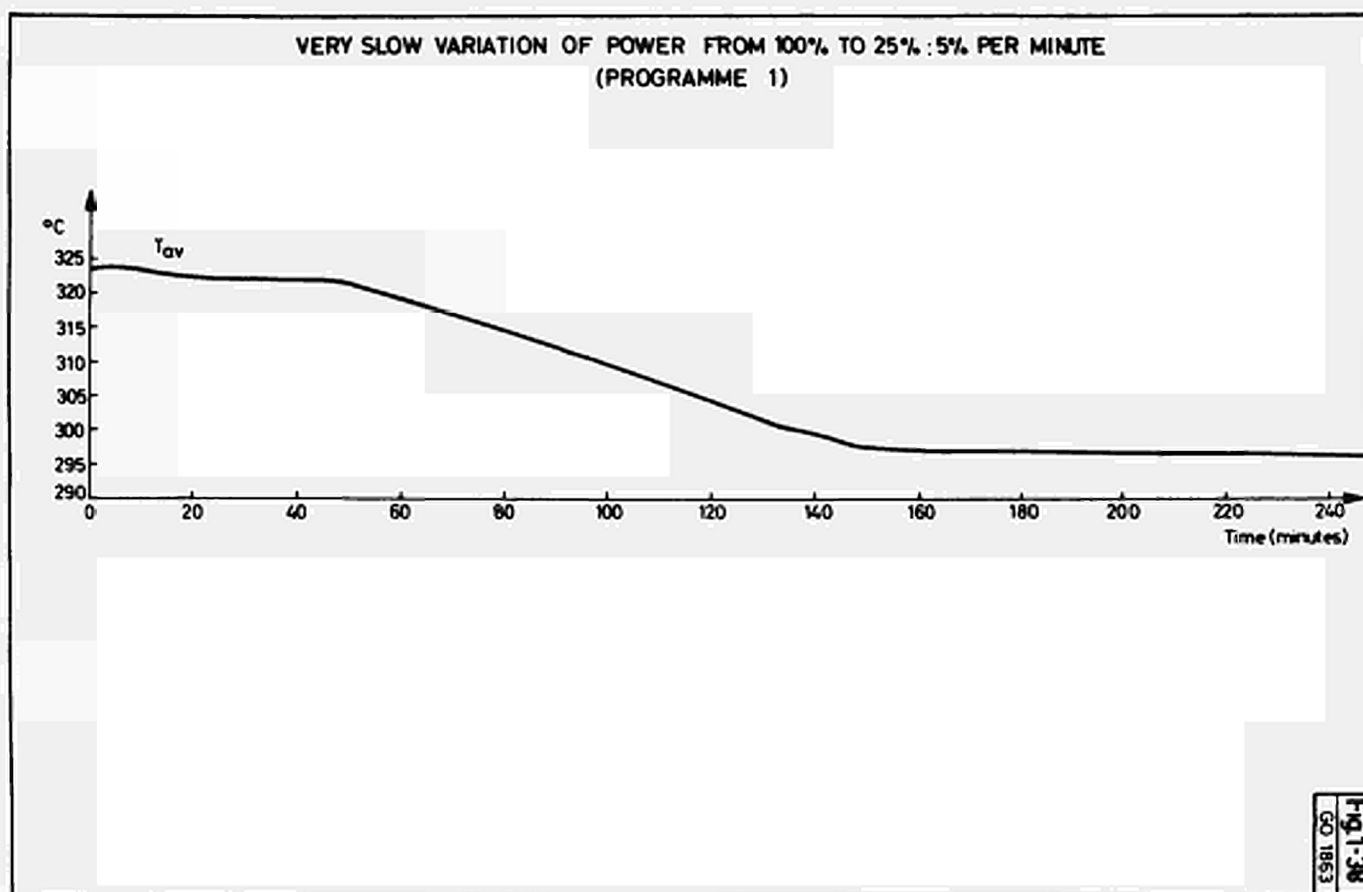
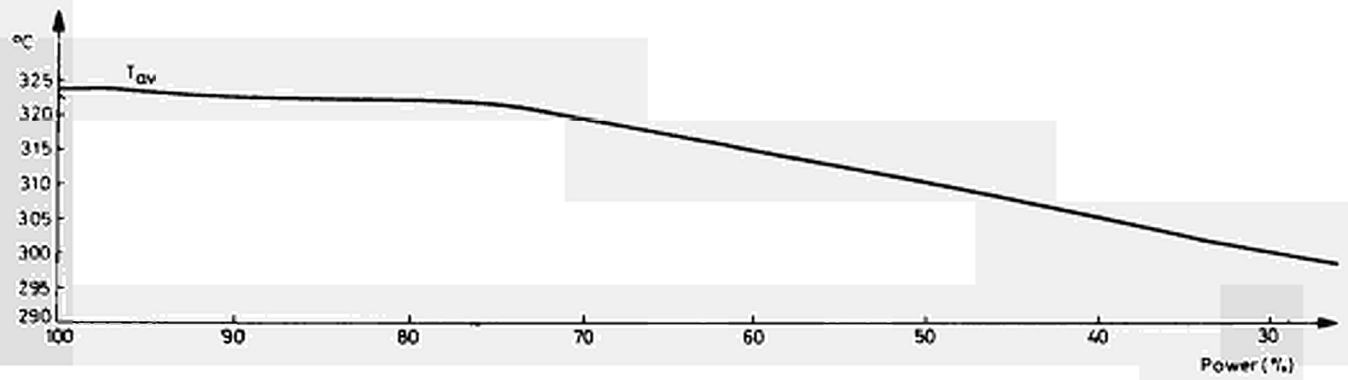
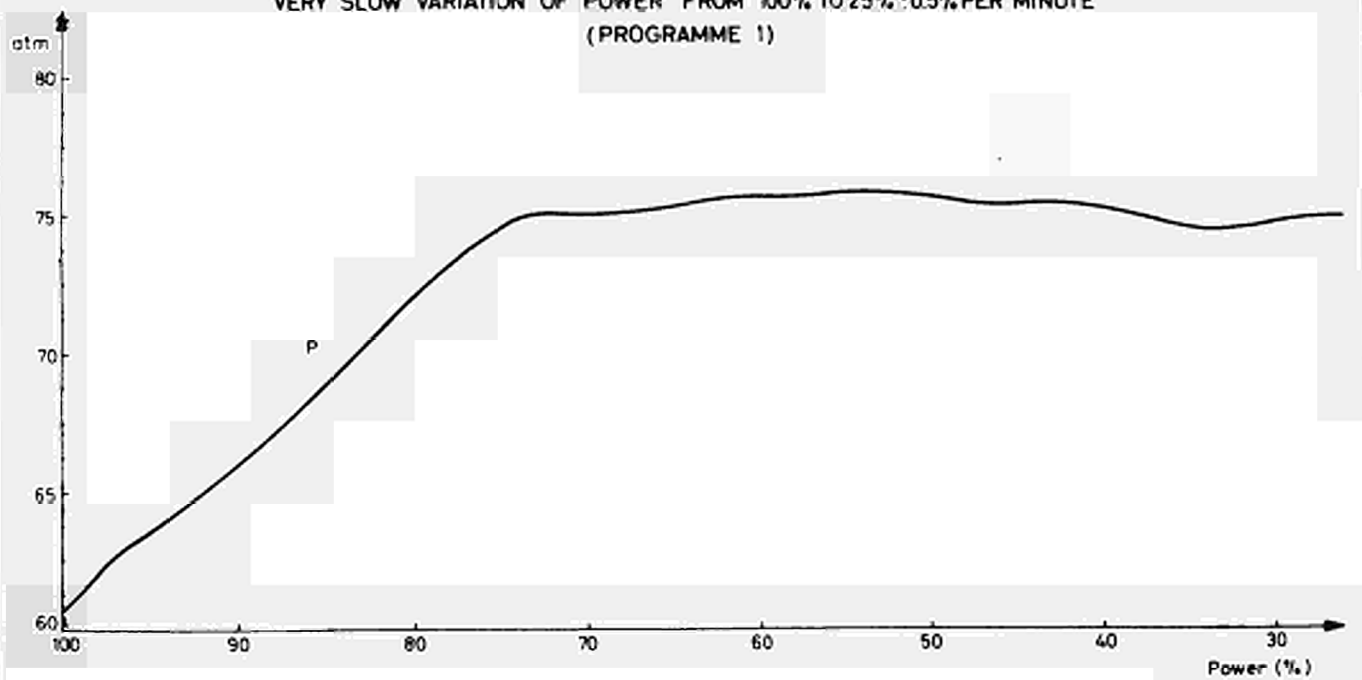
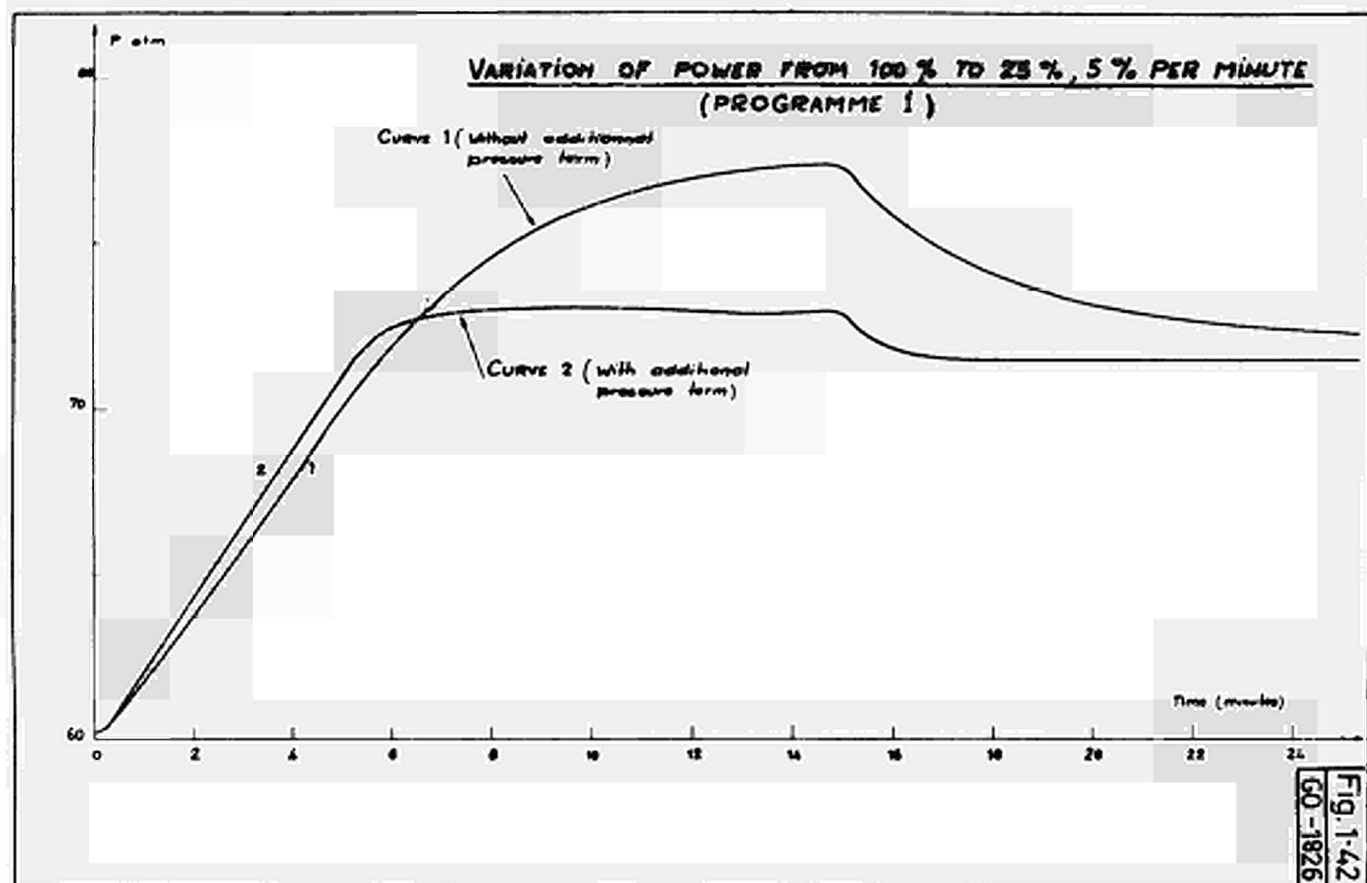


Fig. 1-37
GO-1862



VERY SLOW VARIATION OF POWER FROM 100% TO 25% : 0.5% PER MINUTE
(PROGRAMME 1)Fig 1-40
60 1865VERY SLOW VARIATION OF POWER FROM 100% TO 25% : 0.5% PER MINUTE
(PROGRAMME 1)Fig 1-41
60 1865



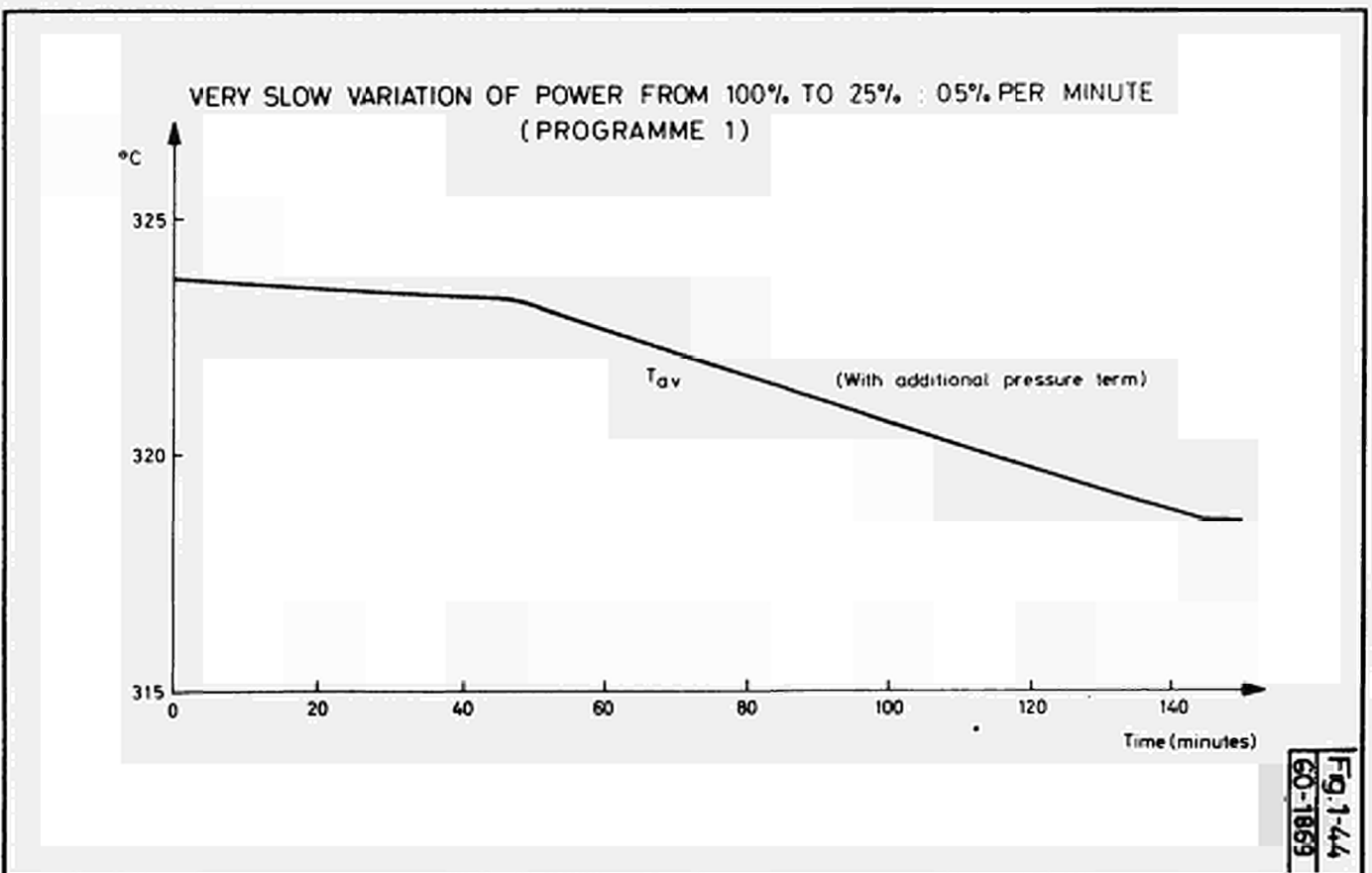
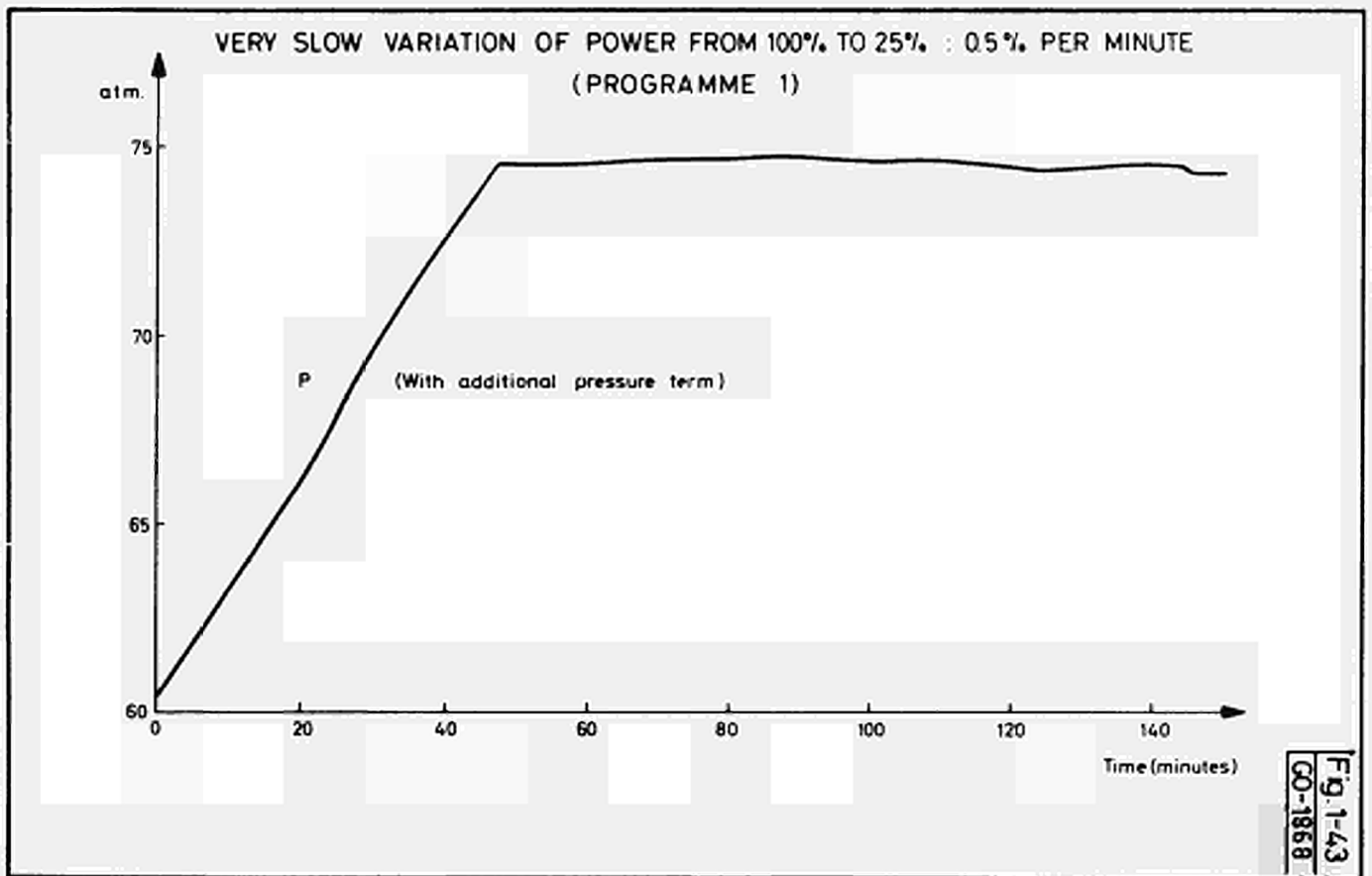


Fig.1-45
GO-1870

VARIATION OF POWER FROM 100% TO 25%.
(PROGRAMME 1)

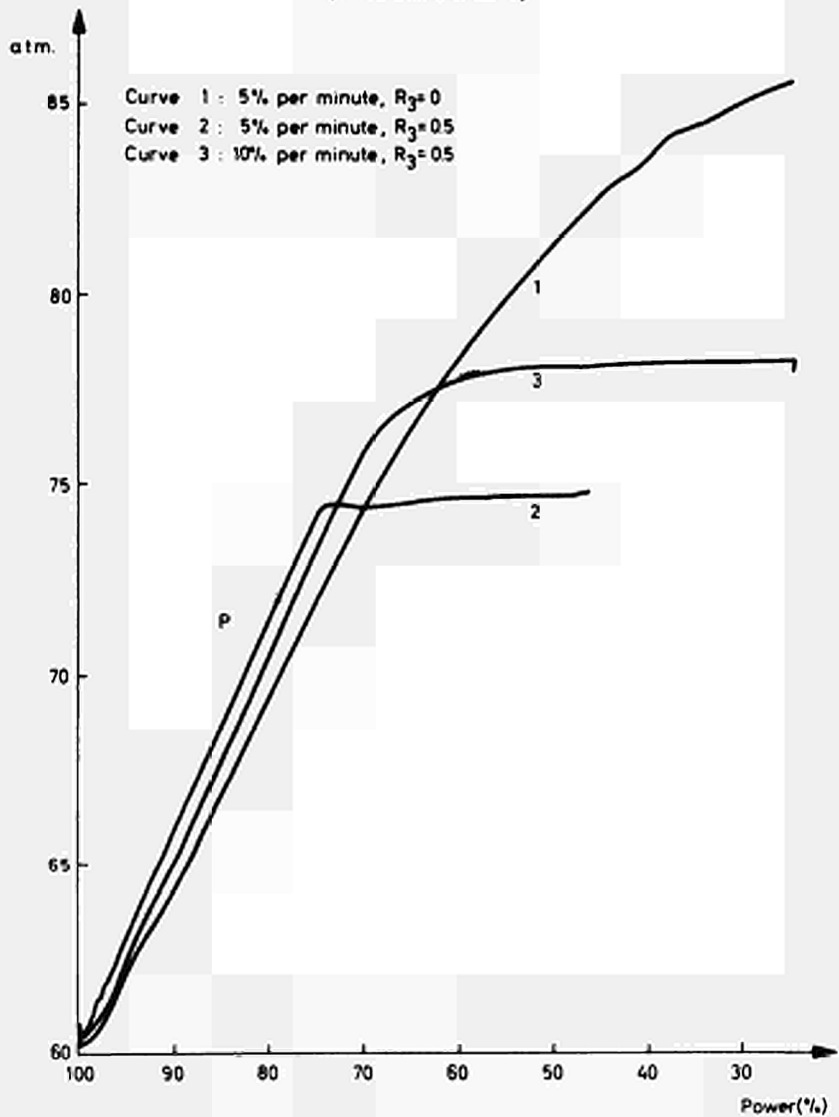
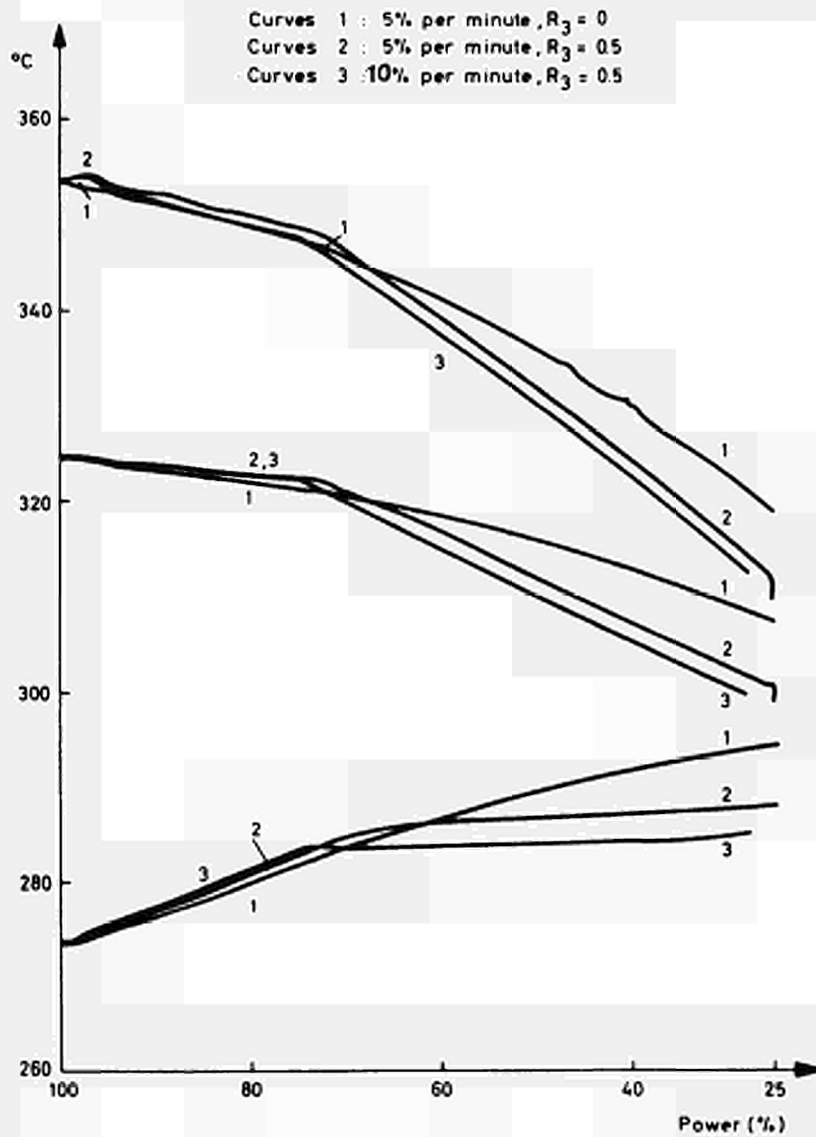


Fig.1-46
GO-1871

VARIATION OF POWER FROM 100% TO 25%.
(PROGRAMME 1)



CONSTANT-STEAM PRESSURE PROGRAM
POWER CHANGE BETWEEN 100 AND 75 % (5%/min.)
WITH PRESSURE TERM ($R_2 = 0.5$)



Fig. 1-47
GO-2059

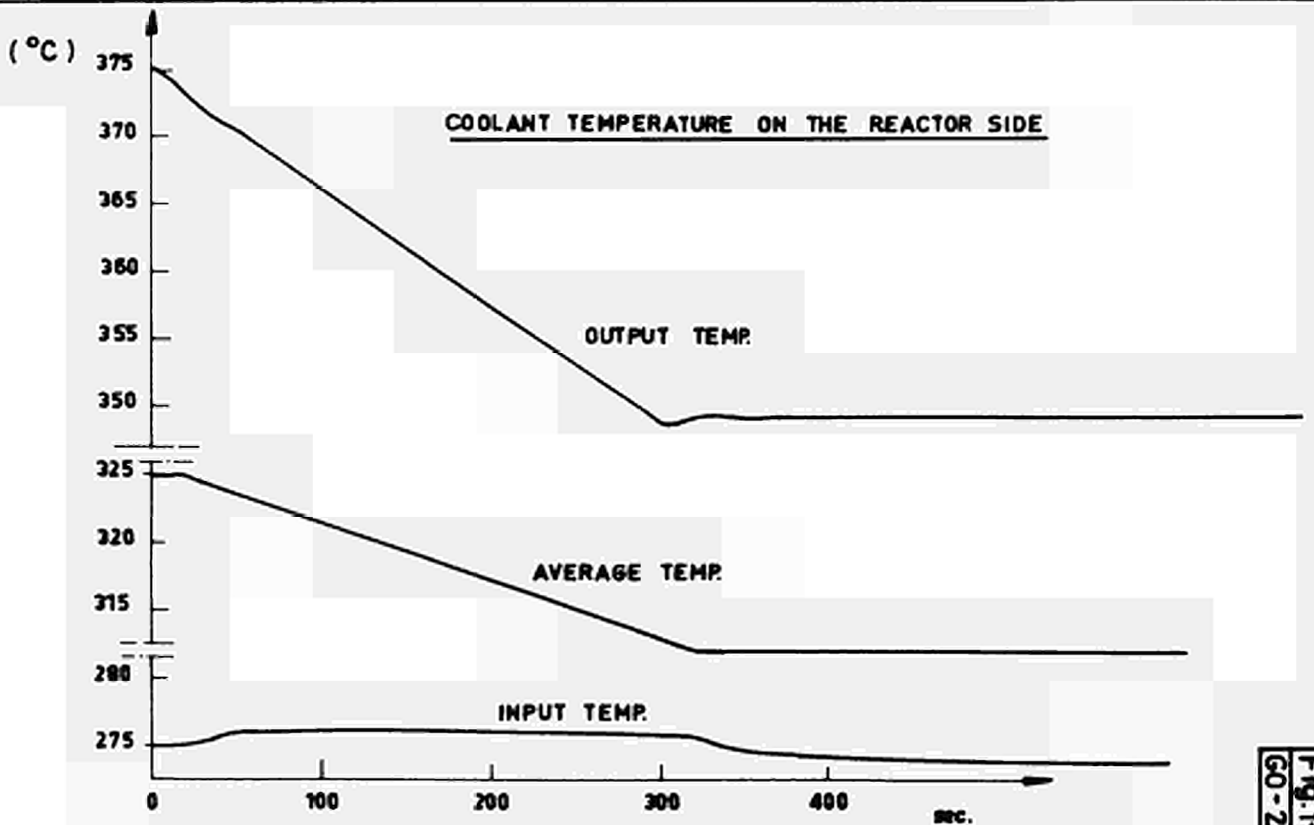
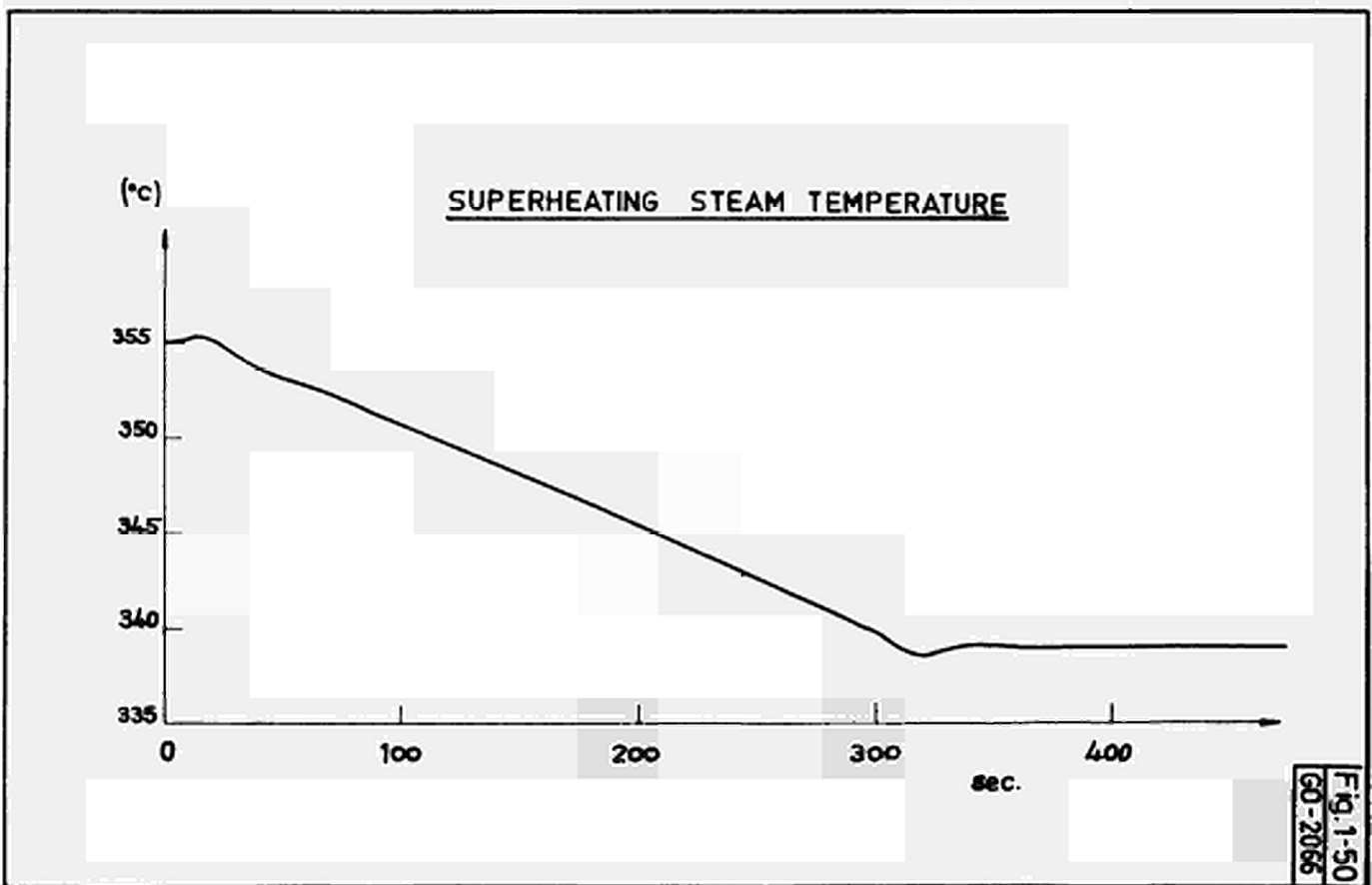
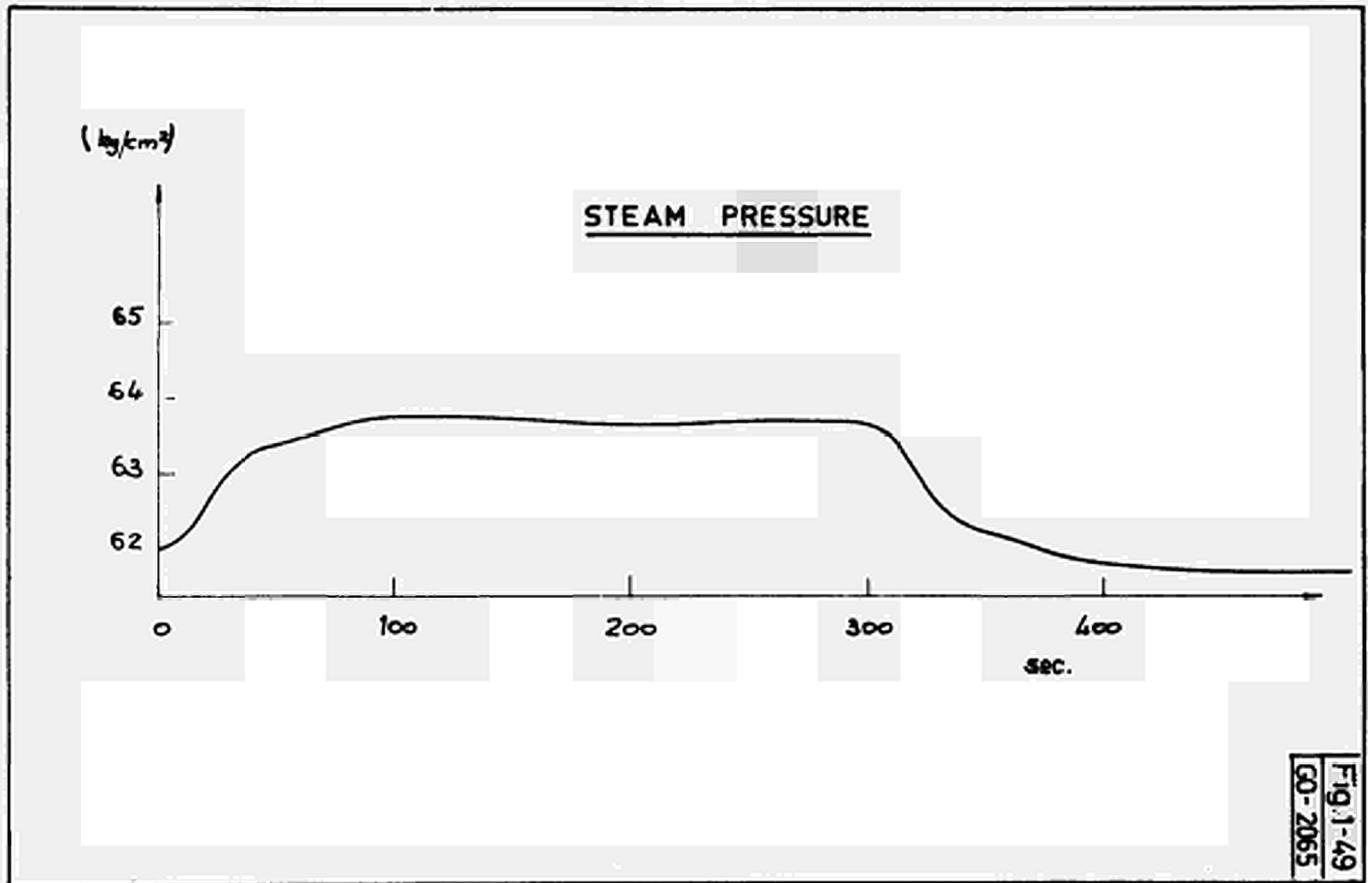
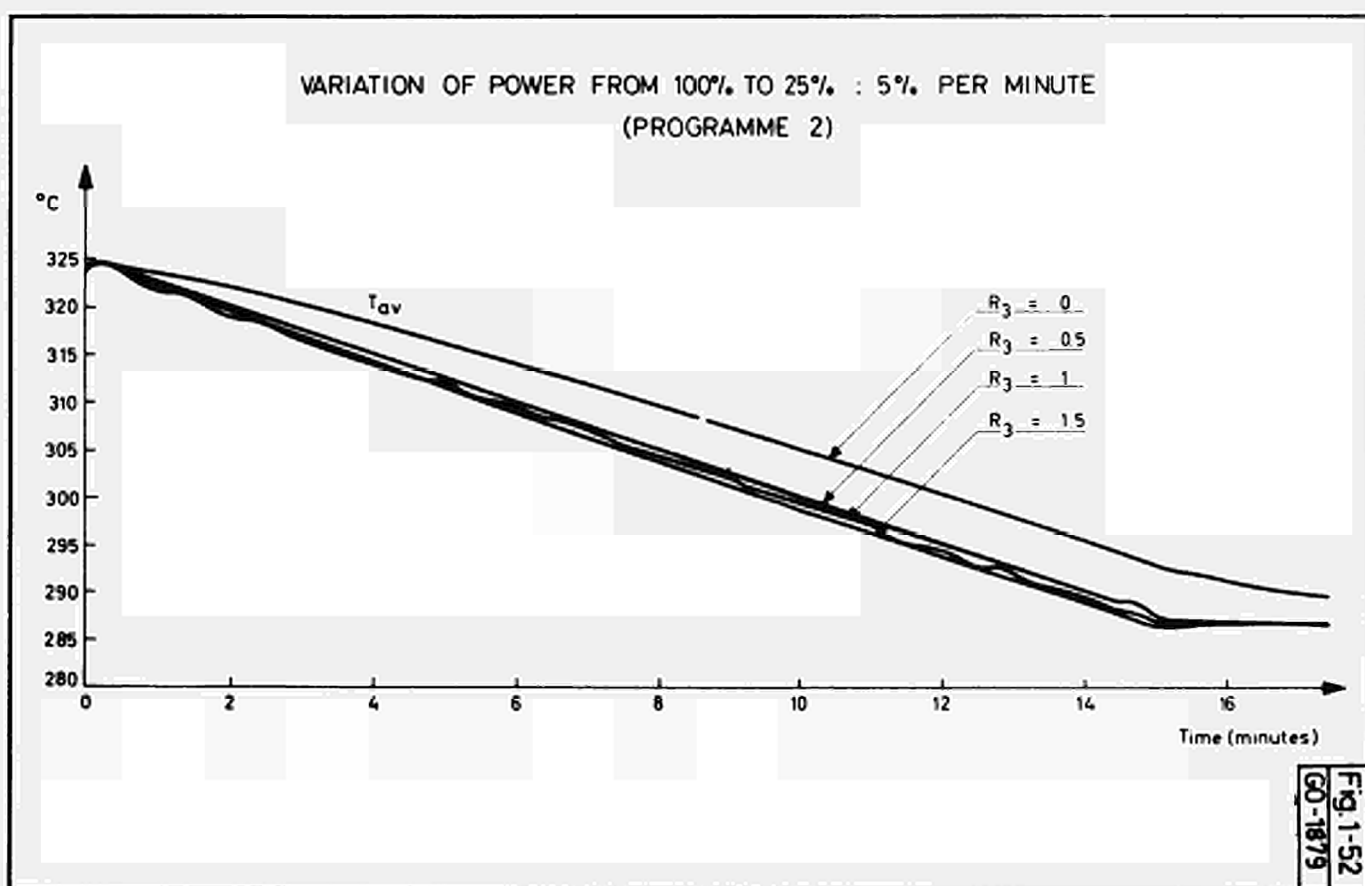
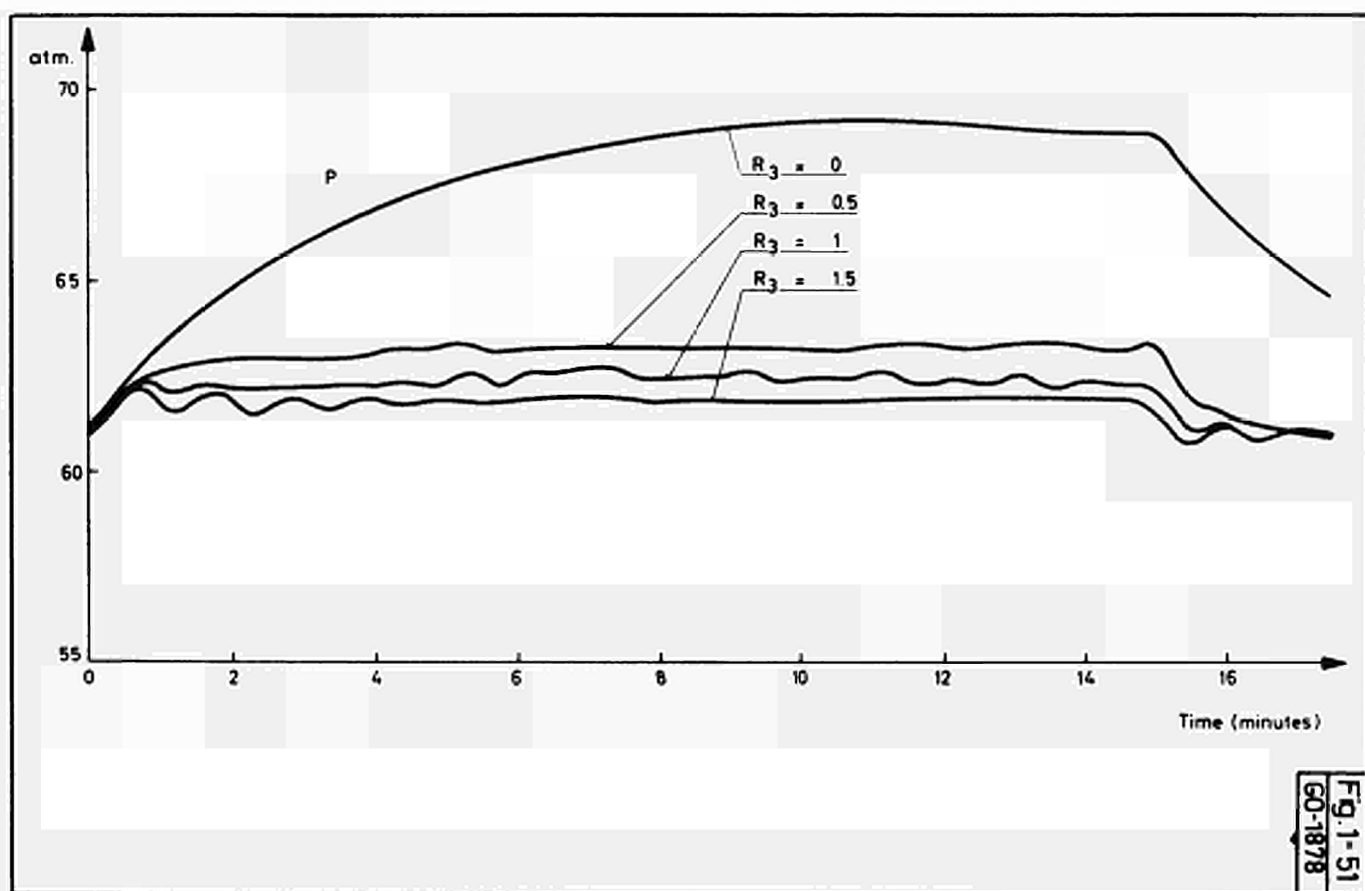
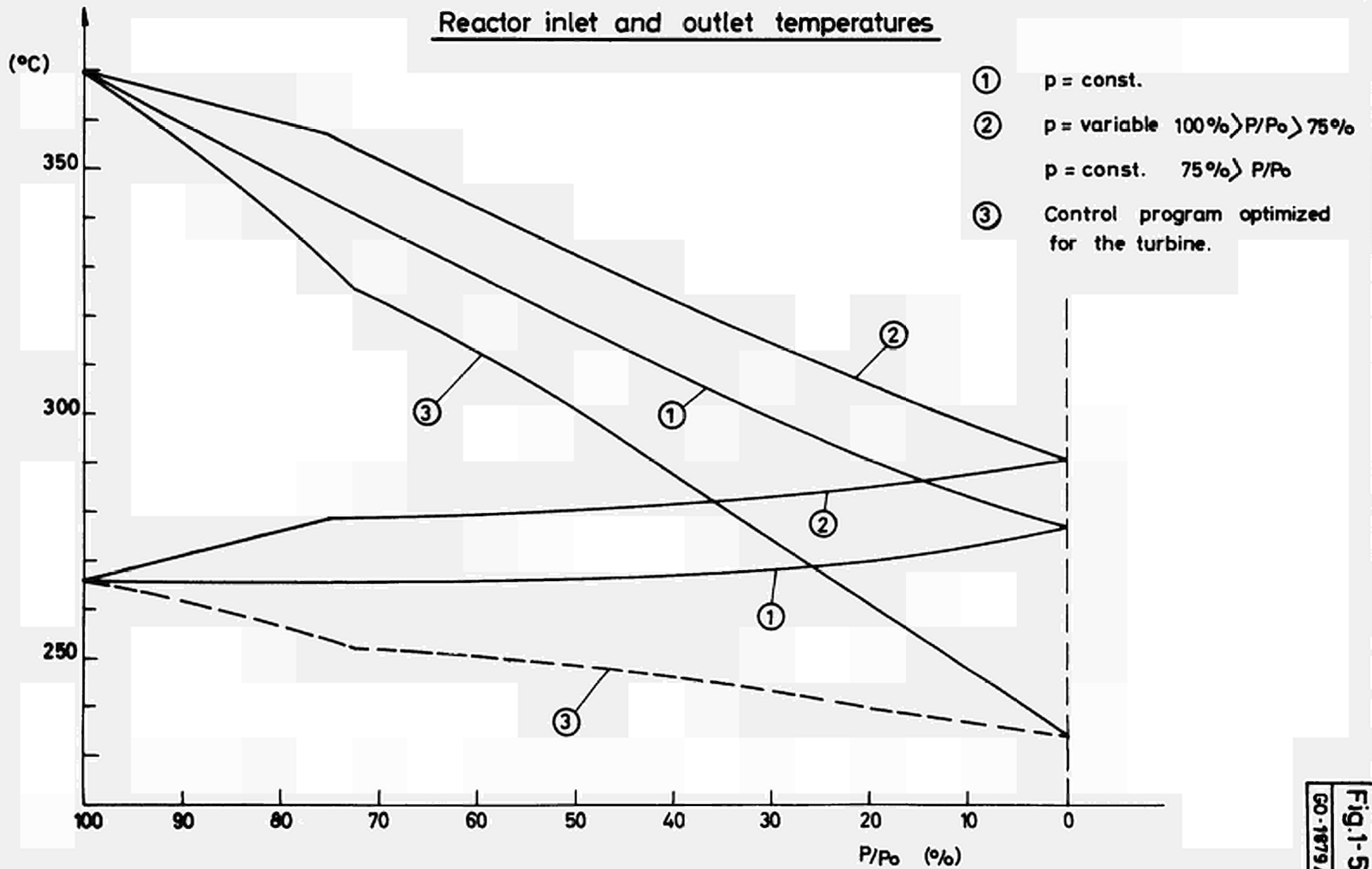


Fig. 1-48
GO-2055





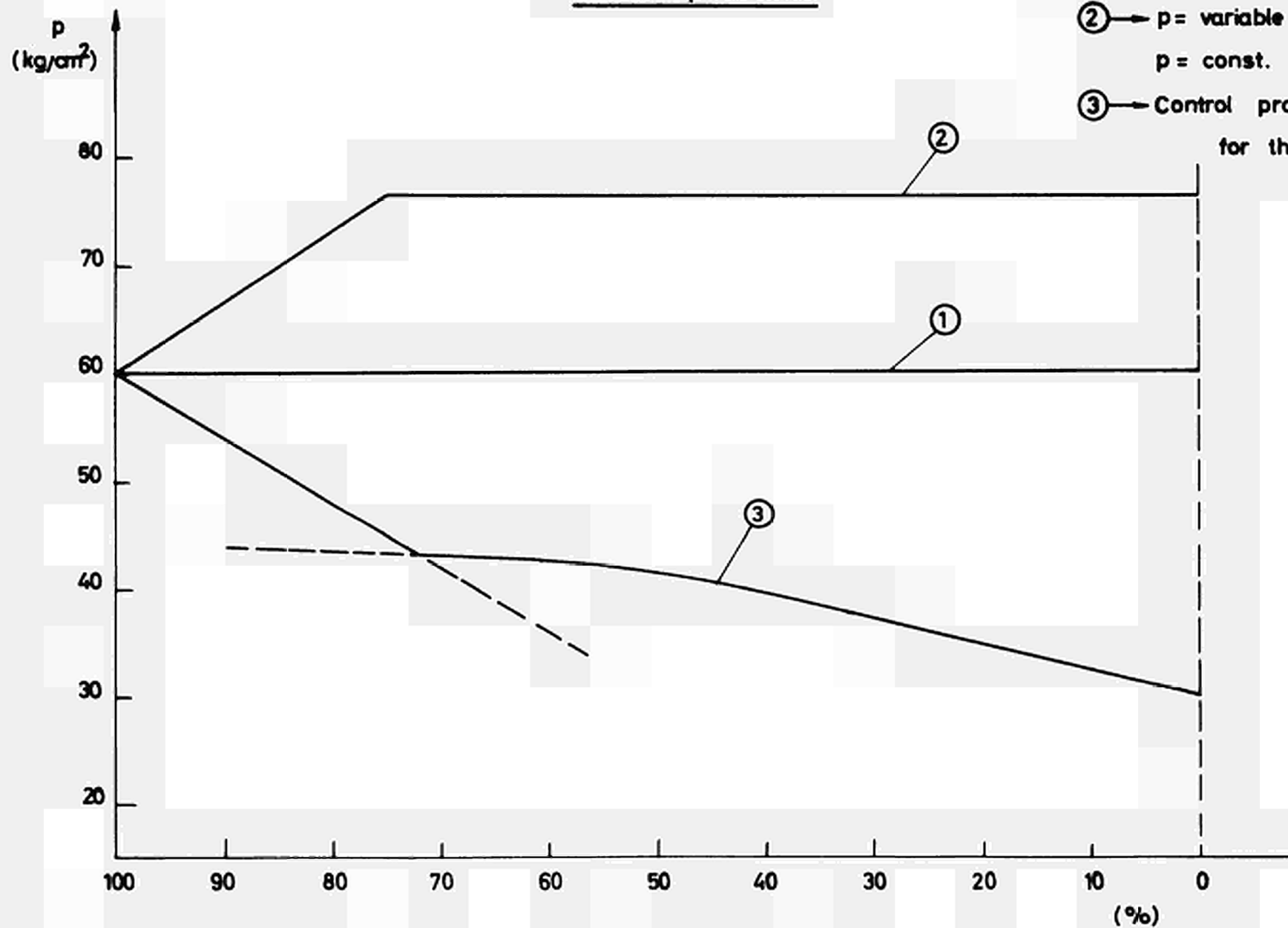
Reactor inlet and outlet temperatures



Steam pressure

p
(kg/cm²)

- ① → $p = \text{const.}$
- ② → $p = \text{variable } 100\% > P/P_0 > 75\%$
 $p = \text{const. } 75\% > P/P_0$
- ③ → Control program optimized
for the turbine



Steam temperature turbine inlet

T_{turb.}
(°C)

350

300

250

100

90

80

70

60

50

40

30

20

10

0

P/P₀ (%)

- ① p = const.
- ② p = variable 100% > P/P₀ > 75%
p = const. 75% > P/P₀
- ③ Control program optimized for the turbine

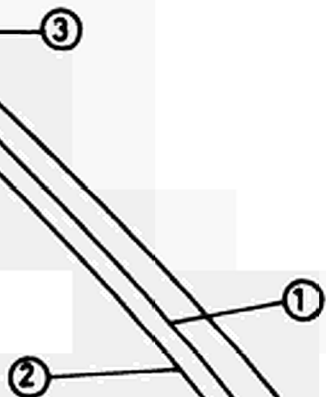
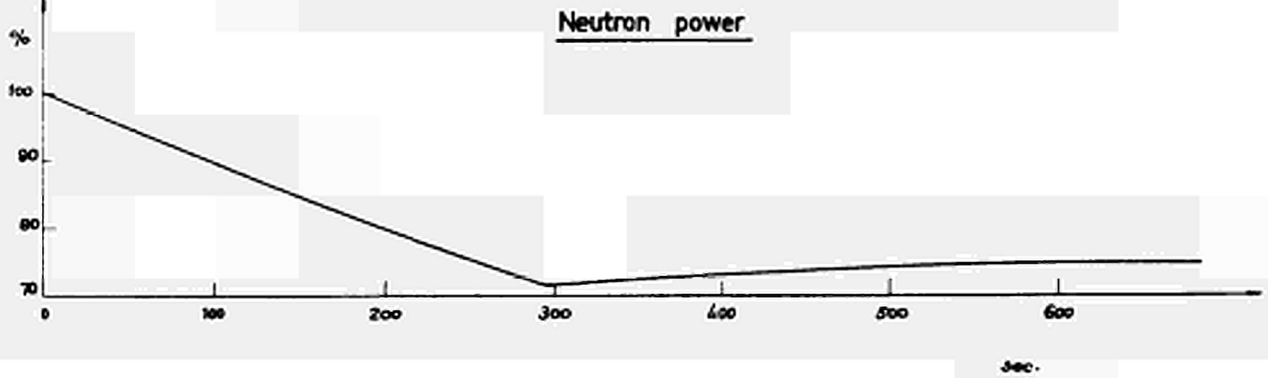
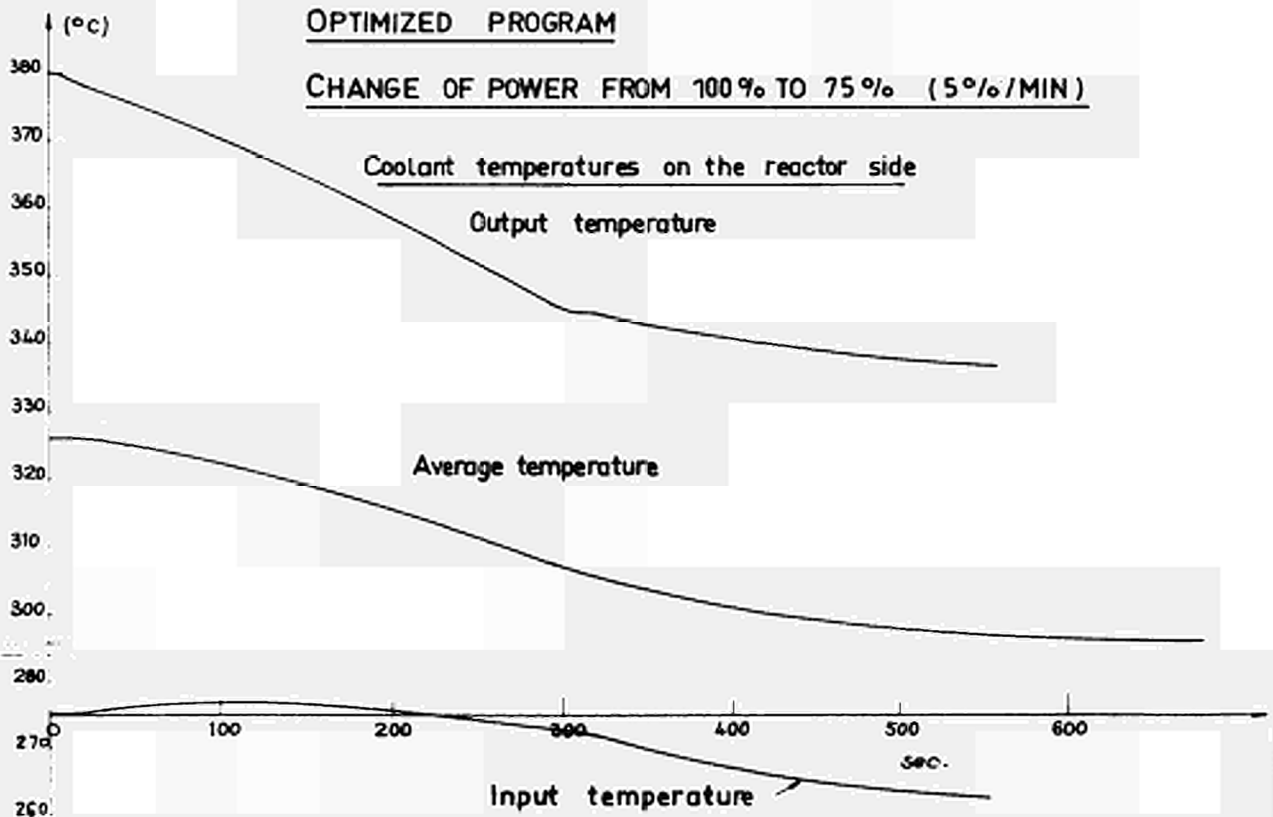
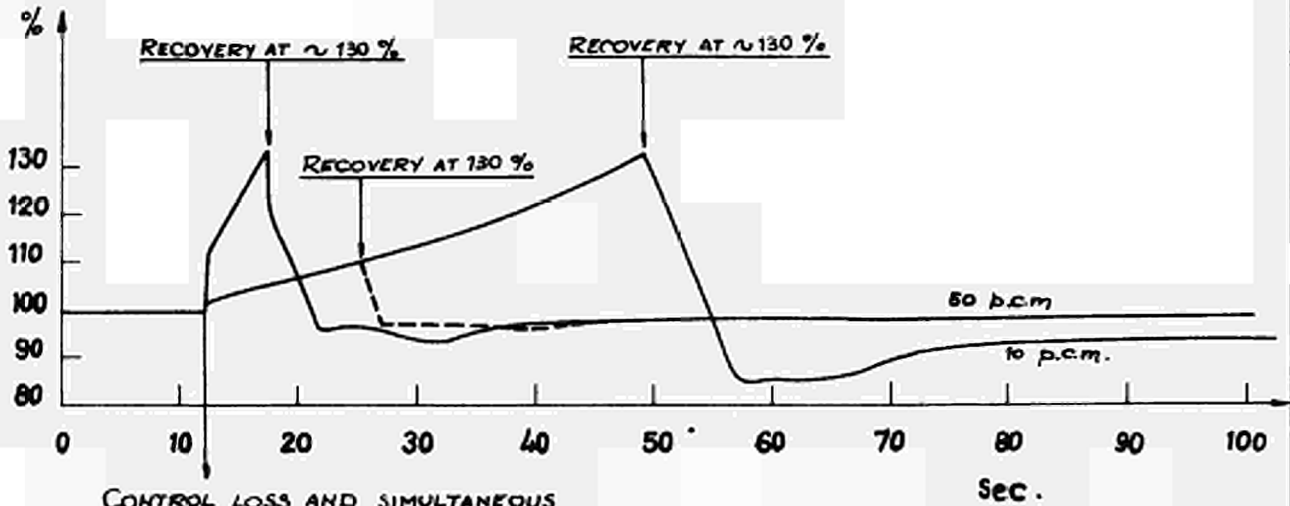


Fig. 1-55
60-1879 C

OPTIMIZED PROGRAMCHANGE OF POWER FROM 100% TO 75% (5%/MIN)Fig. 1-56
GO-2049OPTIMIZED PROGRAMCHANGE OF POWER FROM 100% TO 75% (5%/MIN)Fig. 1-57
GO-2046

CONTROL LOSS AND RECOVERY

NEUTRON POWER



CONTROL LOSS AND SIMULTANEOUS
INJECTION OF 10 OR 50 p.c.m. IN STEP

Fig. 1-58
GO-2061

CONTROL LOSS AND RECOVERY

AVERAGE COOLANT TEMPERATURE ON THE REACTOR SIDE.

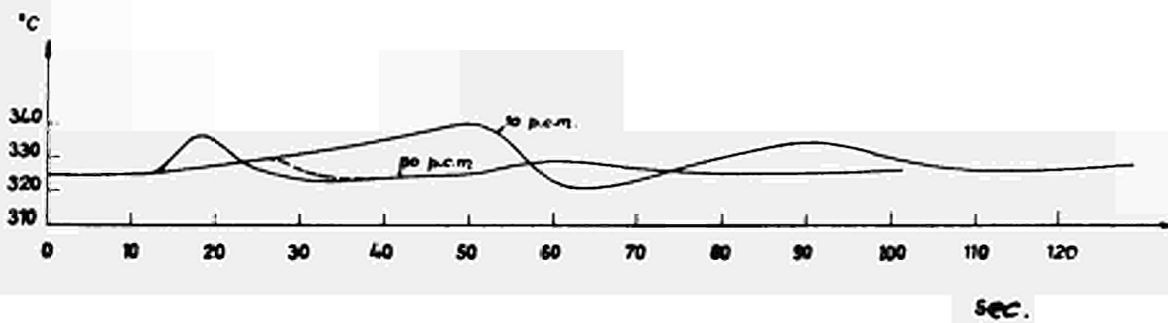
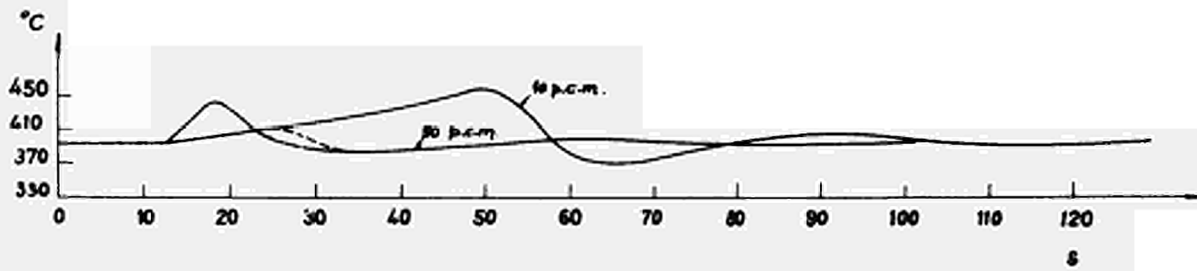
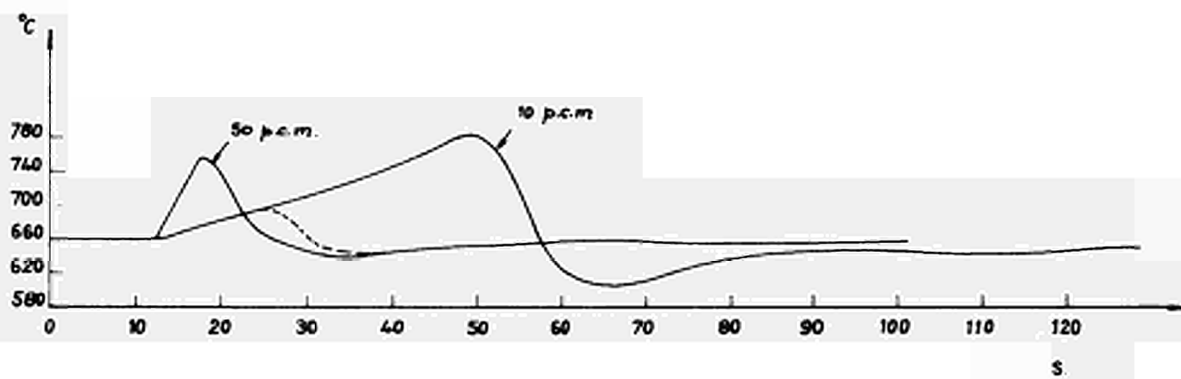


Fig. 1-59
GO-2052

CONTROL LOSS AND RECOVERYAVERAGE CLADDING TEMPERATUREFig. 1-60
GO-2051CONTROL LOSS AND RECOVERYAVERAGE FUEL TEMPERATUREFig. 1-61
GO-2050

SCRAM

NEUTRON POWER

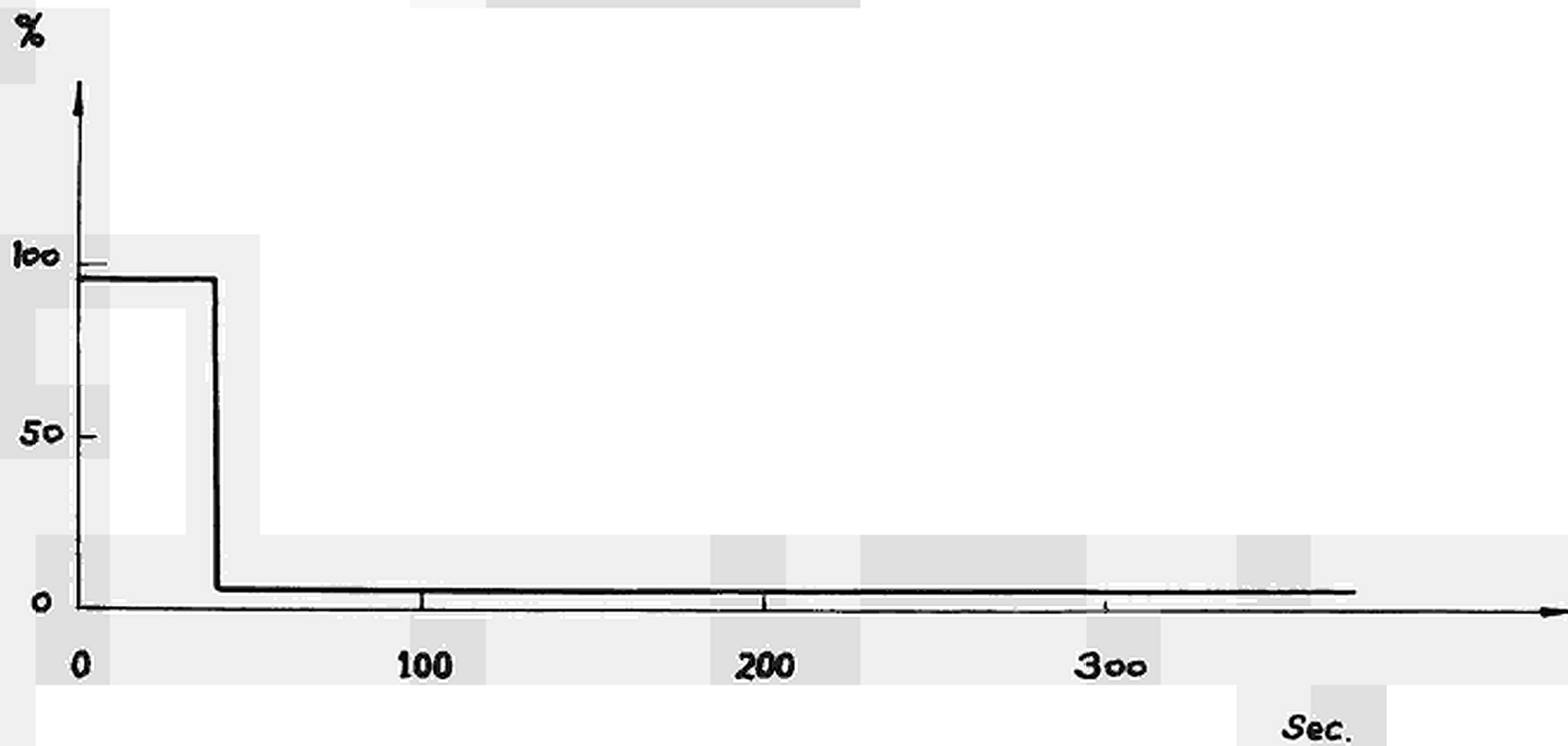


Fig. 1-62
40-2064

SCRAM

COOLANT TEMPERATURES

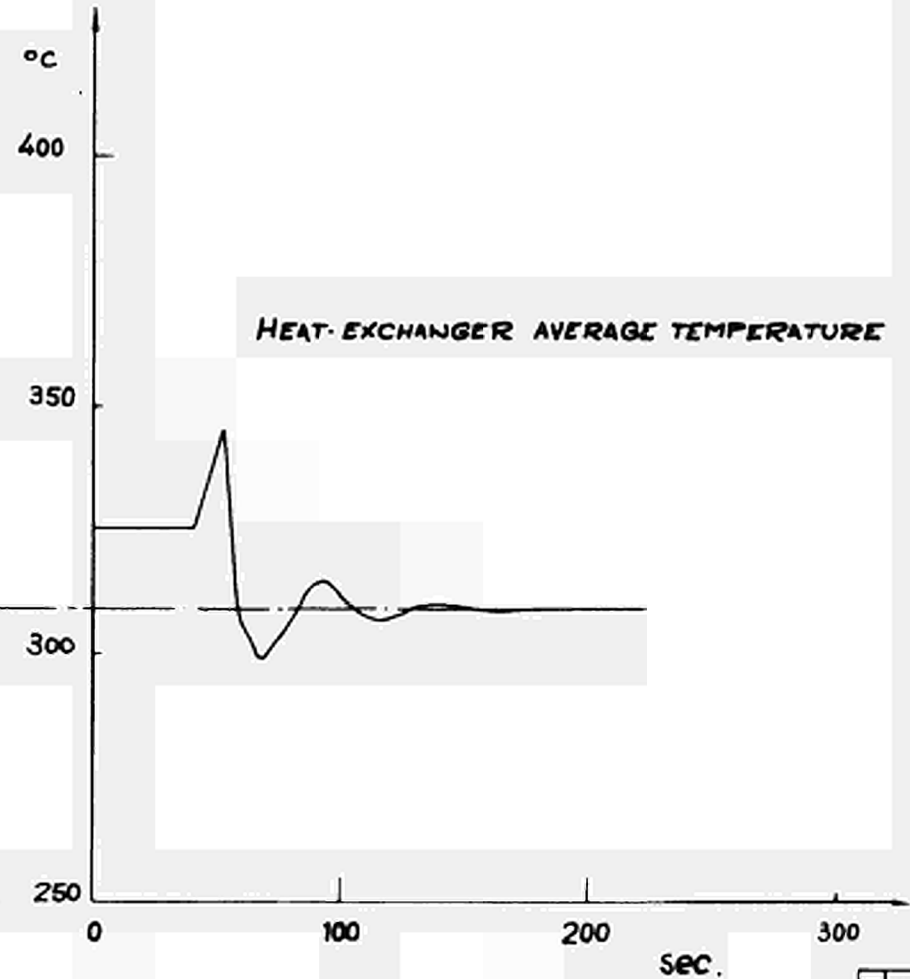
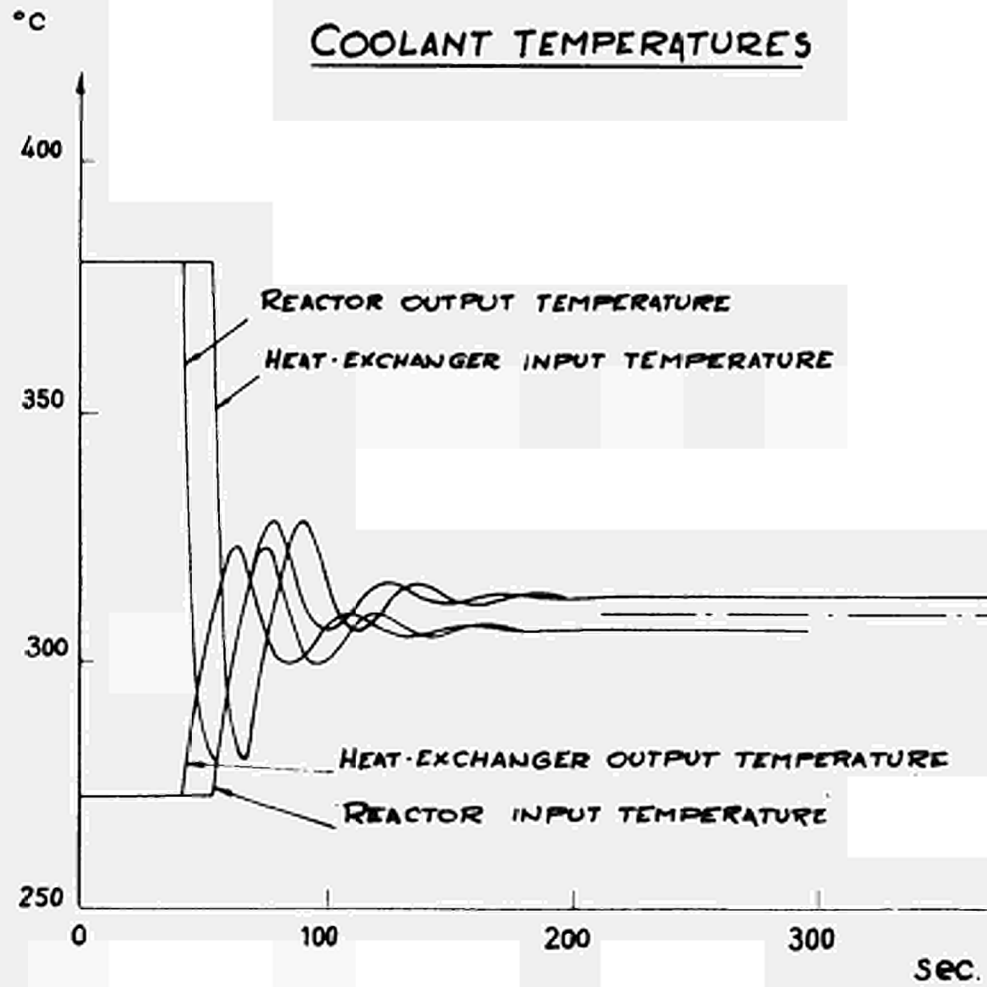
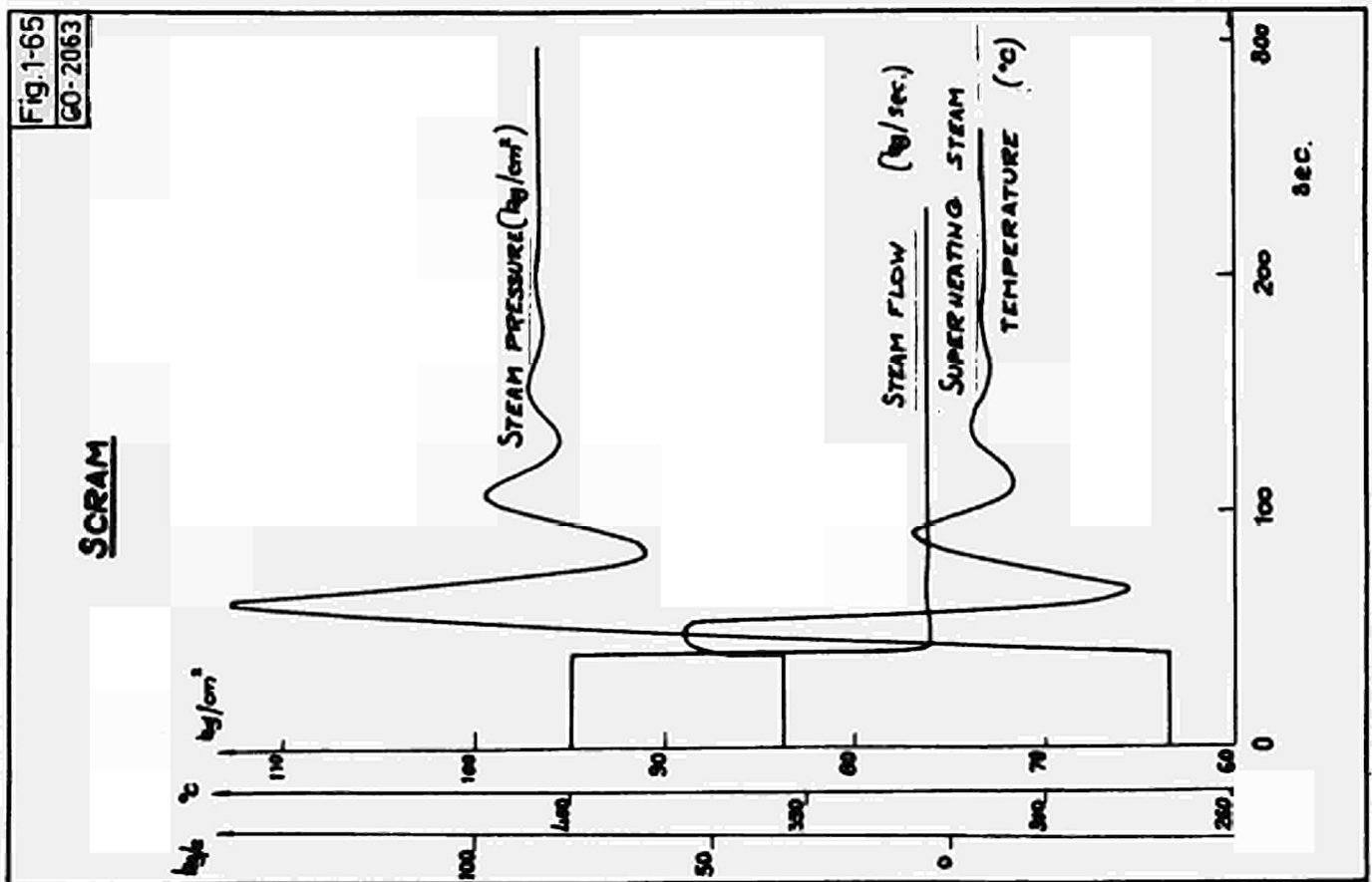
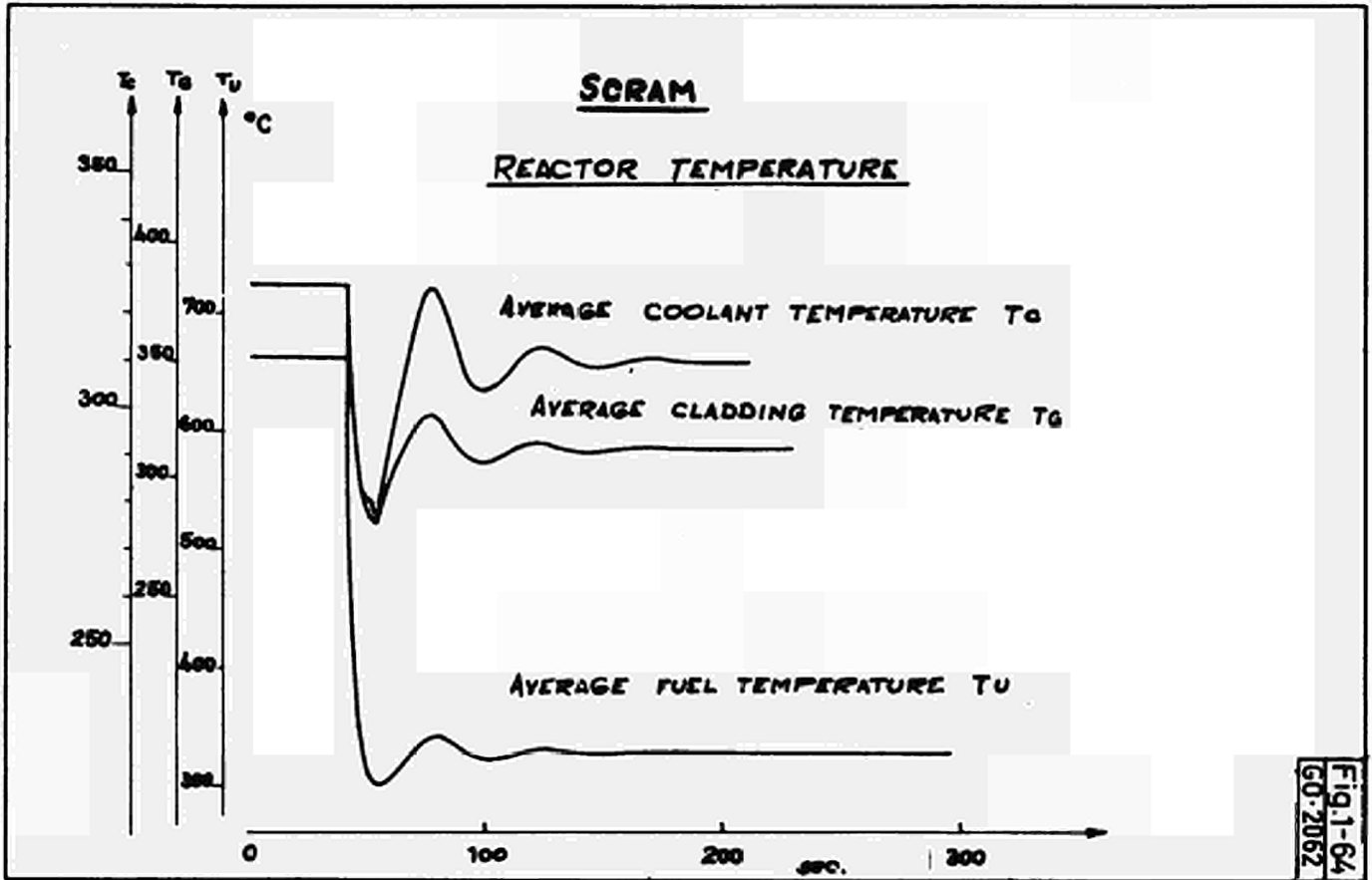
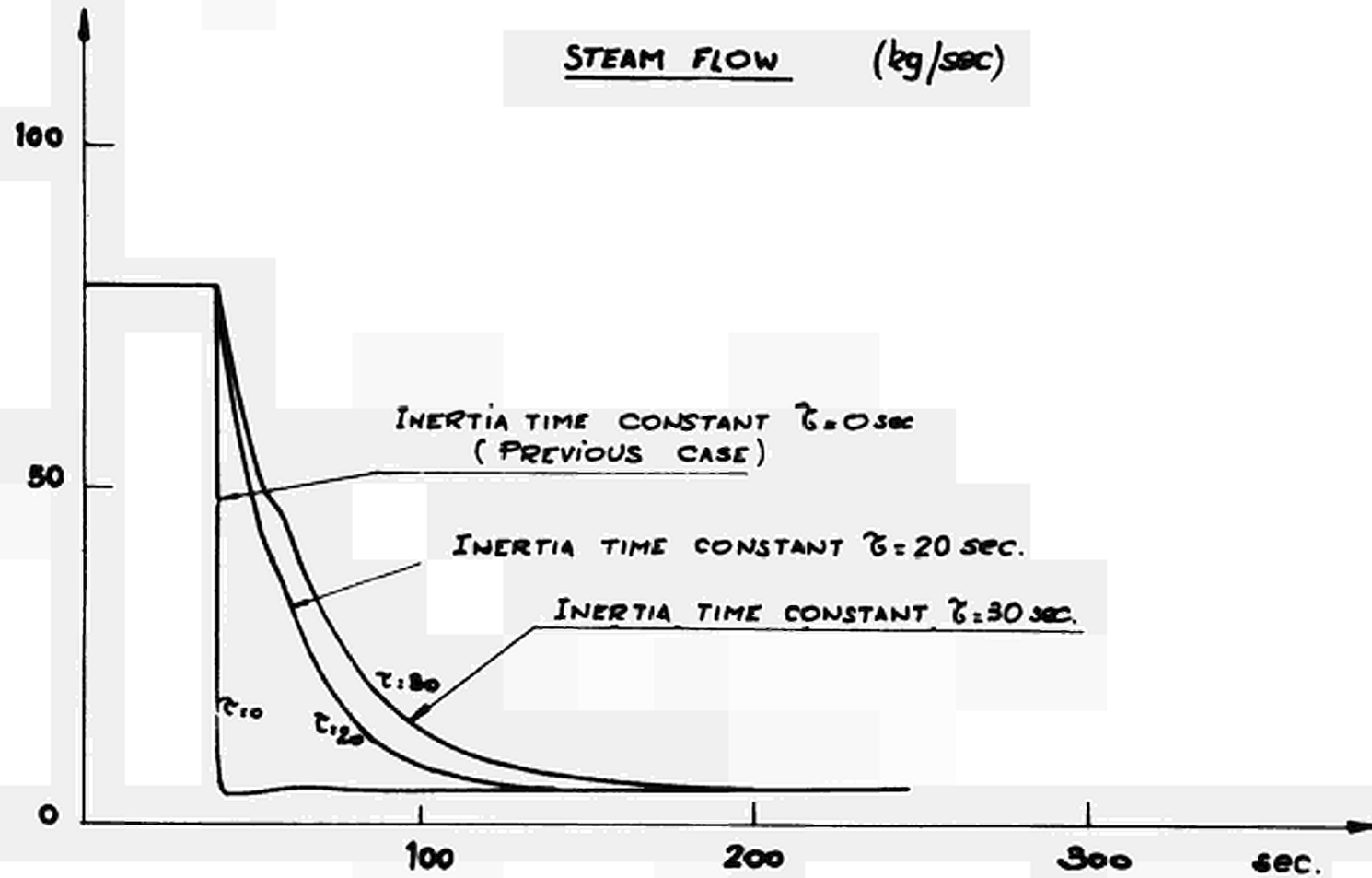


Fig 1-63
CO-2053



SCRAM WITH THROTTLE CLOSING



SCRAM WITH THROTTLE CLOSING

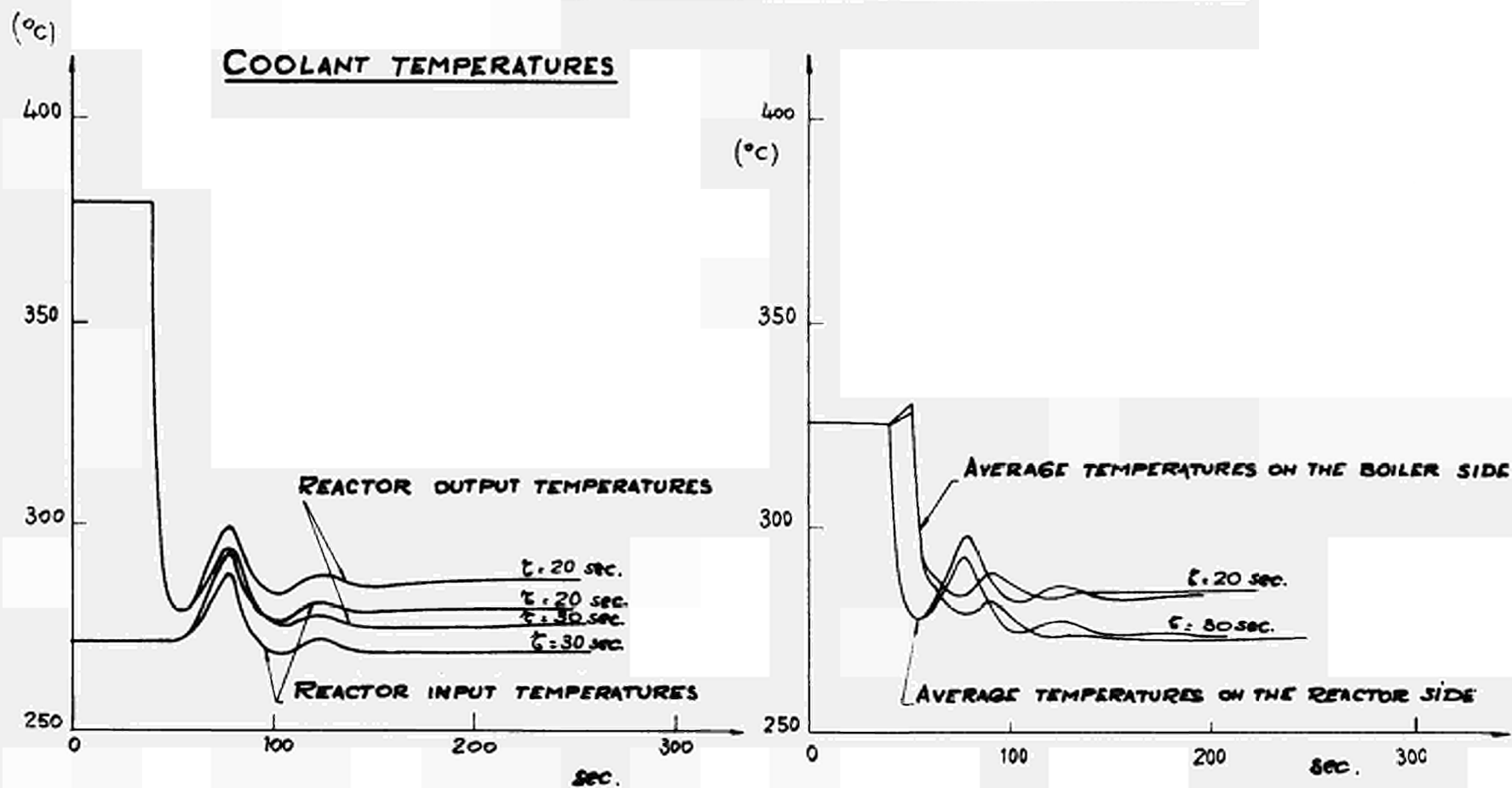


Fig. 1-67
G02056

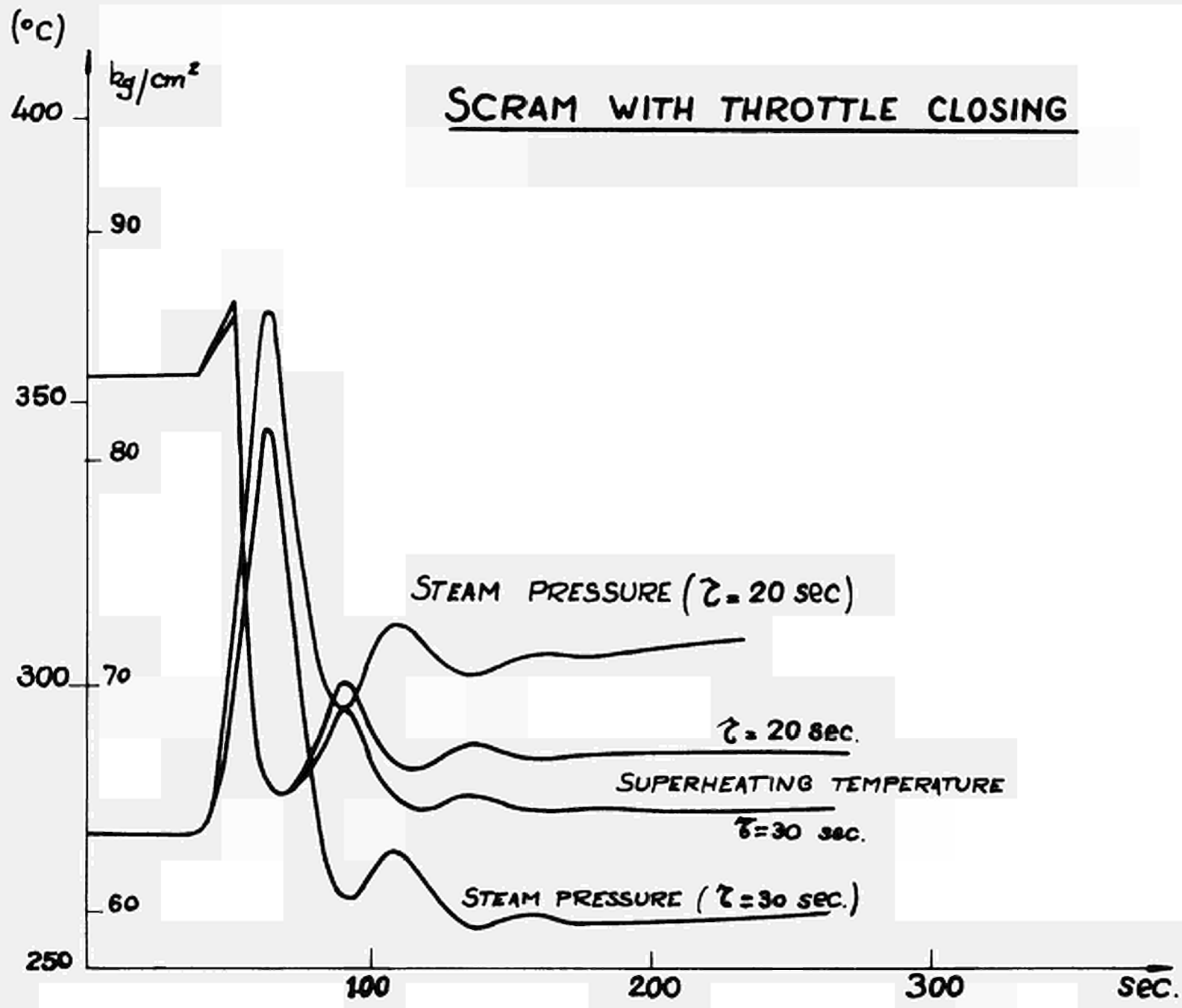


Fig. 1-68
00.2057

Fig. 1-70
GO-2069

RESPONSE TO A LIKESTEP CHANGE
IN REACTIVITY OF 50 p.c.m.

AVERAGE COOLANT TEMPERATURE ON THE BOILER
SIDE

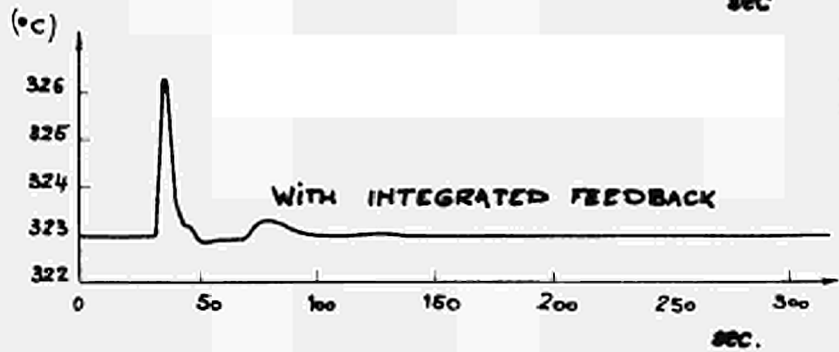
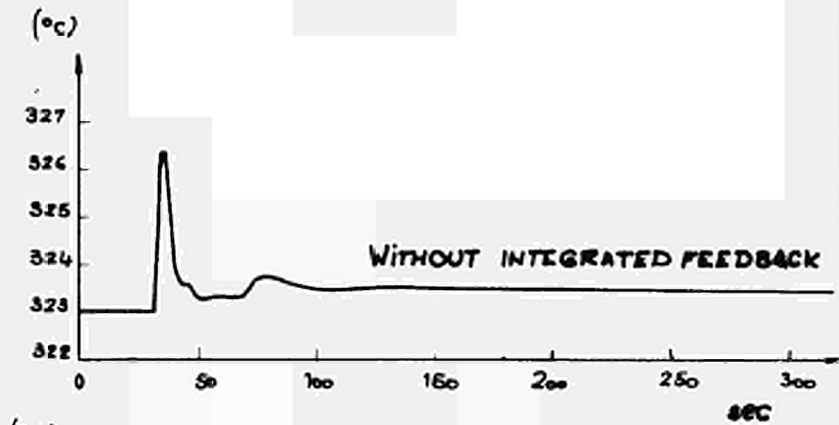


Fig. 1-69
GO-2068

RESPONSE TO A LIKESTEP CHANGE
IN REACTIVITY OF 50 p.c.m.

NEUTRON POWER

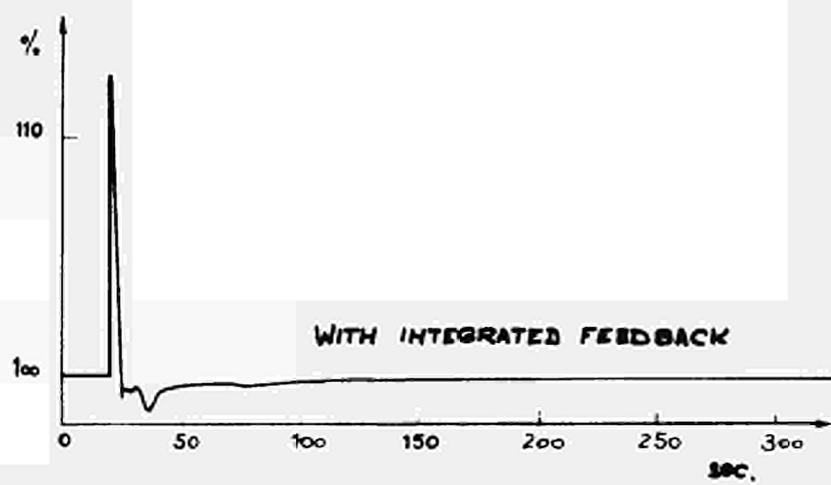
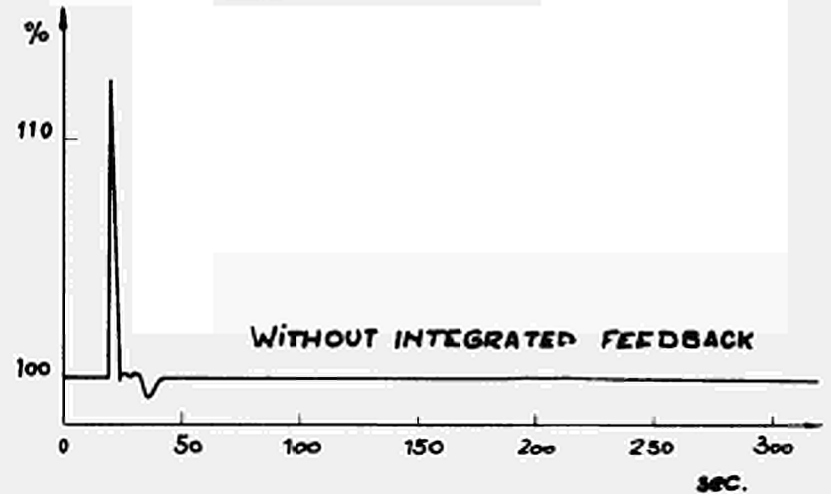
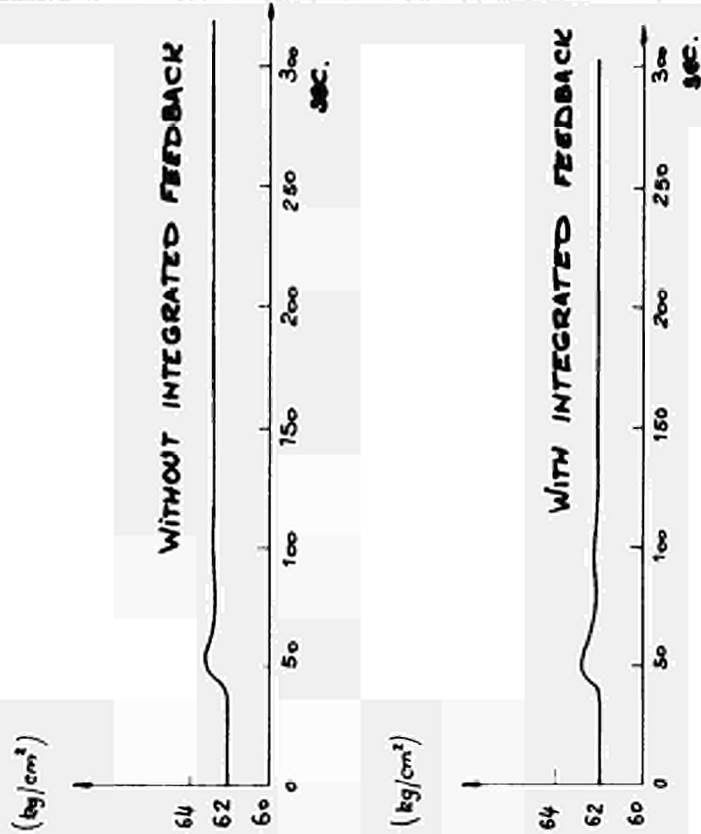


Fig.1-71
GO-2070

**RESPONSE TO A LIKESTEP CHANGE
IN REACTIVITY OF 50 P.C.M.**

STEAM PRESSURE



**STABLE REACTOR: CASE 1 WITH ON-OFF CONTROL
RESPONSE TO A STEP OF 50 P.C.M.**

DEAD ZONE : ±1%
INERTIVE TIME CONSTANT OF THE BAR : 2 SEC.
VARIABLE VELOCITY OF THE BAR

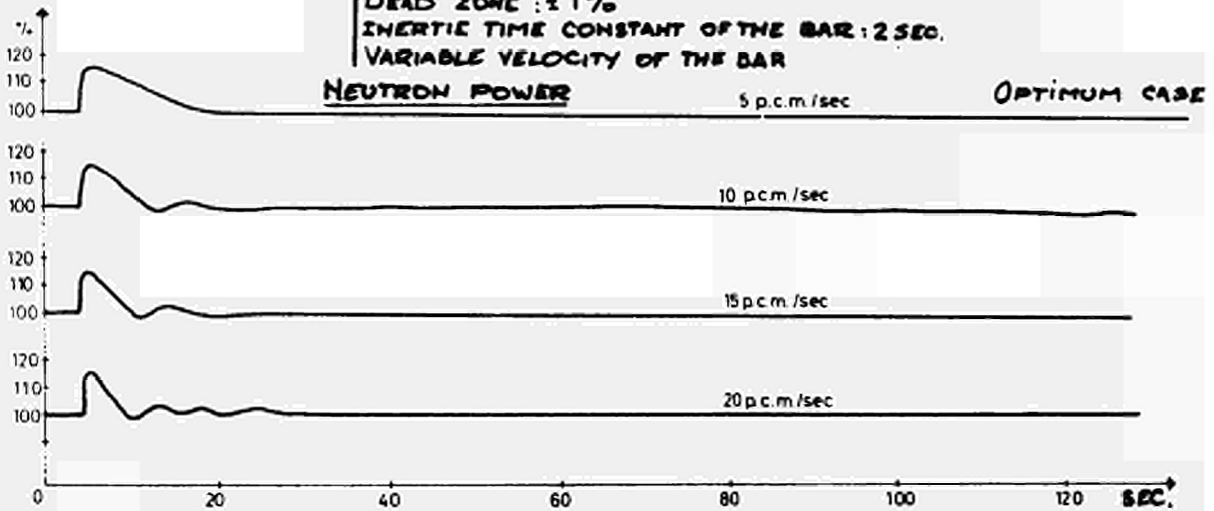
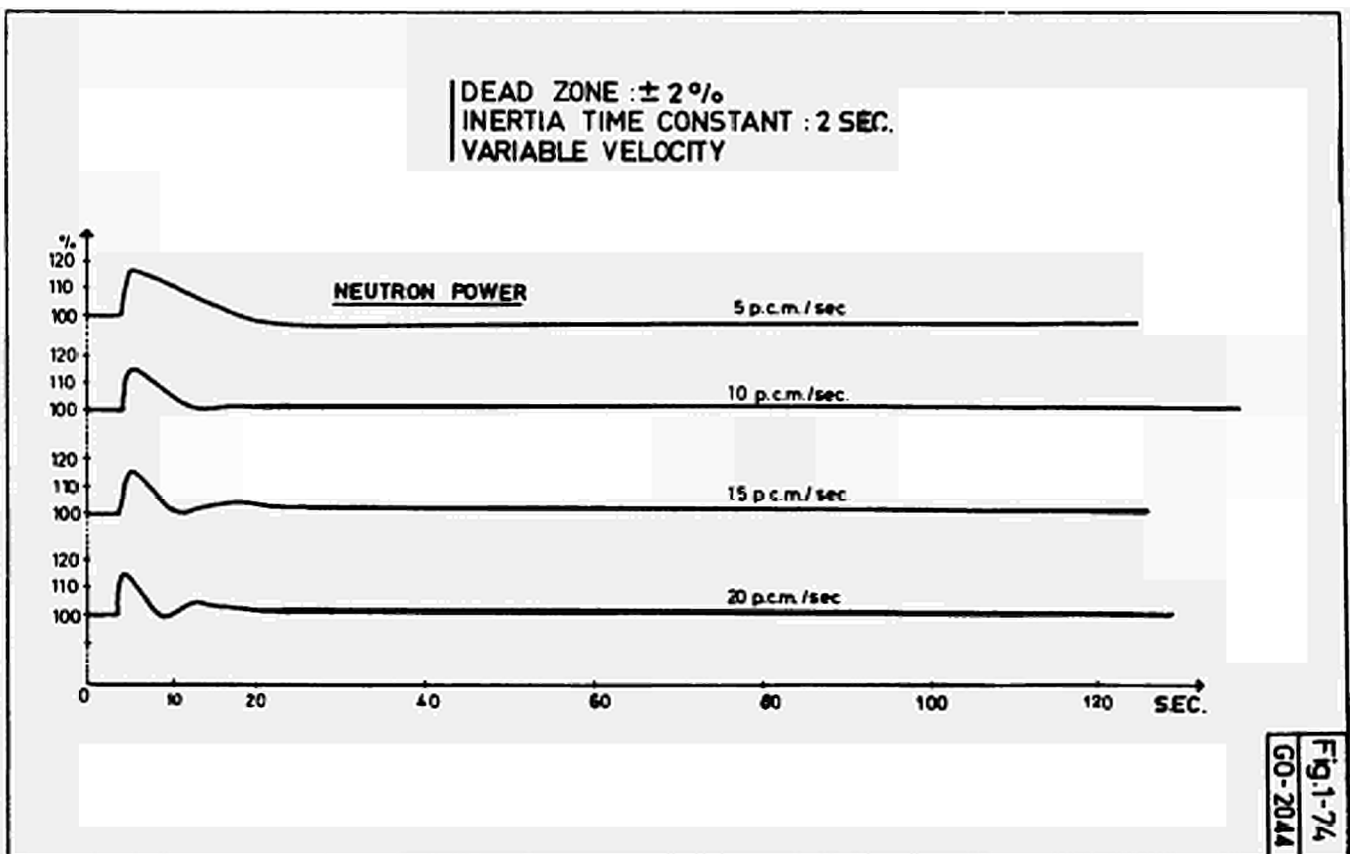
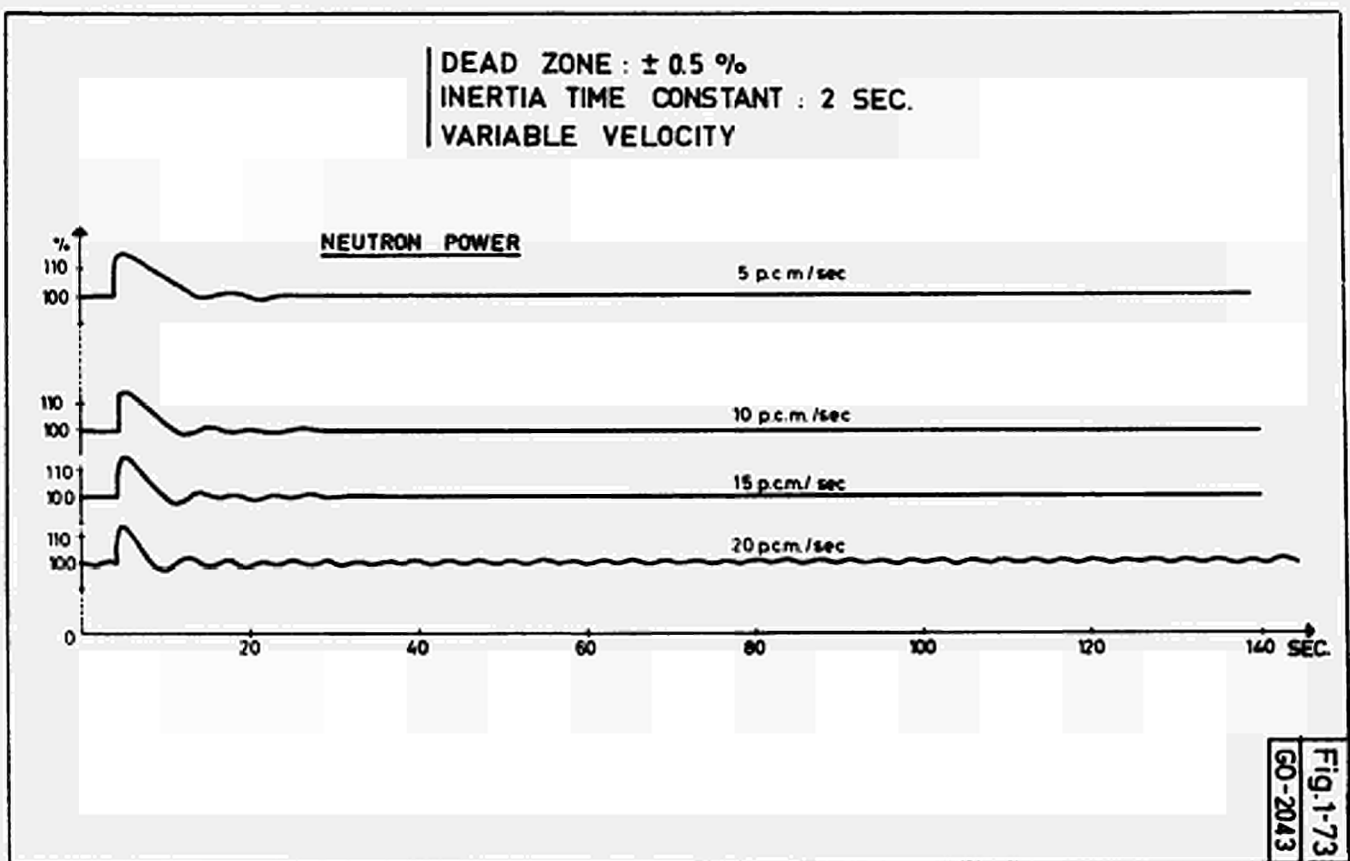
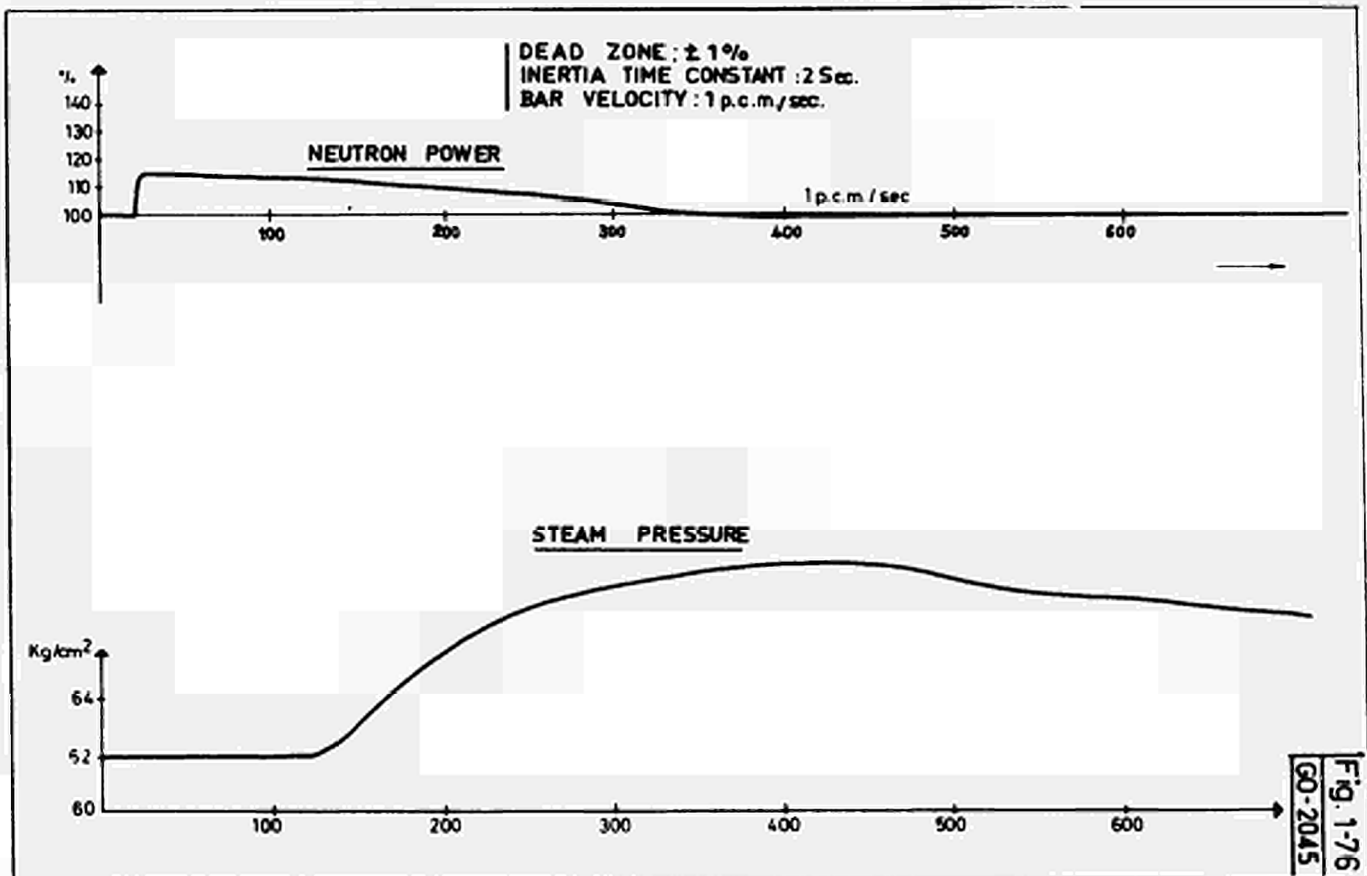
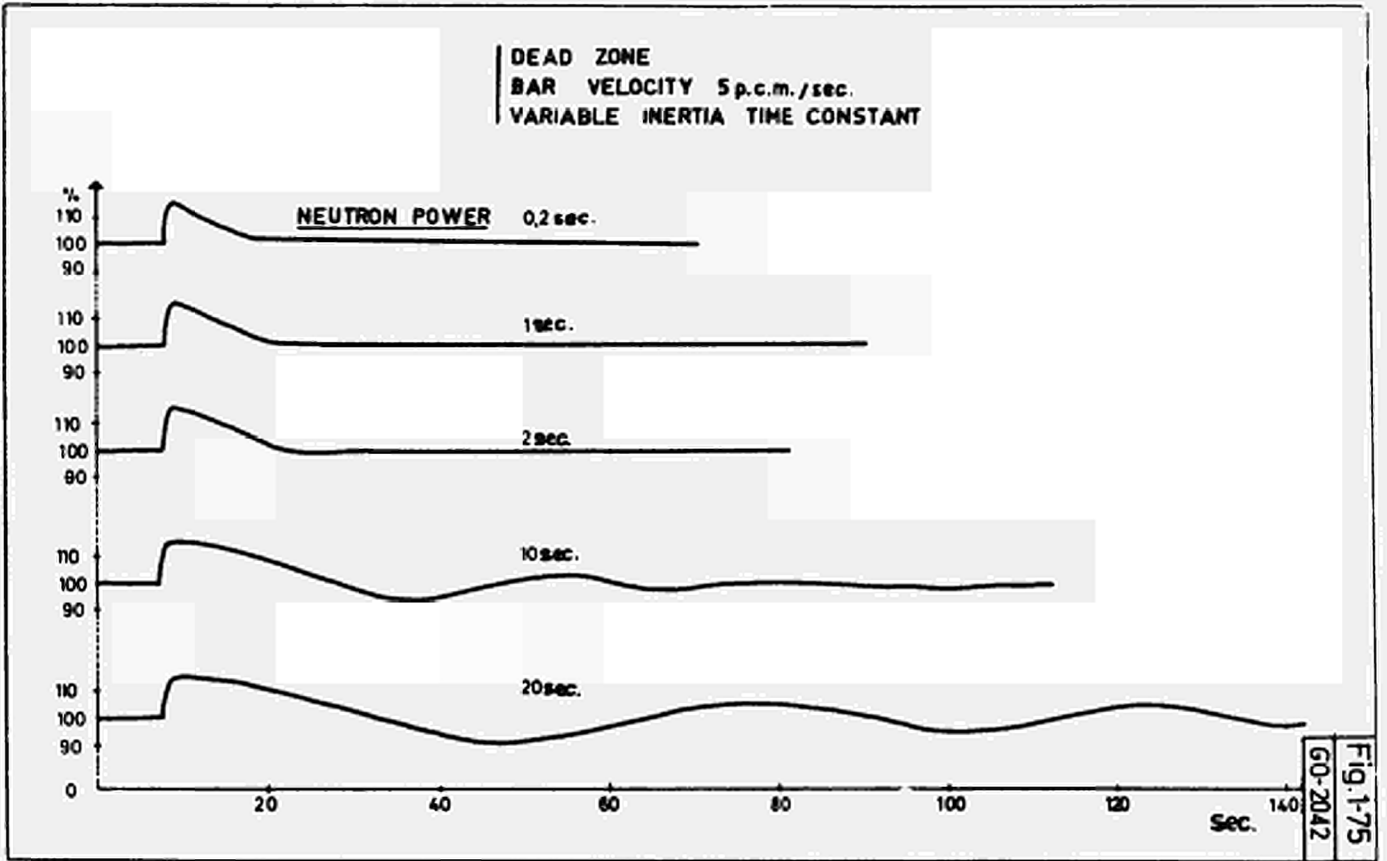
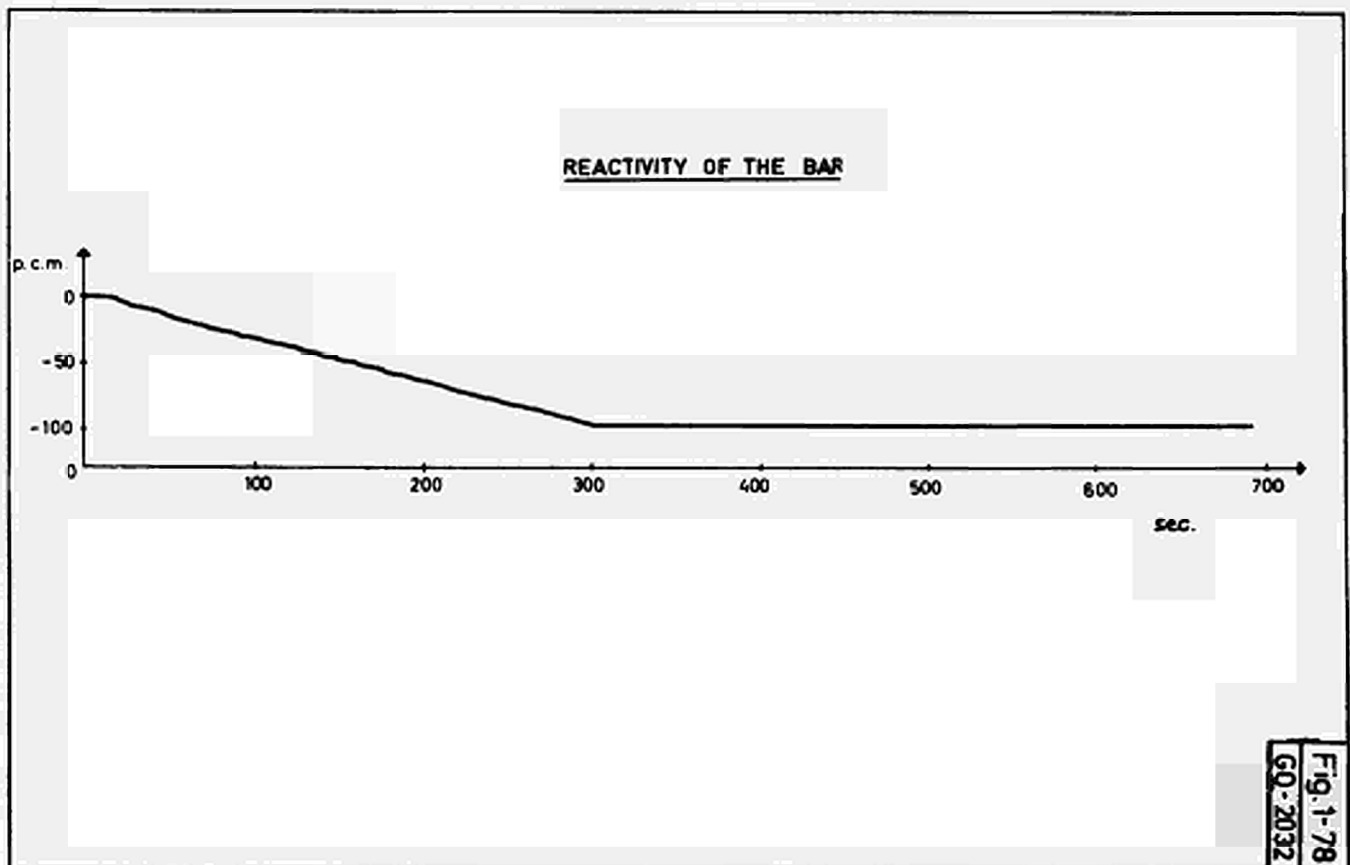
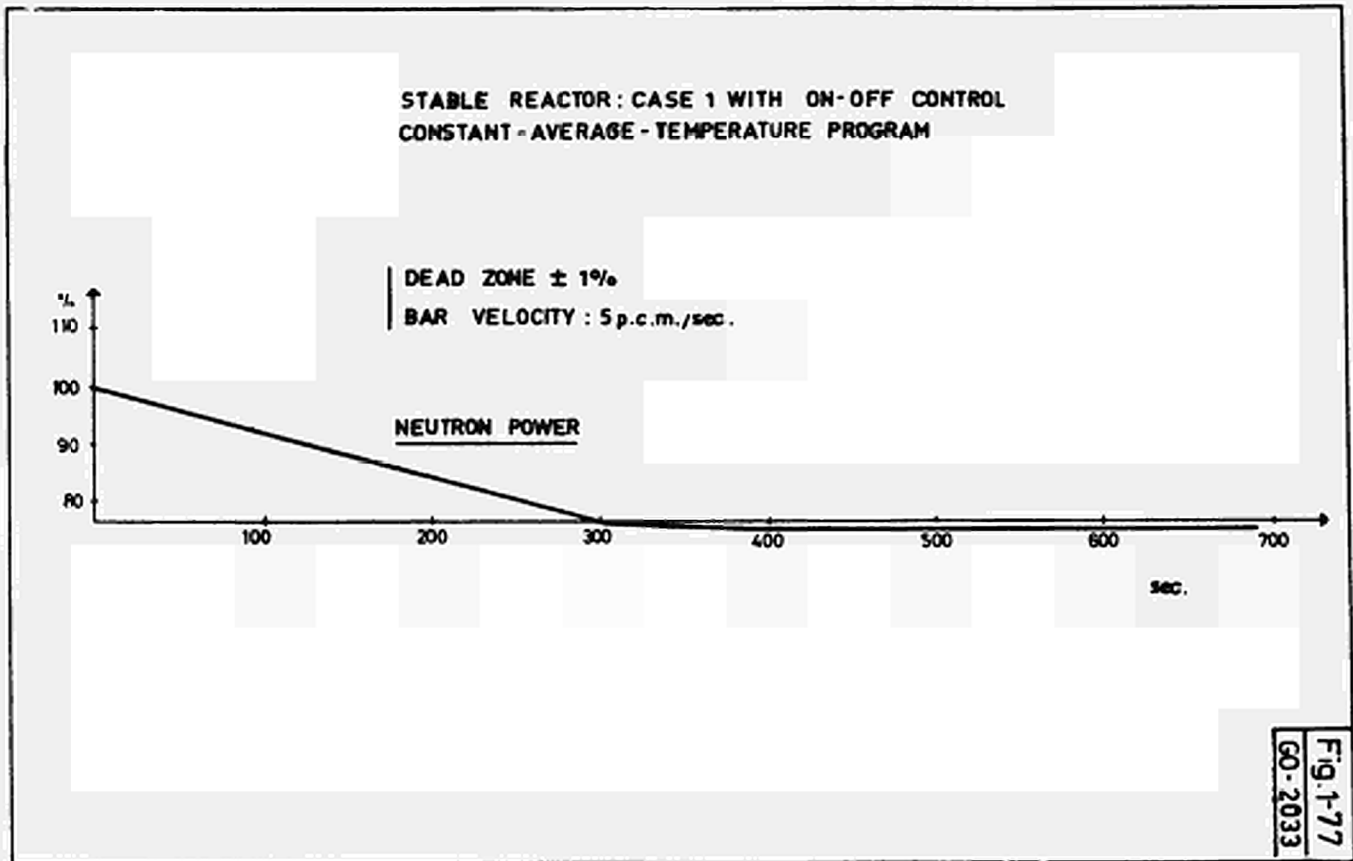
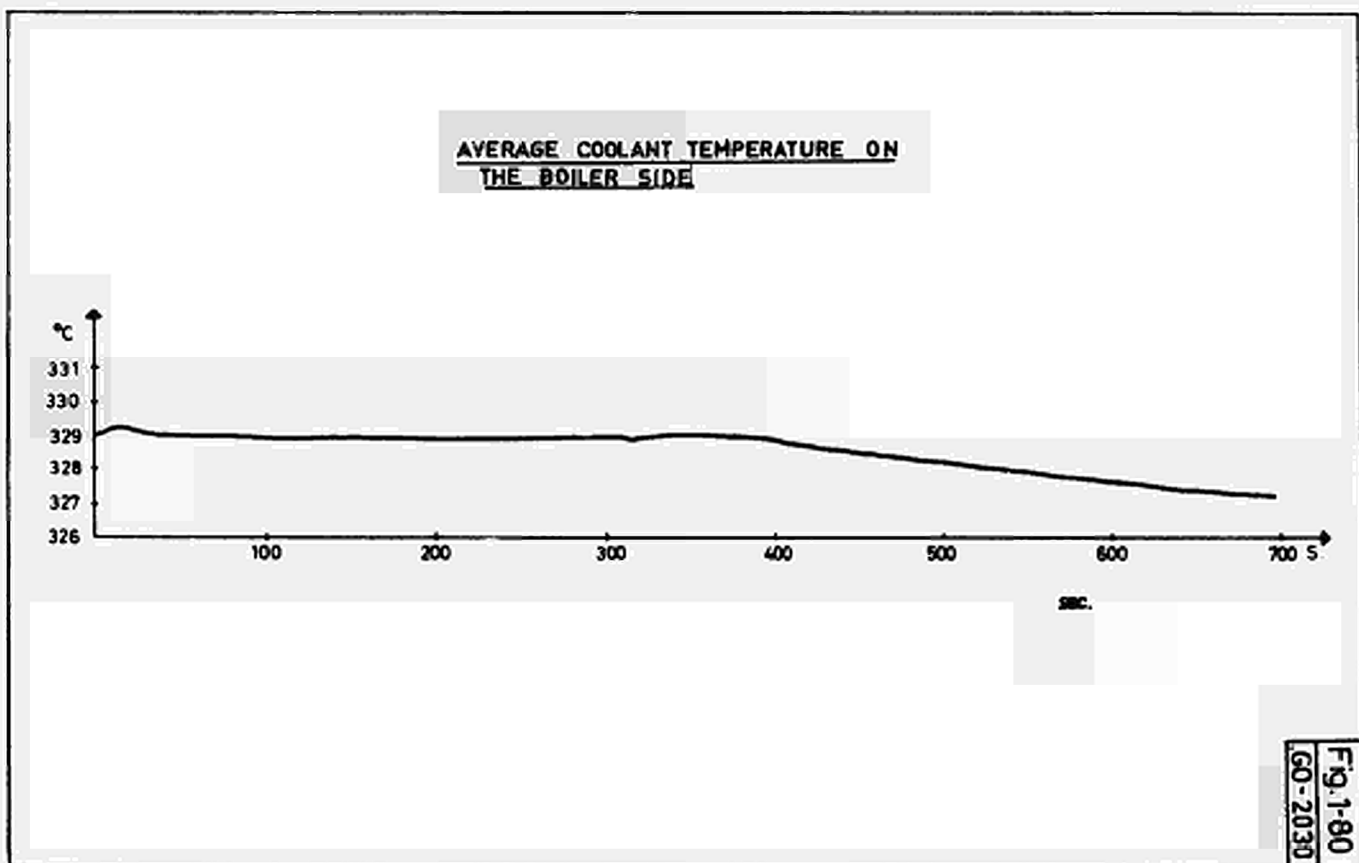
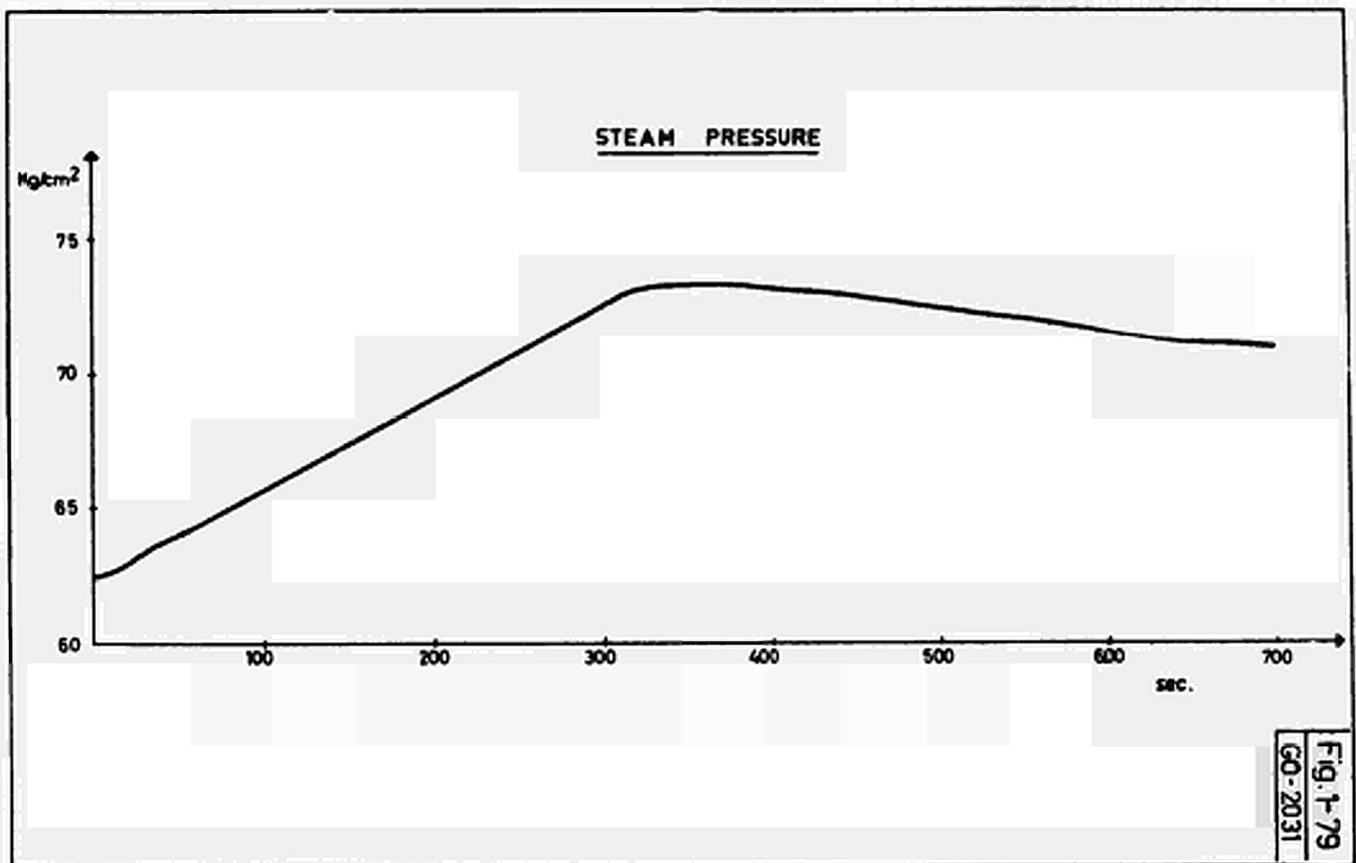


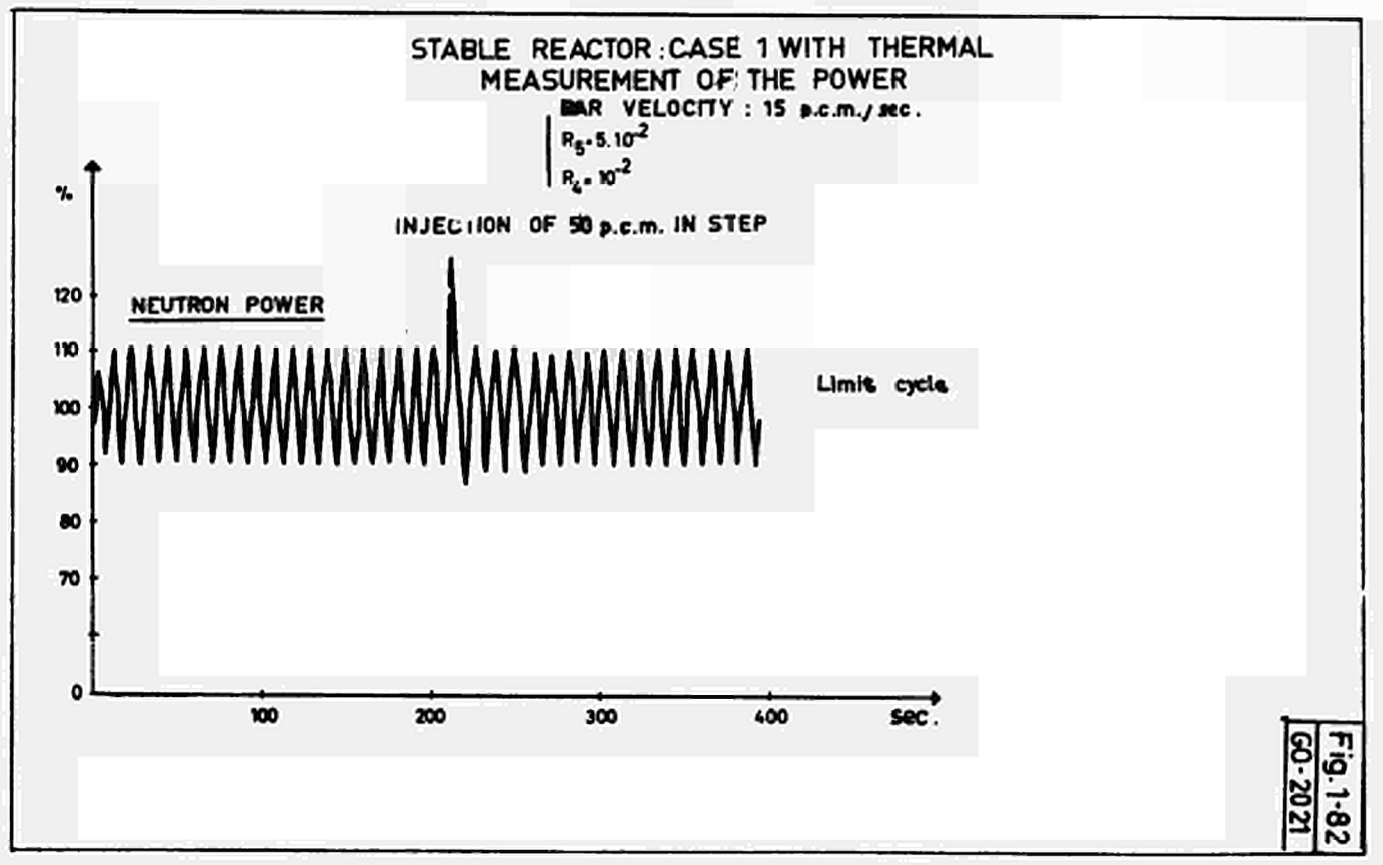
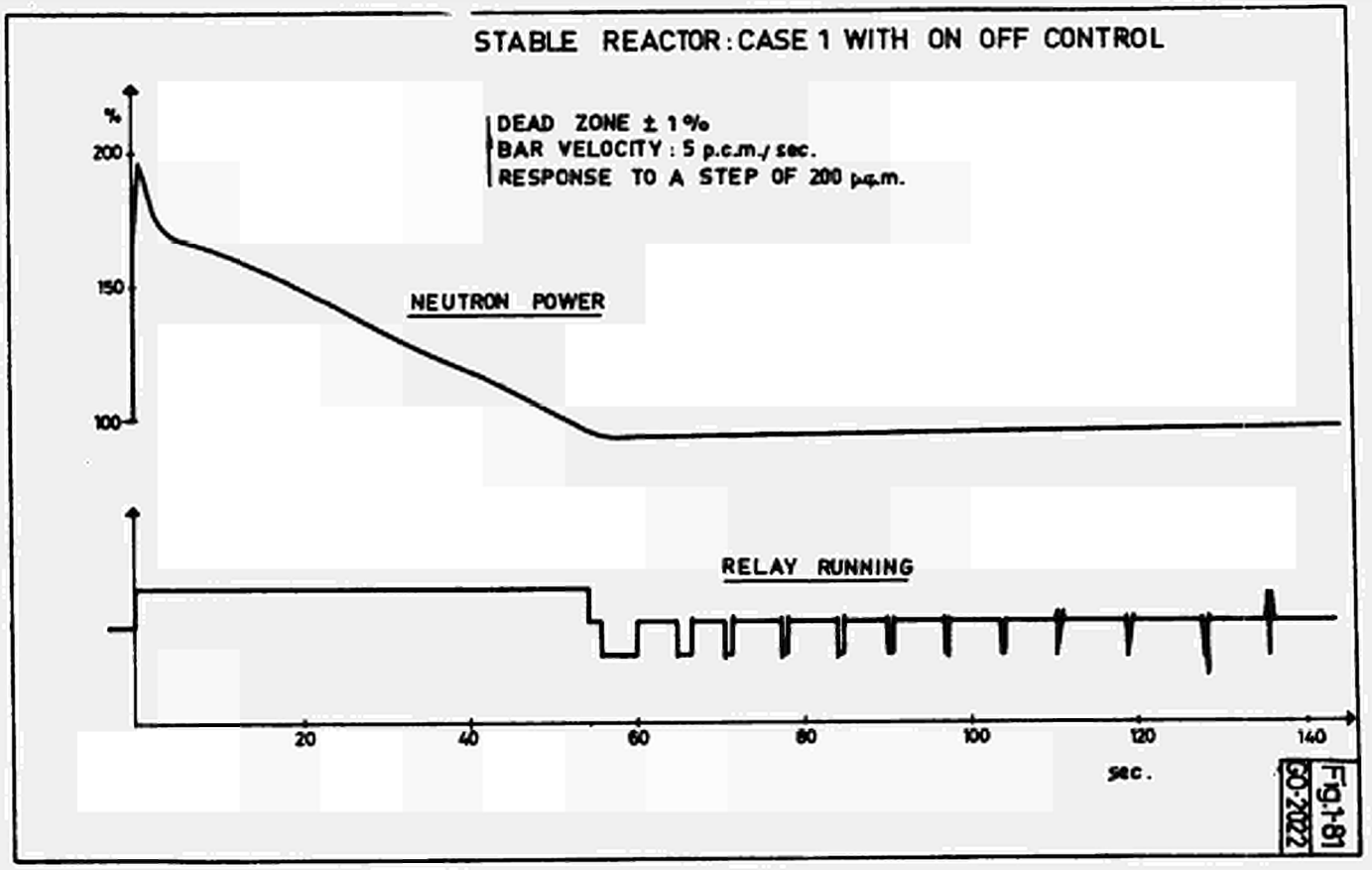
Fig.1-72
GO-2041











RESPONSE TO 50 p.c.m. IN STEP
 BAR VELOCITY : 5 p.c.m./sec. (optimum)
 DELAY IN THE TEMPERATURE MEASURE : 4 sec.

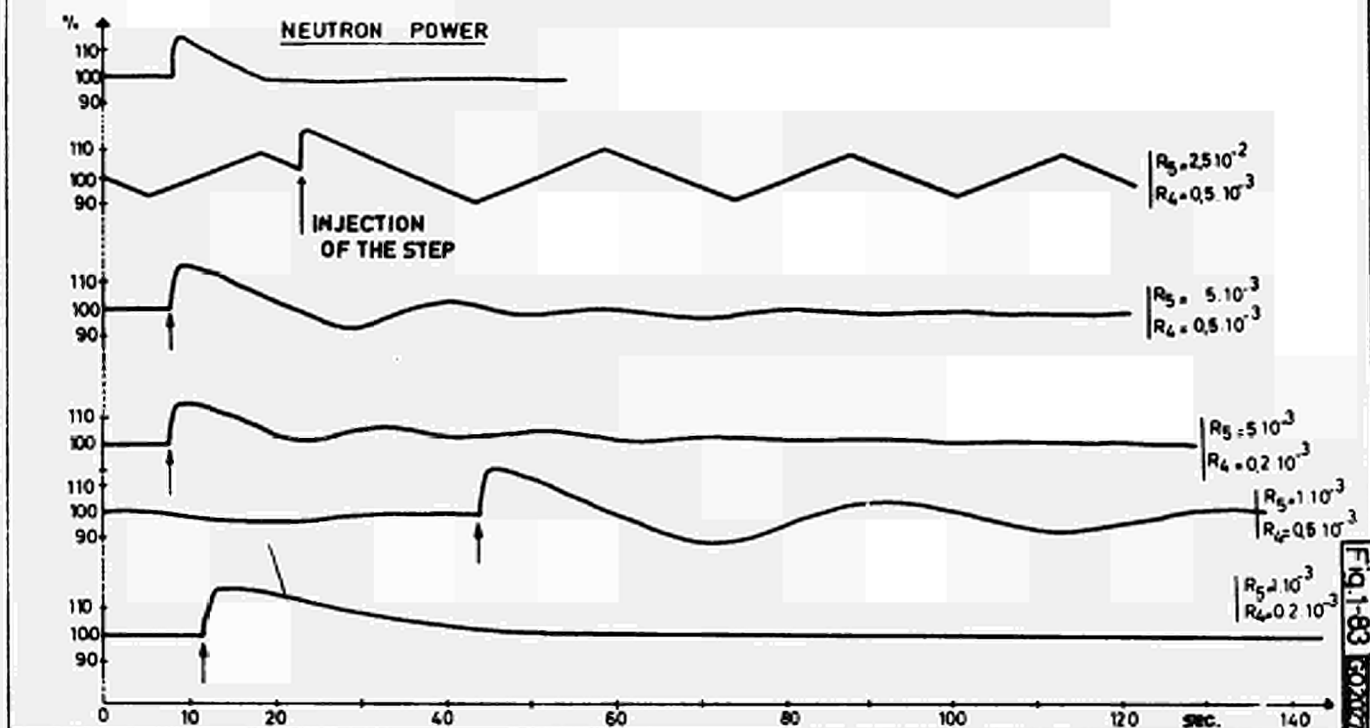


Fig. 1-83

STABLE REACTOR : CASE 1. CONTROL LOSS WITH
 INJECTION OF 50 p.c.m. IN STEP, WITHOUT RECOVERY
 BUT WITH STEAM DISCHARGE AT 80 Kg/cm²

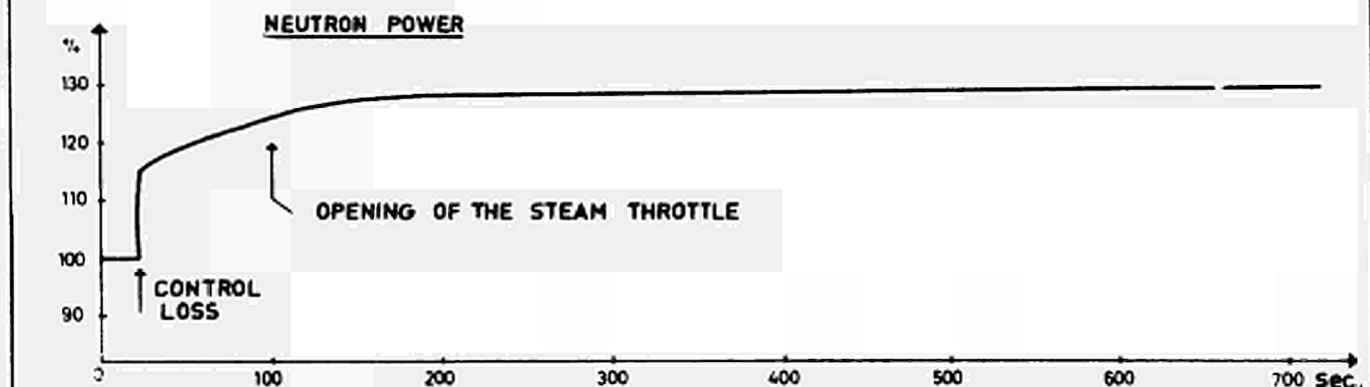
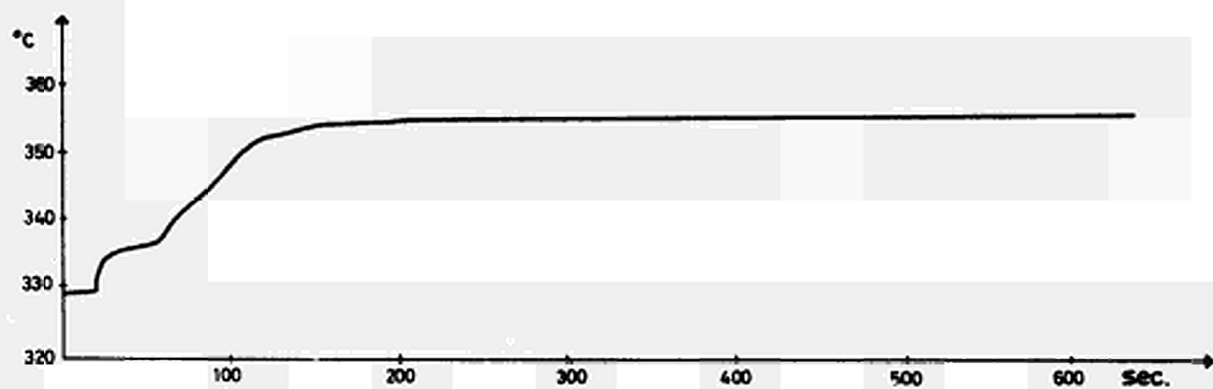
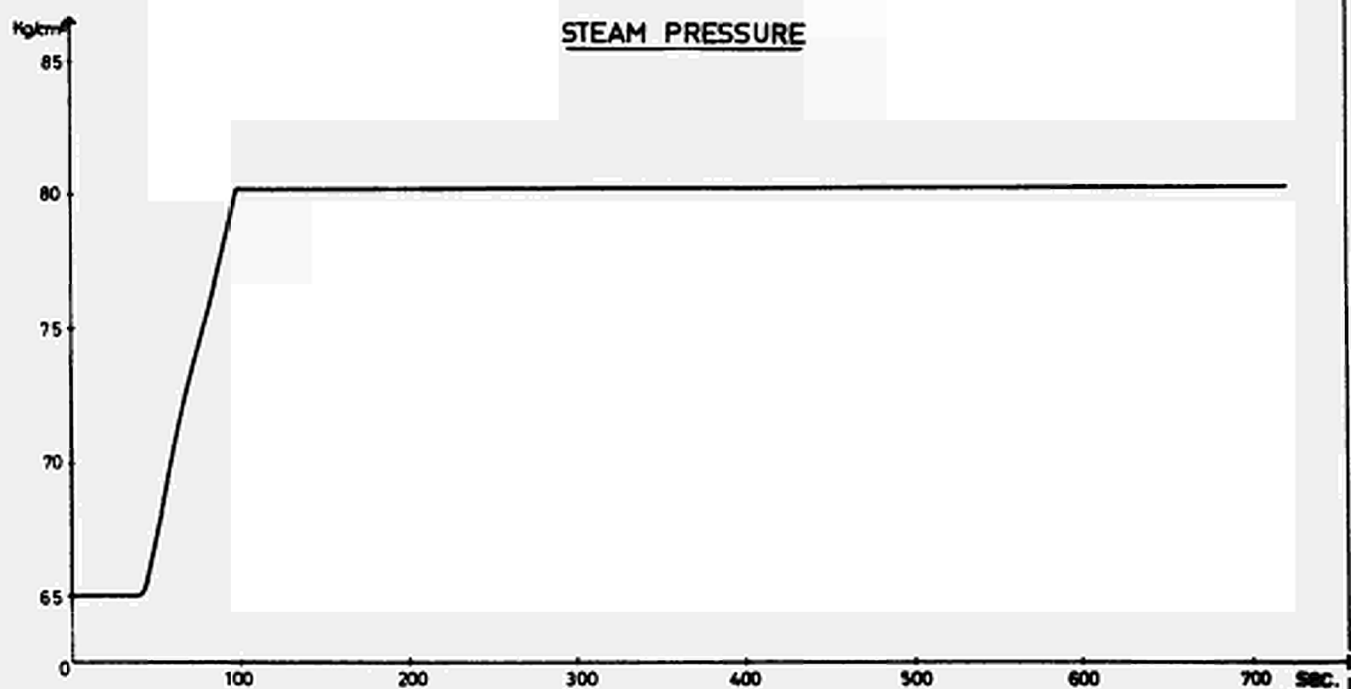
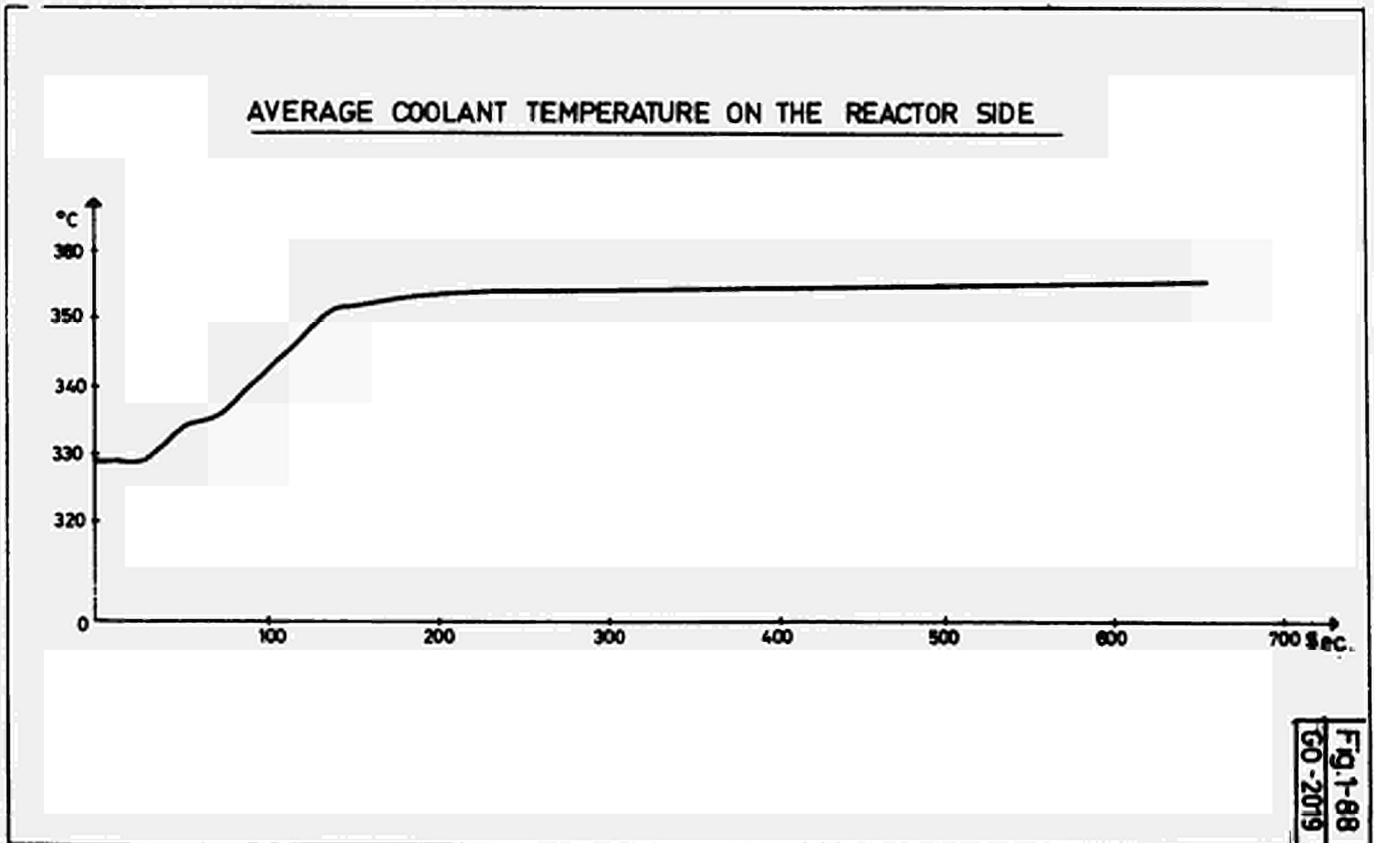
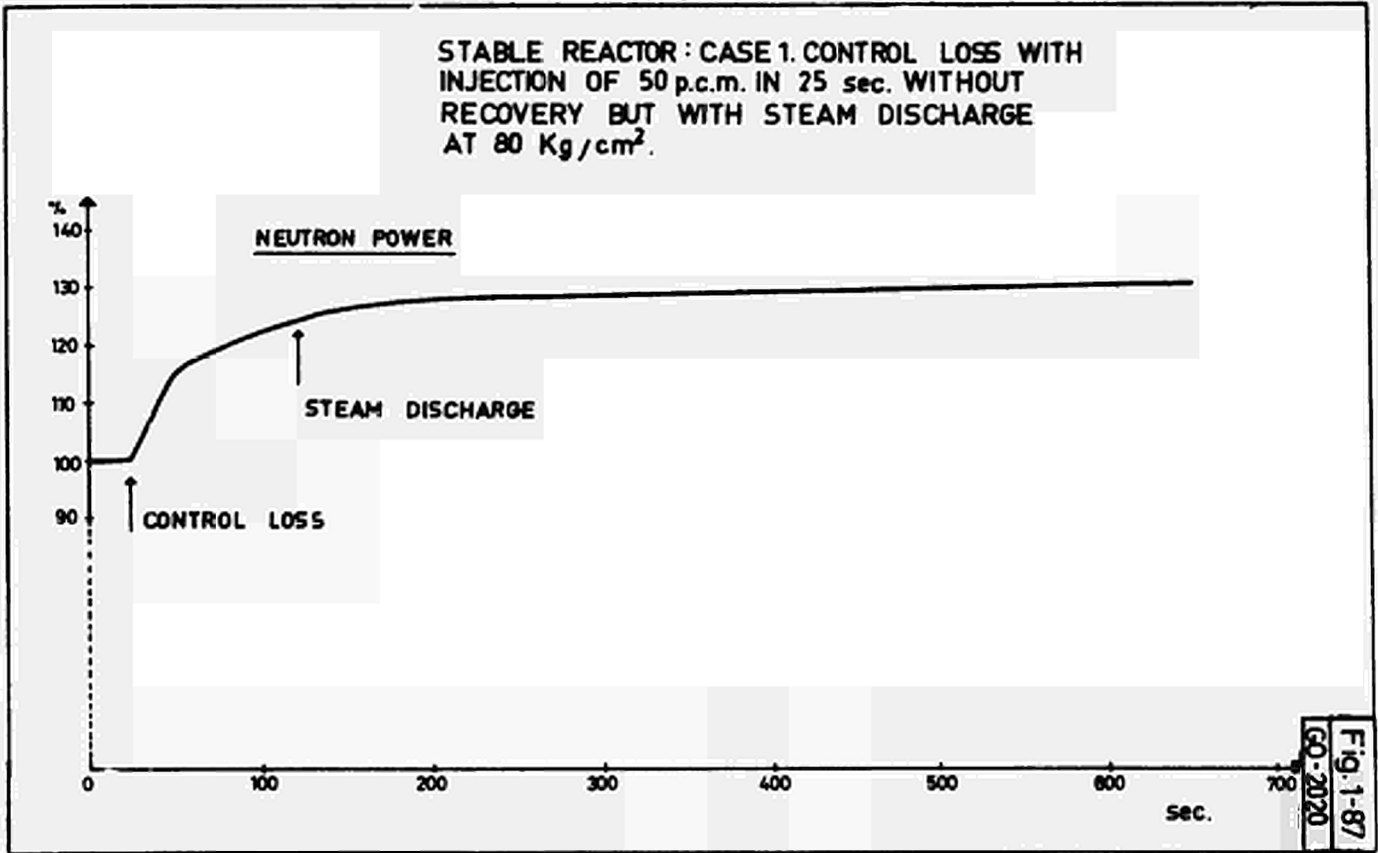
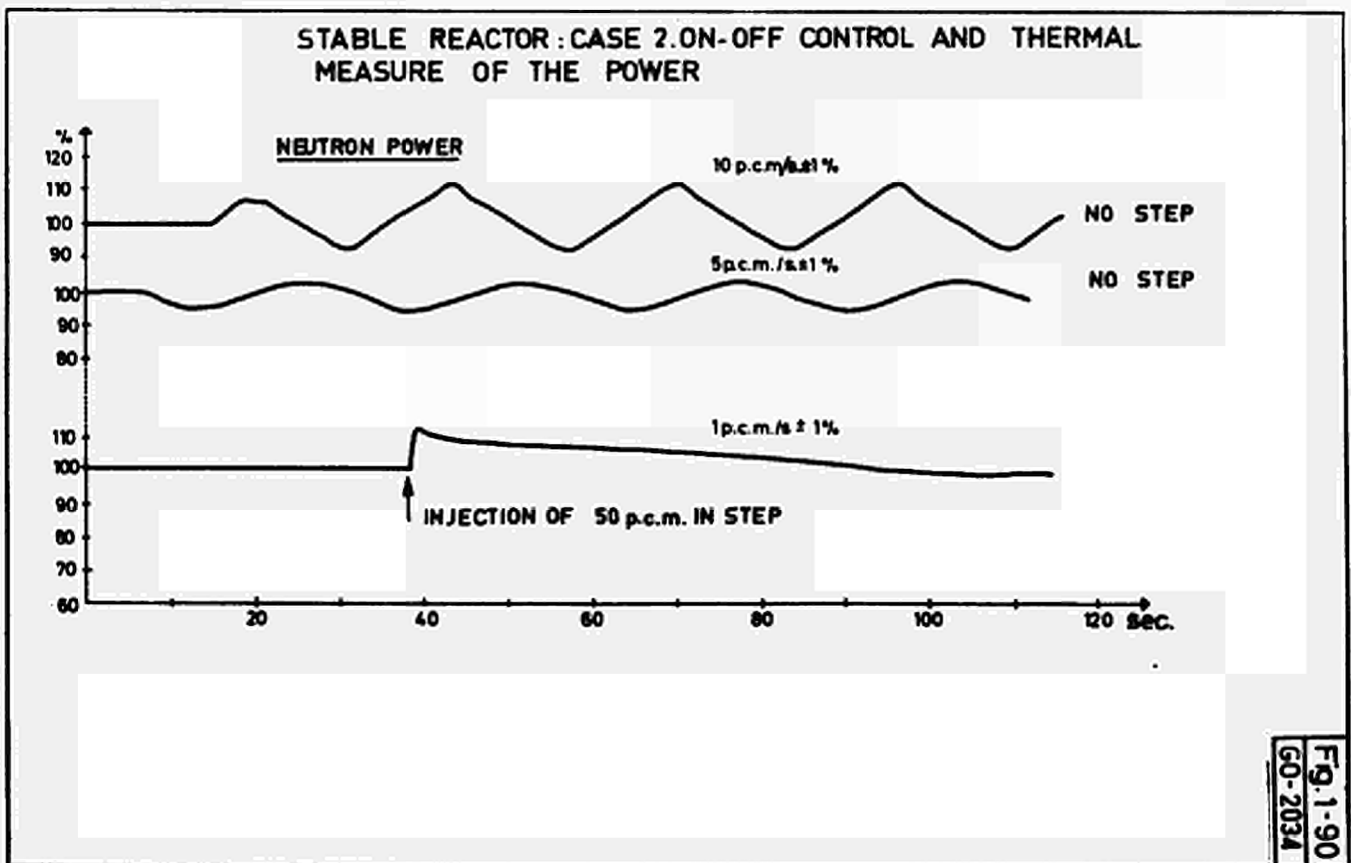
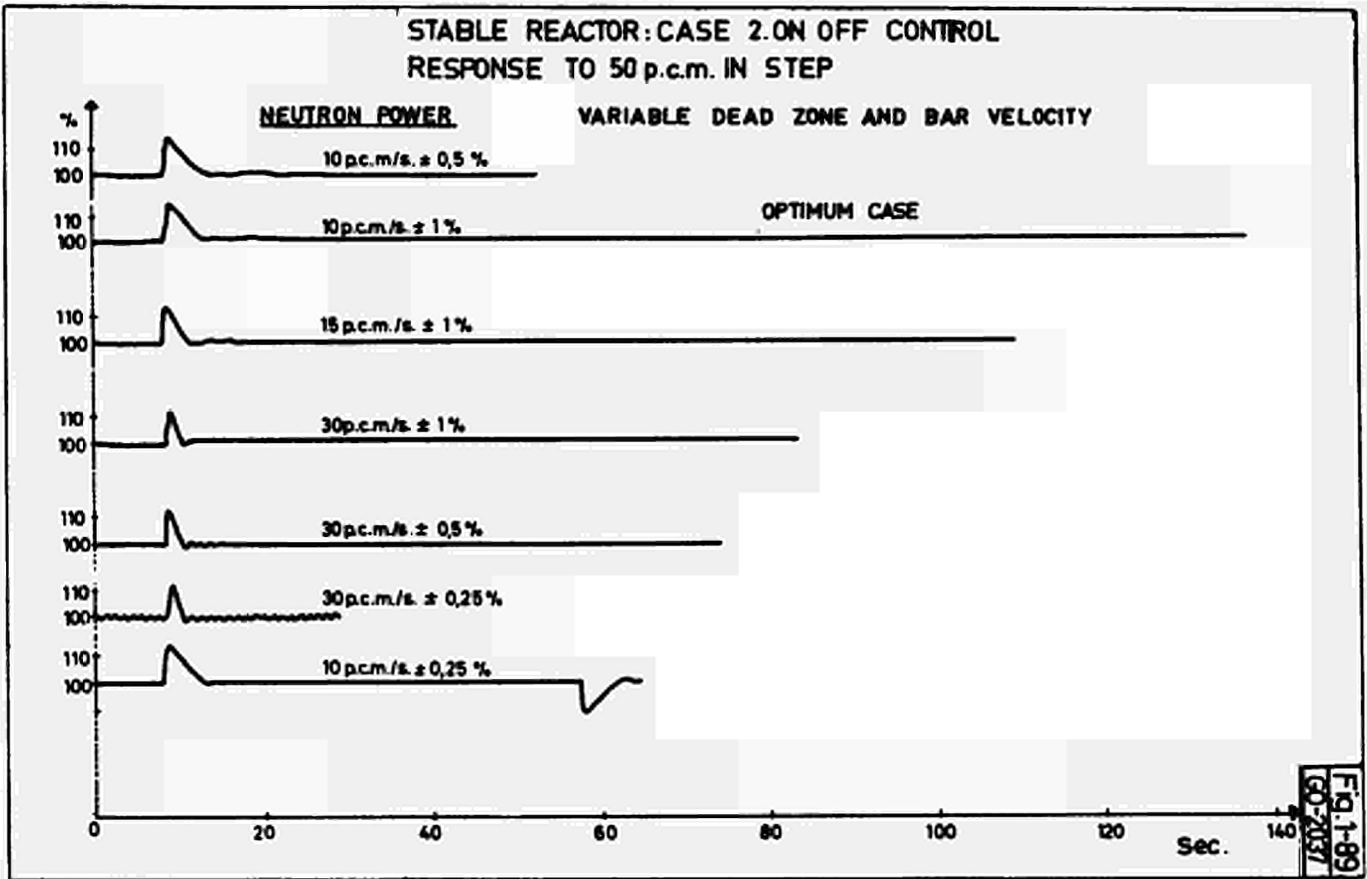


Fig. 1-84
 GO-2029

AVERAGE COOLANT TEMPERATURE ON THE REACTOR-SIDEFig. 1-85
GO-2028STEAM PRESSUREFig. 1-86
GO-2028





POWER CHANGE FROM 100 TO 75 % (5%/min.)
CONSTANT AVERAGE TEMPERATURE PROGRAM
DEAD ZONE $\pm 1\%$
BAR VELOCITY : 1 p.c.m. / sec.

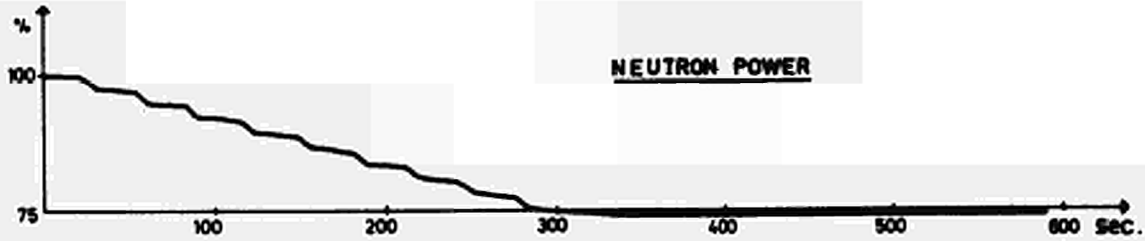


Fig. 1-91
GO-2035

AVERAGE COOLANT TEMPERATURE ON THE BOILER SIDE

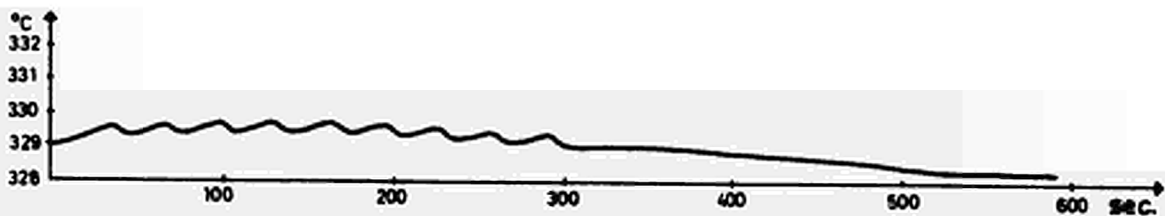
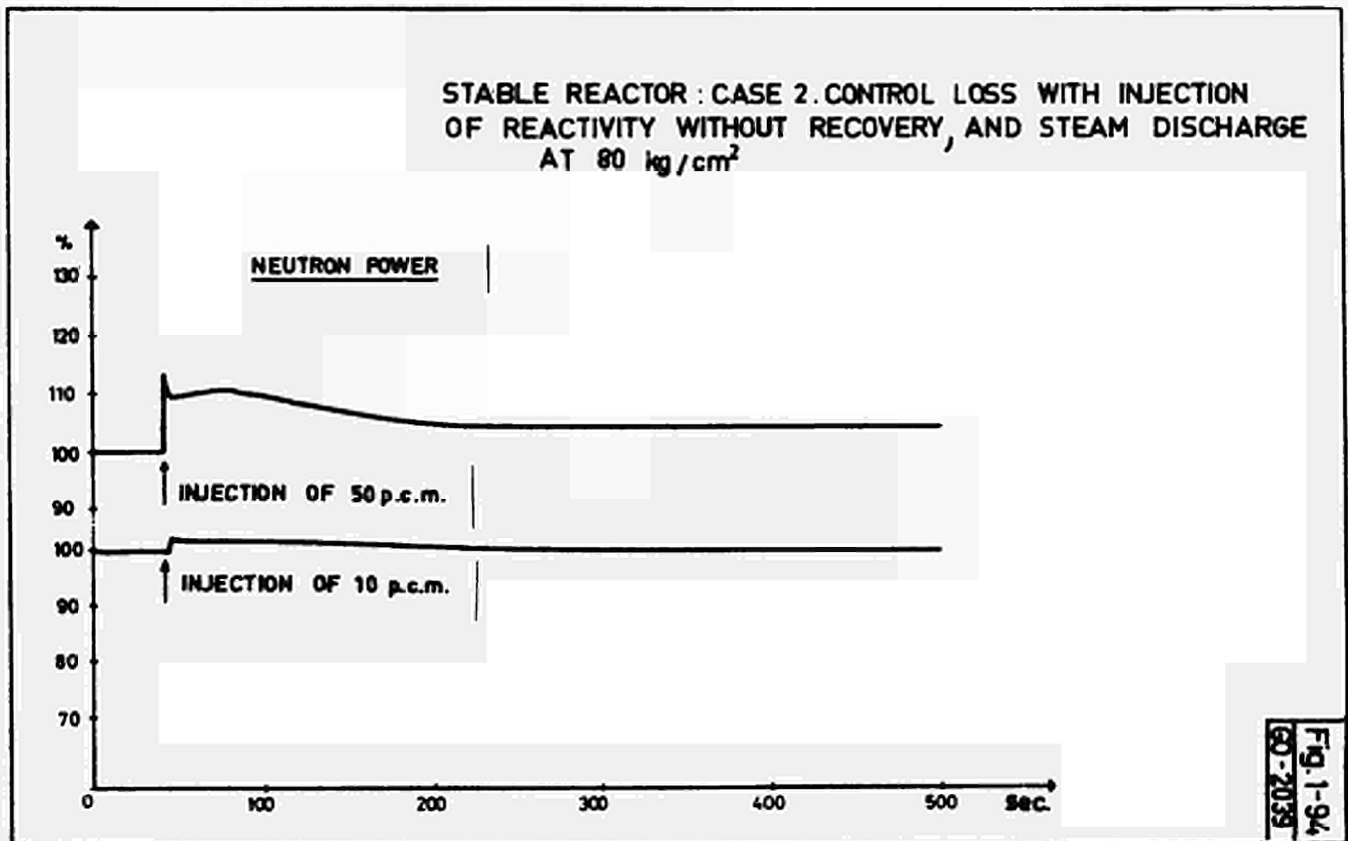
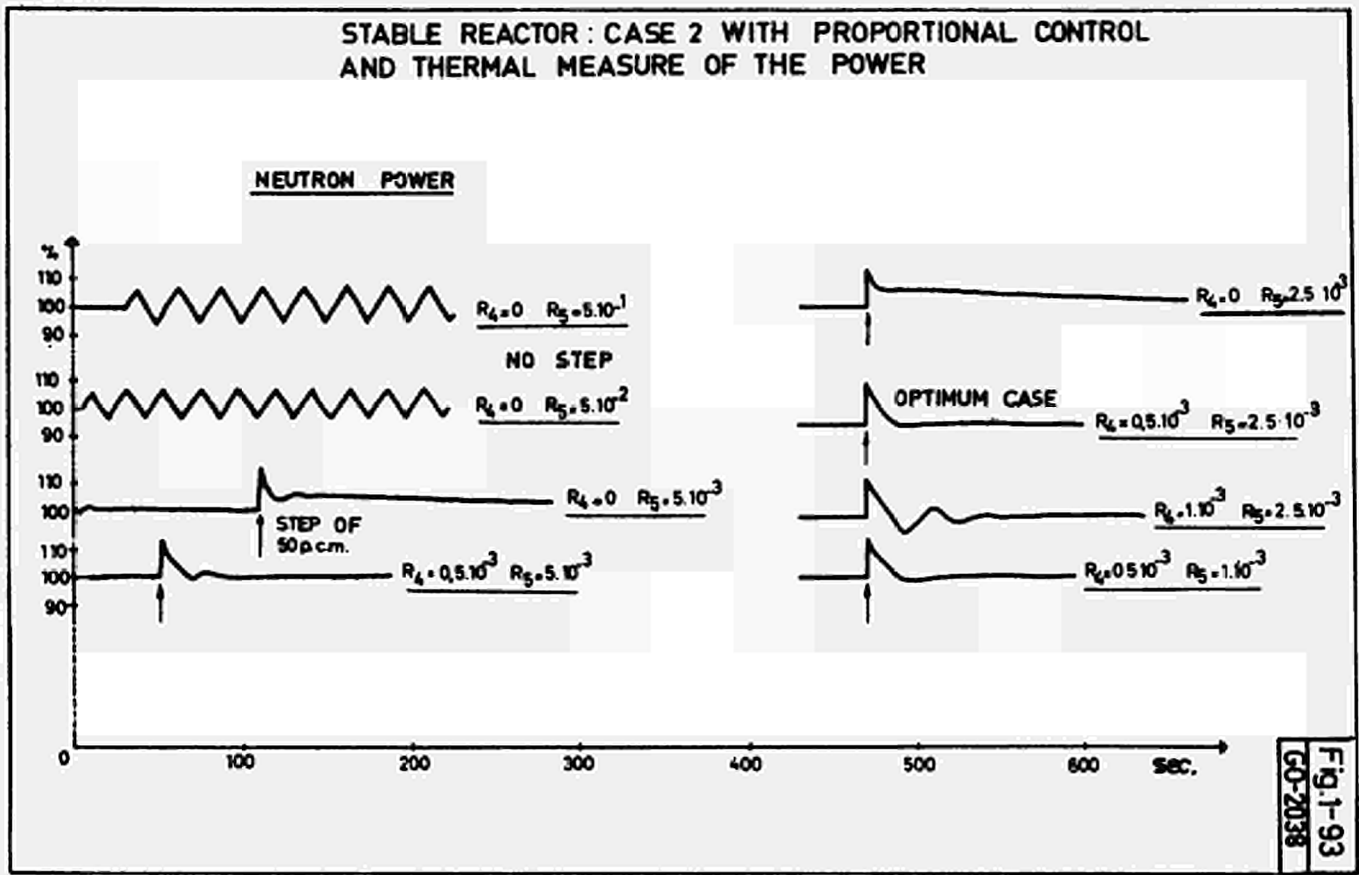
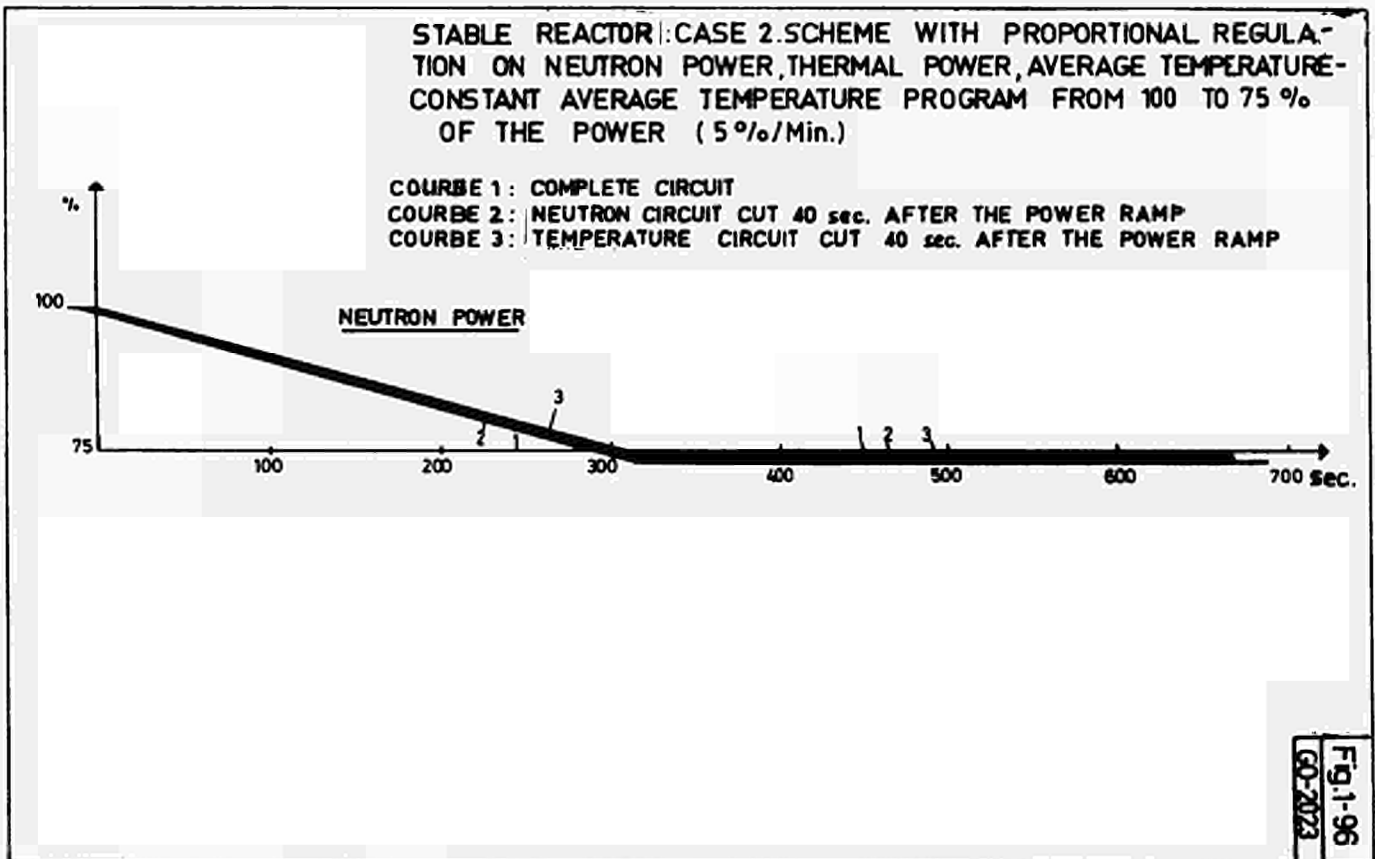
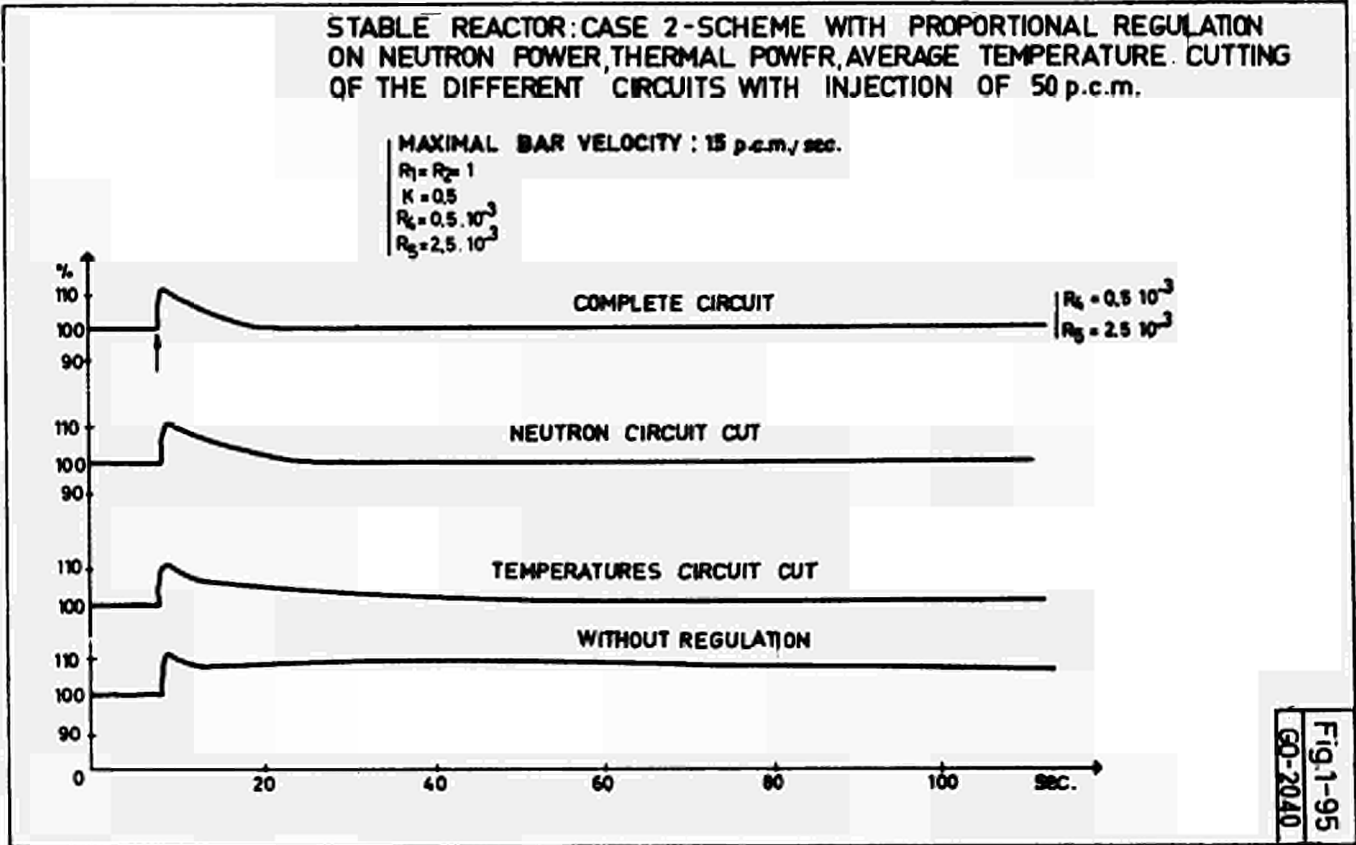


Fig. 1-92
GO-2036





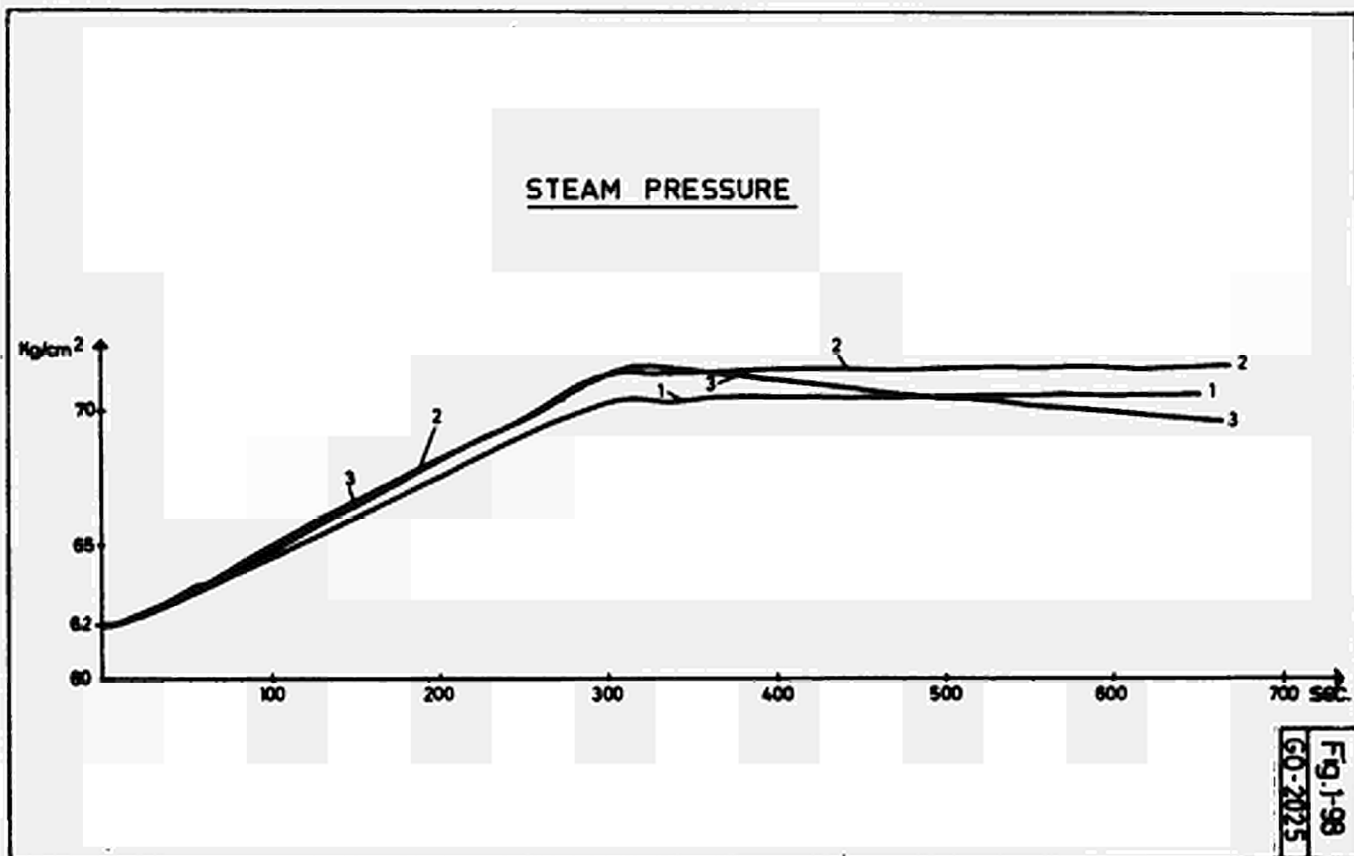
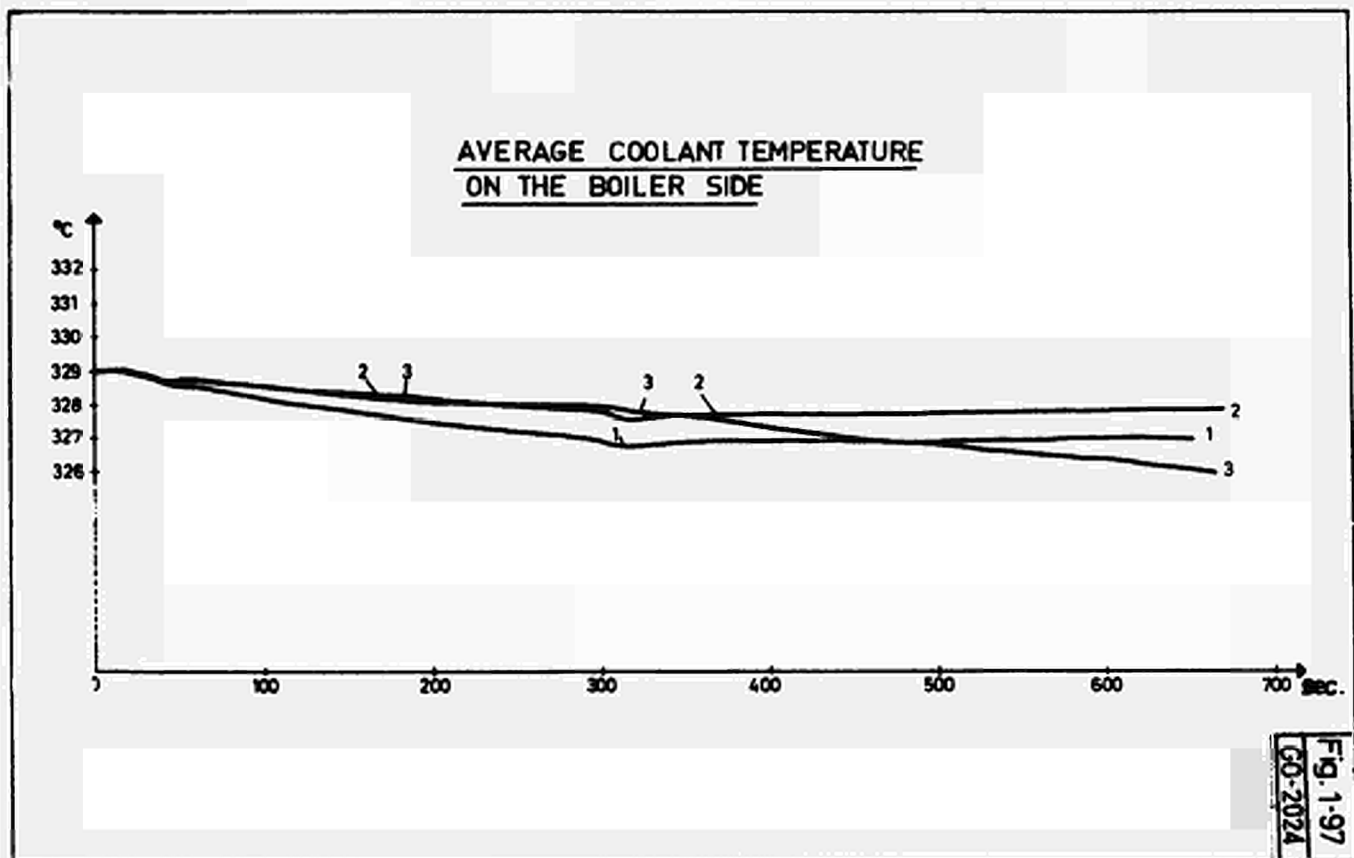


FIG. 2-1

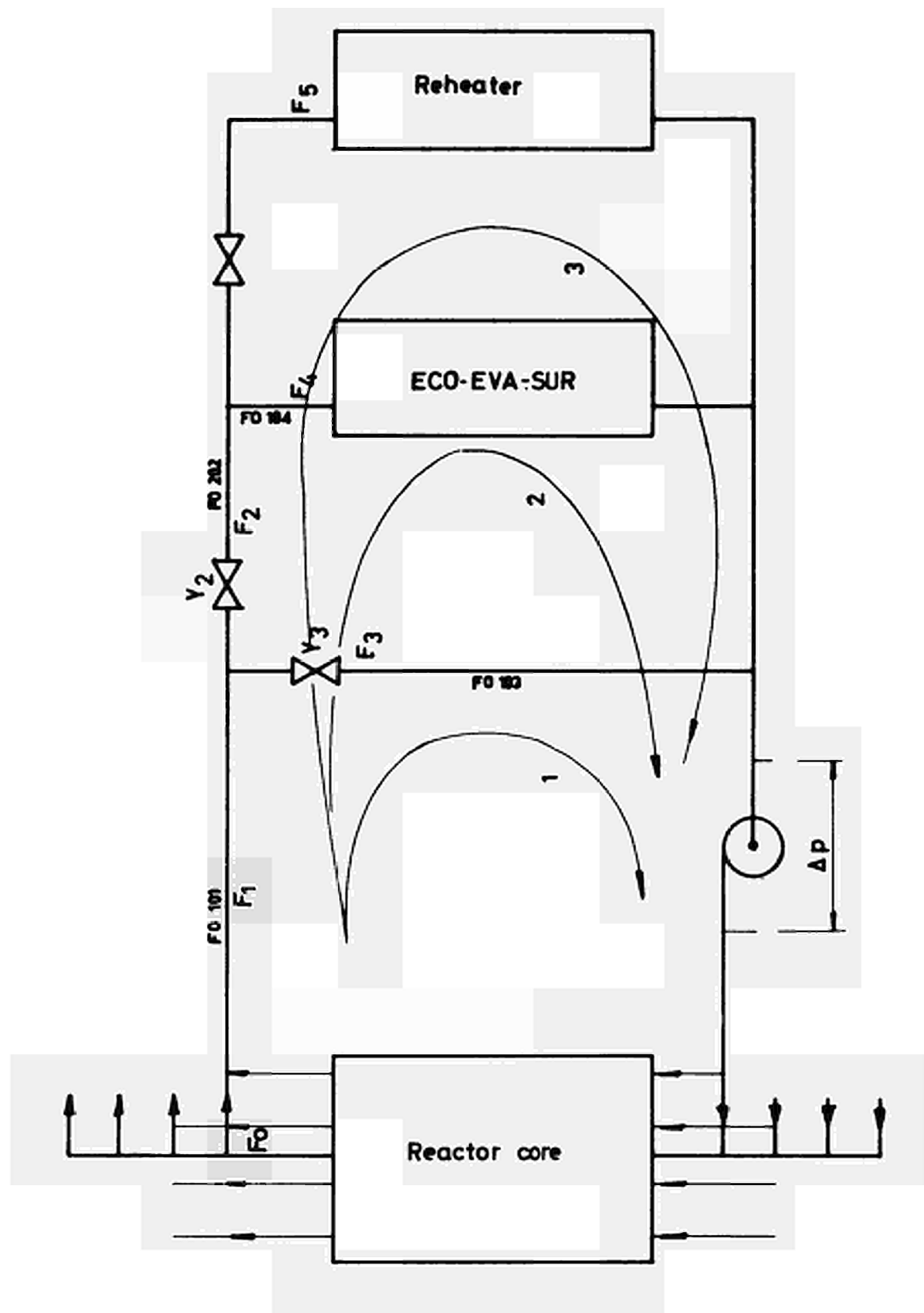


FIG 2-2

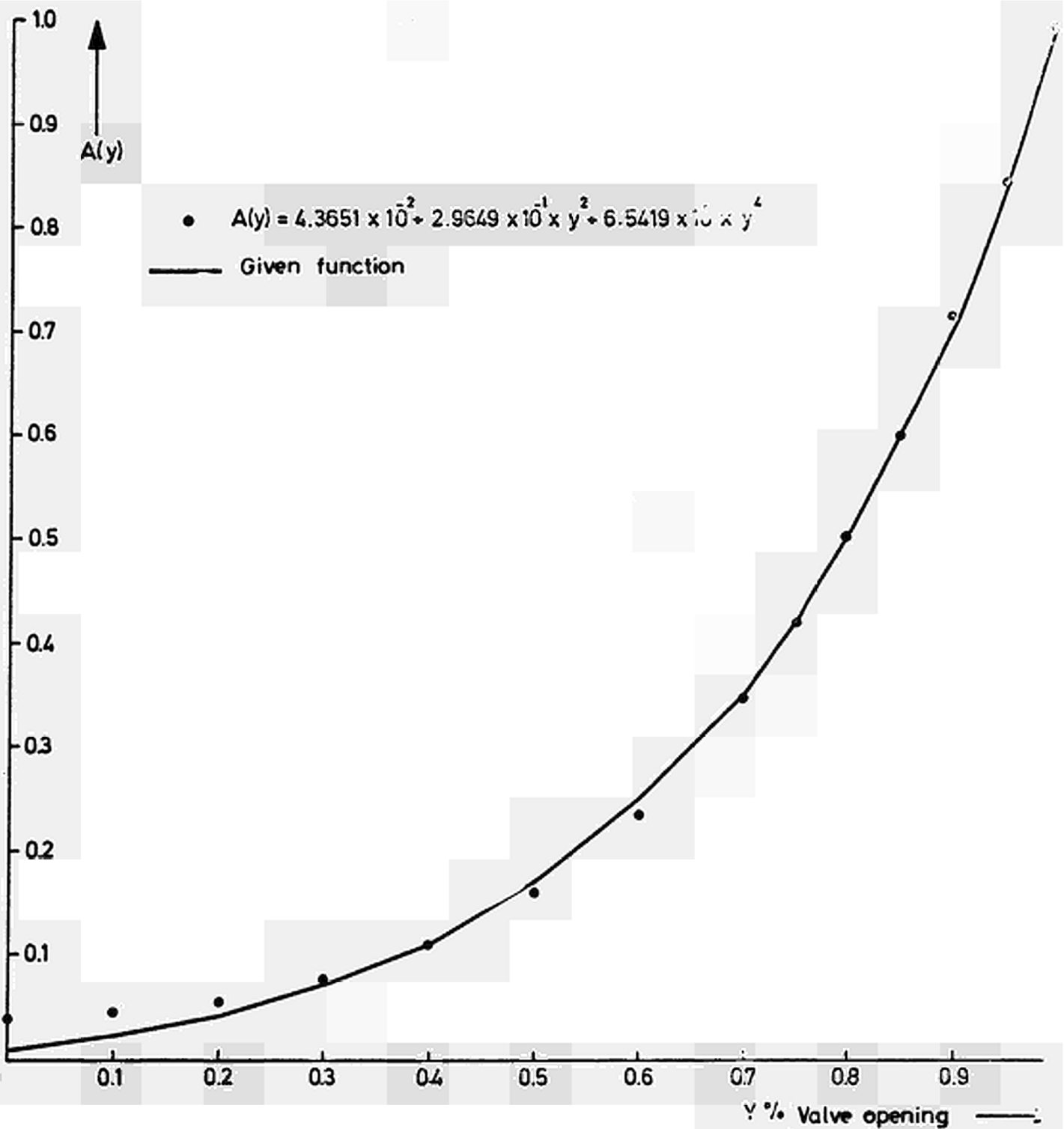
Characteristics of the primary valves

FIG 2-3

Characteristics of the primary pumps

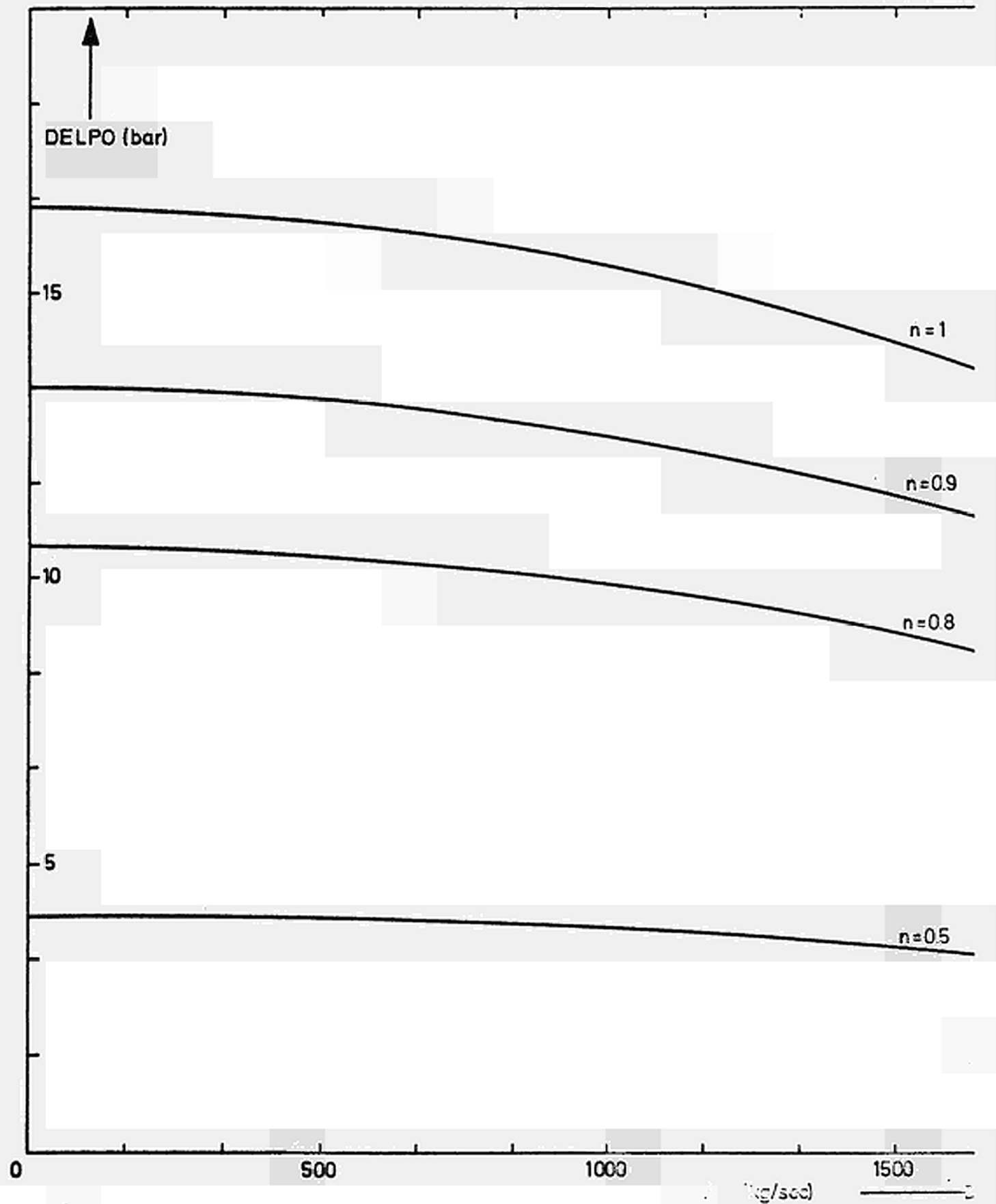


FIG. 2-4

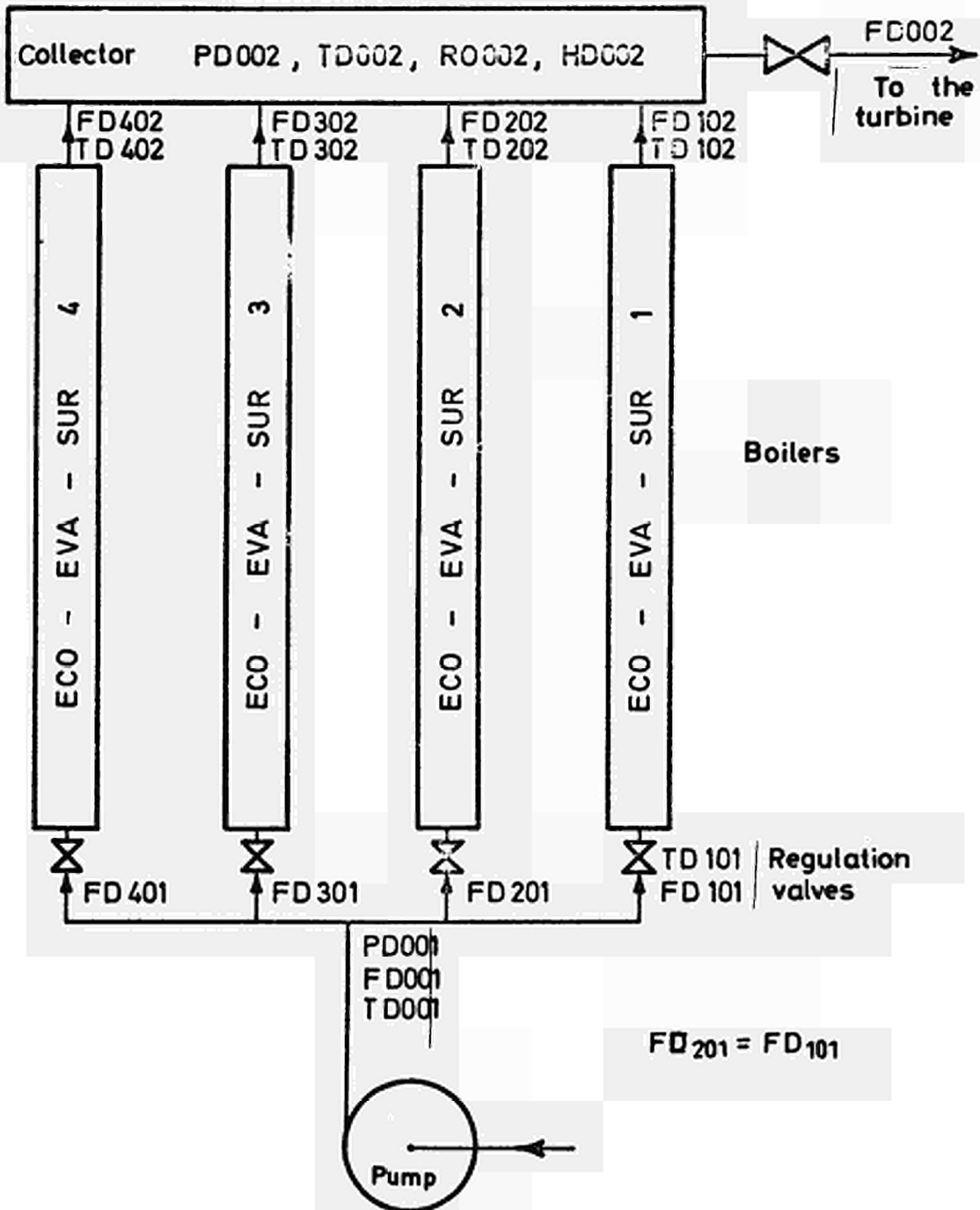


FIG. 2-5

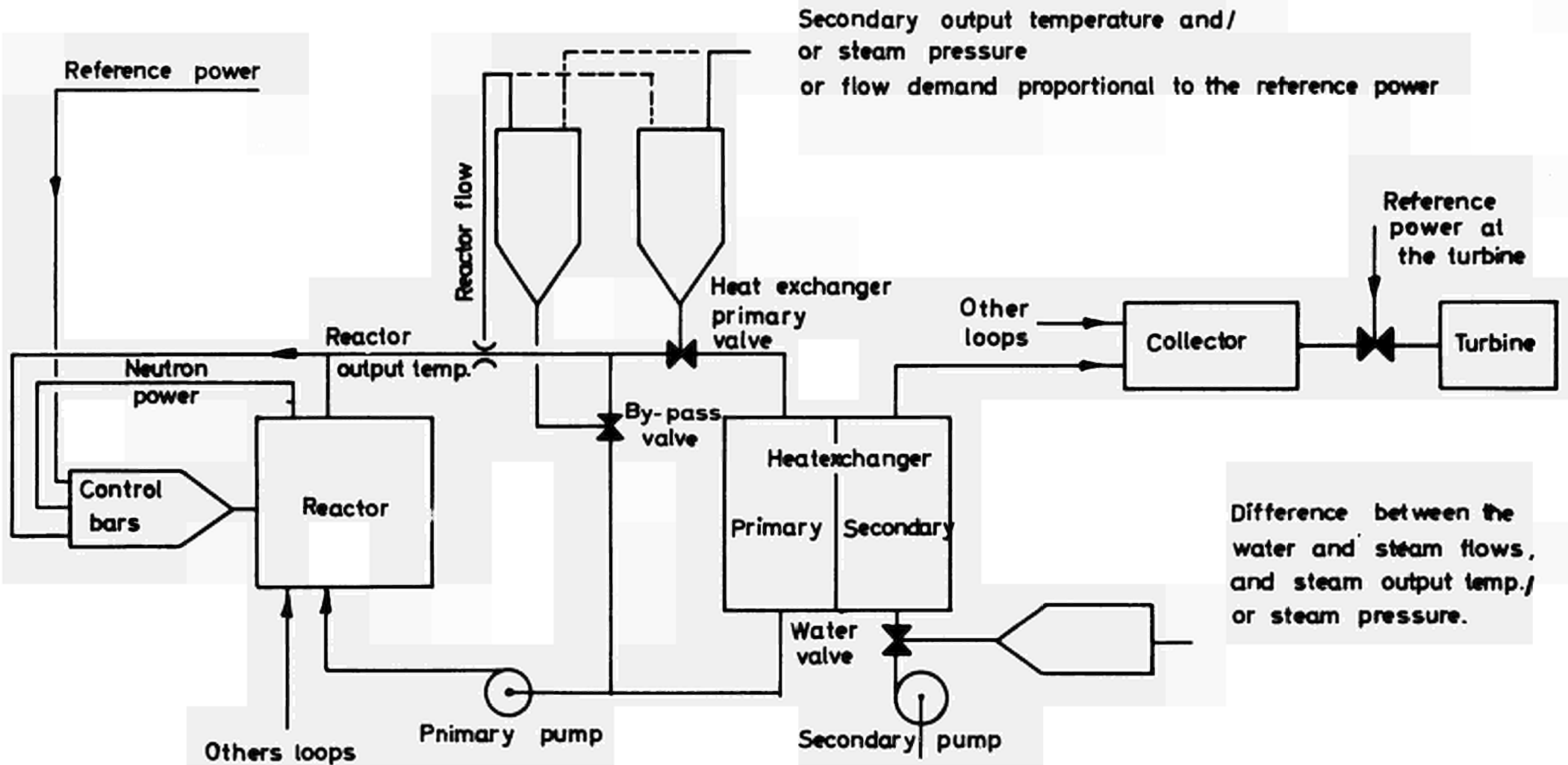


FIG 2-6

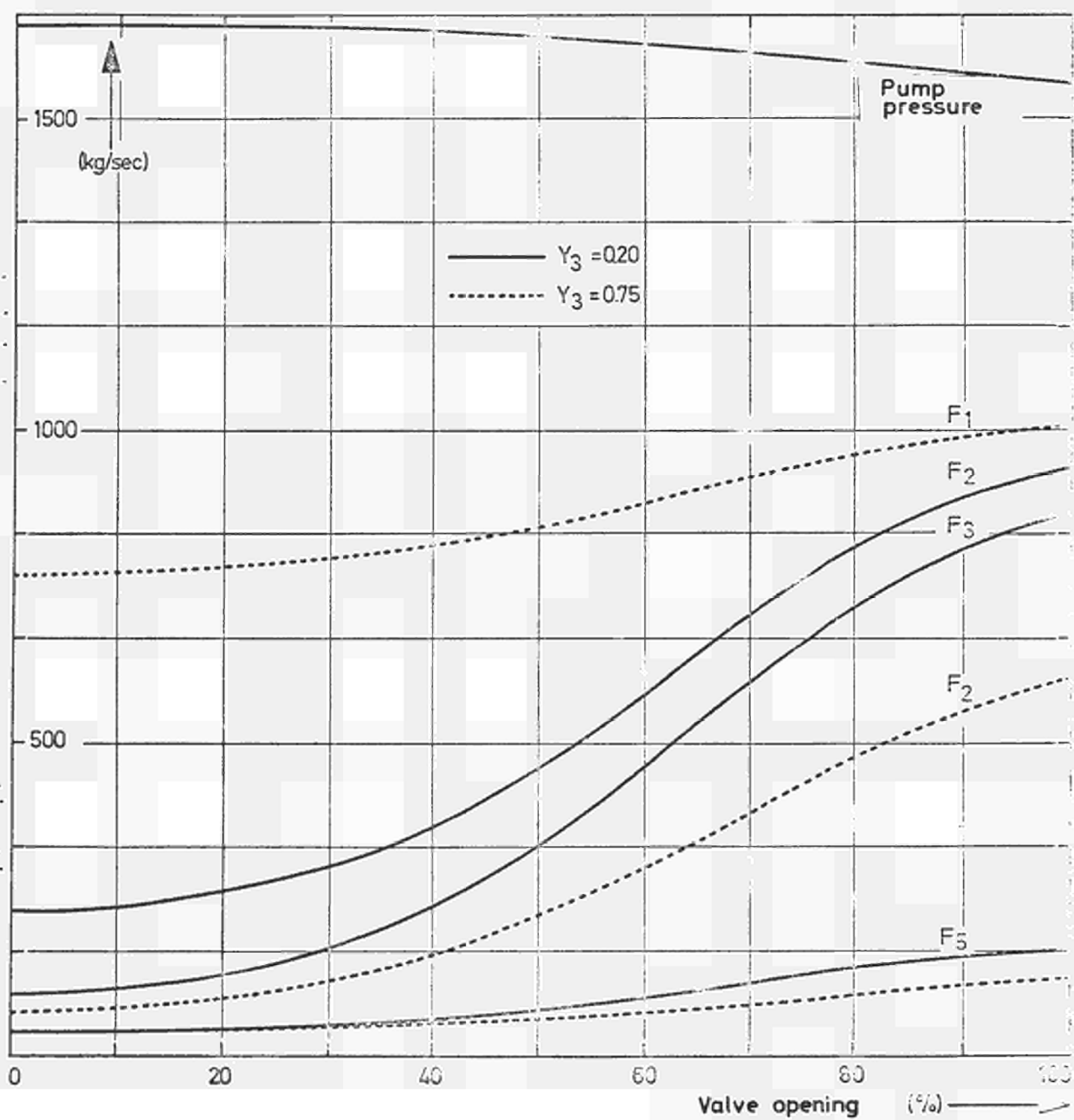
F₁ F₂ F₃ as function of Y₂

FIG. 2-7

Position of Y_3 vs Y_2 for F_1 constant
 F_1 is constant Y_5 completely open

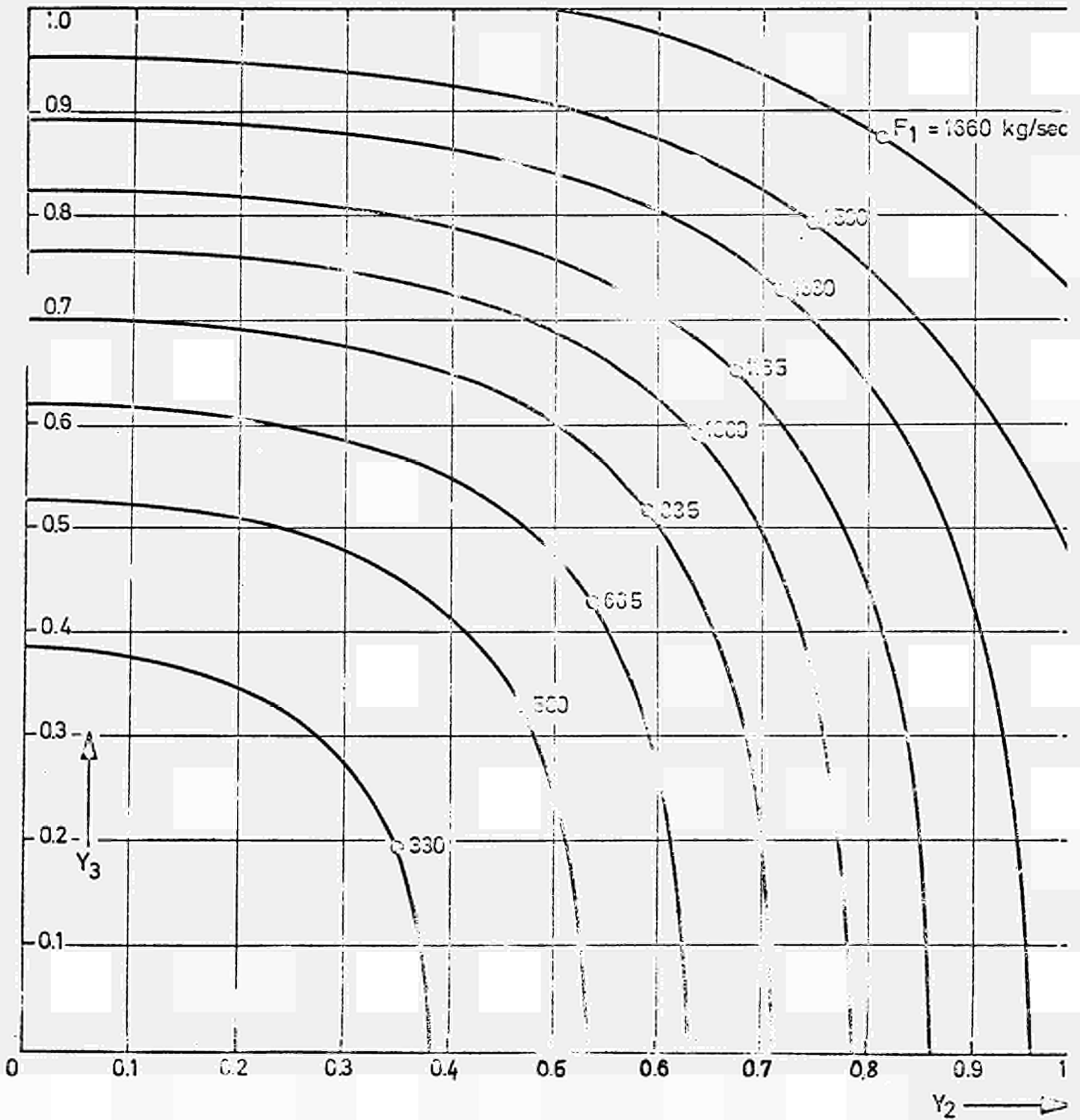


FIG. 2-8

Flow in the heat exchanger and in the reheater (F_2) as function of the total flow F_1

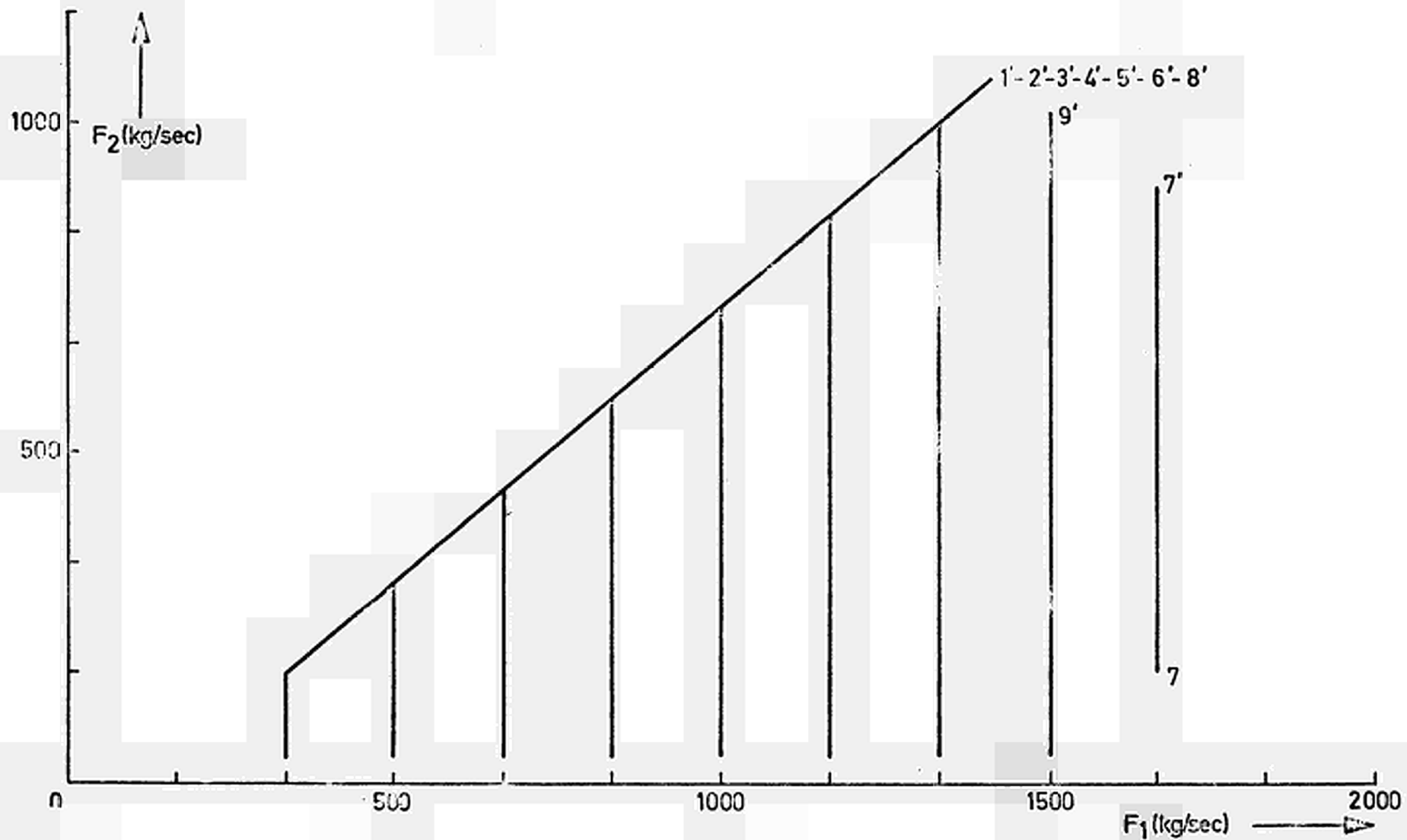


FIG. 2-9

Flow in the reheater (F_5) as function of the total flow F_1

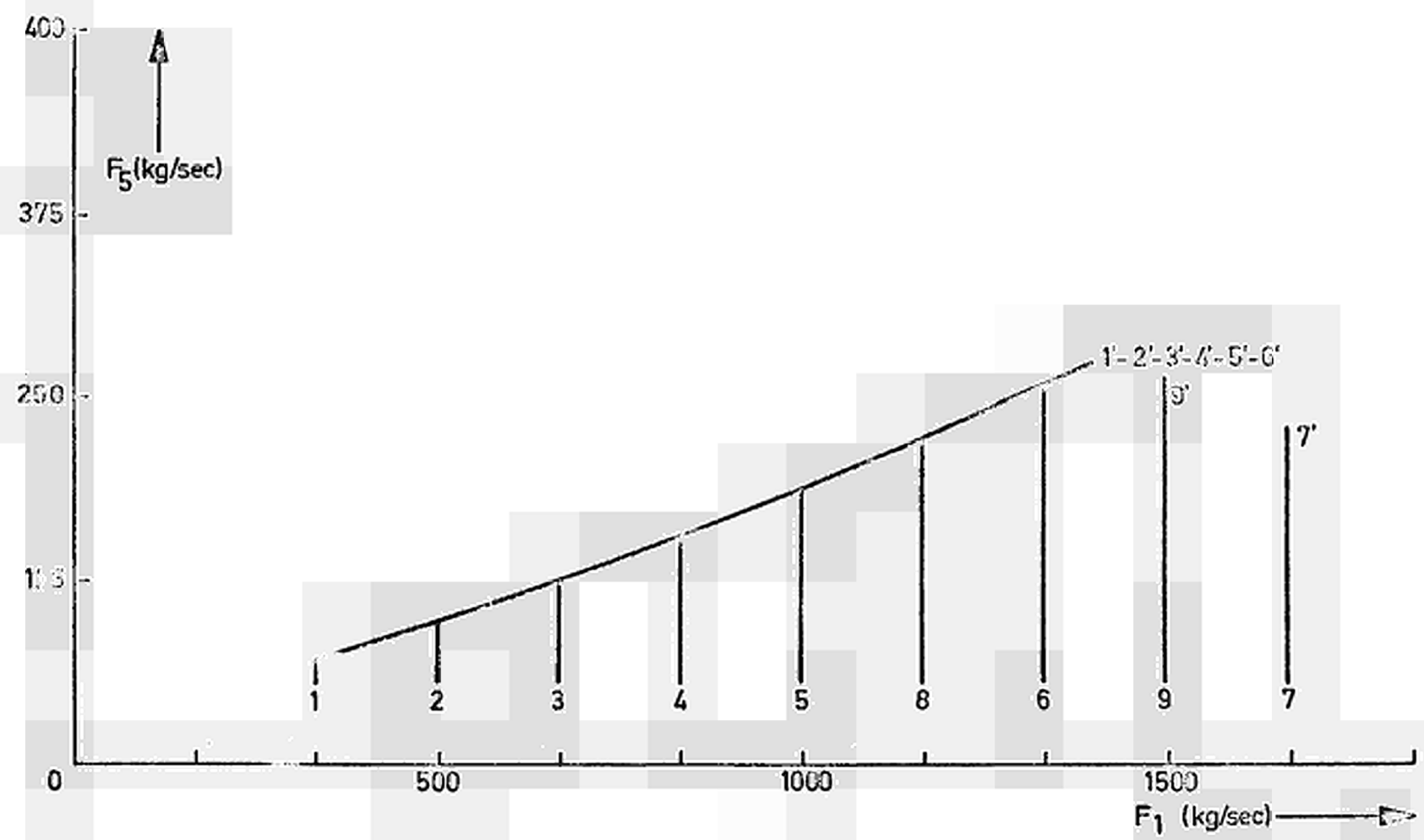


FIG.2-10

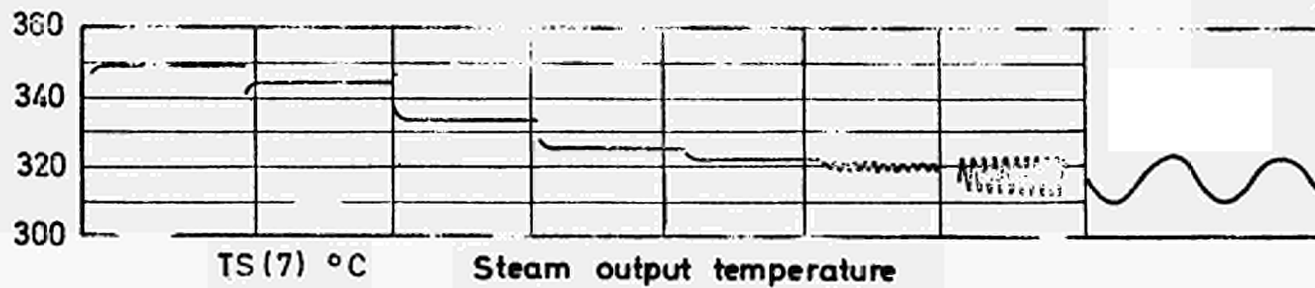
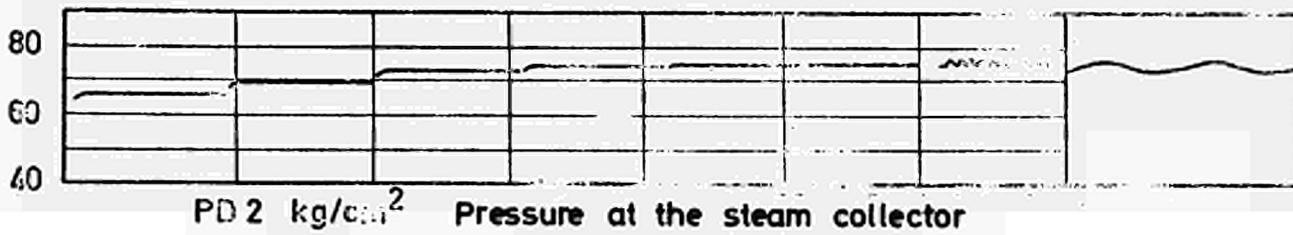
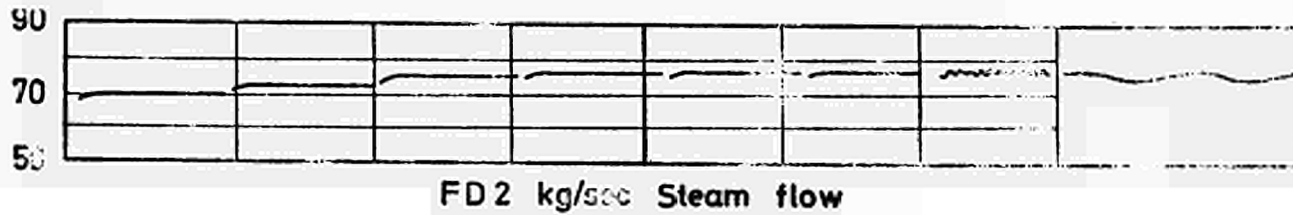
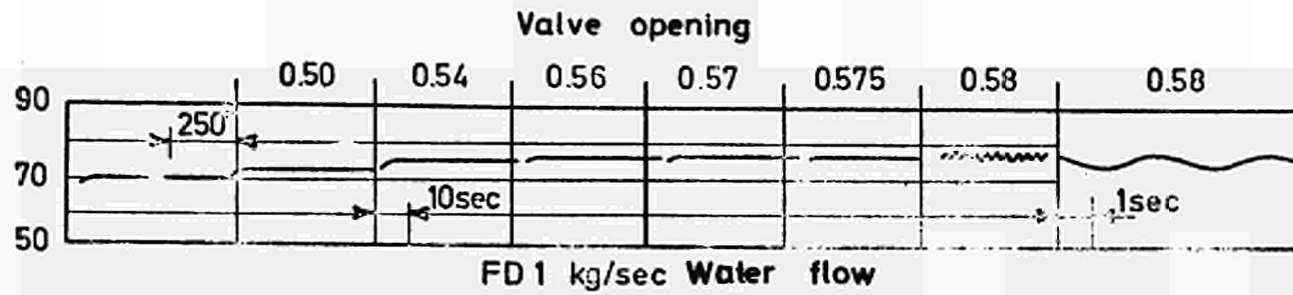


FIG. 2-11

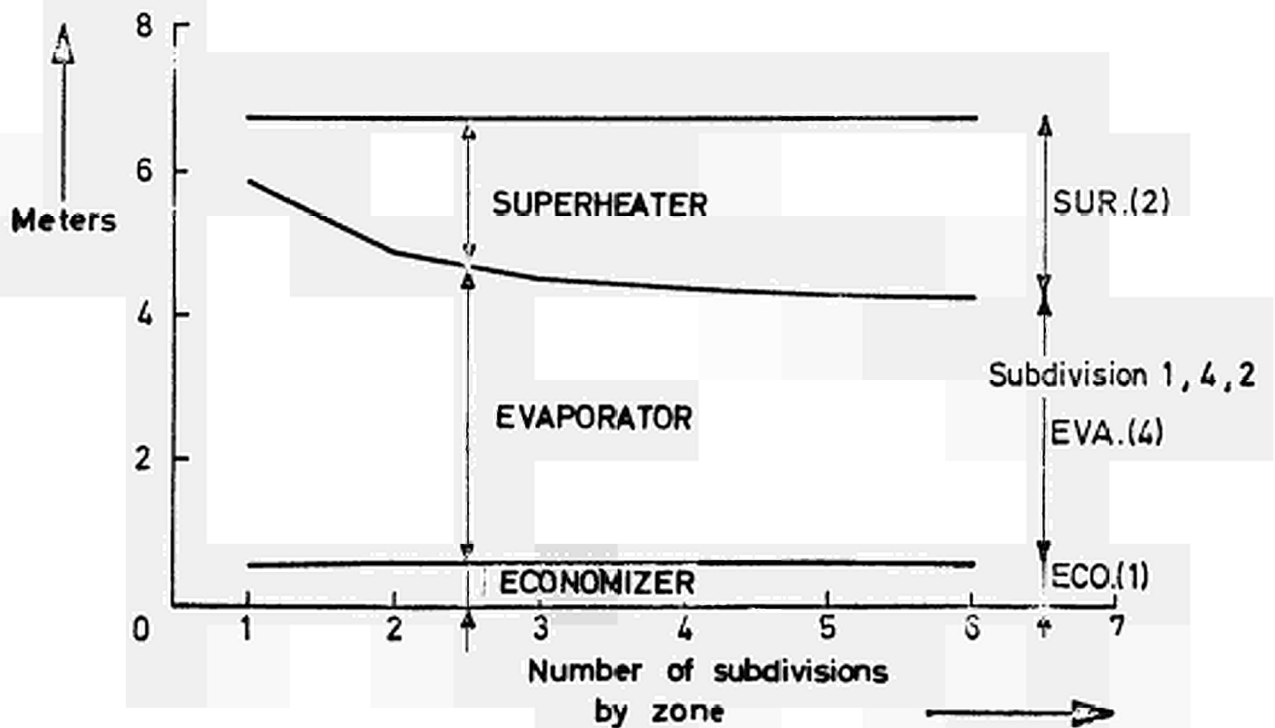
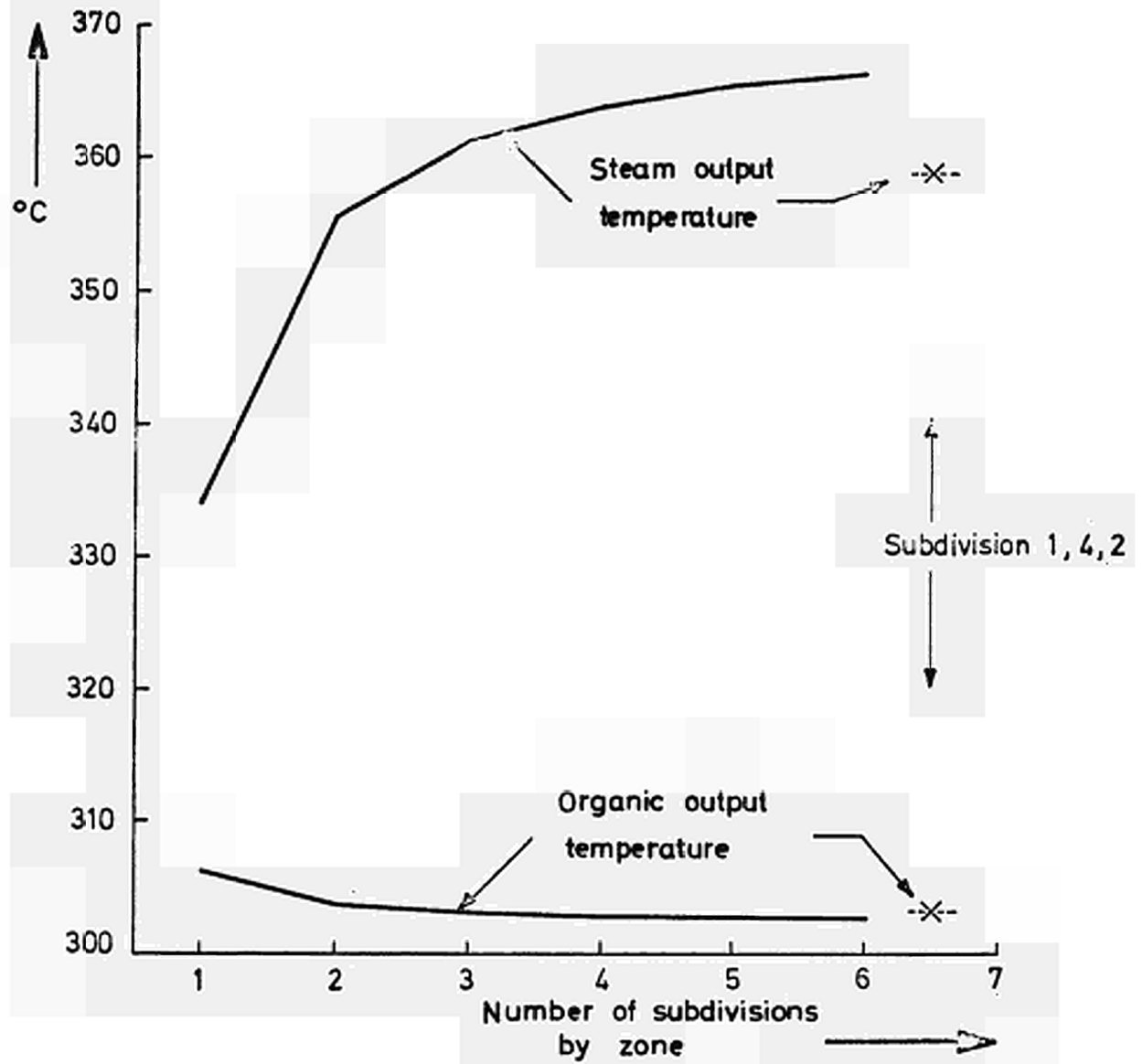


FIG. 2-12

Constant organic input temperature

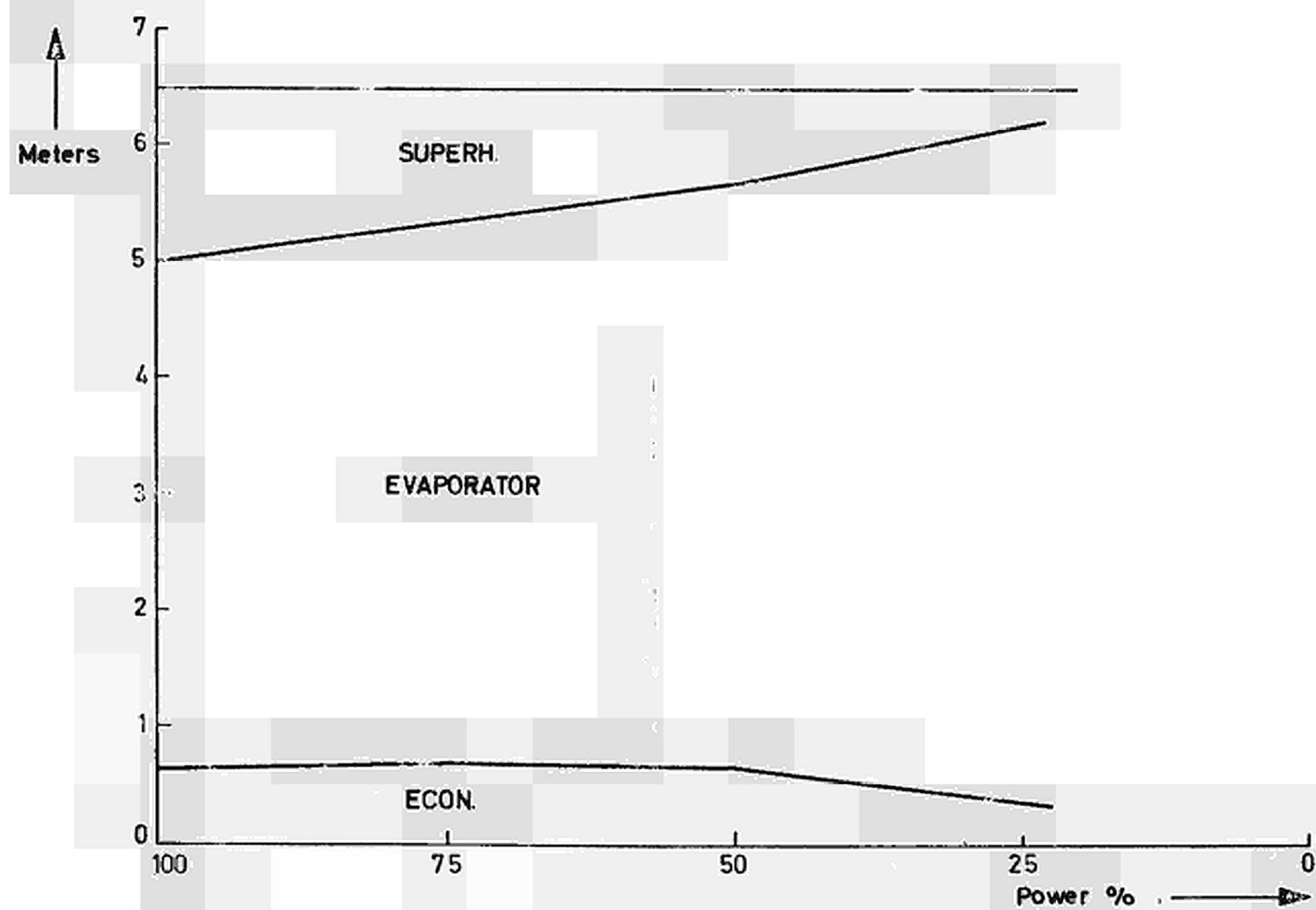


FIG. 2-13

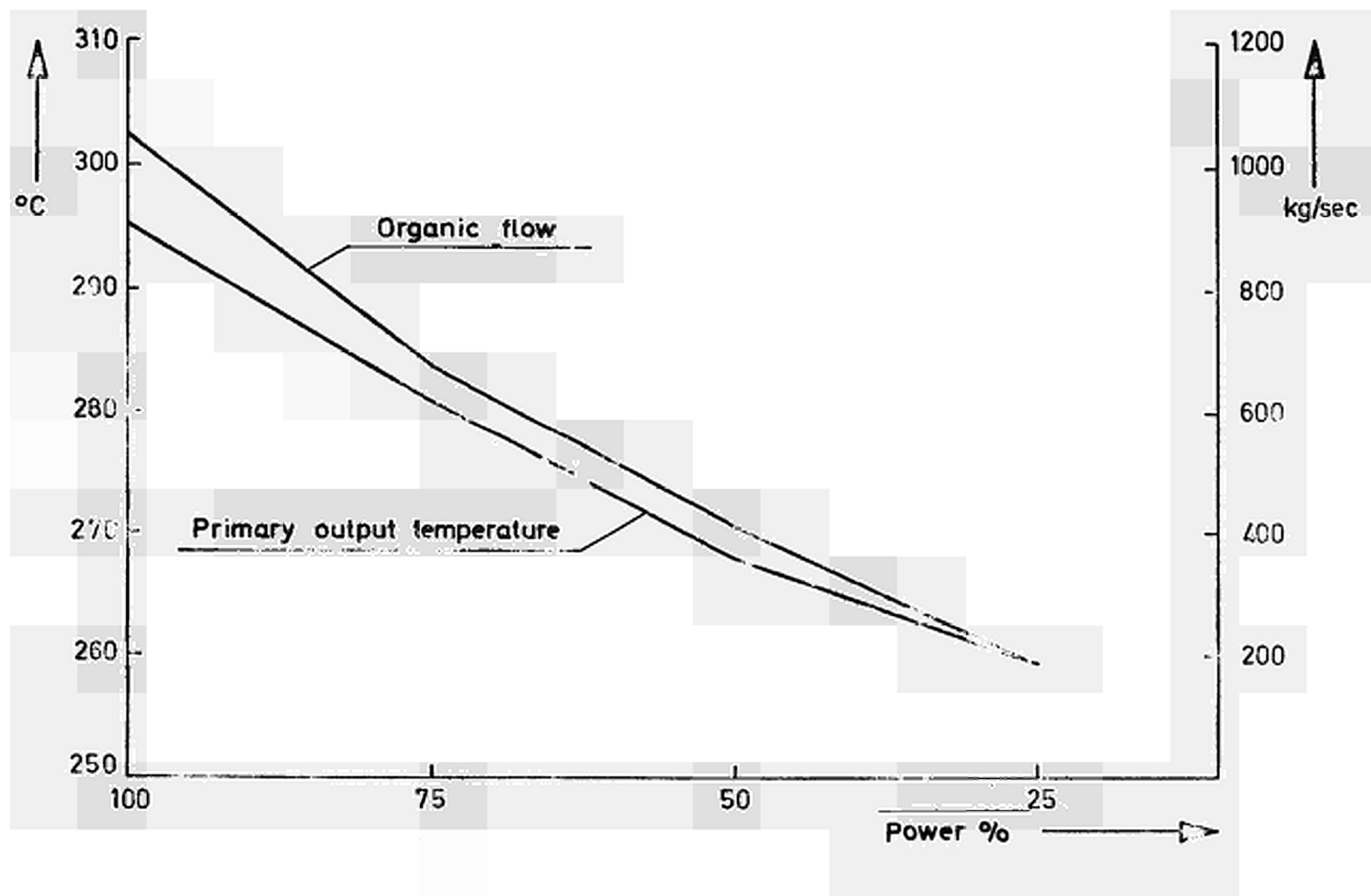


FIG.2-14

Constant primary flow

Meters ↑

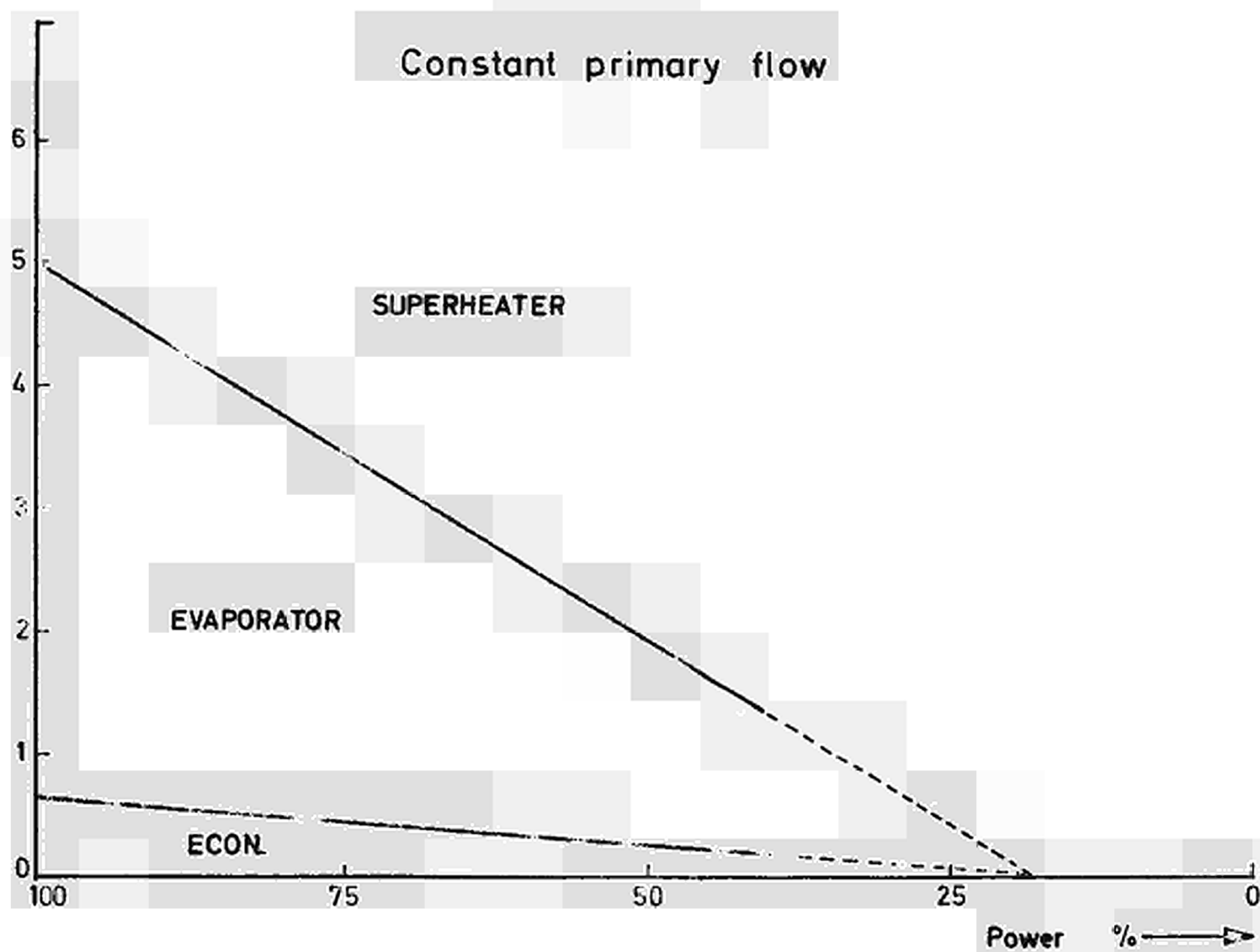


FIG. 2-15

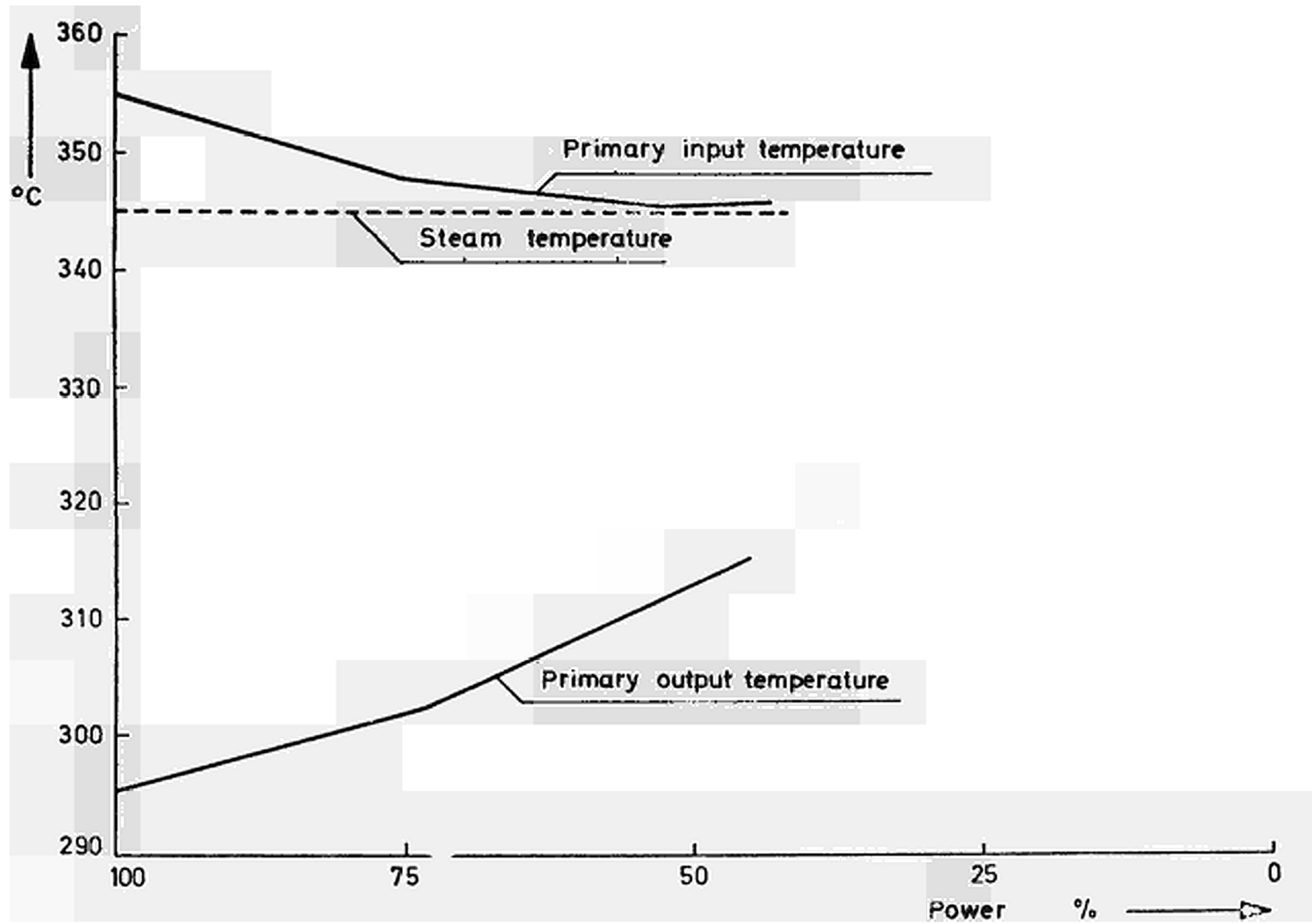


FIG. 2-16

Organic input temperature and
variable primary flow

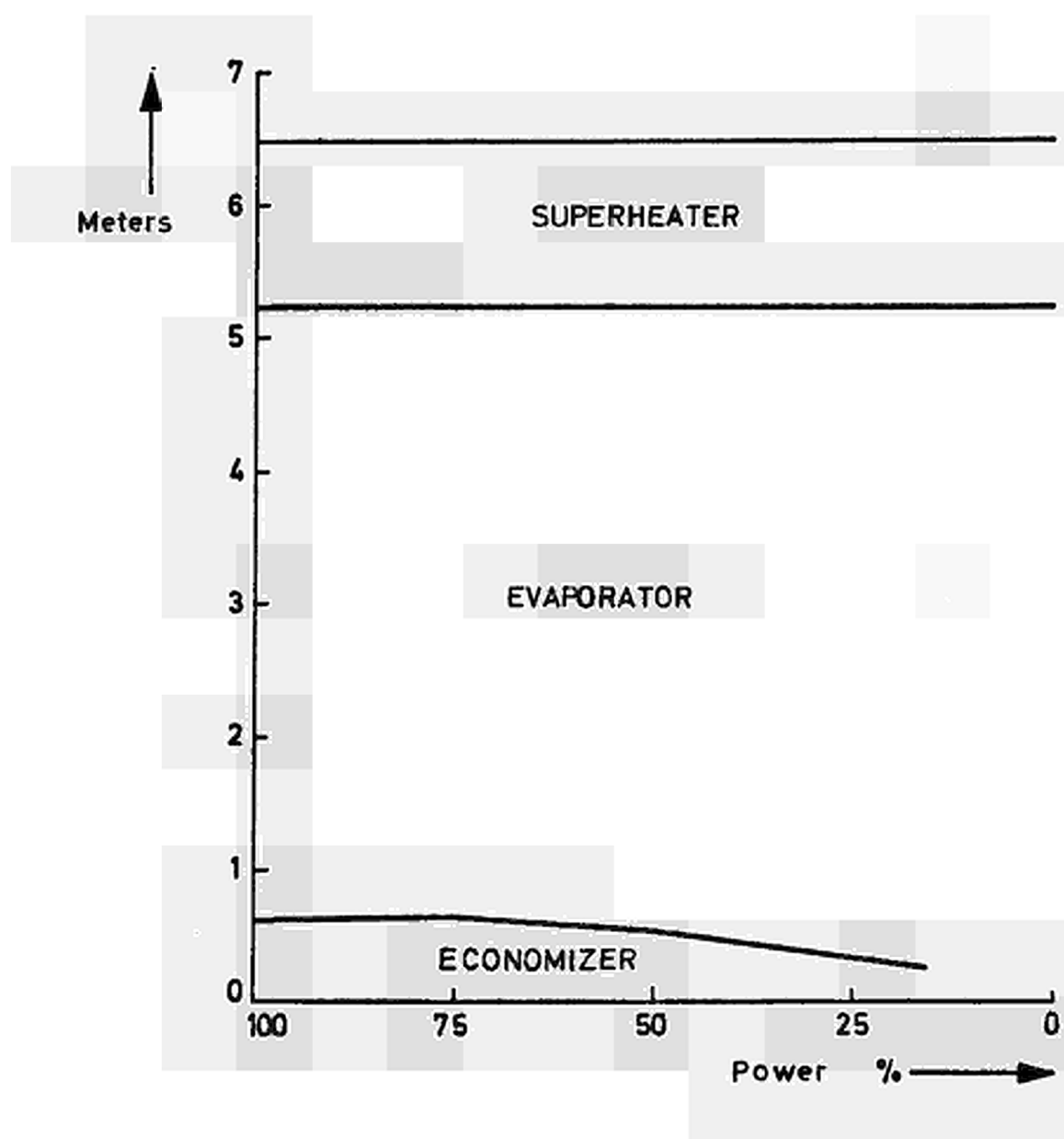
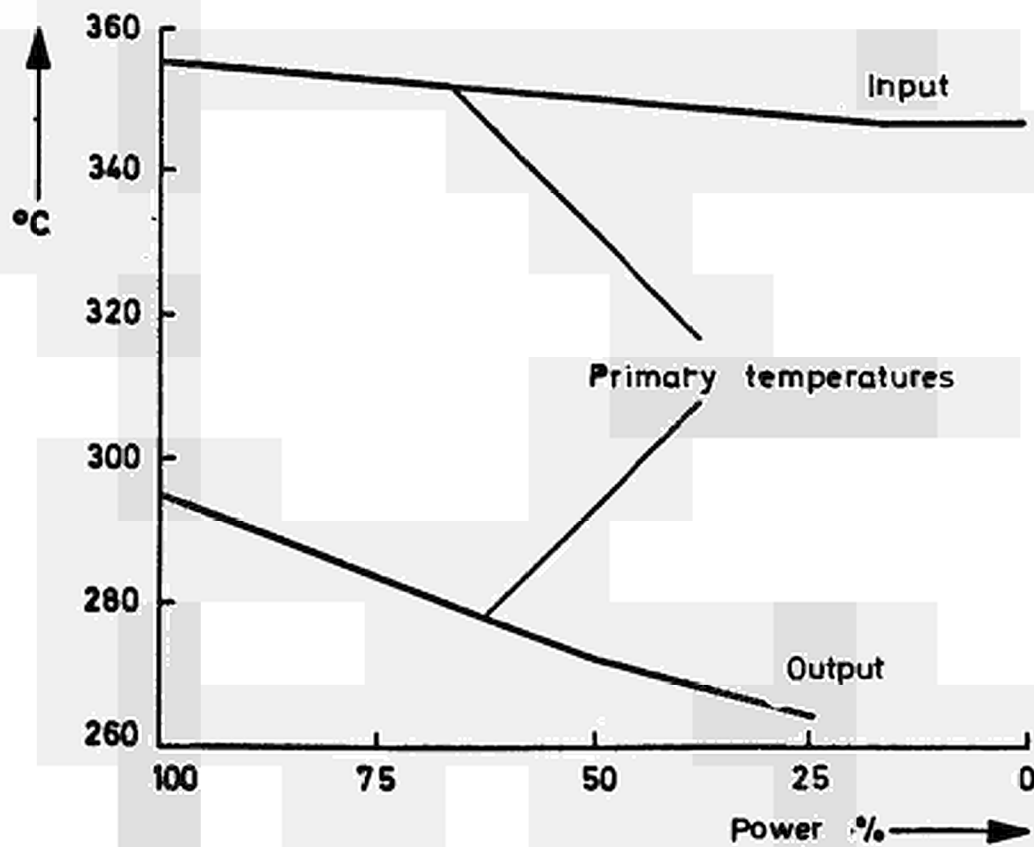
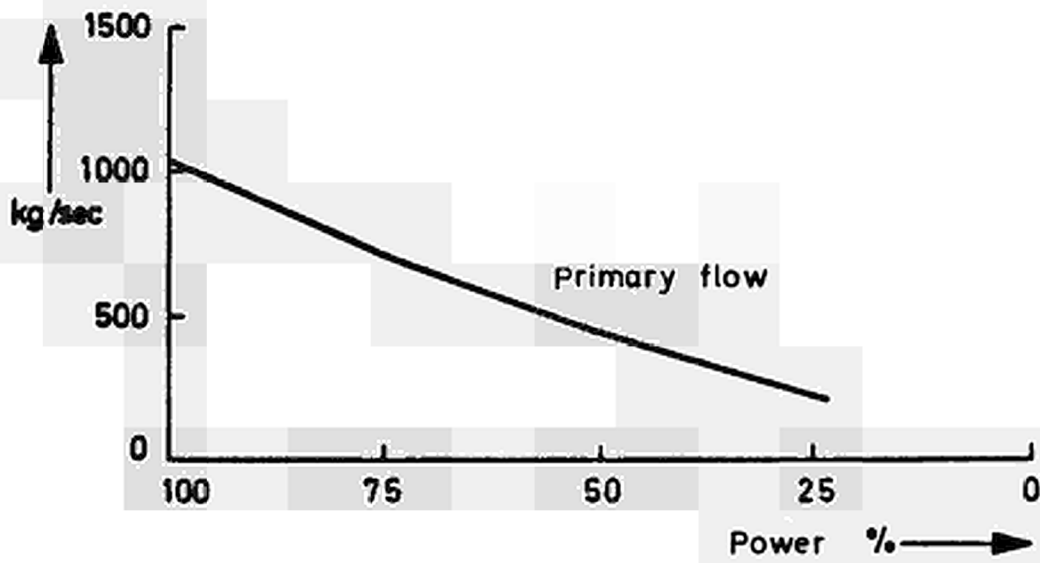
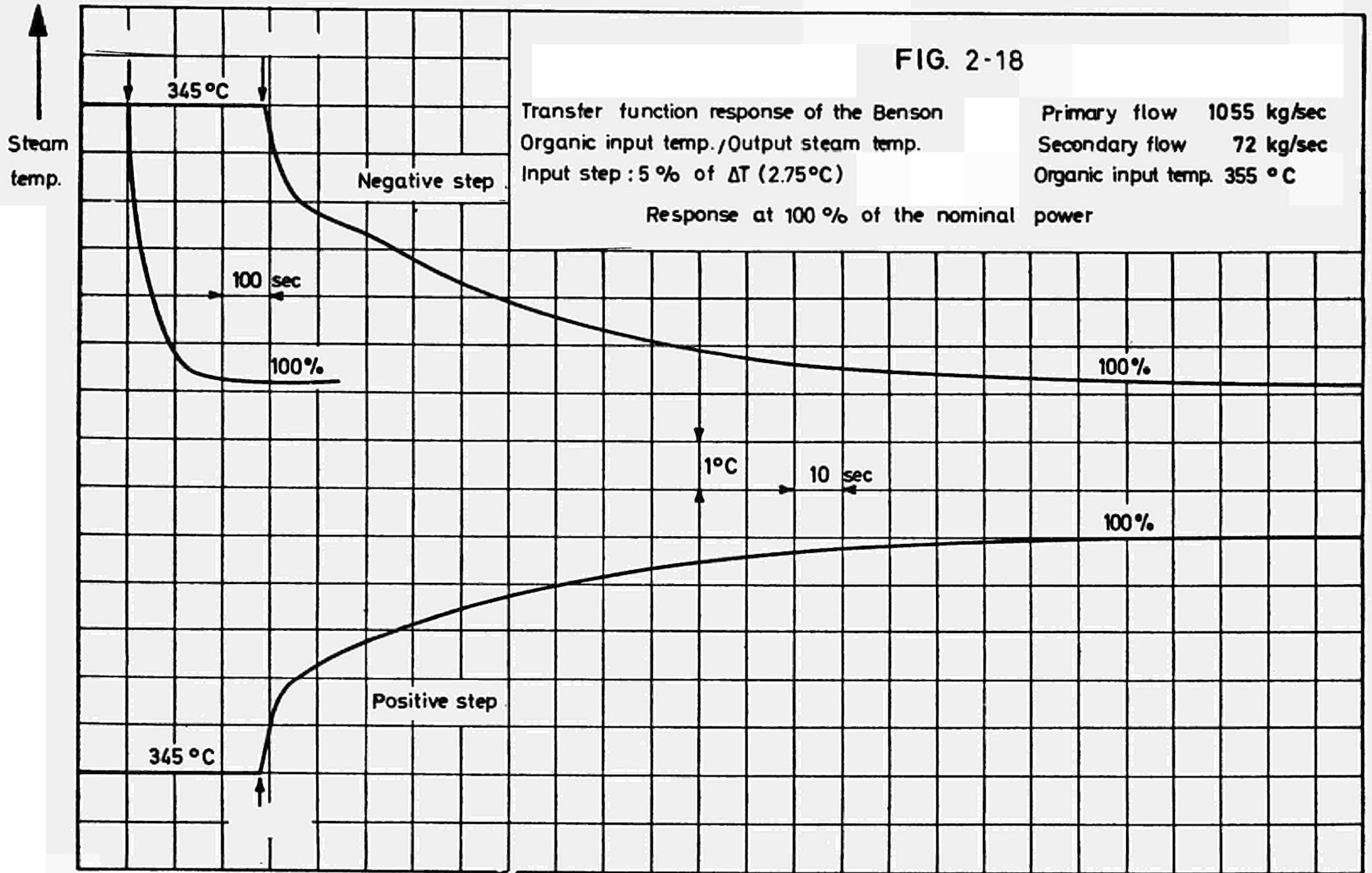


FIG. 2-17





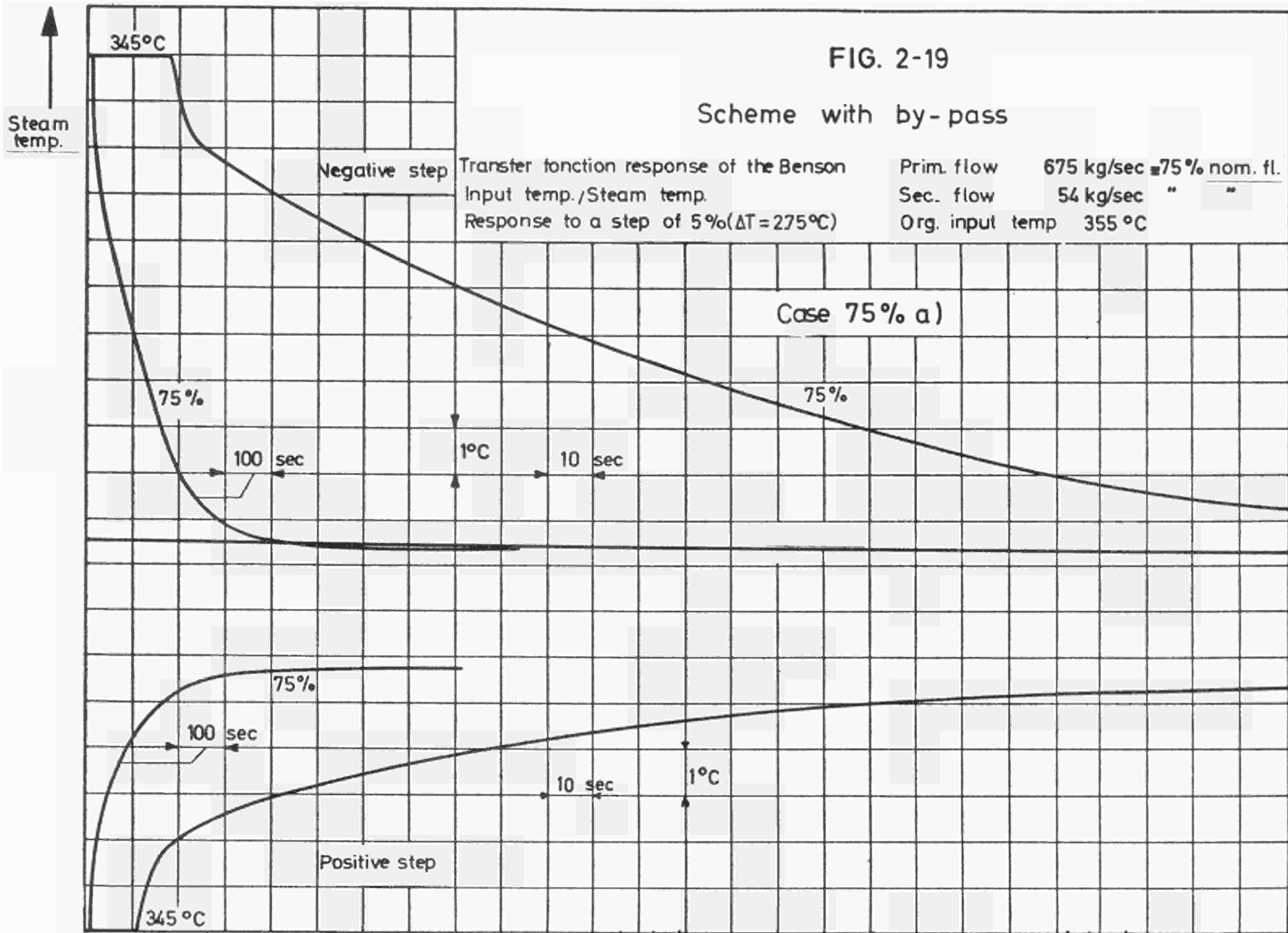


FIG. 2-20

Scheme with by pass

Transfer function of the Benson
 Input temp./ Output temp.
 Response to a step of 5%=2.75°C

Primary flow 408 kg/sec
 Secondary flow 36 kg/sec
 Org. input temp. 355 °C

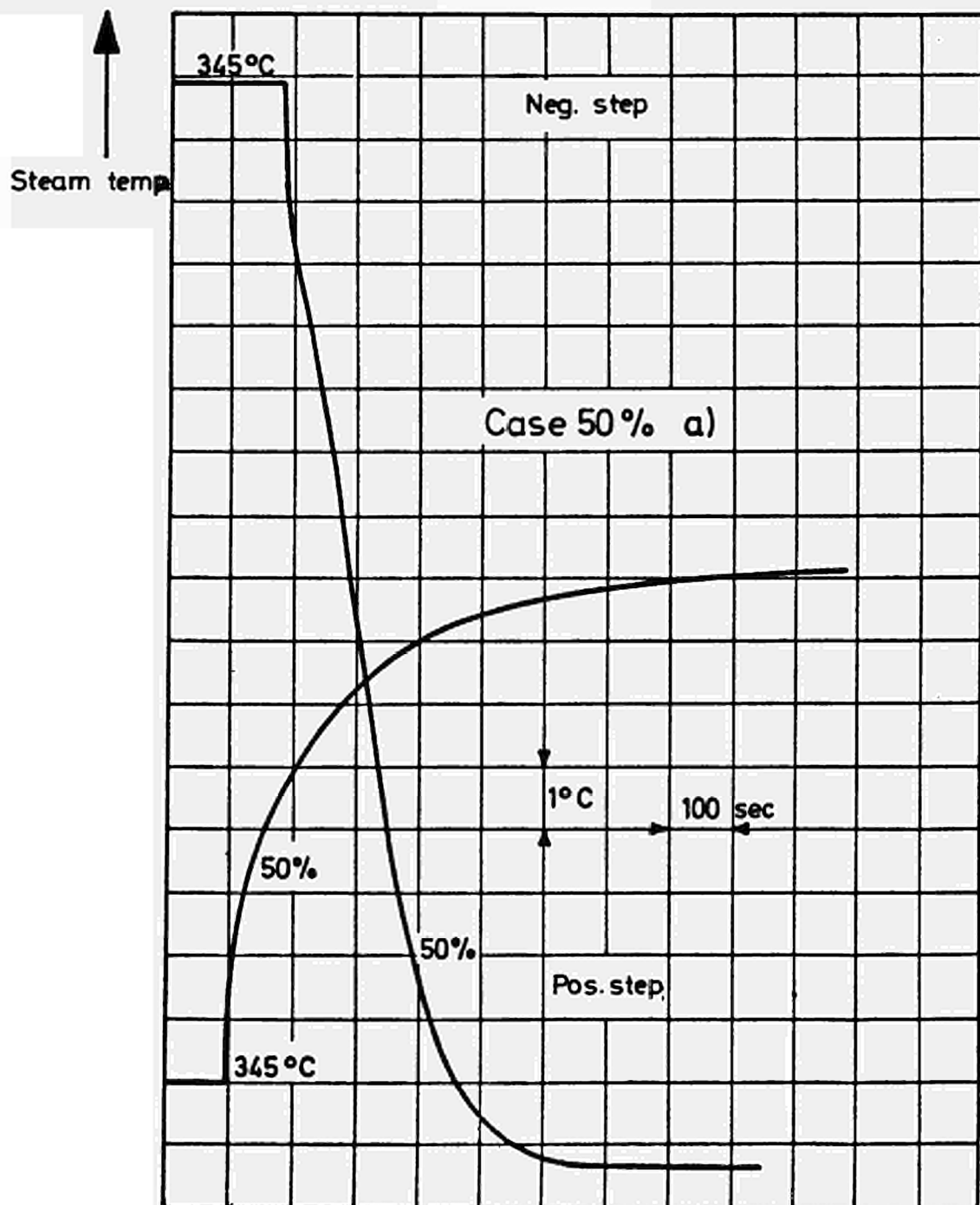


FIG. 2-21

Scheme with by-pass

Transfer function of the Benson
Input flow / Output temperature
Response to a step of 2%

Primary flow 1055 kg/sec.
Secondary flow 72 "
Org. input temp. 355 °C

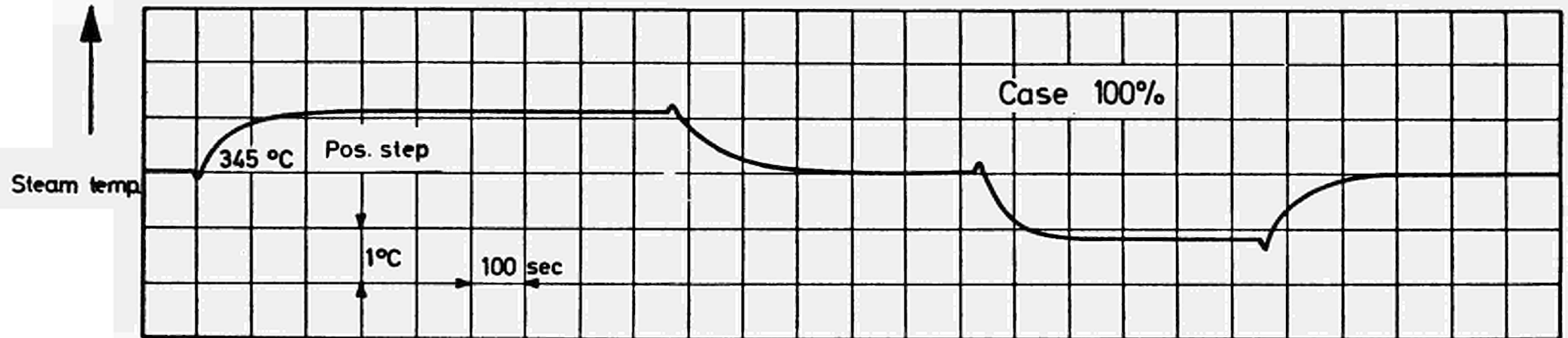


FIG. 2-22

Scheme with by-pass

Transfer function of the Benson
Primary flow/Secondary temperature
Response to a step of 2%

Primary flow 675 kg/sec.
Secondary flow 54 "
Prim. input temp. 355 °C

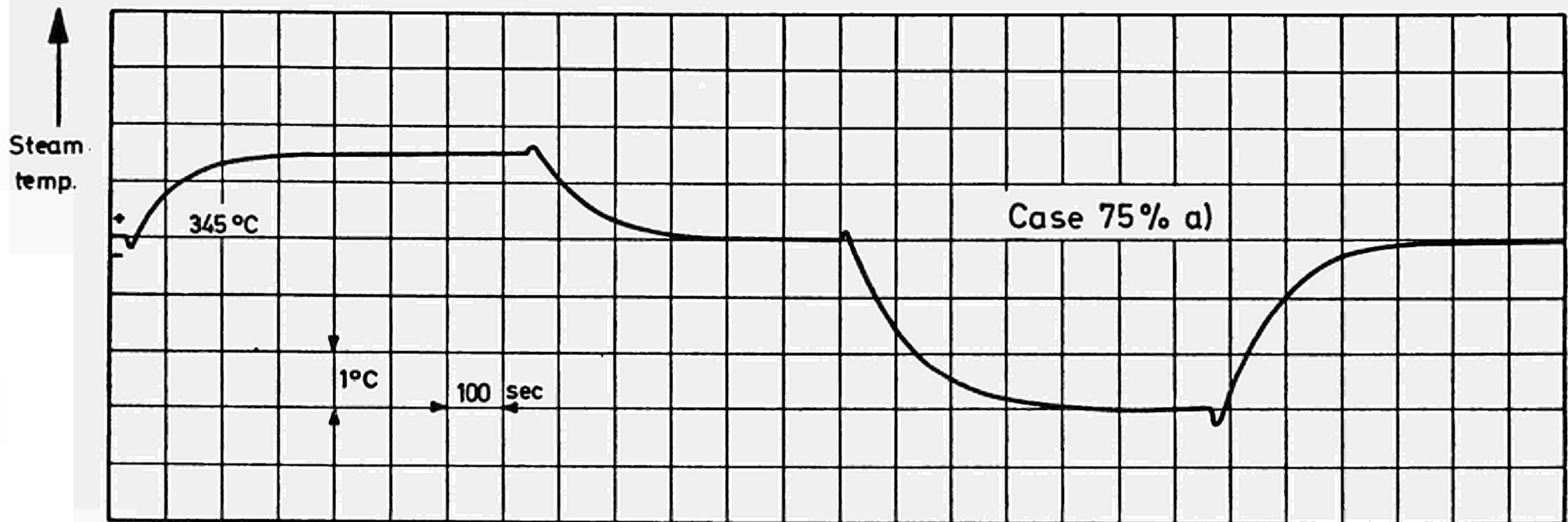


FIG. 2-23

Scheme with by pass

Transfer function of the Benson
Primary flow/Secondary temperature
Response to a step of 2%

Primary flow 408 kg/sec
Secondary flow 36 "
Primary input temp. 355 °C

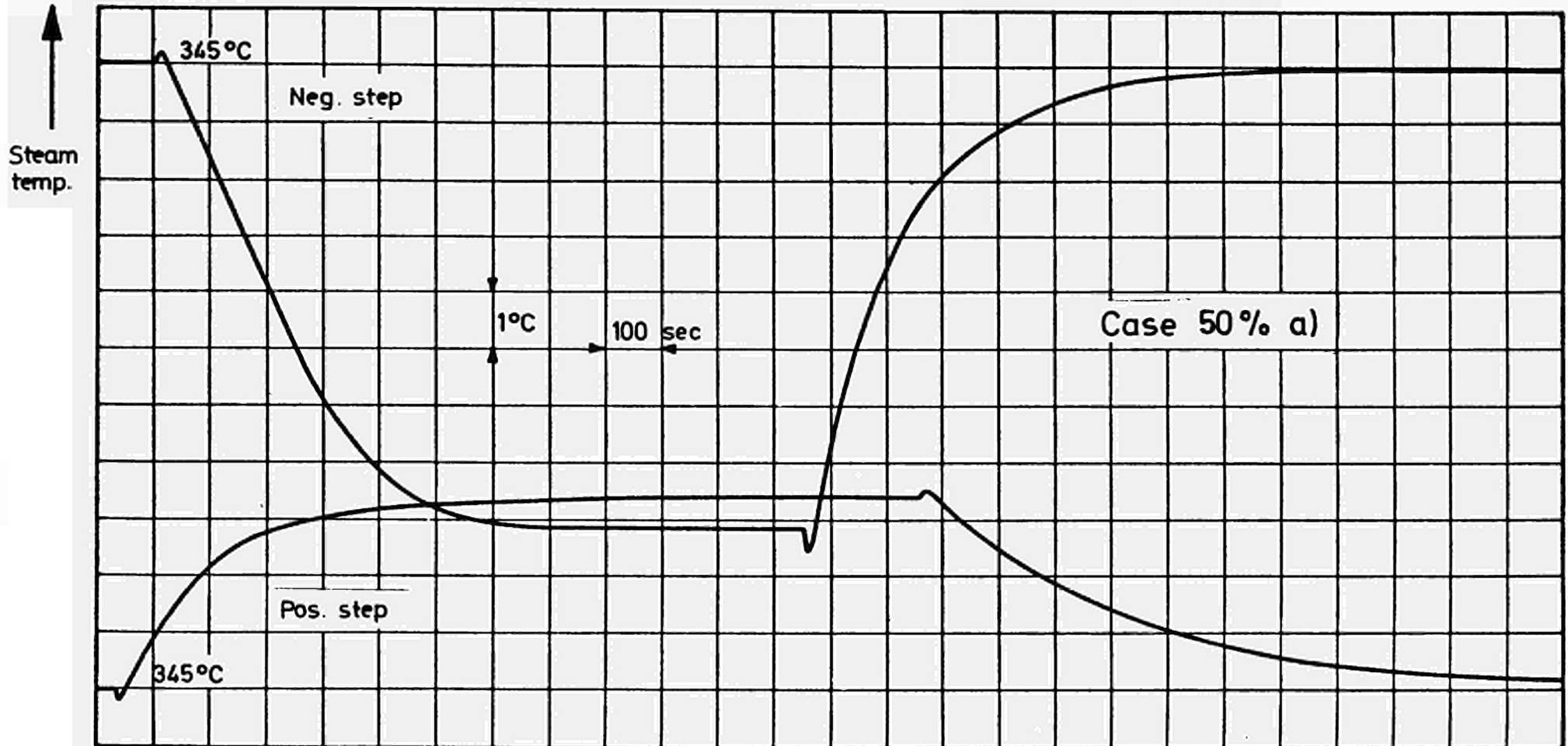


FIG. 2-24

Scheme without by pass

Transfer function of the Benson
Input temp./Output temp.
Response to a step of 5% = 2.4 °C

Primary flow 1055 kg/sec
Secondary flow 54 kg/sec
Org. input temp. = 348 °C

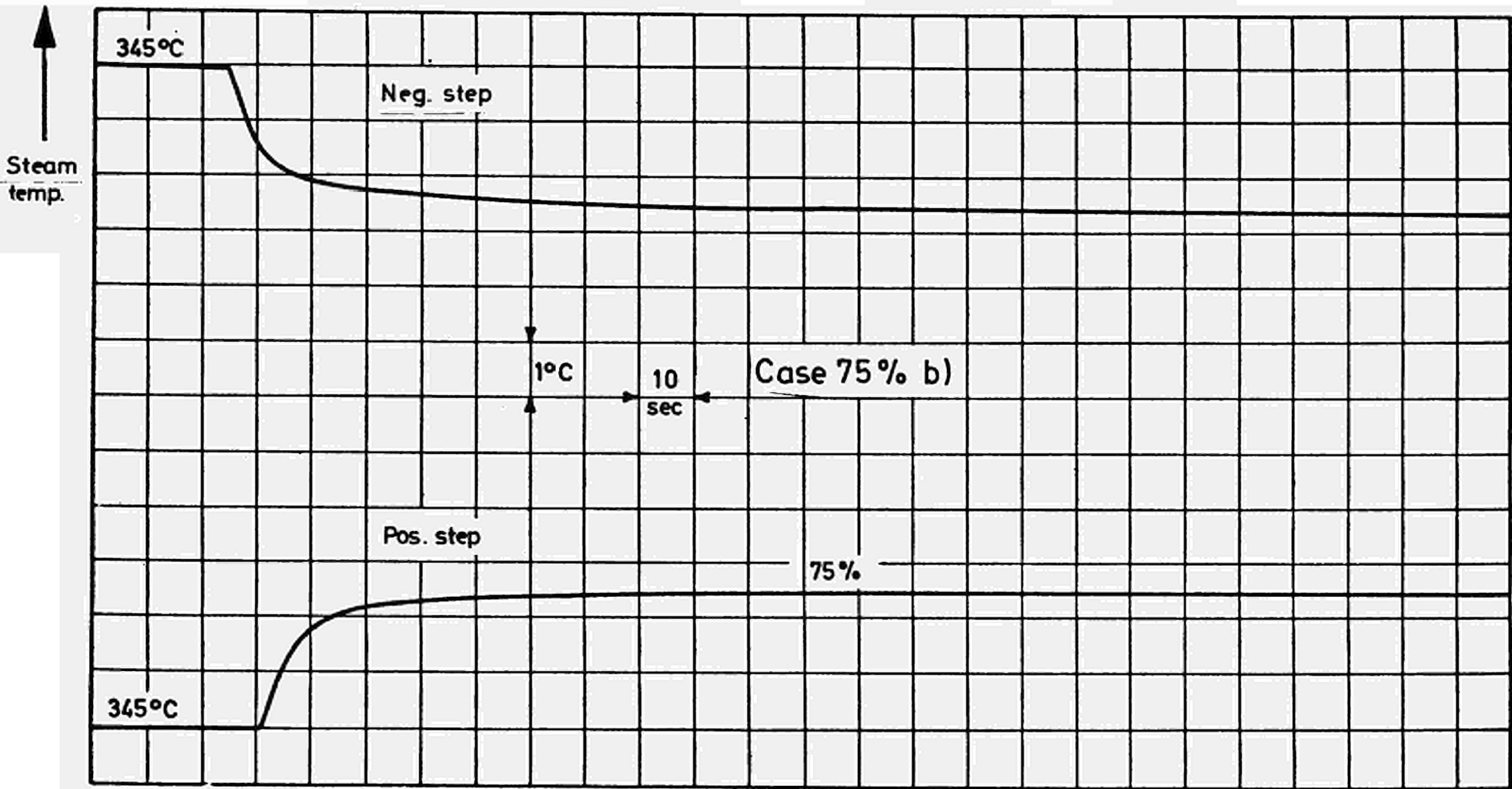


FIG. 2-25

Scheme without by pass

Transfer function of the Benson

Input temp. / Output temp.

Response to a step of 5% \cong 2.27 °C

Primary flow 1055 \cong max. flow

Secondary flow 36 kg/sec.

Org. input temp. \cong 345,5 °C

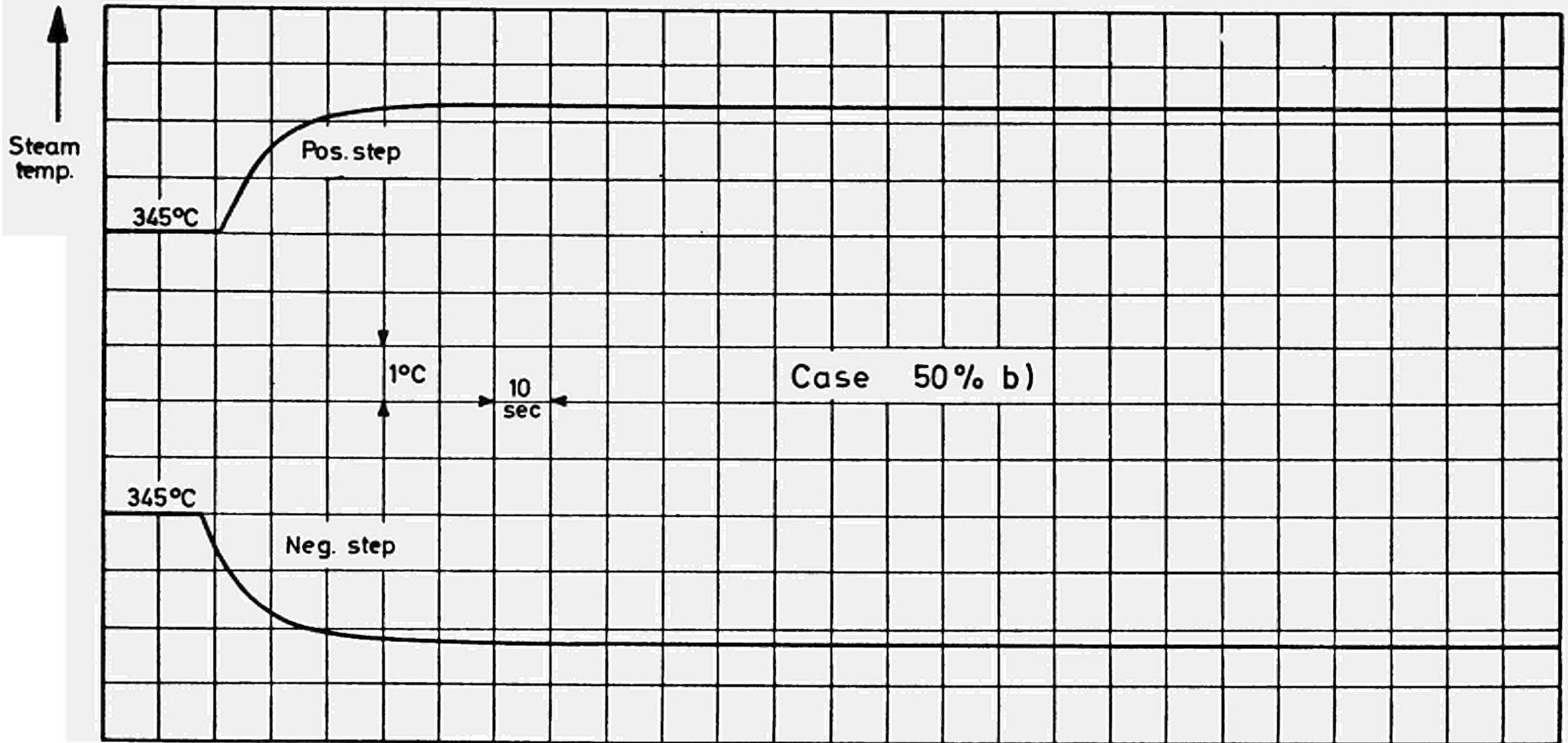


FIG. 2-26

Response to a primary flow step of 2%
for different power levels varied according to
the scheme C.

The primary flow and the organic temp.
are varied in the same time in order to
maintain the reheater height in the Benson
and the steam output temperature constant.

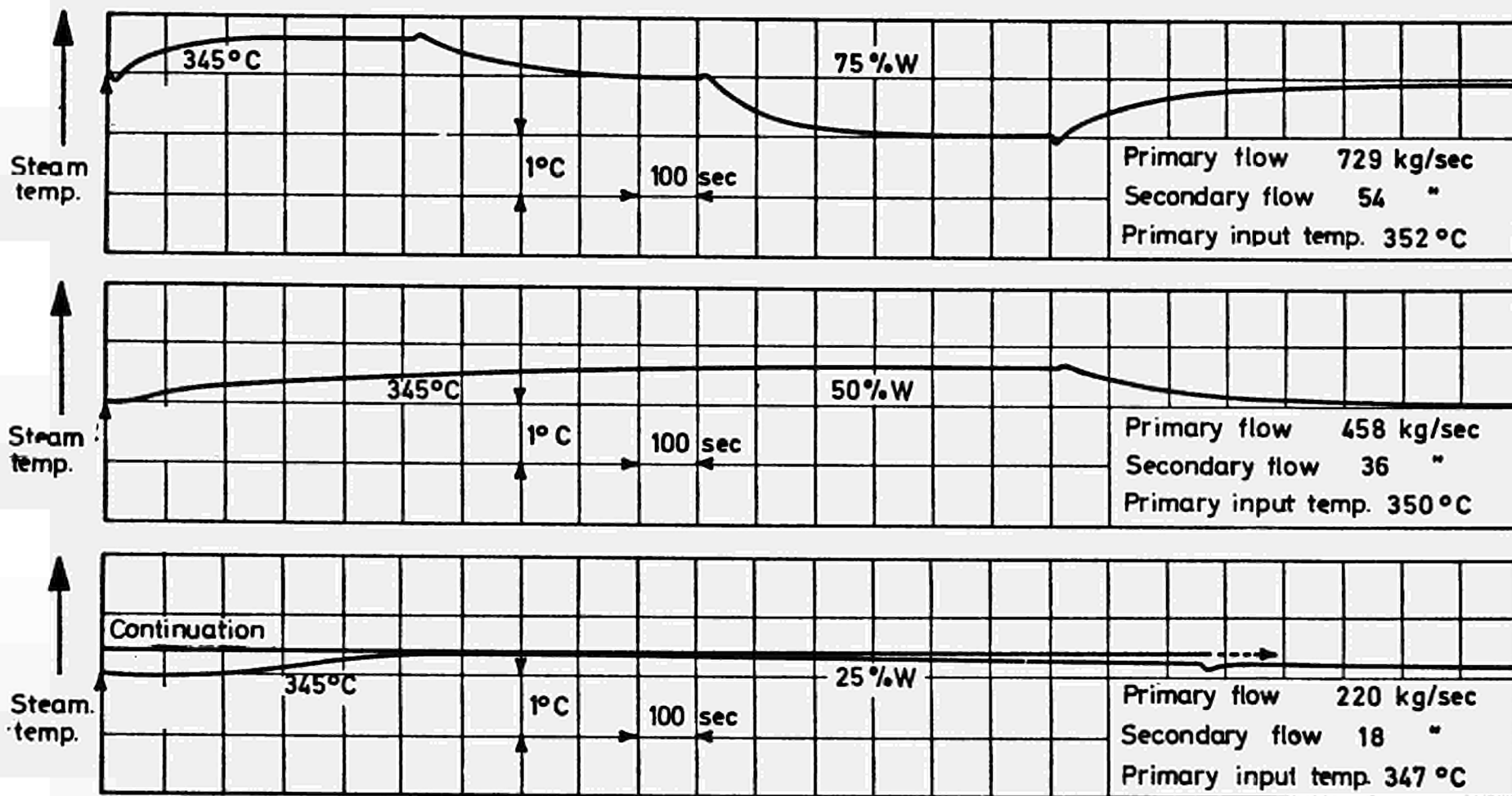


FIG. 2-27

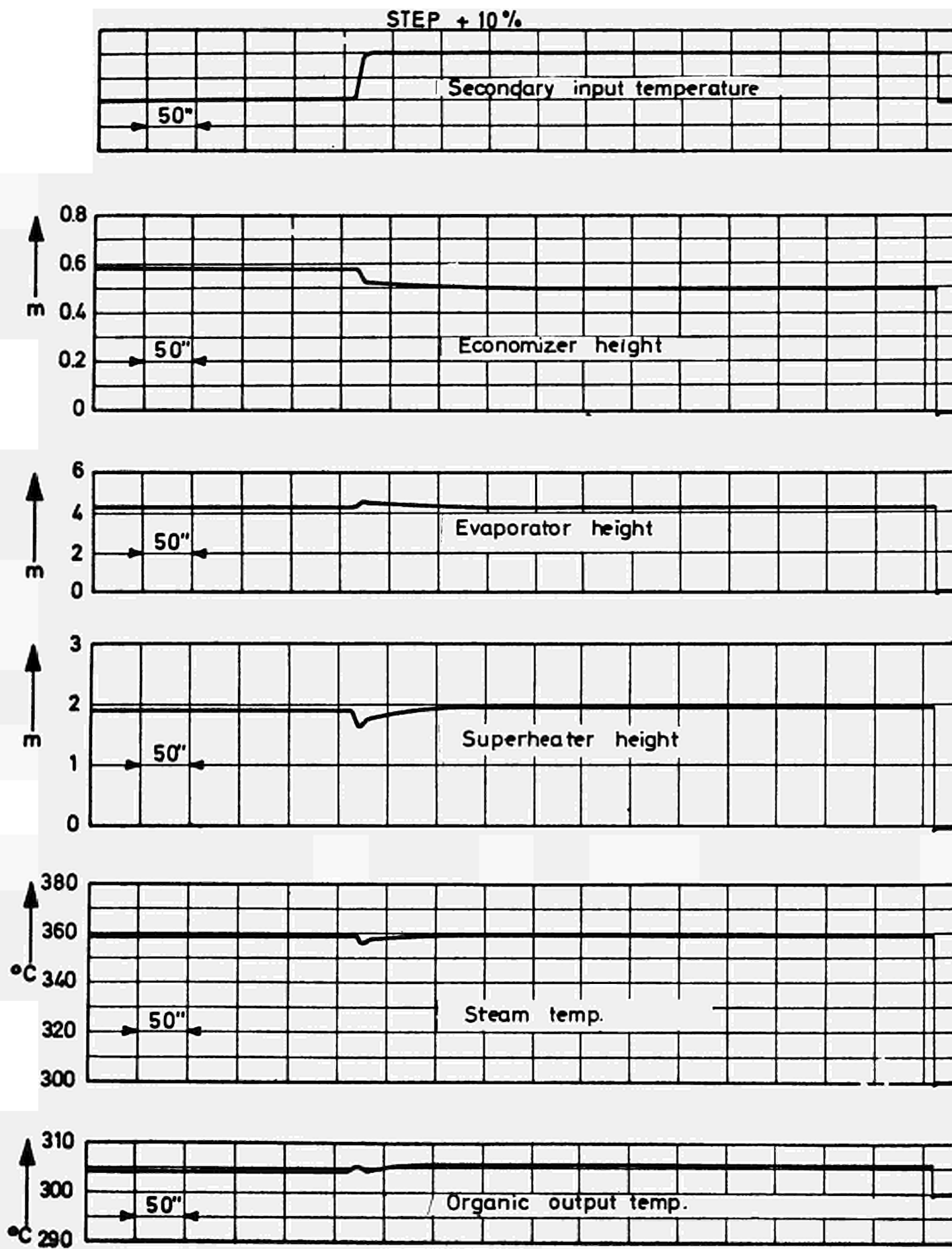


FIG. 2-28

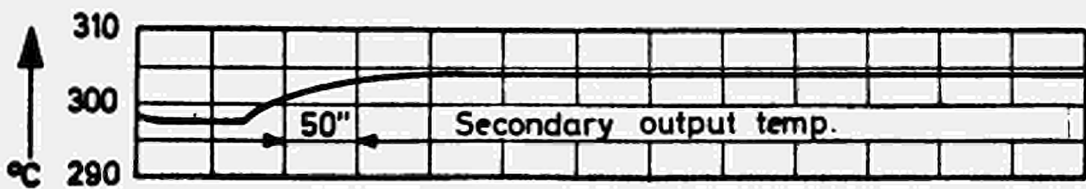
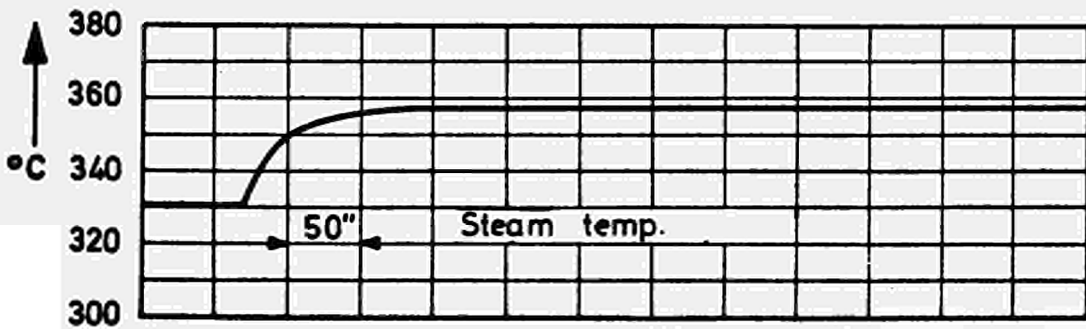
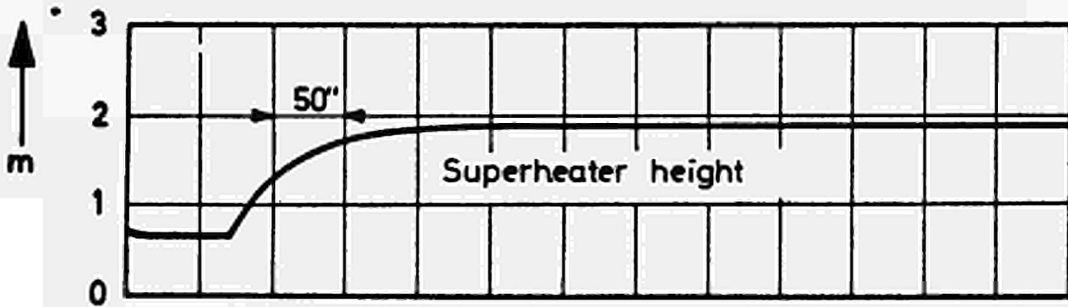
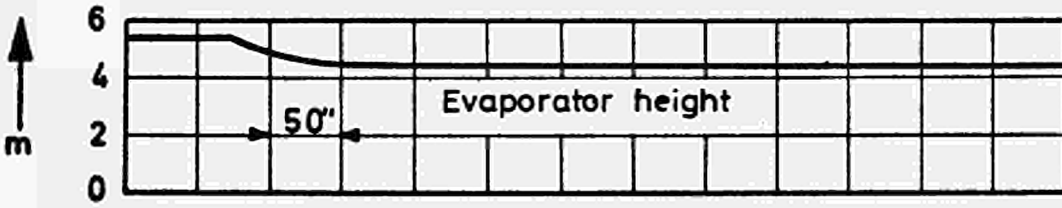
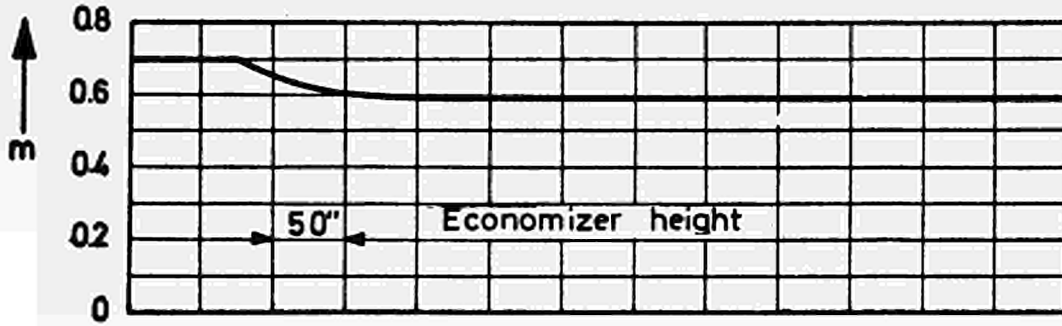
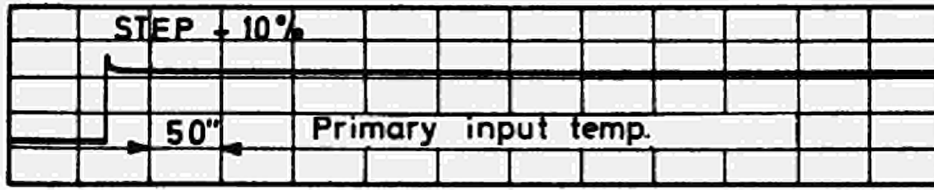
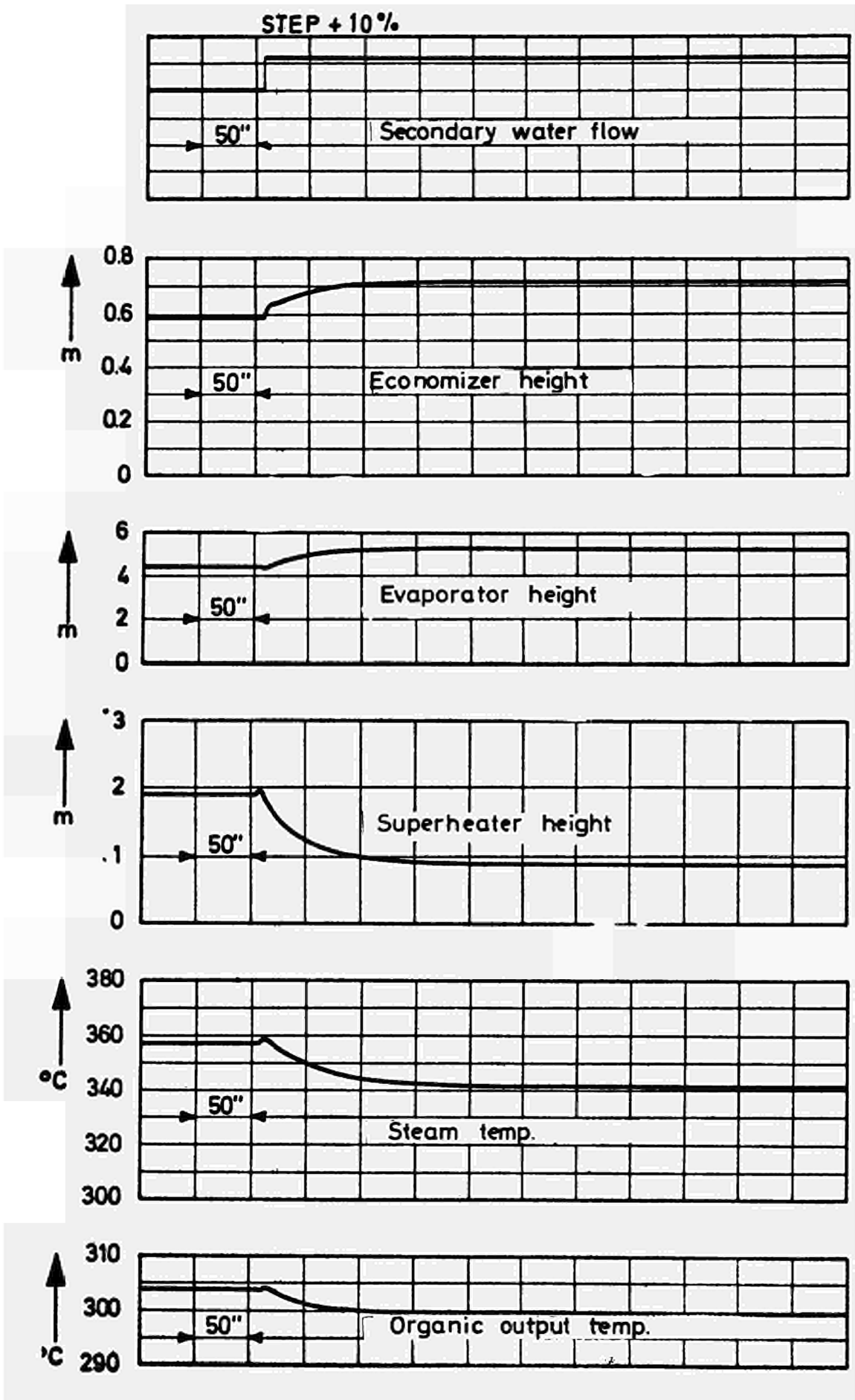
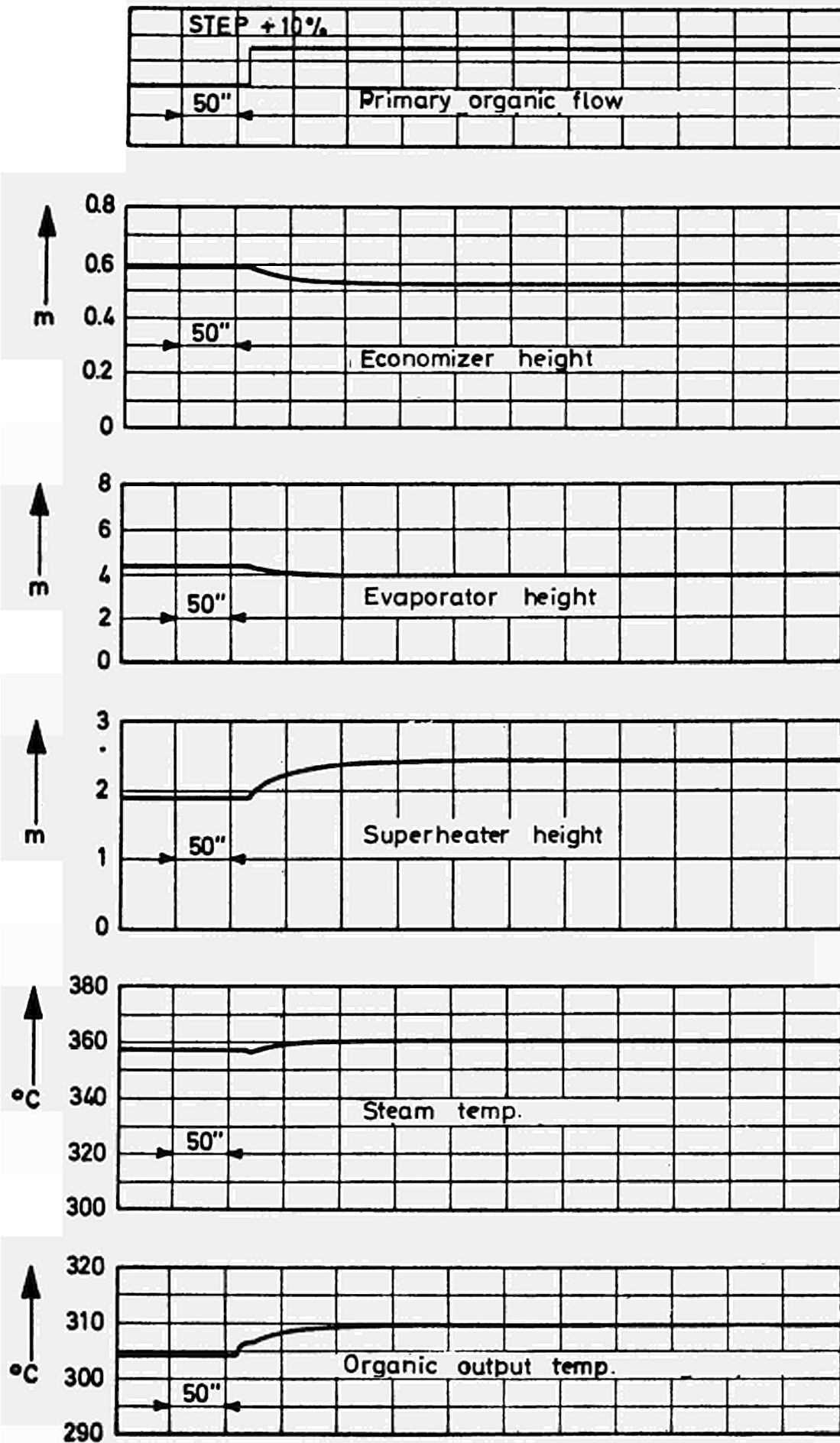


FIG. 2-29



I79
FIG. 2-30



APPENDIX ASERVO-MECHANISM ANALYSIS
OF THE
ORGEL REACTOR CONTROL SYSTEM1. INTRODUCTION

The scope of this study is to complete and generalize some results concerning the control loop system, given by the analogue simulation.

The mathematical tool used is the servo theory; this theory assumes that the studied physical systems are described by sets of linear differential equations with constant coefficients; this is not the case for the kinetic equations of a reactor, which is why this study is valid only for small variations around a specified steady state. The method is not so restrictive as it would seem; the stability problems are described by equations of small variations which are actually linear; on the other hand, it presents the great advantage to give the analytic relations which link the different parameters of stability and, even to a certain degree, the transient response, which is not possible when using a numerical method; moreover, one must check the validity of the theory on the particular cases of the 100 and 250 MWe prototypes studied previously by analogue or digital methods. In fact, the real limit of the method is on the transient response when the limitations on the reactivity and velocity of the control rod are reached: obviously, these limitations cannot be examined when only the linear phenomena are taken into account.

Thus, the same sets of reactor equations used already in the analogue simulation are retaken, but they

are linearized in order to obtain the complete description of the reactor as a control element; then this element is used in a control system and the entire system may again be examined for stability and transient response. The type of transient apt to be more disturbing for a nuclear power plant is usually not a change in the power level demand which can be limited externally to any desired value, but an internal change in reactivity during which the thermodynamical quantities of the power plant do not shift perceptibly because of the important time-delays involved in the circulation of the coolant; this justified the fact that, in this study, no plant is attached to the reactor to remove the power, which is however impossible without a good transfer function representation of the heat exchanger.

2. THE REACTOR AS A CONTROL ELEMENT

2.1. Solution of kinetic equations for sinusoidal reactivity input

The response of the reactor is studied from a one-point black-box type of approach, i.e. the only significant reactor constants that are present are βK , λ and n in a multiplying medium; the temperature coefficients will be presumed to be zero.

The kinetic equations are the familiar ones:

$$\frac{dn}{dt} = \frac{K_{\text{eff}} (1 - \beta) - 1}{\lambda} n + \sum_{i=1}^6 \lambda_i C_i$$

where $\beta = \sum_{i=1}^6 \beta_i$

$$\frac{dC_i}{dt} = \frac{K_{\text{eff}} \beta_i}{\lambda} n - \lambda_i C_i$$

let us take $\delta K = \frac{K_{\text{eff}} - 1}{K_{\text{eff}}}$ with $K_{\text{eff}} \neq 1$

then:

$$\frac{dn}{dt} = \frac{\delta K}{1} n - \sum_{i=1}^6 \frac{dC_i}{dt}$$

$$\frac{dC_i}{dt} = \frac{\beta_i}{1} n - \lambda_i C_i$$

This set of linear equations has no constant coefficients, but, if we assume sufficiently small sinusoidal excursions of n around the static value n_0 , these equations can be approximated by a set of constant coefficients. This calculation is trivial and developed for instance in Ref. 1. The searched transfer function, indicated in Fig.2.1., is the following:

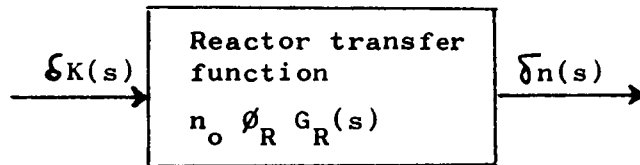


Fig. 2.1.

$$\frac{\delta n(s)}{n_0 \delta K(s)} = \phi_R G_R = \frac{1}{s1 \left[1 + \sum_{i=1}^6 \frac{\beta_i}{1(s+\lambda_i)} \right]}$$

where s is the Laplace operator; it becomes, in expanded form:

$$\frac{\delta n}{n_0 \delta K} = \frac{a_0 + a_1 s + \dots + a_6 s^6}{b_1 s + b_2 s^2 + \dots + b_7 s^7}$$

For a single group of delayed neutrons:

$$\frac{\delta n}{n_0 \delta K} = \frac{s + \lambda}{s1(s + \lambda \beta/l)}$$

where $\lambda = \beta / \sum_{i=1}^6 \frac{\beta_i}{\lambda_i}$

and in expanded form:

$$\frac{\delta n}{n_0} \frac{\delta K}{\delta K} = \phi_{RGR}^G = \frac{A_0 + A_1 s}{B_1 s + B_2 s^2} \quad (2.1.)$$

where:

$$\left| \begin{array}{l} A_0 = \lambda/1 \\ A_1 = 1/1 \end{array} \right. \quad \left| \begin{array}{l} B_1 = \lambda + \beta/1 \\ B_2 = 1 \end{array} \right.$$

Fig. 1 and 2 show the amplitude and phase frequency response (substituting s by $j\omega$) of the 250 MWe prototype in the two cases of a single group and six groups of delayed neutrons when the power level is 100% and the reactor irradiated.

The calculations have been achieved with the help of a FORTRAN code. As it can be seen, the transfer function (2.1.) is a good approximation, easy to use for later determining analytical expressions; besides, it will not change the general results of the study.

If δK is a step function, when $t \rightarrow +\infty$ $\frac{\delta n}{n} \sim \frac{A_0}{B_1 s} \rightarrow +\infty$, i.e. when a small amount of positive reactivity is inserted into the reactor, the power level rises infinitely.

2.2. Feedback loop due to temperature coefficients

The physical effects of the temperature coefficients will be translated in servo-loop feedback which modifies the elementary reactor transfer function. Because of the presence of this feedback, the problem of stability will exist.

Two-path temperature coefficient feedback is considered according to the block diagrams of Fig. 2.2., which are equivalent.

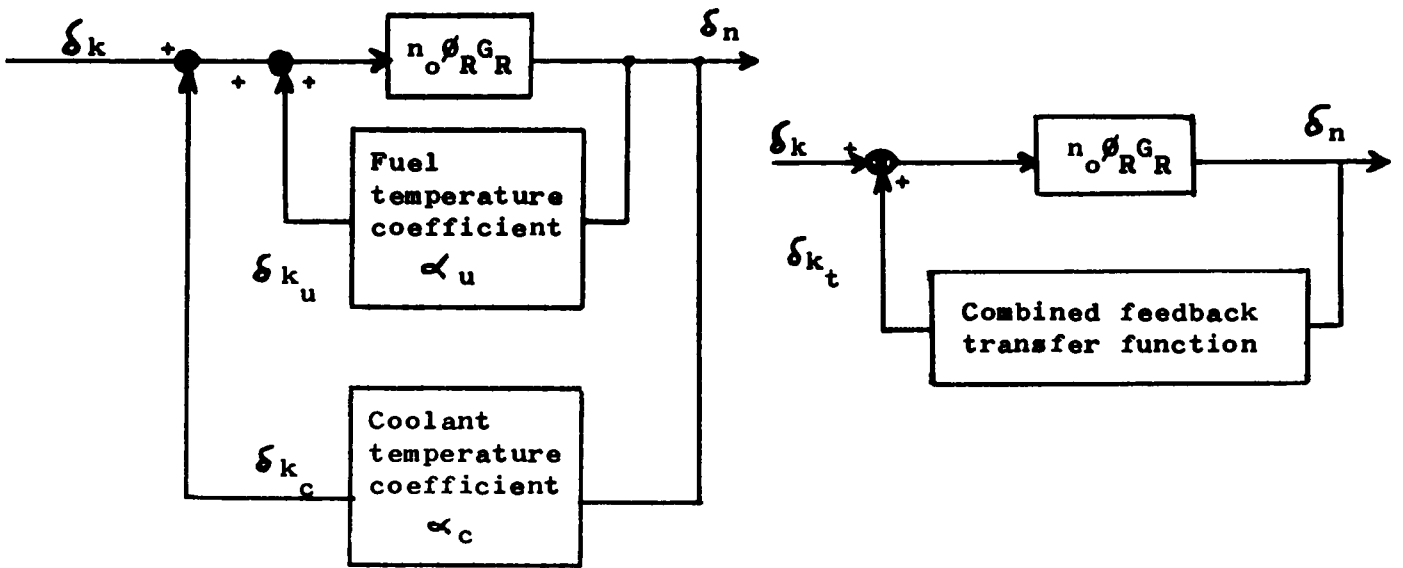


Fig. 2.2.

The total feedback reactivity is:

$$\delta K_t(s) = \delta K_u(s) + \delta K_c(s)$$

Assuming that the steady-state program of the reactor is a constant coolant flow with a constant inlet coolant temperature T_i (which is not restrictive because of the insensibility of the thermodynamical quantities during an internal change of reactivity), and taking again the equations of the heat transmission of the analogue reactor model, we get:

$$\delta K_t(s) = \alpha_u \delta T_u^*(s) + \alpha_c \delta T_c^*(s) \tag{2.2.}$$

where $\delta T_u^* = \gamma_c \delta T_c + \gamma_u (\delta T_u - \delta T_c)$ (2.3.)

$$\delta T_c^* = \gamma_c \delta T_c \tag{2.4.}$$

δT_u and δT_c are small variations about the steady-state values of the average fuel and coolant temperatures of the representative channel, the representative channel being included between the central channel and the channel of medium power and defined by its radius r_o , so that:

$$n(r_o) = \frac{\int_0^R n^3(r) r dr}{\int_0^R n^2(r) r dr}$$

where $n(r)$ is the radial thermal flux and R the reactor radius. Combining the Eqs. (2.2.), (2.3.) and (2.4.) gives:

$$\delta K_t(s) = \alpha_u \gamma_u \delta T_u(s) + [\alpha_u (\gamma_c - \gamma_u) + \alpha_c \gamma_c] \delta T_c(s)$$

and using the notations:

$$\alpha_u^* = \alpha_u \gamma_u \quad (2.5.)$$

$$\alpha_c^* = \alpha_c \gamma_c - \alpha_u (\gamma_u - \gamma_c) \quad (2.6.)$$

$$\delta K_t(s) = \alpha_u^* \delta T_u(s) + \alpha_c^* \delta T_c(s) \quad (2.7.)$$

The variations in the time of δT_u and δT_c are given by the following set of differential equations:

$$\begin{cases} \mu_u \frac{d \delta T_u}{dt} = K \delta n - A (\delta T_u - \delta T_g) \\ \mu_g \frac{d \delta T_g}{dt} = A (\delta T_u - \delta T_g) - B (\delta T_g - \delta T_c) \\ \mu_c \frac{d \delta T_c}{dt} = B (\delta T_g - \delta T_c) - C \delta T_c \end{cases}$$

where A , B and C are heat transfer coefficients obtained from the steady-state with $W^0 = Kn_0$ power of the representative channel:

$$A = \frac{W^0}{T_u^0 - T_g^0} \quad (2.8.)$$

$$B = \frac{W^0}{T_g^0 - T_c^0} \quad (2.9.)$$

$$C = \frac{W^0}{T_c^0 - T_i} \quad (2.10.)$$

Taking the Laplace transforms gives:

$$\delta T_u (\mu_u s + A) = K \delta n + A \delta T_g \quad (2.11.)$$

$$\delta T_g (\mu_g s + A + B) = A \delta T_u + B \delta T_c \quad (2.12.)$$

$$\delta T_c (\mu_c s + B + C) = B \delta T_g \quad (2.13.)$$

Combining Eqs. (2.7.), (2.11.), (2.12.) and (2.13.), the transfer function indicated in Fig. 2.3. is:

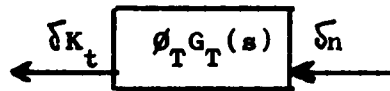


Fig.2.3.

$$\frac{n_o \delta K_t}{\delta n} = \phi_{TG_T} = \frac{C_0 + C_1 s + C_2 s^2}{D_0 + D_1 s + D_2 s^2 + D_3 s^3} \quad (2.14.)$$

where:

$$\left. \begin{aligned} C_0 &= \frac{\alpha_u^* W^o}{\mu_u} \left[\frac{A(B+C) + BC}{\mu_g \mu_c} + \frac{\alpha_c^*}{\alpha_u^*} \cdot \frac{AB}{\mu_g \mu_c} \right] \\ C_1 &= \frac{\alpha_u^* W^o}{\mu_u} \left(\frac{A+B}{\mu_g} + \frac{B+C}{\mu_c} \right) \\ C_2 &= \frac{\alpha_u^* W^o}{\mu_u} \\ D_0 &= \frac{ABC}{\mu_u \mu_g \mu_c} \\ D_1 &= \frac{AB}{\mu_u \mu_g} + \frac{A(B+C)}{\mu_u \mu_c} + \frac{A(B+C)+BC}{\mu_g \mu_c} \\ D_2 &= \frac{A}{\mu_u} + \frac{A+B}{\mu_g} + \frac{B+C}{\mu_c} \\ D_3 &= 1 \end{aligned} \right\} \quad (2.15.)$$

2.3. Reactor stability

Fig. 2.4. represents the block diagram of the reactor and its overall temperature feedback:

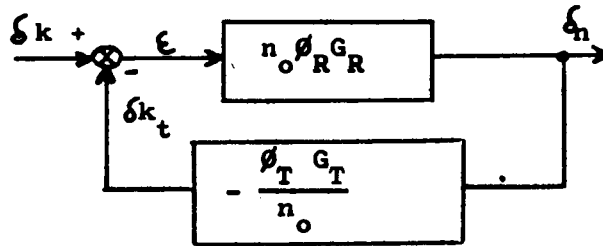


Fig. 2.4.

The sign $\phi_T G_T$ has been reversed in order to conserve the usual servo-language convention for the closed-loop feedback transfer equation.

$$\frac{\xi_n}{n_o \delta k} = \phi_{RT} G_{RT} = \frac{\phi_R G_R}{1 + \phi_R \phi_T G_R G_T} \quad (2.16.)$$

To examine the reactor stability, it is necessary to employ the Nyquist plots of the open-loop transfer function: $\phi_R \phi_T G_R G_T$.

Eqs. (2.1.) and (2.14.) give with a reversed sign for (2.14.)

$$\phi_R \phi_T G_R G_T = \frac{E_0 + E_1 s + E_2 s^2 + E_3 s^3}{F_1 s + F_2 s^2 + F_3 s^3 + F_4 s^4 + F_5 s^5} \quad (2.17.)$$

where:

$$\left| \begin{array}{l} E_0 = -A_0 C_0 \\ E_1 = -(A_0 C_1 + A_1 C_0) \\ E_2 = -(A_0 C_2 + A_1 C_1) \\ E_3 = -A_1 C_2 \end{array} \right. \quad \left| \begin{array}{l} F_1 = B_1 D_0 \\ F_2 = B_1 D_1 + D_0 \\ F_3 = B_1 D_2 + D_1 \\ F_4 = B_1 + D_2 \\ F_5 = 1 \end{array} \right.$$

In Figs. 3 and 4 are reported the Bode diagrams of the open-loop transfer functions of the 250-MWe prototype with initial core and equilibrium core.

Fig. 2.5. gives the shapes of the corresponding Nyquist plots:

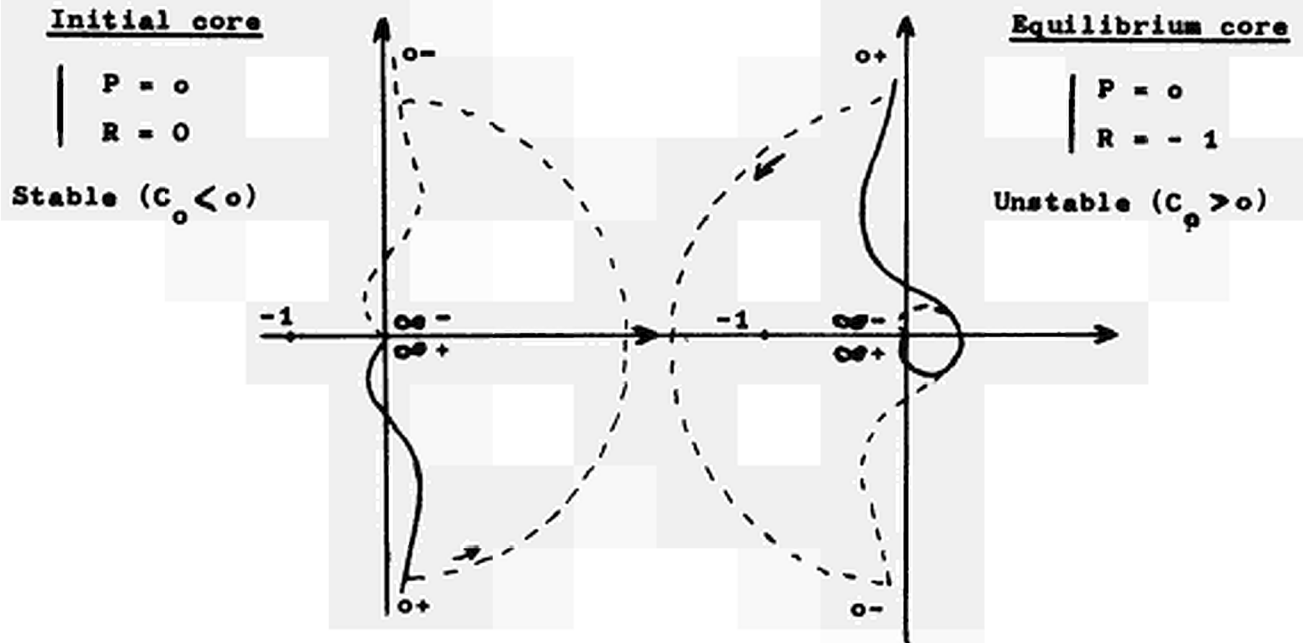


Fig. 2.5.

It can be seen that the initial core is stable, the equilibrium core unstable, the stability depending only on the sign of C_o .

Indeed, when $s = j\omega \rightarrow +\infty$

$$\phi_{RT} \phi_{RT}^{G_T} \sim \frac{E_o}{F_1 s} = \frac{A_o C_o j}{B_1 D_o} \rightarrow \infty$$

A_o, B_1, D_o are positive quantities; thus:

$$\text{si } C_o > 0 \quad \phi_{RT} \phi_{RT}^{G_T} \rightarrow +\infty$$

$$\text{si } C_o < 0 \quad \phi_{RT} \phi_{RT}^{G_T} \rightarrow -\infty$$

The closure of the diagram from $\omega = +0$ and $\omega = -0$ is always achieved in the counterclockwise sense with an angular rotation of π ($F_1 \neq 0$).

The stability condition is: $C_0 = 0$. Taking again the expression of C_0 (Eq. 2.15.), this condition becomes:

$$-\frac{\alpha_c^*}{\alpha_u^*} = 1 + C \left(\frac{1}{A} + \frac{1}{B} \right)$$

Substituting the values of A, B and C given by the Eqs. (2.8., 2.9. and 2.10.):

$$-\frac{\alpha_c^*}{\alpha_u^*} = \frac{T_u^0 - T_i}{T_c^0 - T_i} \quad (2.18.)$$

and combining Eqs. (2.5.), (2.6.) and (2.18.),

the stability condition is thus:

$$-\frac{\alpha_c}{\alpha_u} < l_s \quad (2.19.)$$

where $l_s = 2 \frac{\gamma_u}{\gamma_c} \cdot \frac{T_u^0 - T_c^0}{T_o^0 - T_i} + 1$

The stability is independent of the reactor power level for a constant flow steady-state program. It can be verified that this limit is unchanged for six groups of delayed neutrons. For a negative fuel temperature coefficient and a positive coolant temperature coefficient, the greater is the fuel temperature and the smaller is the coolant span ($\Delta T = T_o - T_i$), the more the reactor is stable.

The γ_u and γ_c coefficients take the axial statistical weight of the temperatures into account and the "representative" channel take the radial statistical weight of the temperatures into account; the coolant temperatures are independent of the radial statistical weight because of the constant coolant temperature span in every channel.

For a cosine axial flux:

$$\left| \begin{array}{l} \gamma_u = \frac{4}{3} \\ \gamma_c = 1 \end{array} \right.$$

$$\text{and } l_s = \frac{8}{3} \cdot \frac{T_u^o - T_c^o}{\Delta T} + 1 \quad (2.20.)$$

In this case, the coolant temperatures are thus independent from the radial and axial statistical weight; as the fuel temperature coefficient is negative, the statistical weight of the fuel temperatures has a stabilizing effect.

In Fig. 5 are reported the stability limits in the following cases:

Representative channel: $\gamma_u = \frac{4}{3}$, $\gamma_c = 1$
(with axial statis. weight)

Averaged channel (with axial statistical weight): $\gamma_u = \frac{4}{3}$, $\gamma_c = 1$

Averaged channel (without axial statistical weight): $\gamma_u = \gamma_c = 1$

In a logarithm plot, the difference between these cases is small, and a good pessimistic and easy approximation is to take the second case. The numerical results are given in the following table:

250-MWE prototype

$$T_i = 266^\circ\text{C}$$

$$T_c^o = 318^\circ\text{C}$$

$$T_u^o = 672,5^\circ\text{C} \text{ for the "representative" channel} \\ = 658^\circ\text{C} \text{ for the averaged channel}$$

	case 1	case 2	case 3
l_s	10.1	9.7	7.5

In Fig. 6 are reported the stability limits of the 100- and 250 MWe prototypes comparatively with the numerical previous results. The agreement is good.

100 MWe-prototype

$$T_i = 292^\circ\text{C}$$

$$T_c^o = 328^\circ\text{C}$$

$$T_u^o = 762^\circ\text{C}$$

$$l_s = 15.8$$

2.4. Reactor power coefficient

Taking again the reactor closed-loop transfer function (2.16.), and developing it with (2.1.) and (2.17) gives:

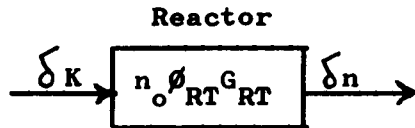


Fig. 2.6.

$$\frac{\delta n}{n_o \delta K} = \phi_{RT} G_{RT} = \frac{G_0 + G_1 s + \dots + G_5 s^5}{H_0 + H_1 s + \dots + H_6 s^6} \quad (2.21.)$$

where:

$G_0 = A_0 F_1$	$H_0 = E_0 B_1$
$G_1 = A_0 F_2 + A_1 F_1$	$H_1 = E_0 + (E_1 + F_1) B_1$
$G_2 = A_0 F_3 + A_1 F_2$	$H_2 = (E_1 + F_1) + (E_2 + F_2) B_1$
$G_3 = A_0 F_4 + A_1 F_3$	$H_3 = (E_2 + F_2) + (E_3 + F_3) B_1$
$G_4 = A_0 + A_1 F_4$	$H_4 = (E_3 + F_3) + F_4 B_1$
$G_5 = A_1$	$H_5 = F_4 + B_1$
	$H_6 = 1$

When C_0 is negative, the reactor is stable and all the coefficients H_0, H_1, H_2, H_3 and H_4 are positive (H_5 and H_6 are always positive) or all the roots of $(H_0 + H_1s + \dots + H_6s^6 = 0)$ are negative.

When C is positive, the reactor is unstable, H_0 at least is negative and the equation $(H_0 + \dots + H_6s^6 = 0)$ has at least one positive root.

$$(H_0 + H_1s + \dots + H_6s^6) = (B_1 + B_2s)(h_0 + h_1s + \dots + h_5s^5)$$

where

$$\left. \begin{aligned} h_0 &= E_0 \\ H_1 &= E_1 + F_1 \\ h_2 &= E_2 + F_2 \\ h_3 &= E_3 + F_3 \\ h_4 &= F_4 \\ h_5 &= 1 \end{aligned} \right\}$$

The problem comes to study the sign of the roots of the equation $(h_0 + h_1s + \dots + h_5s^5) = 0$.

For a reactivity input in step function:

when $t \rightarrow \infty$

where:

$$\frac{\delta n}{n_0 \delta K} \rightarrow \frac{G_0}{H_0} = - \frac{D_0}{C_0}$$

$$\frac{\delta K}{\delta n/n_0} = - \frac{C_0}{D_0}$$

Substituting the expressions of C_o and D_o gives (Eq. 2.15.):

$$\begin{aligned} -\frac{C_o}{D_o} &= \alpha_u^* \left[\frac{1}{A} + \frac{1}{B} + \frac{1}{C} \cdot \frac{\alpha_c^*}{\alpha_u^*} \right] \\ &= \alpha_u^* \left[\left(\frac{1}{A} + \frac{1}{B} + \frac{1}{C} \right) + \frac{1}{C} \cdot \frac{\alpha_c^*}{\alpha_u^*} \right] \\ &= -\alpha_u^* (T_u^o - T_i) - \alpha_c^* (T_c^o - T_i) \end{aligned}$$

then:

$$\frac{\delta K}{\delta n/n_o} = -\frac{\gamma_c (T_o - T_i)}{2} \cdot (\alpha_c + \alpha_u 1_s) \quad (2.22.)$$

Doing $\delta n/n_o = 1\%$, δK is the reactor power coefficient α_w :

$$\alpha_w (\text{p.c.m.}\%) = 10^{-2} \cdot \frac{\Delta T}{2} (\alpha_c + \alpha_u 1_s) \quad (2.23.)$$

with α_c and α_u in p.c.m./°C.

α_w is constant in the temperature coefficients plan on any parallel to the stability limit straight.

α_w is a measure of the reactor stability degree; it is negative for a stable reactor, positive for an unstable reactor.

Prototype	100 MWe		250 MWe	
	Initial	Equilibrium	Initial	Equilibrium
α_c pcm/°C	+ 1	+ 6	- 0.25	+ 5.0
α_u pcm/°C	- 1	- 0.26	- 1.5	- 0.45
α_w pcm/%	- 6	+ 1.45	- 8	+ 0.24

For a stable reactor, the power coefficient has an immediate signification: if a small and given amount of

positive reactivity δk is inserted into a stable reactor, the power, if allowed to be free, will stabilize itself at a superior level, the variation power being given by:

$$\delta n/n_0 = -\delta k/\alpha_w.$$

Example: in the case of the initial core of the 250-MWe prototype, when $\delta k = 50$ pcm, $\delta n/n_0 = 6,25\%$; Fig. 5 gives the lines corresponding to $\alpha_w = \pm 1, -10, -100$ pcm/%; Figs. 7 and 8 give the amplitude and phase of the closed-loop transfer functions of the initial and equilibrium core; Fig. 9 gives some analogue cases of verification of the power coefficient.

It should be recalled (Ref. 1, p.206-7) that the maximum initial value for $\delta n/n_0$ is given by:

$$\delta n_{\max}/n_0 = \frac{\delta k}{\beta - \delta k} \quad (2.24.)$$

when δk is small with respect to β , and neglecting, during this small initial time, the influence of the temperature coefficients.

In the present case,

$$\begin{aligned} \text{with } \beta &= 395.5 \text{ pcm} \\ l &= 5.4 \cdot 10^{-4} \text{ s} \\ \text{and when } \delta k &= 10 \text{ pcm:} \end{aligned}$$

$\delta n_{\max}/n_0 \approx 2.6\%$, the time constant of the initial peak being $1/(\beta - \delta k) = 0.14\text{s.}$; therefore, very small with respect to the fuel rod thermal time constant, that is 2 sec.

3. THE REACTOR CONTROL LOOP

An external control loop is needed, when the reactor is unstable. It can be operated as a proportional regulating system or an on-off type of regulating system. In a

proportional regulating system, the position of the control rod is changed proportionally to any error created, either by a power demand change, or by an internal system transient; in a discontinuous regulating system, no control is attained unless an error, which is greater than some fixed percentage, is set up in the control rod. It is known, and this has been verified on occasion of the analogue computation, that the on-off type control system is inadequate when the reactor by itself is inherently unstable, the presence of a dead zone involving the control system to be in continuous oscillation. Fig. 3.1. shows the servo-block diagram of reactor control loop used for stability analysis:

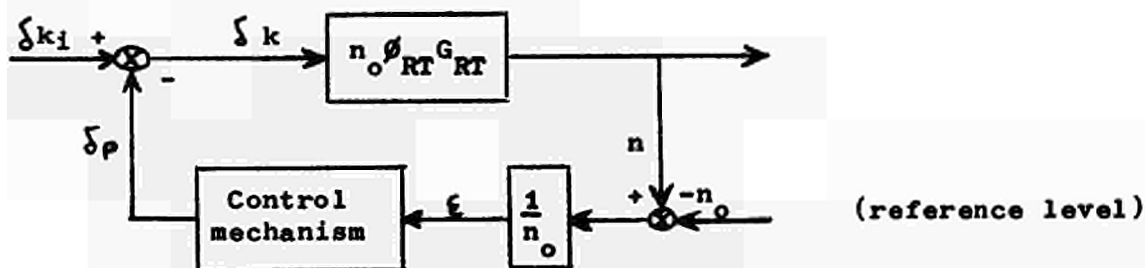


Fig. 3.1.

The reactor output is measured by a neutron detector; this power n is then compared with the reference power level, the activating error $\epsilon = \frac{n - n_0}{n_0}$ is amplified and finally controls an activator which moves the rod in order to obtain the necessary antireactivity to eliminate ϵ . During the reactivity change Δk_1 , it can be assumed that the power level demand n_0 does not change. The rod is affected by a time constant τ .

We can assume that the reactivity to be inserted is generated according to the general equation:

$$\Delta \rho = \frac{R_1 + \frac{R_2}{s} + R_3 s}{1 + \tau s} \epsilon \quad (R_1, R_2, R_3 > 0)$$

where:

R_1 is a proportional term

R_2 is an integral term

R_3 is a differential term

The problem consists in determining the terms or a combination of these necessary terms to stabilize the reactor.

3.1. Effect of a proportional term

We only have:

$$\phi_c G_c = \frac{\delta p}{\xi} = \frac{R_1}{1 + \tau s} \quad (3.1.)$$

Considering the block diagram of Fig. 2.1. where

$$\left\{ \begin{array}{l} \delta k = \delta k_i - \delta p \\ \delta p = \xi \phi_c G_c \\ \xi = \delta n / n_o \\ \delta n = n_o \phi_{RT} G_{RT} \delta k \end{array} \right.$$

the closed-loop transfer function of the reactor control system is:

$$\frac{\delta n}{n_o \delta k_i} = \frac{\phi_{RT} G_{RT}}{1 + \phi_c \phi_{RT} G_c G_{RT}} \quad (3.2.)$$

For stability problems, it is necessary to study the Nyquist plots of the open-loop transfer function:

$$\frac{\delta n}{n_o \xi} = \phi_c \phi_{RT} G_c G_{RT}$$

Eqs. (2.21.) and (3.1.) give:

$$\frac{\delta n}{n_o \xi} = \frac{R_1 (G_o + G_1 s + \dots + G_5 s^5)}{(1 + \tau s) (H_o + H_1 s + \dots + H_6 s^6)}$$

or using the following notation:

$$\frac{\sum n}{n_0 \varepsilon} = \frac{R_1 (G_0 + \dots + G_5 s^5)}{J_0 + \dots + J_7 s^7} \quad (3.3.)$$

where:

$$\left. \begin{aligned} J_0 &= H_0 \\ J_1 &= \tau H_0 + H_1 \\ J_2 &= \tau H_1 + H_2 \\ J_3 &= \tau H_2 + H_3 \\ J_4 &= \tau H_3 + H_4 \\ J_5 &= \tau H_4 + H_5 \\ J_6 &= \tau H_5 + H_6 \\ J_7 &= \tau H_6 \end{aligned} \right\}$$

The study of the limits of $G_c G_{RT}$ and of $\operatorname{tg} (\varphi_c \varphi_{RT})$ when $s \longrightarrow +0$ or $+\infty$ gives in all cases the following elements of the Nyquist diagram:

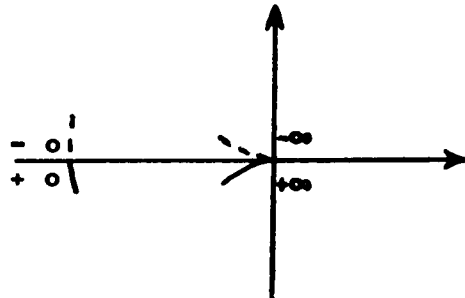


Fig. 3.2.

Fig. 3.3. gives the complete shape of the Nyquist diagrams in the case of the 250-MWe prototype for two values of τ : 1 and 10 sec.

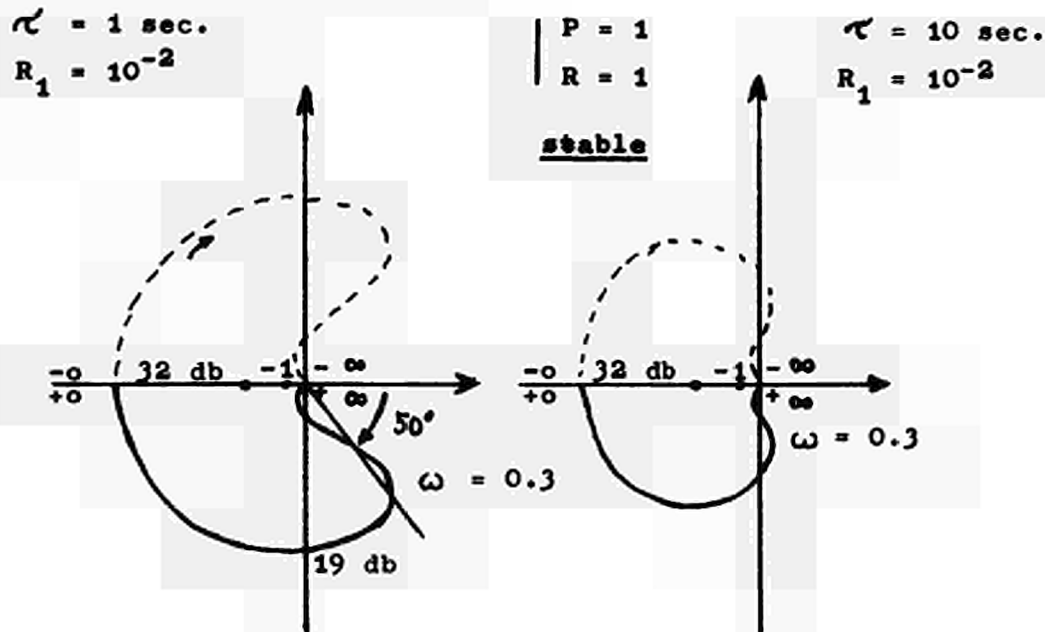


Fig. 3.3.

There is stability if the point (-1) is enclosed or when $s \rightarrow +0$

$$\frac{\int_{\omega} \frac{D_n}{n_o \xi} \rightarrow \frac{R_1 G_o}{H_o} = -R_1 \frac{D_o}{C_o} \quad (\text{with } C_o > 0)$$

The stability condition is then:

$$R_1 \frac{D_o}{C_o} > 1 \quad \text{where} \quad R_1 > \frac{C_o}{D_o}$$

In Figs. 10 and 11 are reported the corresponding Bode diagrams. The stability is better for small values of τ because of the greater enclosure of the point (-1); however, the inertia time constant is not a sensitive parameter from a stability point of view. For illustration are reported in Figs. 10 and 11 the Bode diagrams of the 100-MWe prototype: the results are about the same; this allows to conclude that the thermal time constant of the fuel bed (2 sec. in the case of

the 250 MWe, 5 sec. in the case of the 100 MWe) has no significant influence on the inertia time constant of the control rod.

$$\begin{aligned} \frac{\delta n}{n_0 \xi} &= \frac{R_1}{1 + \tau s} \beta_{RT} G_{RT} \\ &= \frac{R_1}{1 - j\omega\tau} \beta_{RT} G_{RT} \end{aligned}$$

Fig. 11 and the previous expression show that the phase loss is equal to 45° when τ is varied from 0 to 1 sec. (for $\omega = 1$); it is equal to $(\arctg 10 - \arctg 1) \approx 40^\circ$ when τ is varied from 1 to 10 sec.

Fig. 3.4. gives an idea of the stability system in function of the inertia time constant of the bar; a reasonable value is τ equal to 1 sec.

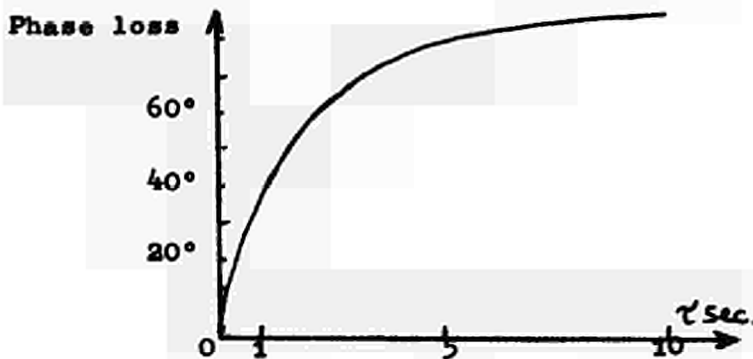


Fig. 3.4.

Taking the reactor control system closed-loop transfer function (3.2.) and developing it, gives:

$$\frac{\delta n}{n_0 \delta k_1} = \beta_{RTC} G_{RTC} = \frac{L_0 + \dots + L_{12} s^{12}}{K_0 + \dots + K_{13} s^{13}} \quad (3.4.)$$

For an input δk_1 in step function, when

$t \rightarrow \infty$

$$\frac{\delta n}{n_0 \delta k_1} \rightarrow \frac{L_0}{K_0} = \frac{G_0 J_0}{H_0 (R_1 G_0 + J_0)}$$

where $\frac{\delta ki}{\delta n/n_0} \rightarrow (R_1 - \frac{C_0}{D_0})$ with R_1 greater than $\frac{C_0}{D_0}$

Substituting the expression of C_0 and D_0 , as it has already been done:

$$10^{-2} \frac{\delta ki}{\delta n/n_0} = R_1 - \alpha_w$$

This relation might be:

$$\alpha'_w = \alpha_w - R_1 \quad (3.5.)$$

where α_w is the power coefficient for the unstable reactor
 α'_w is the power coefficient for the unstable reactor made stable by the proportional term.

For instance, for the equilibrium core of the 250-MWe prototype

$$\alpha_w = + 0.24 \text{ pcm/\%}.$$

If we want to stabilize it in the conditions of the initial core, it must be taken $\alpha'_w = - 8 \text{ pcm/\%}$ and, for this, take $R_1 = 8.24 \text{ pcm/\%} = 0.824 \cdot 10^{-2}$

These relations have been verified by the DYNOR code, as shown in Fig. 12.

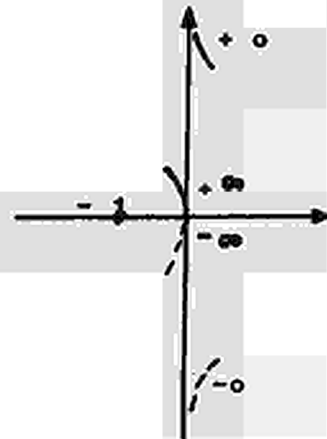
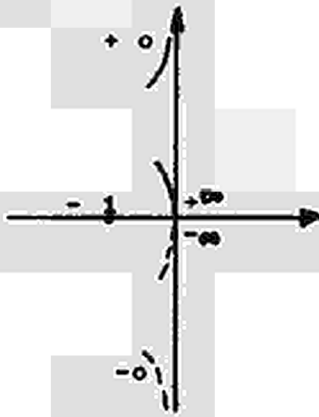
3.2. Effect of an integral term

In this case:

$$\theta_c G_c = \frac{R_2}{s(1 + \tau s)}$$

$$\frac{\delta n}{n_0 \epsilon} = \frac{R_2 (G_0 + \dots + G_5 s^5)}{s (J_0 + \dots + J_7 s^7)}$$

The study of the asymptotic and low frequency limits when $\omega \rightarrow 0$ or $\omega \rightarrow \infty$ gives the following elements of the Nyquist diagram:



$J_1 > 0$ where

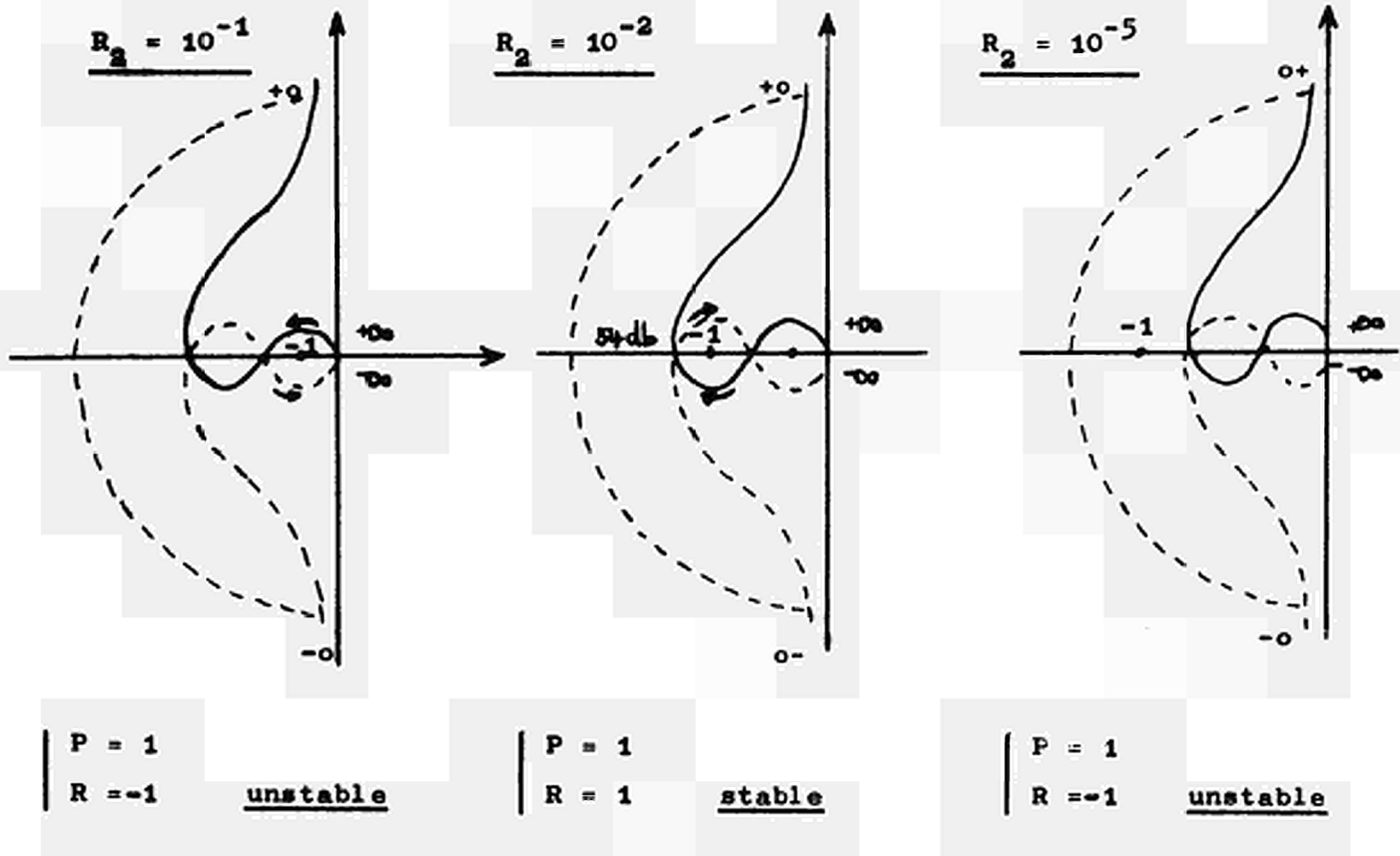
$J_1 < 0$ with $J_0/J_1 < G_0/G_1$

$J_1 < 0$ with $J_0/J_1 > G_0/G_1$

Fig. 3.5.

The following figure gives the shapes of the Nyquist diagram for the 250-MWe prototype:

Fig. 3.6.



The system is stable only for a certain range of amplitude values.

3.3. Effect of a proportional term and an integral term

In this case:

$$\phi_{cc} G_c = \frac{R_1 s + R_2}{s(1 + \tau s)}$$

$$\begin{aligned} \frac{\delta n}{n_0 \xi} &= \frac{(R_2 + R_1 s) (G_0 + \dots + G_5 s^5)}{s(J_0 + \dots + J_7 s^7)} \\ &= \frac{I_0 + \dots + I_6 s^6}{J_0 s + \dots + J_7 s^8} \end{aligned}$$

where

$$\begin{aligned} I_0 &= R_2 G_0 \\ I_1 &= R_1 G_0 + R_2 G_1 \\ I_2 &= R_1 G_1 + R_2 G_2 \\ I_3 &= R_1 G_2 + R_2 G_3 \\ I_4 &= R_1 G_3 + R_2 G_4 \\ I_5 &= R_1 G_4 + R_2 G_5 \\ I_6 &= R_1 G_5 \end{aligned}$$

It can be seen that the amplitude does not change when R_1 is fixed and the ratio R_2/R_1 constant.

The study of the limits when $s \rightarrow 0$ or ∞ gives the following elements:

$$R_2/R_1 < \frac{1}{\tau} + \beta/1$$

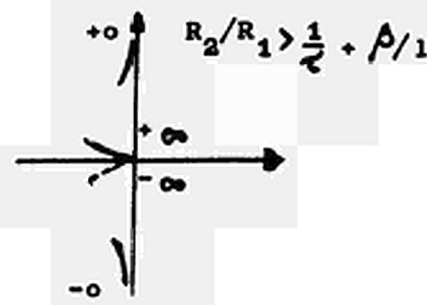
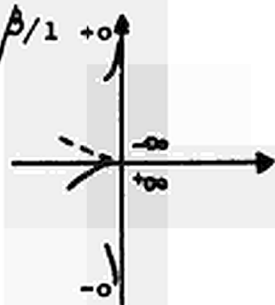
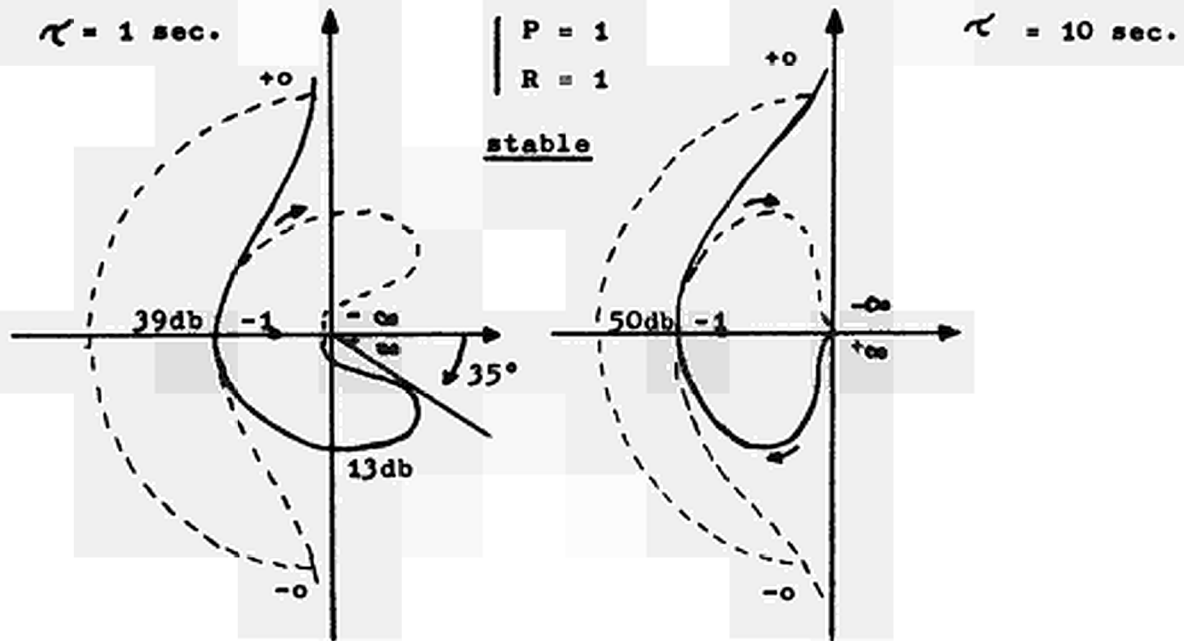


Fig. 3.7.

In Figs. 13 and 14 are reported the Bode diagrams of the 250-MWe prototype for τ equal to 1 and 10 sec. and R_1 equal to 10^{-2} for R_2/R_1 equal to 1/10.

The following figure gives the shape of the corresponding Nyquist diagrams:



A stability limit is at least:

$$\frac{R_2}{R_1} < \frac{1}{\tau} + \beta/1$$

(see Fig. 3.7.)

ORGEL prototype $\tau = 1 \text{ sec.}$	100 MWe	250 MWe
$\frac{1}{\tau} + \beta/1$ in sec.^{-1}	6	8

$$\begin{aligned}
 \phi_C \phi_{RT}^G \phi_C^G \phi_{RT}^G &= \left(R_1 + \frac{R_2}{s} \right) \phi_{RT}^G \phi_{RT}^G \\
 &= R_1 \left(1 - \frac{R_2}{R_1 \omega} \right) \phi_{RT}^G \phi_{RT}^G
 \end{aligned}$$

When R_1 and τ are fixed:

- R_1 determined in order to obtain a reasonable value for α'_w (about - 10 pcm/%);
- τ chosen as minimum possible mechanical value (about 1 sec.);

the amplitude rises and the phase is reduced when the ratio R_2/R_1 increases as it is shown by the previous expression (see also Figs. 13 and 14); a compromise value is then necessary for the R_2/R_1 ratio.

It is interesting to compare Figs. 3.3. and 3.8. (for $\tau = 1$ sec.), where the R_1 value is equal in the two cases: it can be seen that the stability is about the same (similar values are obtained for the amplitude and the phase around the point -1) taking $R_2/R_1 = 1/10$ in the second case; if R_2/R_1 is greater than 1/10, the amplitude rises, but the phase loss is increased; it seems that R_2/R_1 equal to about 1/10 constitutes an optimum value (for $R_2/R_1 = 1/10$ and $\omega = 0,5$, the phase loss is $\arctg \frac{1}{5} \approx 10^\circ$).

Fig. 15 illustrates these results in good agreement with the optimization point of the control loop chosen after analogue computation. Taking again the close-loop transfer function of the reactor (3.2.) where: $\phi_{CC}^G = \frac{1}{s(1 + \tau s)}$ for an input δk_i in step function:

$$\frac{\delta n/n_0}{\delta k_i} \sim \frac{s}{R_2} \rightarrow 0 \text{ when } t \rightarrow \infty$$

The integral term leads back the power level to its initial value.

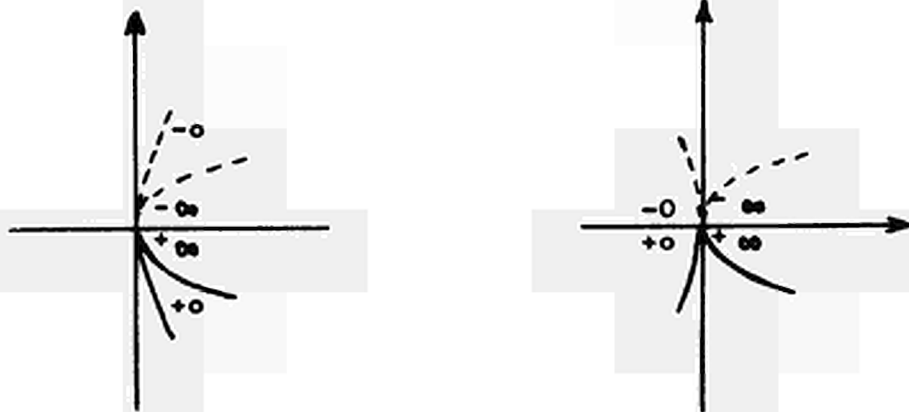
3.4. Effect of a differential term

3.4.1. Differential term alone:

$$\phi_C^{G_C} = \frac{R_3 s}{1 + \tau s}$$

$$\frac{\delta n}{n_0 \xi} = \frac{R_3 s (G_0 + \dots + G_5 s^5)}{J_0 + \dots + J_7 s^7}$$

The study of the amplitude and phase limits give the following elements of diagram:

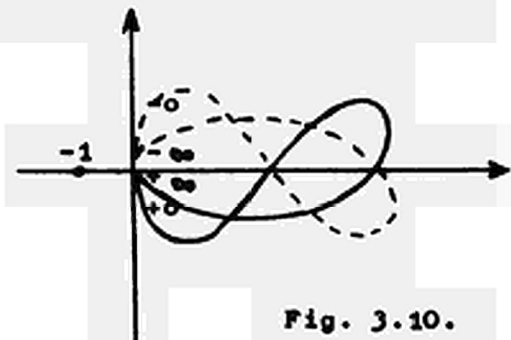


$$\left| \begin{array}{l} J_1 > 0 \text{ where} \\ J_1 < 0 \text{ with } J_1/J_0 < G_1/H_0 \end{array} \right.$$

$$\left| \begin{array}{l} J_1 < 0 \text{ with } J_1/J_0 > G_1/H_0 \end{array} \right.$$

Fig. 3.9.

The corresponding Nyquist plot of the 250-MWe prototype is the following:



The system is always unstable.

Fig. 3.10.

3.4.2. Combination of a proportional and differential term

$$\phi_C^{G_C} = \frac{R_1 + R_3 s}{1 + \tau s}$$

$$\frac{\delta n}{n_o \xi} = \frac{(R_1 + R_3 s) (G_o + \dots + G_5 s^5)}{J_o + \dots + J_7 s^7}$$

when $\omega \rightarrow +0$

$$\frac{\delta n}{n_o \xi} \rightarrow \frac{R_1 G_o}{H} = -R_1 \frac{D_o}{C_o} \quad (\text{identical limit for the proportional term alone}).$$

When $\omega \rightarrow +\infty$

$$\frac{\delta n}{n_o \xi} \sim -\frac{R_3 G_5}{J_7} \cdot j \rightarrow -\infty$$

$$\text{tg}(\phi_C \phi_{RT}) \sim \frac{-\omega}{(H_5 + 1/\tau) - (R_1/R_3 + G_4/G_5)} \rightarrow -\infty$$

when $(H_5 + 1/\tau) > (R_1/R_3 + G_4/G_5)$

The following Nyquist plot can be obtained:

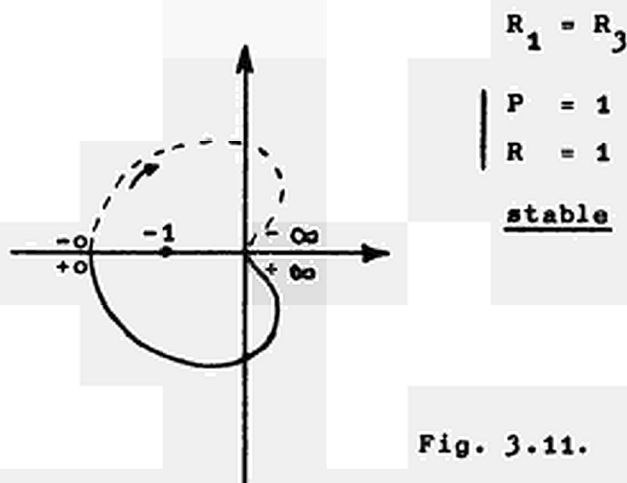


Fig. 3.11.

The system is stable if the condition $R_1 > \frac{C_o}{D_o}$ is satisfied (closure condition of the point -1).

3.4.3. Combination of proportional, integral and differential terms

$$\phi_{CC}^{GC} = \frac{R_1 + R_2/s + R_3 s}{1 + \tau s}$$

$$\frac{\delta n}{n_o \xi} = \frac{(R_2 + R_1 s + R_3 s^2) (G_o + \dots + G_5 s^5)}{s (J_o + \dots + J_7 s^7)}$$

A first necessary stability condition is $R_2/R_1 < \frac{1}{\tau} + \frac{\beta}{1}$ because of the instability of the differential term.

When $\omega \rightarrow + 0$

$$\frac{\delta n}{n_o \xi} \rightarrow +\infty \quad (J_o < 0)$$

$$\text{tg} (\phi_{C\phi_{RT}}) \rightarrow -\infty$$

When $\omega \rightarrow + \infty$

$$\frac{\delta n}{n_o \xi} \rightarrow -0$$

$$\text{tg} (\phi_{C\phi_{RT}}) \sim \frac{\omega}{R_1/R_2 - (\frac{1}{\tau} + \frac{\beta}{1})} \quad \text{when}$$

$$\frac{R_1}{R_2} < \frac{1}{\tau} + \frac{\beta}{1}$$

For $R_1 = P = R$ we have obtained the following Nyquist plot, always in the \dots :

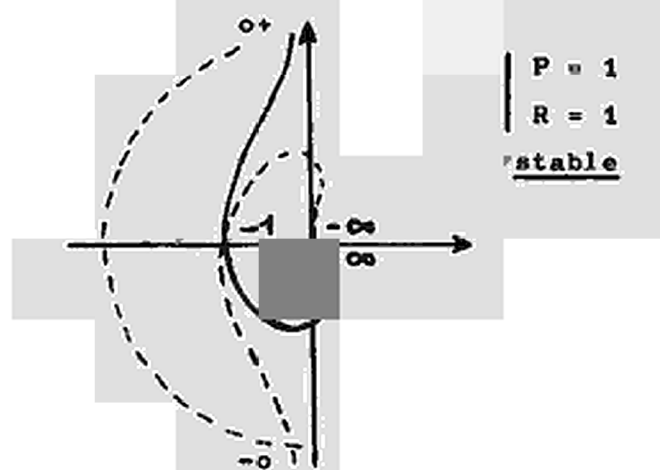


Fig. 3.12.

3.5. Conclusions

They are resumed in the following table:

Transfer function of the control mechanism (inertia = 0)	Stability	Stability conditions	Permanent response to a step function δk_i
R_1	stable	$R_1 > \alpha_w$	$\frac{\delta n}{n_0} = \frac{\delta k_i}{R_1 - \alpha_w}$
R_2/s	stable	stable only in a certain range of amplitude values	$\frac{\delta n}{n_0} = 0$
$R_1 + R_2/s$	stable	$\frac{R_2}{R_1} < \frac{1}{\tau} + \frac{\beta}{1}$	$\frac{\delta n}{n_0} = 0$
R_3s	unstable		
$R_1 + R_3s$	stable	$R_1 > \frac{C_0}{D_0}$	$\frac{\delta n}{n_0} = \frac{\delta k_i}{R_1 - \alpha_w}$
$R_1 + R_2/s + R_3s$	stable	$\frac{R_2}{R_1} < \frac{1}{\tau} + \frac{\beta}{1}$	$\frac{\delta n}{n_0} = 0$

It appears that:

- the proportional term is the stabilizing term;
- the integral term leads back the power level to its initial value (reset);
- the differential term is without interest for stability point of view (it brings nothing).

**4. STUDY OF THE TRANSIENT RESPONSE OF THE REACTOR WITHOUT CONTROL
TO A REACTIVITY STEP**

Let us now search the transient response of the reactor to its noise.

The transfer function of the reactor is the following (Eq. 2.21.):

$$\phi_{RT}^{G_{RT}} = \frac{\delta n(s)/n_0}{\delta k(s)} = \frac{G_0 + \dots + G_5 s^5}{H_0 + \dots + H_6 s^6}$$

The reactor noise is simulated by a unit-step function of amplitude δk , so that:

$$\delta k(s) = \frac{\delta k}{s}$$

$$\delta n(s)/n_0 = \delta k \cdot \frac{G_0 + \dots + G_5 s^5}{s(H_0 + \dots + H_6 s^6)}$$

The inverse transform of this equation will give the transient response of the reactor.

We have:

$$s(H_0 + \dots + H_6 s^6) = s(B_1 + s)(h_0 + \dots + h_5 s^5)$$

$$\delta n(s)/n_0 = \frac{Z_0}{s} + \frac{Z_1}{s + s_1} + \frac{Z_2}{s + s_2} + \frac{Z_3}{s + s_3} + \frac{Z_4}{s + s_4} + \frac{Z_5}{s + s_5} + \frac{Z_6}{s + s_6}$$

where:

$$s_1 = B_1 > 0$$

s_2, s_3, s_4, s_5, s_6 are the roots with reversed signs of the equation $(h_0 + \dots + h_5 s^5) = 0$

s_2, s_3, s_4, s_5 are positive values and s_6 is a positive value for the unstable core.

The solutions are the following:

For the initial stable core:

$$\delta n(t)/n_0 = \delta k(Z_0 + \sum_{i=1}^6 a_i e^{-s_i t})$$

where Z_0 is $\frac{G_0}{H_0} = -\frac{D_0}{C_0} = -\frac{1}{\alpha_w}$, then:

$$\delta n(t)/n_0 = -\frac{\delta k}{\alpha_w} + \delta k \sum_{i=1}^6 a_i e^{-s_i t}$$

When $t \rightarrow +\infty$, $\delta n/n_0 \rightarrow -\frac{\delta k}{\alpha_w}$, we have again the relation (2.22.), as expected.

For the unstable equilibrium core:

$$\delta n(t)/n_0 = -\frac{\delta k}{\alpha_w} + \delta k \left(\sum_{i=1}^5 a_i e^{-s_i t} + a_6 e^{-s_6 t} \right) \quad (4.1.)$$

where s_6 has alone a negative value.

This last case is the most important one and has been studied numerically: the calculation of the roots of the equation $(h_0 + \dots + h_5 s^5) = 0$ has allowed to check that the time constants $1/s_1, 1/s_2, 1/s_3, 1/s_4, 1/s_5$ are inferior to the second and very small with respect to $-1/s_6$; this signifies that, in expression (4.1.), after a time near but superior to the second, the sum $\sum_{i=1}^6 a_i e^{-s_i t}$ becomes negligible with respect to the other terms and that the power variation is then only given by:

$$\delta n/n_0 \approx -\frac{\delta k}{\alpha_w} + \delta k a_6 e^{-s_6 t} \text{ for } t > 1 \text{ sec.}$$

It is verified that the time constant $\theta = 1/s_6$ is about equal to $-\frac{h_1}{h_0} \approx \frac{B_1 D_0}{A_0 C_0} = \frac{1}{C_2 \alpha_w}$ where C_2 is a constant (for an averaged group of delayed neutrons).

We then have:

$$\left(\delta n/n_0 + \frac{\delta k}{\alpha_w} \right) \approx c_1 \delta k e^{c_2 \alpha_w t} \quad \text{for } t > 1 \text{ sec.}$$

c_1 and c_2 being two characteristical constants of the reactor, where c_1 must be taken as $1/\beta$ for $\delta k \ll \beta$ (see 2.24.).

In a semi-logarithmic plot, the representation of the quantity $(\delta n/n_0 + \delta k/\alpha_w)$ as function of the time is then linear, the slope of the representative straight line being proportional to the power coefficient and its ordinate to the origin being proportional to the amplitude step; these properties are checked effectively in Fig. 16 where are reported for the 250 MW-e prototype the power variations (given by the digital DYNOR code) which result from a loss of control simultaneously with a reactivity injection for two power coefficients about double: the searched linearity is verified well until power variations reaching 20%; it must be seen that an overpower of 10% is reached in 15 sec. when the power coefficient is equal to 0.25 pcm/% and in about 12 sec. when this power coefficient is double, this for a reactivity step of 10 pcm.

5. VARIATION OF THE POWER COEFFICIENT IN FUNCTION OF THE COOLANT FLOW

It has been assumed till now that the coolant input temperature and flow are constant. Let us search what is the variation of the power coefficient when the coolant flow is reduced because of the stop of a primary pump.

5.1. The reactor power is constant

At the equilibrium: Δt has increased in an inversely proportional manner to the flow; the difference $(T_U - T_G)$, proportional to the power, remains unchanged; the difference $(T_G - T_C)$ has

increased inversely as the flow (which is the same as assuming the cladding-coolant transfer coefficient to be proportional to the flow).

Using again expression (2.20.) gives:

$$(l_s - 1) = \frac{8}{3} \left(\frac{T_U^\circ - T_G^\circ}{\Delta T} + \frac{T_G^\circ - T_C^\circ}{\Delta T} \right)$$

$$(l_s - 1) \neq C_3 M + C_4$$

where C_3 and C_4 are two constants

then:

$$dl_s = \frac{dM}{M} (l_s - m)$$

$$\text{with } m = \left(1 + \frac{8}{3} \cdot \frac{T_G^\circ - T_C^\circ}{\Delta T} \right) \quad (5.1.)$$

The differentiation of expression (2.23.) giving α_w leads finally, after reducing, to the following relation, valid for small flow variations:

$$\alpha_M = - \frac{d\alpha_w / \alpha_w}{dM/M} = \frac{1 + \frac{\alpha_u}{\alpha_c} m}{1 + \frac{\alpha_u}{\alpha_c} l_s} \quad (5.2.)$$

m being given by (5.1.).

5.2. The reactor power varies like the flow

At equilibrium, Δt is unchanged; the drop $(T_U - T_G)$ varies like the power; the drop $(T_G - T_C)$ is unchanged if the heat transfer coefficient varies directly as the flow; the same expression is found for dl_s , the stability limit not being related to the power.

Finally, we obtain the following relation giving the relative variation of the power coefficient for small variations of flow:

$$\alpha_{MW} = - \frac{d\alpha_W / \alpha_W}{dM/M} = \frac{-\frac{\alpha_u}{\alpha_c} (l_s - m)}{1 + \frac{\alpha_u}{\alpha_c} l_s} \quad (5.3.)$$

For the initial core of the 250 MWe prototype, to a decrease in flow of 10% corresponds a relative variation of α_M and α_{MW} , of about 2.5%. For the equilibrium core, to a decrease in flow of 10% corresponds a double value for the power coefficient.

5.3. Discussion

α_M and α_{MW} have been plotted in Fig. 17 in the logarithmic plan of the temperature coefficients for a negative decrement dM of flow.

- If the reactor is unstable:

The plot shows that α_M and α_{MW} are positive: $d\alpha_W / \alpha_W$ is then positive like $d\alpha_W$ since α_W is positive in the unstable zone: the new value of the power coefficient has then the same sign and a greater absolute value; the reactor instability can only increase in the event of a flow decrement, and this the more the nearer the running point in the temperature coefficient plan is located to the stability limit.

- If the reactor is stable:

Let us consider the case where α_M and α_{MW} are negative, then $d\alpha_W$ is positive since α_W is negative in the stable zone: α_W and $d\alpha_W$ having inversed signs, the reactor stability decreases and even, if the absolute value of $d\alpha_W$ becomes superior to that of α_W , the reactor initially stable can become unstable; in reality, this can happen only if the reactor stability is very weak; indeed, to obtain $d\alpha_W / \alpha_W = +1$ corresponding to a flow decrement of 10% for example, it is

necessary to take α_M or $\alpha_{MW} = -10$ and it can be seen in Fig.17 that the running point is located very near to the stability limit.

In the case where α_M is positive, the reactor stability increases weakly in the event of flow decrement, but this variation is not significant.

We can conclude that, generally, a flow decrement makes the reactor more unstable or less stable than the simultaneous effect of the power is not significant and that it is always of interest to take a couple of temperature coefficients not too closely situated to the stability limit.

6. CONCLUSIONS

In the following, we give the main results obtained in this study. The stability condition of the reactor is given by:

$$-\alpha_c / \alpha_u < l_s$$

where

$$l_s = \frac{8}{3} \cdot \frac{T_U - T_C}{\Delta T} + 1$$

T_U and T_C are the averaged temperatures of fuel and coolant in the representative channel; a good approximation is to take T_U and T_C as averaged temperatures of the averaged channel. ΔT is the coolant temperature span. The axial neutron flux is a cosine flux.

The reactor power coefficient is:

$$\alpha_w = 10^{-2} \cdot \frac{\Delta T}{2} (\alpha_c + \alpha_u l_s)$$

with α_w in pcm/% when α_c and α_u are in pcm/°C; in the temperature coefficients plan, α_w is constant on any parallel to the stability limit given by $-\alpha_c / \alpha_u = \frac{1}{l_s}$.

A proportional term R_1 in the control system is necessary to stabilize the unstable core. R_1 must be adjusted in order to obtain for the reactor a negative power coefficient of desired value α'_w so that:

$$R_1 = \alpha'_w - \alpha'_w$$

The inertia time constant of the bar is not a sensitive parameter for stability point of view. Usually, the thermal time constant of the fuel rod has not a significant influence on the inertia time constant of the control rod.

When the proportional term and the time constant of the bar are adjusted, an integral term R_2 is necessary to lead back the power level to its initial value.

In the case of the 100 and the 250 MWe studied prototypes, an optimum value for the ratio R_2/R_1 is about 1/10.

A differential term is without interest for stability point of view.

In case of control loss with a simultaneous injection of reactivity, the power of the unstable core after a time of about one second increases exponentially with a time constant varying inversely as the power coefficient.

A reduction of the coolant flow makes the reactor ^{less} stable or more unstable.

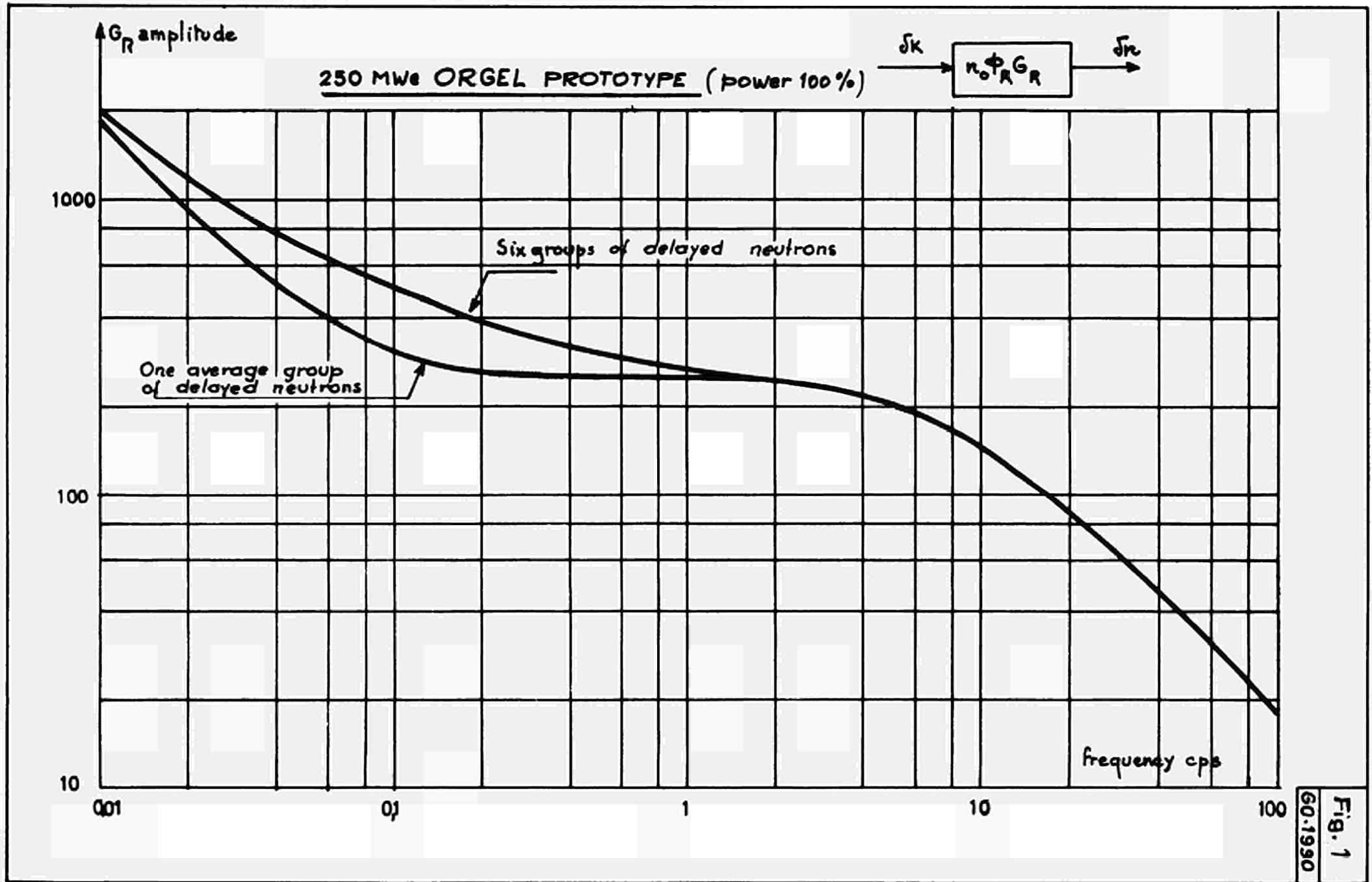
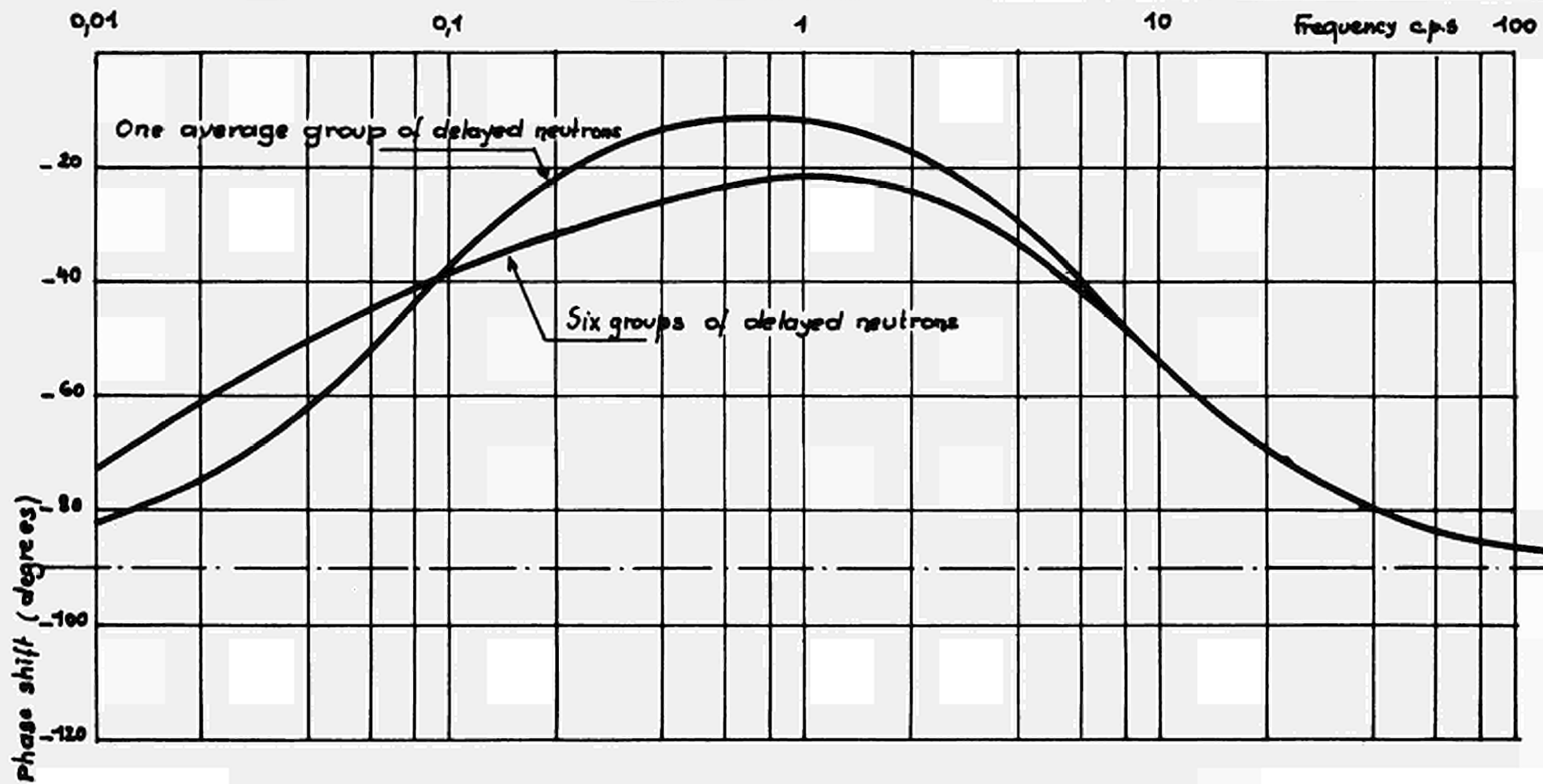


Fig. 1
 GO-1990

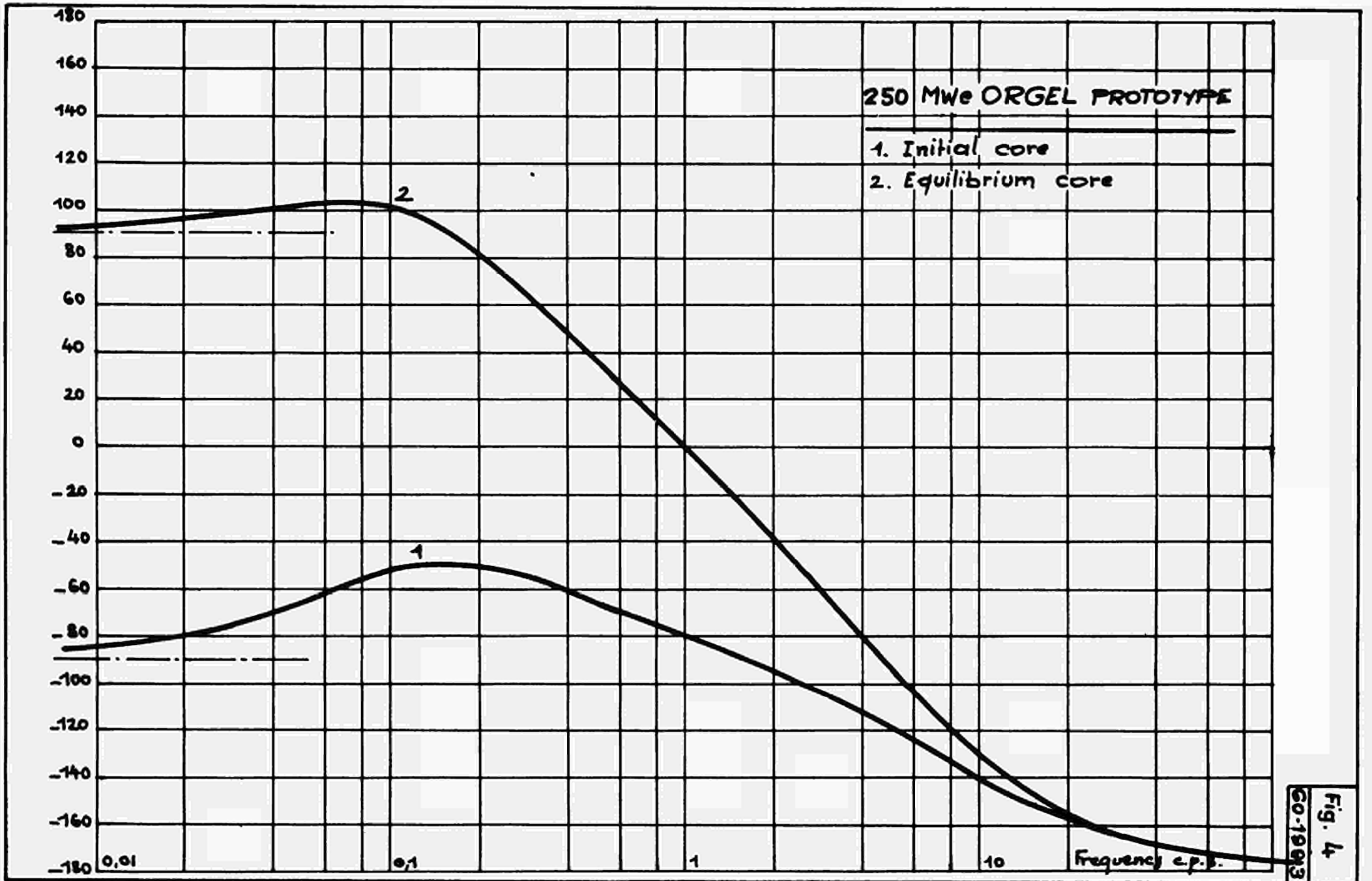


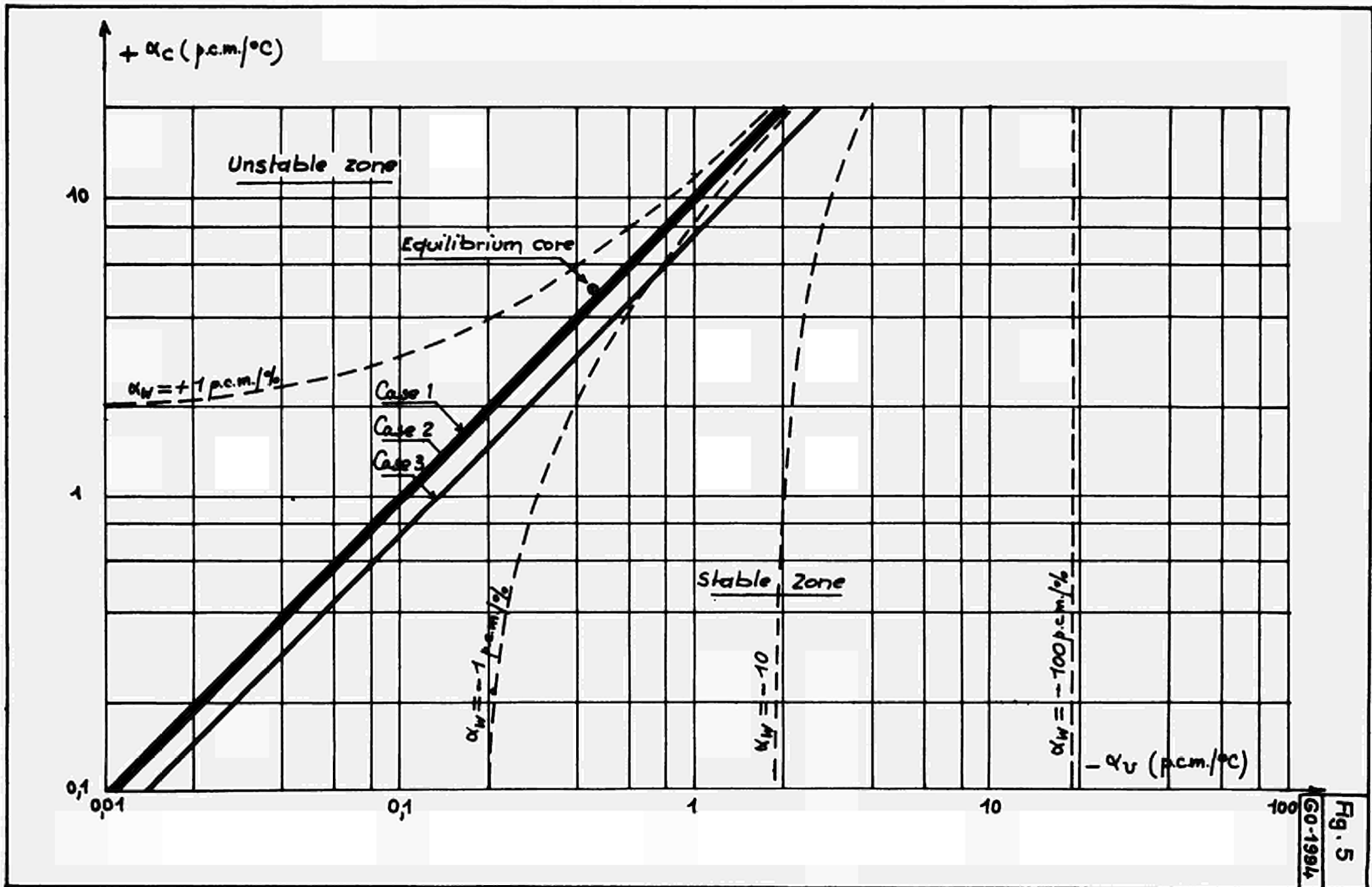
250 MW ORGEL PROTOTYPE (power 100%) $\delta K \rightarrow$ $K_0 + \beta_R G_R$ $\rightarrow \delta n$

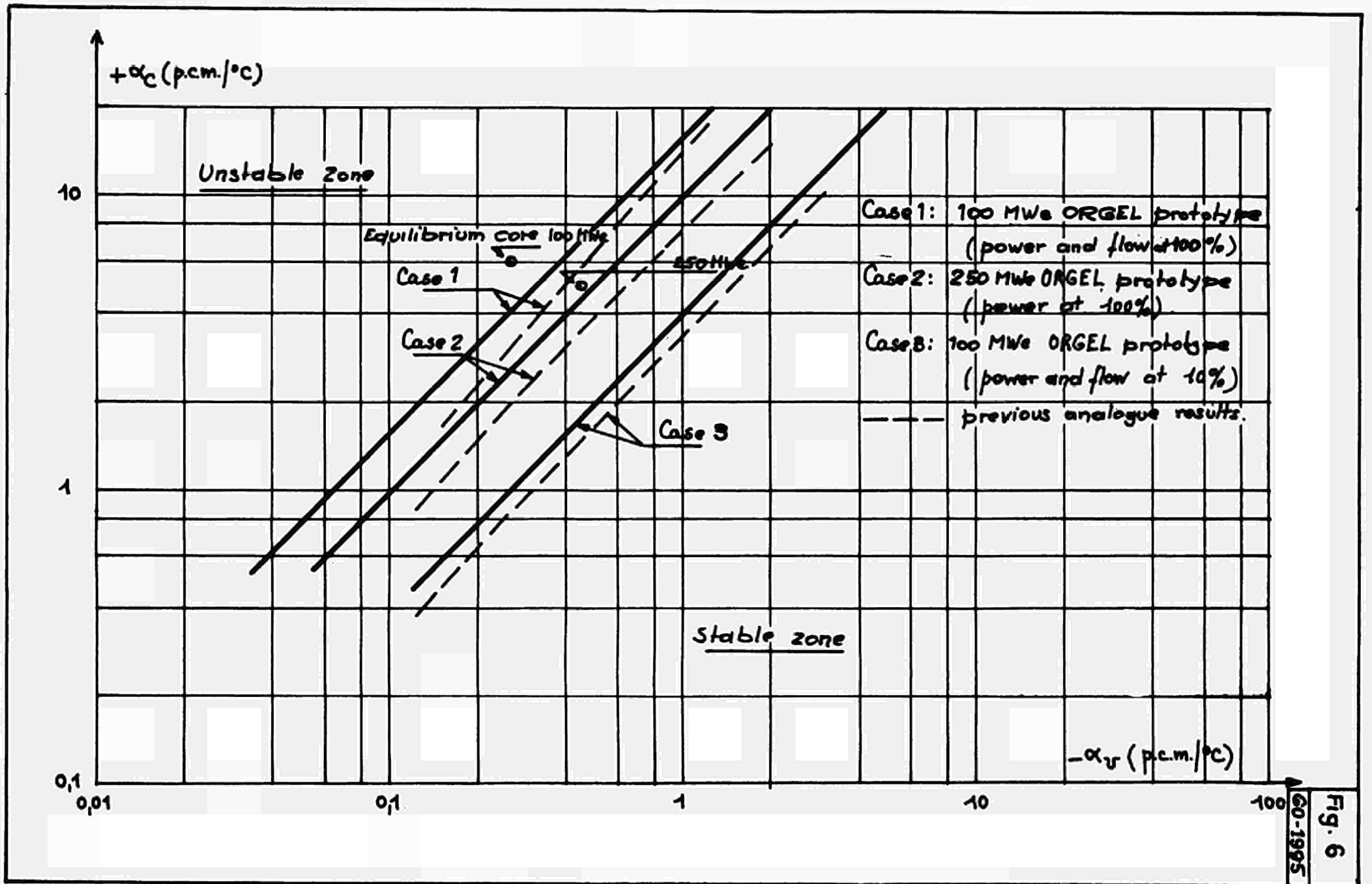
250 MWe ORGEL PROTOTYPE



- 1. Initial core
- 2. Equilibrium core







60-1995
Fig. 6

250 MWe ORGEL PROTOTYPE

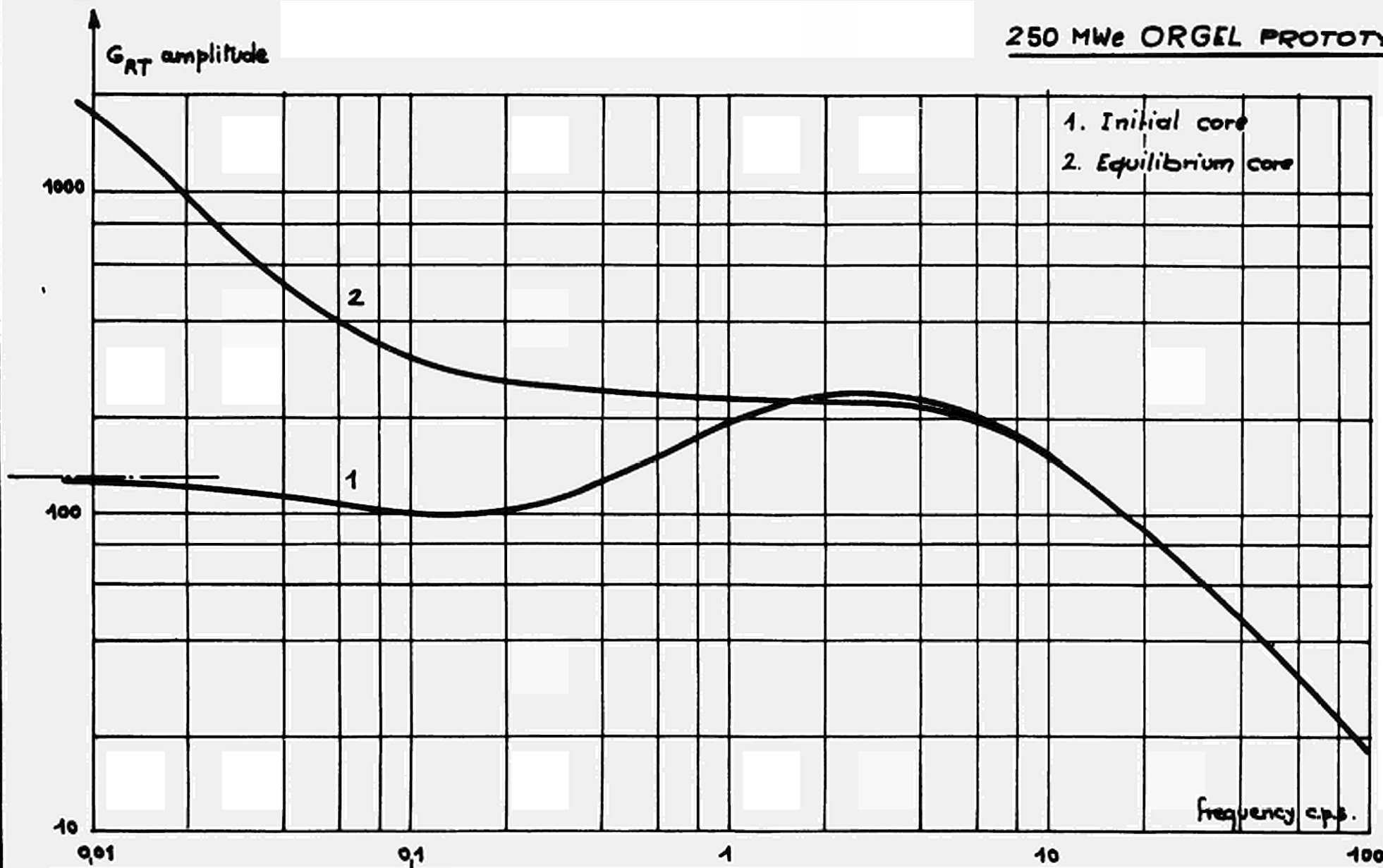


Fig. 7
GO-1996

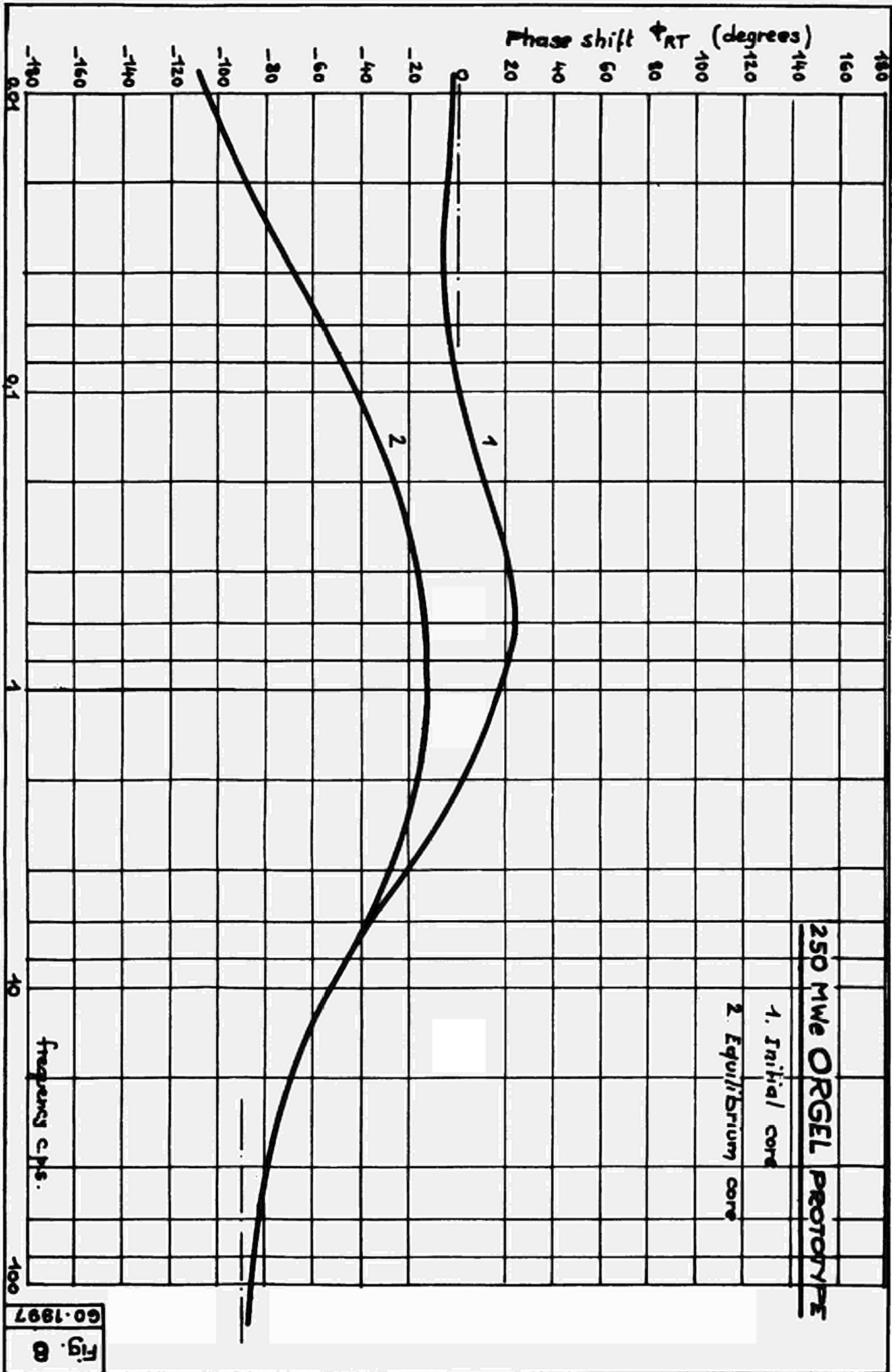
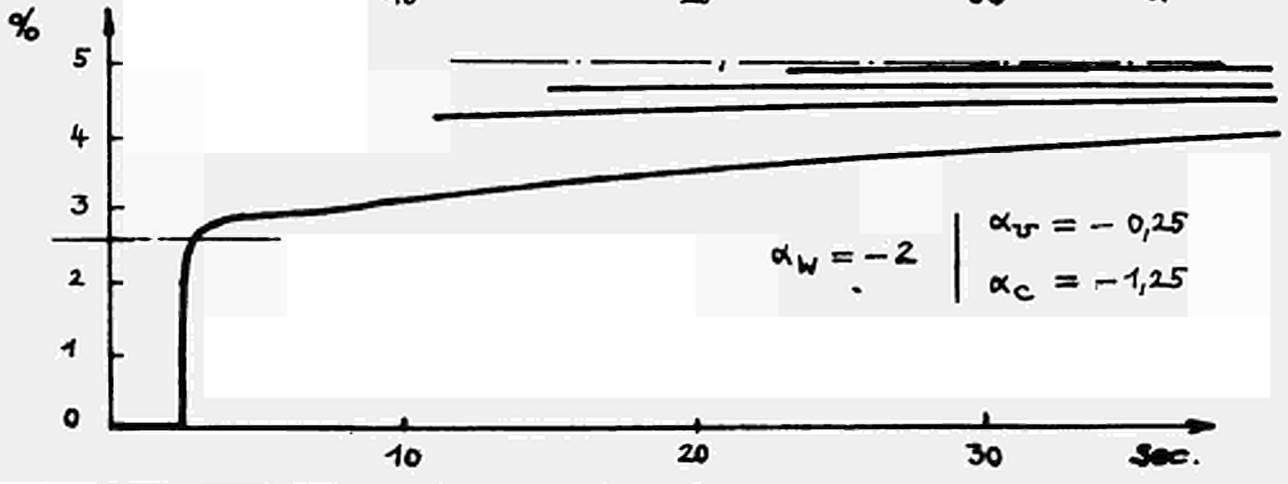
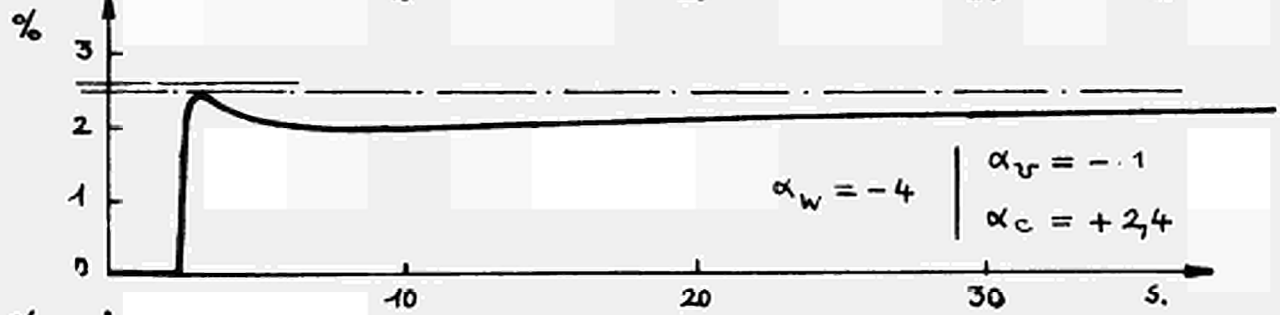
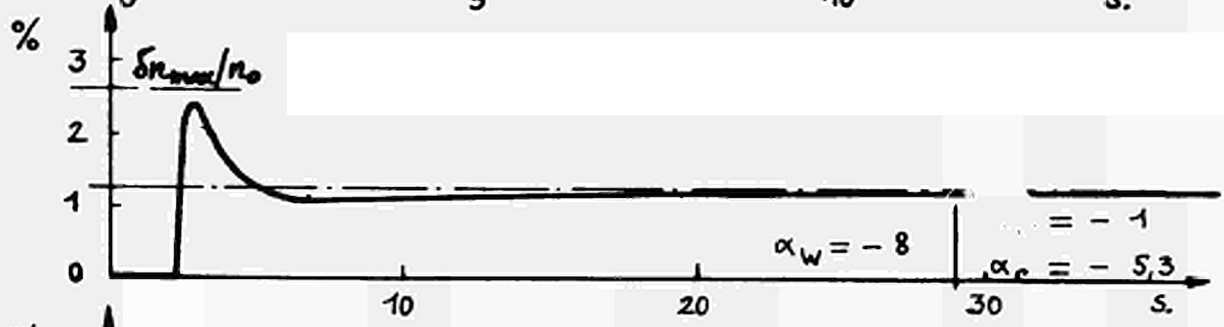
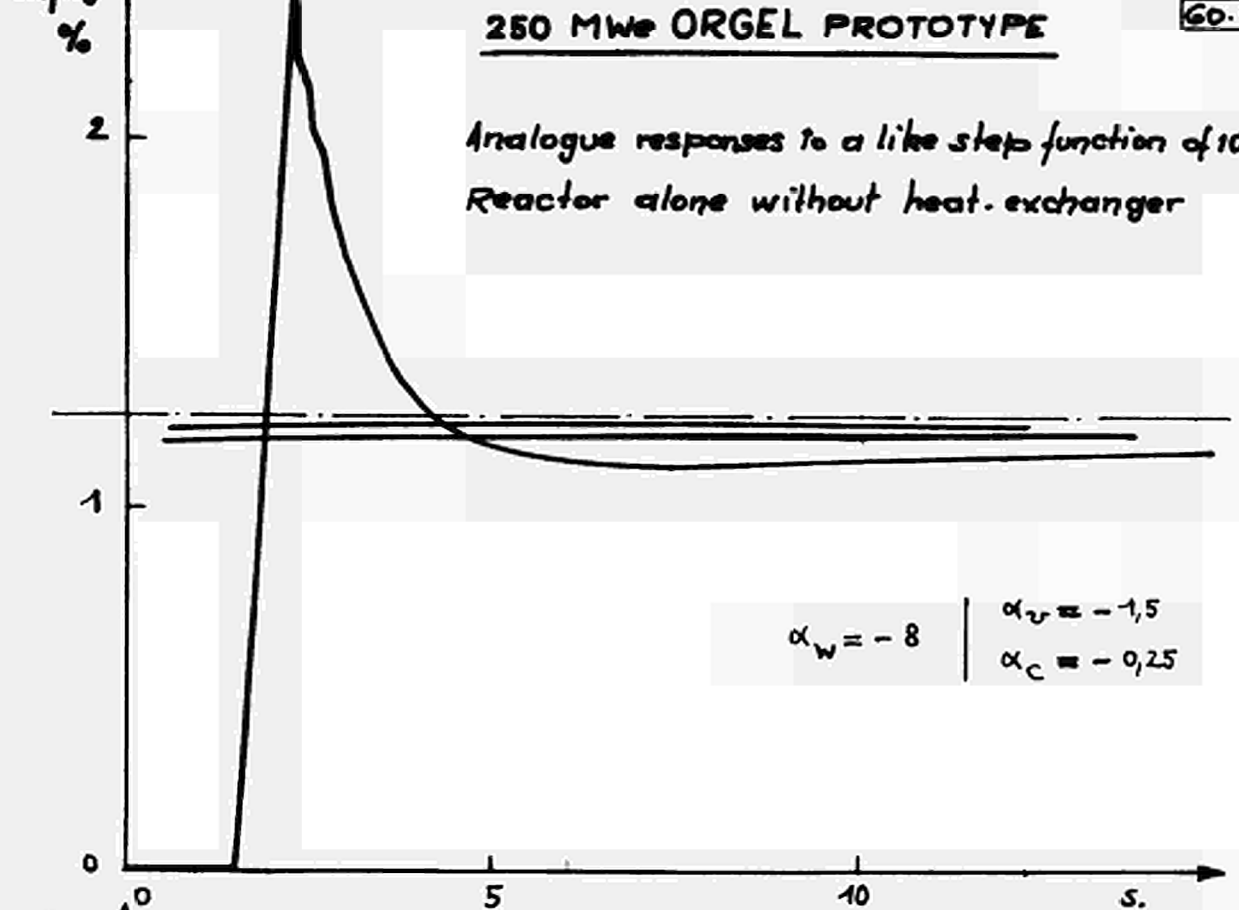


Fig. 8
60-1897

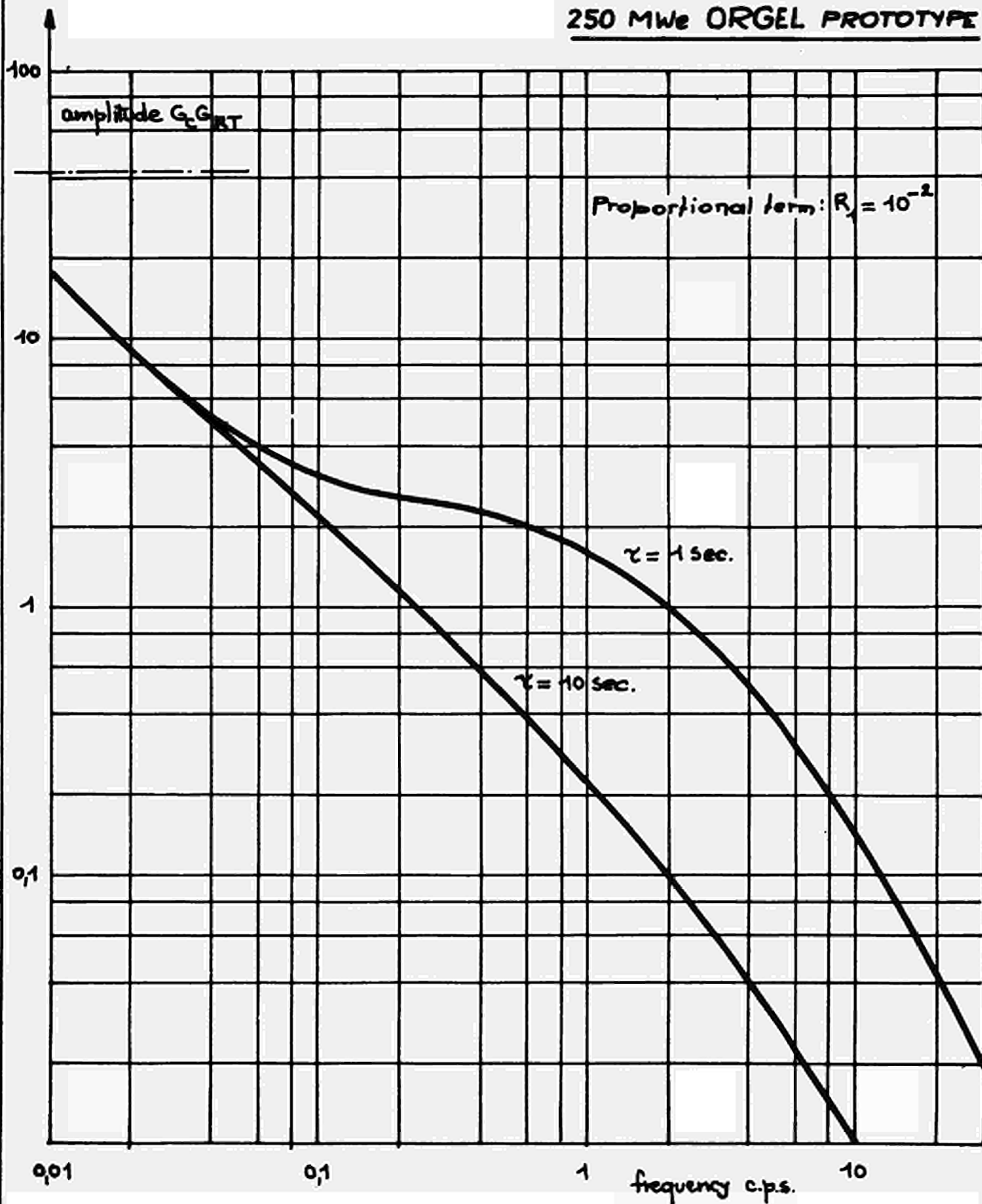
250 MWe ORGEL PROTOTYPE

Analogue responses to a like step function of 10 p.c.m.
Reactor alone without heat-exchanger

$$\frac{\delta n_{max}}{n_0} = \frac{\delta k}{\beta - \delta k}$$



250 MWe ORGEL PROTOTYPE



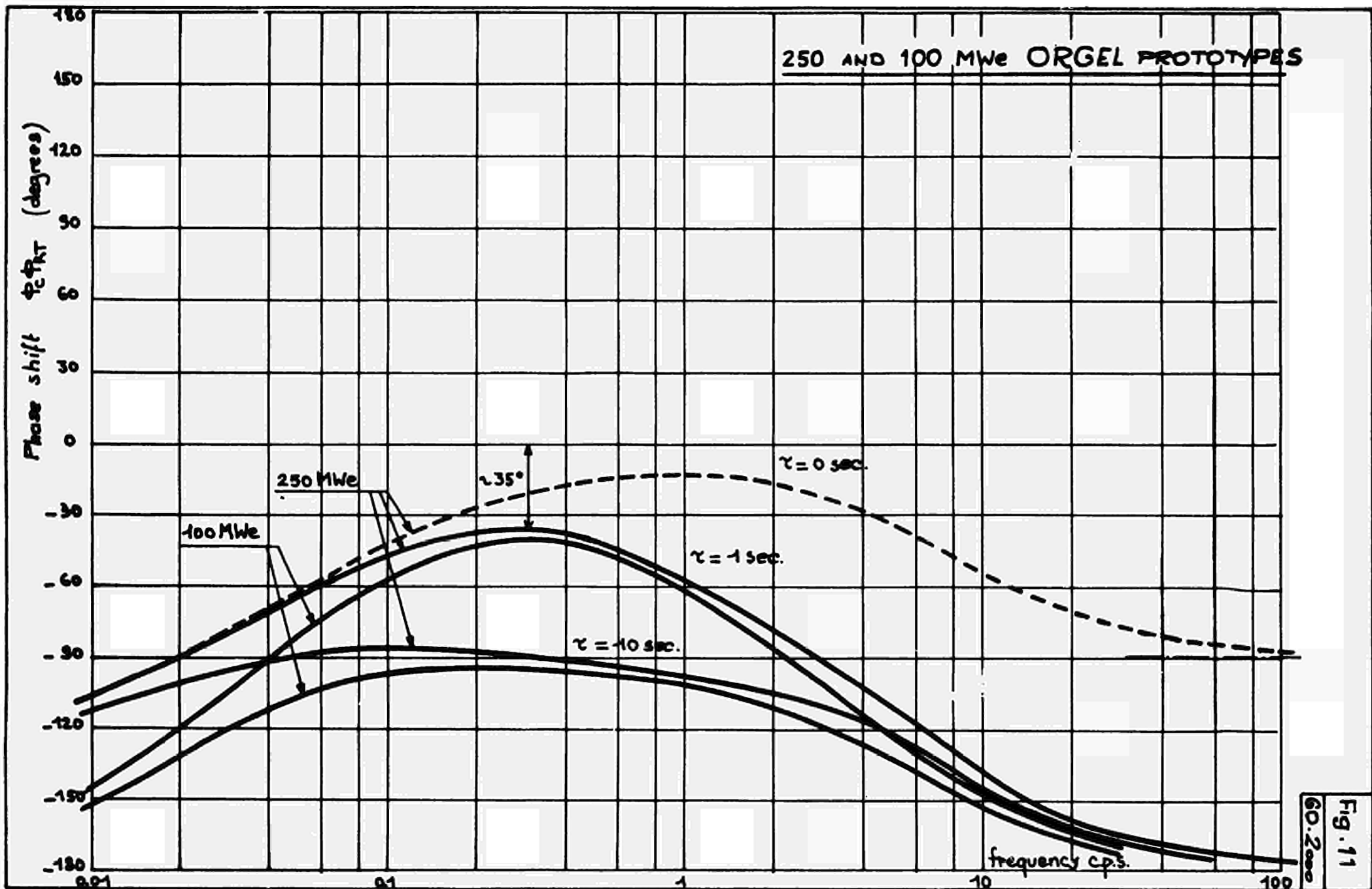


Fig. 11
60.2 sec

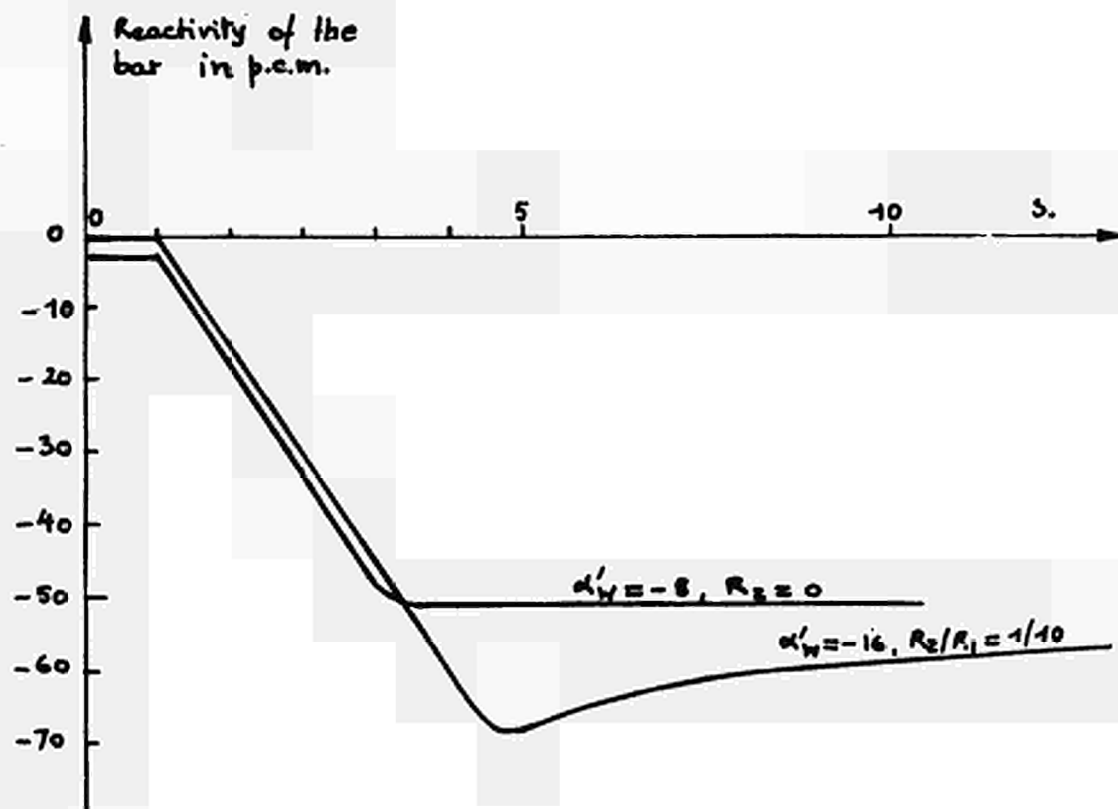
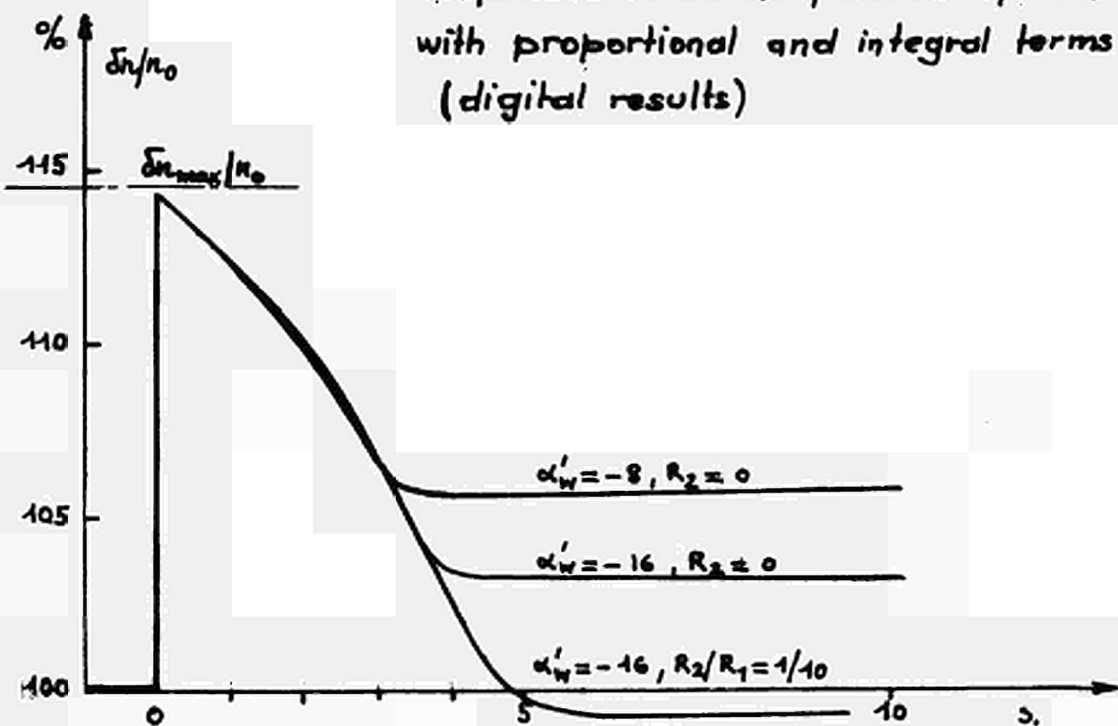
250 MWe ORGEL PROTOTYPE

Fig. 12

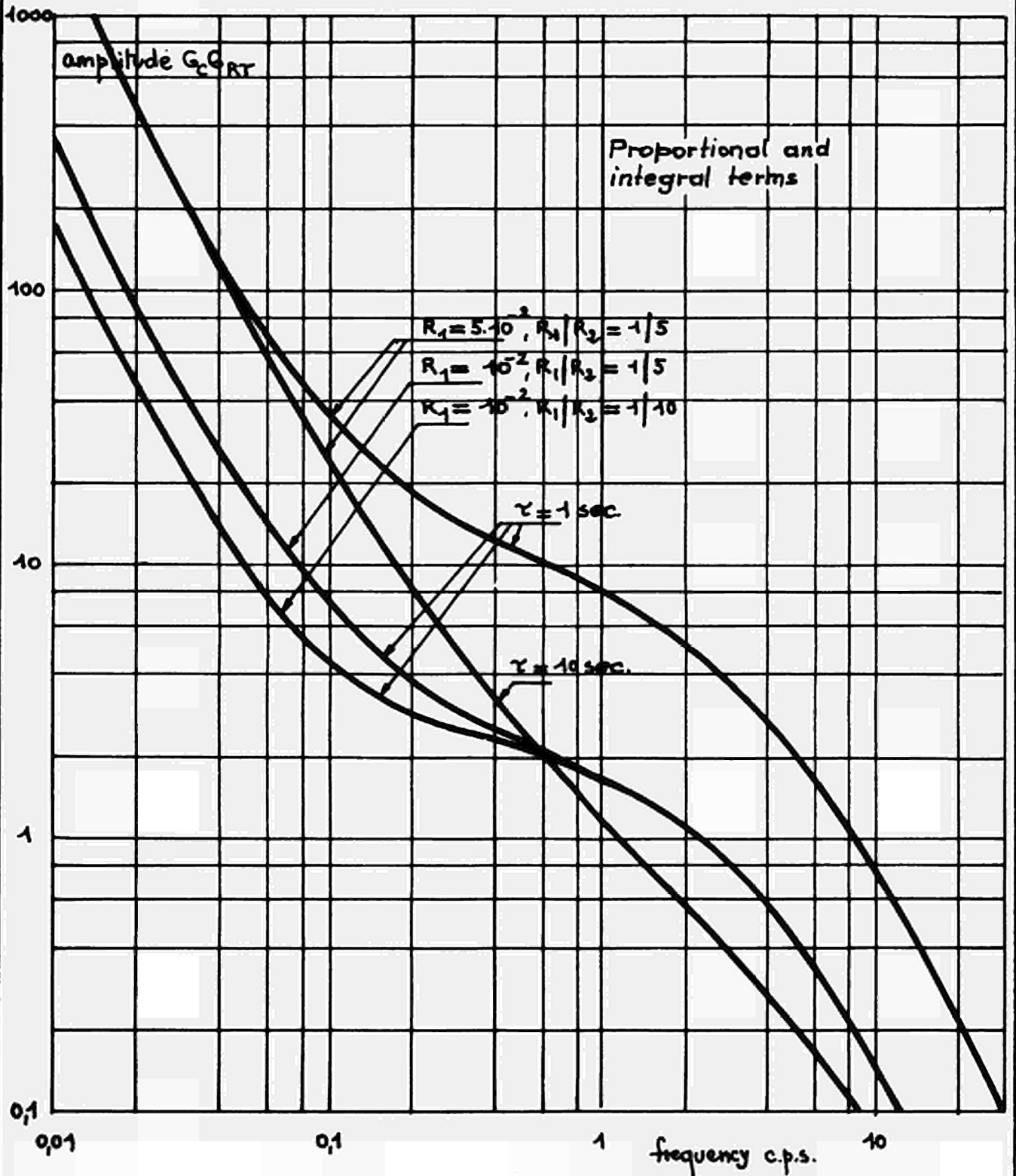
G.O.2001

Unstable equilibrium core

Responses to a step function of 50 p.c.m.
with proportional and integral terms
(digital results)



250 MWe ORGEL PROTOTYPE



250 MWe ORGEL PROTOTYPE

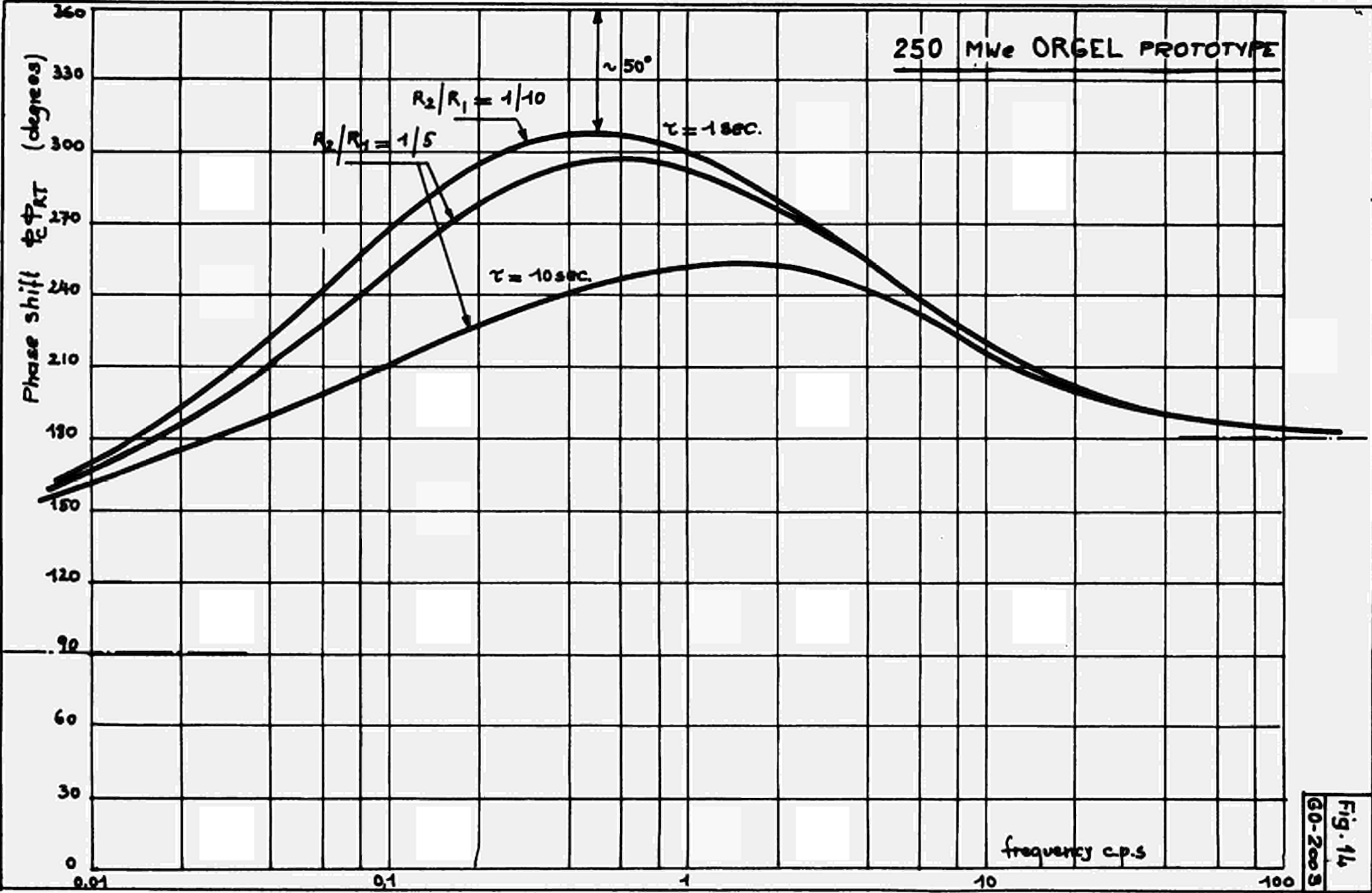
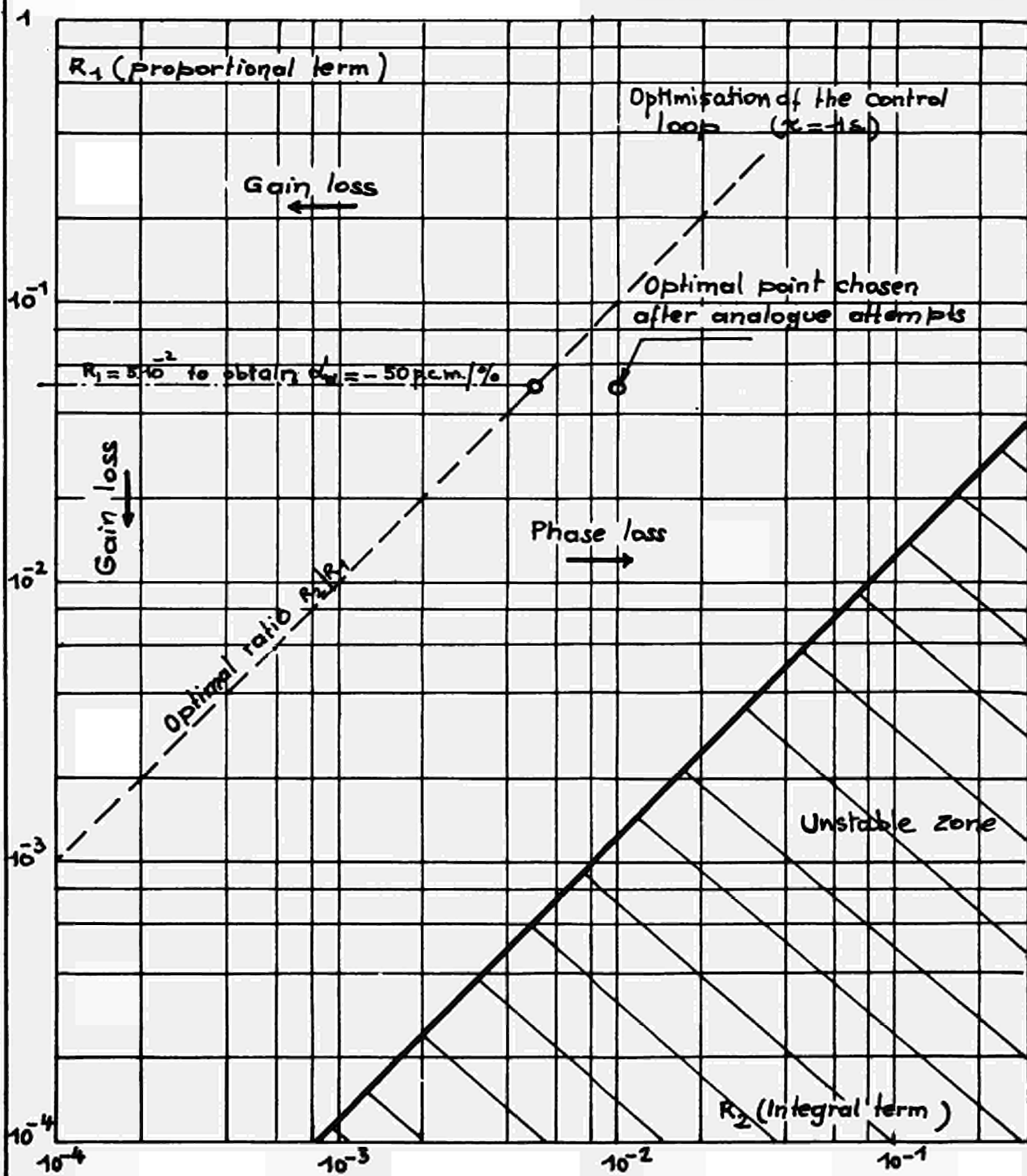


Fig. 14
GO-2009

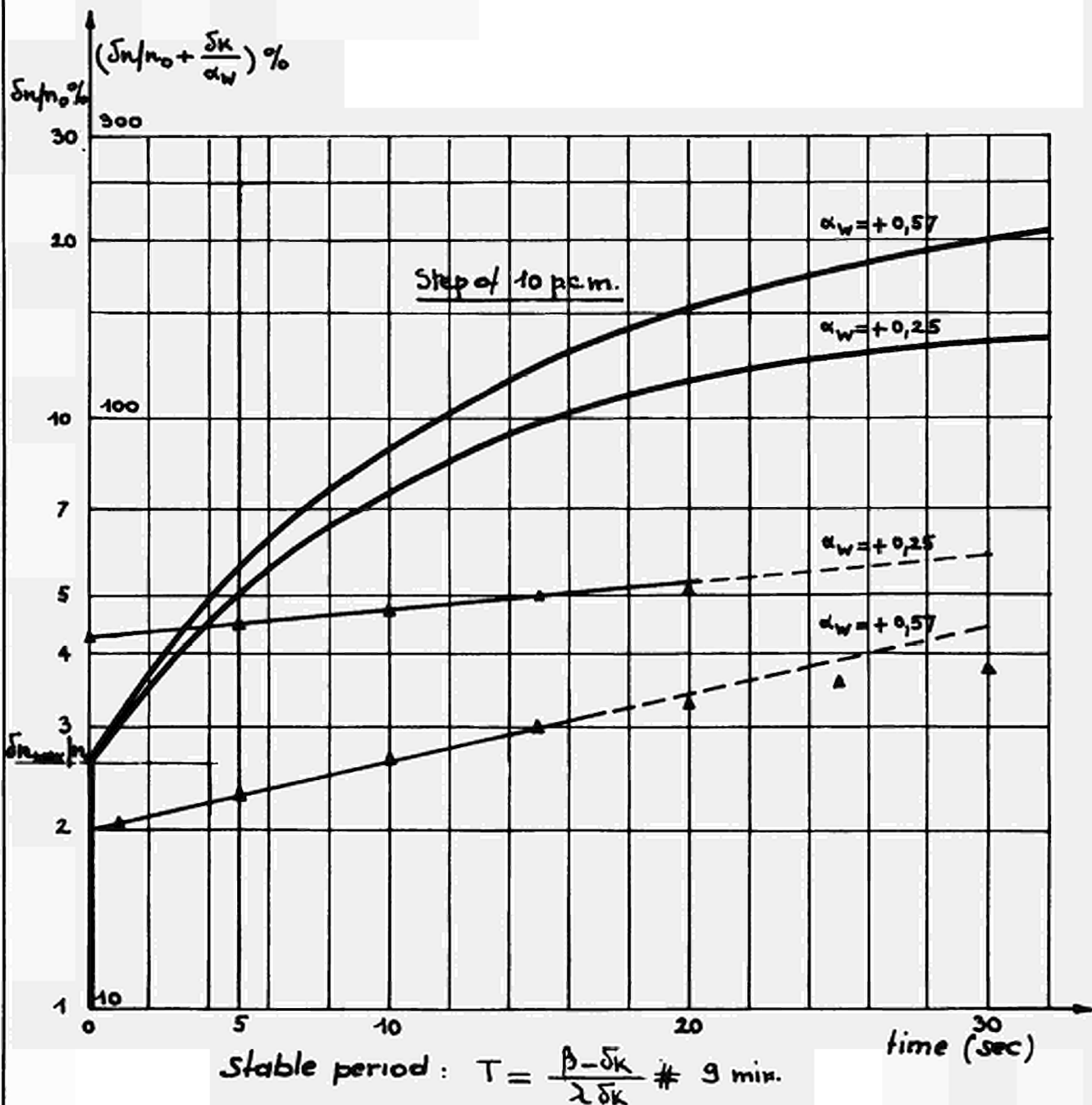
250 MWe ORGEL PROTOTYPE



250 MWe ORGEL PROTOTYPE

Simultaneous control loss and reactivity step for
variable power coefficients.

Digital results



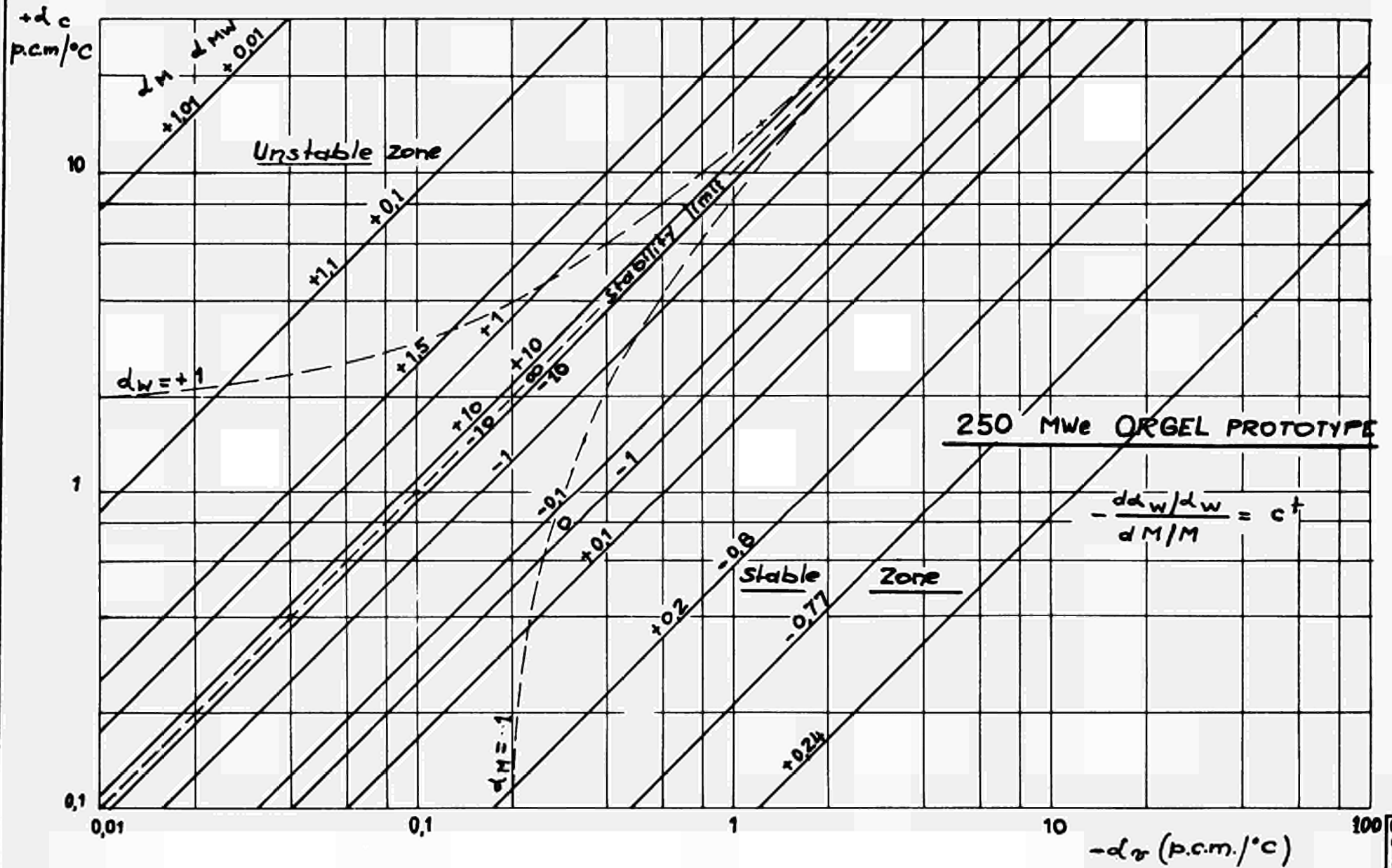


Fig. 17
 GO-2006

APPENDIX BD Y N O R

A numerical program for the DYNamic simulation of an ORGEL power plant

1. INTRODUCTION

The DYNOR code was made with the intention to investigate the behavior of an ORGEL power station under a great variety of circumstances, such as:

- variation of power level;
 - reactivity, temperature or coolant flow disturbances;
 - different temperature coefficients;
 - different regulator arrangements;
 - different arrangements of the heat exchanger;
- etc.

For this reason, the DYNOR code was written using the more general simulation program SAHYB 2 (Ref. 2), which accepts the problem description in a language close to the mathematical formulae, and handles integration and input-output in a standard way.

As a consequence. DYNOR is made of 10 subroutines, which are called by SAHYB-2. Changes in the formulation corresponding to the required investigations are done modifying some of these routines which contain substantially the physical formulae.

The description which follows will thus refer to a standard version of DYNOR that will be modified according to the investigation needed. The standard DYNOR, given in Appendix II, computes the dynamical evolution towards a steady state.

2. GENERAL ORGANIZATION OF DYNOR

The block diagram of the power station is given in Fig. B-1; as in all programs using an integration routine, the integrated variables are expressed in vector notation X_i or $X(I)$. The correspondence between the $X(I)$ and the physical variables is given in the following sections and is resumed in Fig. 1. In all subroutines, the derivatives are noted $DX(I)$ and time is noted T . A differential equation is thus noted:

$$DX(I) = \dots\dots \text{expression}$$

The correspondence between physical parts of the system and the subroutines of DYNOR is also given in Fig. 1.

The reader should note the exact correspondence between Fig. 3.1. and Fig. 1.21a. The finite differences partition of the heat exchanger is identical to the one described in 1.3.

3. THE SUBROUTINE DER

This subroutine contains the description of the reactor and of the primary loop, including the wall equations of the heat exchanger.

DER only is called by the program SAHYB-2, and all other routines of DYNOR are called by DER, directly or indirectly.

The arguments of DER are:

T the time (independent variable)
 X the integrated vector
 DX the vector of the derivatives

PAR a parameter vector, not utilized here*

The first part of DER, up to the statement 200 CONTINUE, is executed only once, and contains the physical parameters** and intermediate computations.

The equations following statement number 200 are equations*** (1.1.), (1.2.), (1.8.), (1.9.), (1.10.), (1.27.) for the reactor, and (1.29.), (1.30.) for the heat exchanger.

Equation (1.1.) has been approximated by a sequence of equilibrium states, assuming the derivative always equal to zero. This is necessary to ensure numerical stability with reasonable long integration steps, since this equation has very fast time constants.

The subroutine DER calls subroutines VARIAT, SECOND, REGUL, to be explained later.

The functions DELAY and SIGMAP are standard SAHYB-2 functions, performing respectively delay simulation and multiple summation (see SAHYB-2 operating manual).

The use of indices for the vectors X and DX can clearly be understood examining Fig. B-1.

PAR is a vector of parameters (maximum 100) that can be read in the input data (see section 9). It has not been used in the standard DYNOR because the parameters are too numerous, and the input data deck must be kept reasonably short. Now suppose e.g. that a certain number of computations is wanted varying temperature coefficients AU and AC. The use of DYNOR should then compile subroutine DER replacing instructions n°510 and 520 (of Appendix II) by the following: AU=PAR(1), AC=PAR(2) and then read PAR(1) and PAR(2) in the input data as explained in section 9. The meaning of symbols is given in Appendix I. All equation numbers refer to paragraph 1.

4. THE SUBROUTINE REGUL

This subroutine is called by DER, and contains the description of the regulator, as described in section 1.4. The first section introduces parameters, and after statement number 100 are described equations (1.43.) and (1.44.).

If different control systems need to be tested with the power plant, a new REGUL subroutine may be introduced in DYNOR.

The arguments are the same as for DER.

The function COMPAR is a standard SAHYB-2 function* which introduces the non-linearities (limitations of speed and displacement). COMPAR is used here in a similar way as a comparator in an analogue set-up.

5. THE SUBROUTINE SECOND

This routine is called by DER, and contains the equations of the secondary side of the heat exchanger, except the super - heater equations, which are in subroutine SUPHTR, called by SECOND.

As in DER and REGUL, the first section, up to statement number 300, contains the parameter definitions and preliminary computations which are executed only once.

The equations are those given in Figs. 1.8. and 1.10. and Eqs. (1.33.), (1.34.), (1.36.), (1.37.), (1.39.), (1.40.) and (1.41.).

COMPAR(A,i) is equal to 1 when A is positive, and zero for A negative; when the transition from one state to another occurs, this is indicated in the output, and COMPAR resets the starting procedure of the integration routine, avoiding the errors due to the discontinuity.

The economizer equations (Fig. 1.8.) are solved for their equilibrium state, assuming the derivative always equal to zero, in order to ensure numerical stability with a reasonable long integration step (as for Eq. 1.1.).

The approximation given in section 1.3. for the thermodynamical functions (saturation temperature, enthalpies and specific volume) are linked with the scaling range of the analogue computation; in DYNOR, these functions have been evaluated by accurate formulae (see section 8).

The subroutine SECOND calls also subroutine RECORD, which is a control on input-output operation. The arguments of second are the same as in DER.

6. THE SUBROUTINE SUPHTR

This subroutine is called by SECOND. It solves the energy conservation equations for the superheater (Fig. 1.18.) as a sequence of equilibrium states (to ensure numerical stability). The equations are solved for the enthalpy of superheated steam $H(J)$ by iterations; this requires the evaluation of the steam temperature, which is function of pressure and enthalpy.

The evaluation of temperature by accurate formulae would require long computer times; the temperature function is therefore stored in tables for a wide range of pressures and enthalpies, and is read by the function FTWOV (which is a standard SAHYB-2 function) which uses linear interpolation (see section 10 and appendix IV). The accuracy of this procedure is maintained within a one percent; if, by any chance, the computed temperature goes outside the stored range, computation is stopped and a diagnostic is given by SAHYB-2.

7. THE SUBROUTINE RECORD

This subroutine is called by SECOND (which is called by DER) and contains the standard SAHYB-2 statements for read-out; they have been grouped here in order to allow a change of the output without modifying or recompiling the other DYNOR sub - programs.

The subroutines that may be called by RECORD to print out results are:

CALL OUTPUT (arg 1, arg 2, ...)

This subroutine enables to print out, either the complete integrated vector and the derivatives, or some of them. Specified labels (given in the input data) are printed out near the results. The arguments are integers, and are the indexes of components which must be printed out.

CALL WRITE (arg₁₁, arg₁₂, ... arg_{i1}, arg_{i2}, ...)

This subroutine prints out variables other than the integrated vector components. These variables must appear at least once in a left-hand side term in the subroutine DER. They are printed out for the same interval as in OUTPUT. The number of arguments is variable with a minimum of two; they are always in pairs, the first one specifying the label, the second one the variable name.

arg_{i1} is a Hollerith field of a maximum of 6 characters, which specify the label that should be printed near the variable;

arg_{i2} is a name of a variable which must be printed out.

In addition, plots may be obtained on the CALCOMP, calling in RECORD the following subroutines:

CALL DRAW (arg₁₁, arg₁₂, arg_{i1}, arg_{i2}, ...)

plots the results as a function of the independent variable T. The arguments have the same arrangement as for WRITE. The subroutine DRAW may be called repeatedly, with different arguments. For each CALL, the curves relative to the arguments will be drawn on the same plot.

CALL DRAWXY (arg₁₁, arg₁₂, ... arg_{i1}, arg_{i2})

plots the results in a phase plane, taking as abscissa the first variable (first two arguments) and as ordinate the successive. The routine may be called repeatedly to obtain different plots in a similar way as DRAW.

For further details on the output procedures, the reader should refer to the SAHYB-2 operating manual. When writing a new RECORD to change the output, care should be taken to see that the variables to be recorded appear in one of the COMMONS.

7. THE SUBROUTINE VARIAT

As it has been illustrated to this point, DYNOR contains a system of differential equations describing the power station; integration would, if carried on a sufficient time, lead to the steady state at nominal power. As the purpose of DYNOR is to allow transient computation under a variety of circumstances, the SUBROUTINE VARIAT has been introduced as an easy way to insert variations (or disturbances) without modifying and recompiling the other DYNOR subroutines. As given in appendix II, VARIAT is a dummy and has no influence. A comment indicates which are the variables that may be programmed in VARIAT: disturbances in reactivity, temperature or flow; variation of power demand, variation on the regulation programs for pressure and temperatures when the power is changed. Since all these inputs have frequently the shape of a step, a pulse or a ramp, SAHYB-2 provides, as a standard feature, the three following functions:

STEP (T)
 PULSE (T)
 RAMP (T1, T2)

simulating respectively a step of unit amplitude, a pulse of unit surface occurring at time T, or a ramp of unity rate (1 unit/second) between times T1 and T2. The synchronisation of the discontinuity with the integration routine is automatically ensured.

For example, a 100 pcm reactivity occurring at time = 5 sec. would need this instruction in VARIAT:

$$CT\phi = 1. + 100.E - 5 * (STEP (5))$$

A temperature disturbance of 5°C/sec. during 2 seconds in the inlet temperature of the heat exchanger would be simulated by:

$$TF = 190. + 5. * (RAMP (0., 2.))$$

As another example, consider a power demand variation following the regulation program given in 1.4.3. and Figs. 1.22. and 1.23.*

The required instructions for VARIAT would be:

$$P\phi WVAR = 1. - 0.0008333 * (RAMP(0., 900.))$$

$$TAVZ = 318. - 0.02222 * (RAMP(300., 900.))$$

When using VARIAT, it must obviously be verified that the variable to be changed is in the common.

Power demand from 100% to 25% in 15 minutes (900 seconds) varying thus of 5% a minute (0.0008333/second). The average temperature must remain constant from 100% to 75% of full power (thus during 300 seconds), and then decrease of 20° in the next 10 minutes (0.02222°C/second).

8. SUBPROGRAMS FOR EVALUATING THERMODYNAMIC QUANTITIES

The functions utilized by DYNOR are:

- FUNCTION TLSAT(P) gives the temperature of saturation, in degrees Centigrades, if P is the pressure in kg/cm²;
- FUNCTION VSVAP (P,TEMP) gives the specific volume of steam, in m³/kg, if P is the pressure in kg/cm² and TEMP is the temperature in degrees Centigrades;
- FUNCTION EVSAT (TSAT) gives the enthalpy of saturated steam, in Kcal/kg, if TSAT is the saturation temperature in degrees Centigrades;
- FUNCTION ELSAT (TSAT) gives the enthalpy of water at saturation, in Kcal/kg, if TSAT is the saturation temperature in degrees Centigrades.

These functions are called by SUBROUTINE SECOND.

9. INTEGRATION SUBROUTINES

These are the standard routines used by SAHYB-2.

Three options may be used, which give comparable results: (the choice of the desired option is made through the input data, see § 10).

Option 4: fixed step 4th order RUNGE-KUTTA integration. Use a time step of about 0.1 second.

Option 1: fixed step predictor-corrector integration. Use a time step of about 0.1 second.

Option 2: variable step predictor corrector. The following characteristics should give a reasonable compromise between accuracy and speed:

MAXIMUM ERROR	10^{-5}
MINIMUM TIME STEP	10^{-3} sec.
MAXIMUM TIME STEP	10^2 sec.
VARIATION FACTOR	0.5
LIMIT BETWEEN ABS. AND RELATIVE ERROR	100
LOWER BOUND TO ERROR	50

Generally, the variable step option will be preferred.

10. INPUT DATA

These follow the standard arrangement for SAHYB-2, adapted to the particular case of DYNOR.

The first card is a comment intended to identify the problem; the first 15 letters of this comment are written on the CALCOMP plots for identification. On the following, there is one numerical information per card: columns 1 to 40 may be used for any comment to be reproduced on the output listing (usually the meaning of that particular datum). The numerical information is contained in column 41 to 50, in fixed or floating-point notation*.

The data cards are, in order:

- 1) identification and comments;
- 2) number of differential equations N (fixed point) $N = 31$ for the standard DYNOR, but may be modified if equations are added;

For fixed point, the reading format is: I 10. For floating point, the reading format is: E 10.6. Thus, for fixed point, the unities should be in column 50; for floating, if the decimal point is explicit, the number may be written in any desired way in columns 41 to 47; column 48 contains eventually the sign of the exponent of 10, columns 49 and 50 this exponent. Blanks are taken as zeroes.

- 3) number of parameters PAR; equal zero, if PAR is not used*
- 4) number of tables to be read in input: N = 7 for the standard DYNOR;
- 5) final time for integration (floating);
- 6) initial or constant integration step (floating); a value around 0.1 is convenient;
- 7) time step for output (floating);
- 8) integration option (see section 9); the numerical information in column 50 should be:
 - 1 for fixed step predictor-corrector
 - 2 for variable step predictor-corrector
 - 3 for variable step predictor-corrector using standard error characteristics**
 - 4 for 4th order Runge-Kutta integration
- 9, 1) initial condition for X(1) in floating; the first six characters of the comment are taken as label on the standard output;

.....
- 9, n) initial condition for X(n);
- 10-i) PAR(i) value, with the same format of initial conditions (only if datum 3 is different than zero)***

Then the following cards (11 to 16) must be placed only when integration option is 2 on datum n.8.

* Datum 3 would be equal to 2 for the case given in footnote of section 3.

** These are: maximum error: 10^{-5}
 minimum time step: 10^{-5}
 maximum time step: 100
 variation factor: 0.5
 level below which the absolute error is considered: 1
 error factor for which a longer step length is taken: 100

*** The numerical values for AU and AC would be introduced in data 10-1 and 10-2 for the case given in footnote of section 3

- 11) maximum relative error (floating);
- 12) minimum time step (floating);
- 13) maximum time step (floating);
- 14) variation factor (floating);
- 15) level below which the absolute error is considered for step variation (floating);
- 16) error factor, specifying a lower bound for which a longer step length is taken (floating);
- 17) number of points in table 1 (100, fixed point);
- 18-1) the following cards contain the abscissae and ordinates of table one: six numbers, per card; respectively $x_1, y_1, x_2, y_2, x_3, y_3$ on the first card, etc. Each number is expressed in floating and uses 10 columns. Thus columns 1 to 60 are used on these cards.
- 19) number of points in table 2 (fixed point)
- 20) abscissae and ordinates of table two
etc.

And so on for the desired number of tables. The last card must always contain END in the first three columns. If the data need to be changed, follow the SAHYB-2 operating manual.

The tables referred to in data 4, 17, 18, 19 etc. are the values of temperature of superheated steam versus enthalpy, for several values of pressure:

Table 1	corresponds to	40	kg/cm ²
" 2	"	60	"
" 3	"	80	"
" 4	"	100	"
" 5	"	130	"
" 6	"	160	"
" 7	"	200	"

These tables are given in appendix 4; they limit the validity domain of the program (see section 5); an example of data deck is given in appendix 3.

APPENDIX IDefinition of symbolsSUBROUTINE DER

X(1) = TU	temperature of uranium
X(2) = TG	temperature of cladding
X(3) = TC	temperature of coolant
X(4) to X(9)	delayed neutrons (6 groups)
{ X(12) = TORG 1 to X(19) = TORG 8	organic temperatures in the primary of the heat exchanger (eight zones, from the hot to the cold end)
{ X(20) = TWALL 1 to X(27) = TWALL 8	wall temperatures in the heat exchanger
PNTR	neutron power
CT	total reactivity
UU, UA, UC	heat capacity per unit of volume of uranium, cladding and coolant
AA, BBB	heat transfer coefficients uranium-cladding and cladding-coolant
CC	transport coefficient
GU, GC	are γ_u , γ_c defined by (2.25.) and (2.22.)
BETA = β	delayed neutrons fraction
VL = ℓ	neutron lifetime
B(i)	β_i / ℓ
AU = α_u	uranium temperature coefficient
AC = α_c	coolant temperature coefficient

SUBROUTINE REGUL

ERROR	actuating error signal
X(10) = INTE	integrated error
X(11) = ROCON	control rods reactivity
TAV	average temperature of organic
TAVZ	reference average temperature
PNOM	nominal power
R4	gain of integrated feedback
R5	gain of proportional feedback

AINERT	inverse of inertia time constant
SPEED	reactivity speed of control rods
SPDLI	speed limit for control rods
UPLI	upper limit for reactivity (mechanical stop of control rod)
DOWNLI	lower limit

SUBROUTINES SECOND and SUPHTR

TSEC(i)	temperature in the secondary (eight zones, from hot to cold)
X(28) - = P	steam pressure
X(29) = RO	steam density in the boiler
X(30) = XX	steam quality in the boiler
X(31) = IDOW	enthalpy in the downcomer
H(i)	enthalpy in the superheater (three zones, from hot to cold)
I	enthalpy in the boiler
ISAT	enthalpy of saturated steam
ILIQ	enthalpy of saturated water
TSAT	temperature of saturation
WREQ	mass flow in the secondary
WR	mass flow in the riser
WC	condensation flow
VS	specific volume of liquid
ROSAT	density of saturated steam
VSPEC	specific volume of steam
POWER	nominal power demand
POWVAR	variation factor for power demand
ROLVE	density of water in the economizer
CLVE	specific heat of water in the economizer
TF	inlet temperature in the economizer
VLIQ	specific volume of water
ROD	density in the downcomer
TAU 1, TAU 2	time delays between reactor and heat exchanger
WOL	organic mass flow
WOLVAR	mass flow variation factor
TOUT	outlet temperature of the reactor
TIN	inlet temperature of the reactor

TOL	inlet temperature of the primary
TOUTEC	oulet temperature of the primary
ALTZE, B, S	height of the economizer, boiler and superheater
VLORE, B, S	volume, organic
VTUE, B, S	volume, tubes
SPORE, B, S	surface, organic side
SPVAE, B, S	surface, secondary side
V	volume upper dome
LR, LD	height of riser and downcomer
VLDO	volume downcomer
HLOE, B, S	heat transfer coefficient organic side for economizer, boiler, superheater
HLVE, B, S	heat transfer coefficient secondary side for economizer, boiler, superheater
ROLOE, B, S	density of organic for economizer, boiler, super - heater
ROPE, B, S	density of wall for economizer, boiler, superheater
CLOE, B, S	specific heat of organic for economizer, boiler, superheater
CPE, B, S	specific heat of wall for economizer, boiler, superheater

APPENDIX IIProgram and deck arrangement

DYNOR may be used with the FORTRAN-4 7090 or FORTRAN-360 monitor, in the following arrangement:

- 1) DYNOR CARDS
- 2) SAHYB-2 CARDS
- 3) DATA CARDS

The DYNOR programs for the 7090 and the 360/60 will practically be identical.

The SAHYB-2 decks are different.

The standard DYNOR is given in the following pages only to facilitate understanding; as in all digital programs changes or corrections could be introduced after publication of the present report.

SAHYB2 CER
EXTERNAL FORMULA NUMBER

SOURCE STATEMENT

04/11/67
INTERNAL FORMULA NUMBER(S)

LSUR = ALTZS / 3e
PLOE = SPORF / ALTZE
PLOB = SPORB / ALTZB
PLOS = SPORS / ALTZS
PLVE = SPVAE / ALTZE
PLVB = SPVAB / ALTZB
PLVS = SPVAS / ALTZS
AD=VLDO/LR
AR=VLVAS/LR

DYNO1120 , 79
DYNO1130 , 80
DYNO1140 , 81
DYNO1150 , 82
DYNO1160 , 83
DYNO1170 , 84
DYNO1180 , 85
DYNO1190 , 86

C
C
C

THERMAL AND HYDRAULIC PARAMETERS

HLOE = 0.696
HLOB = 0.601
HLOS = 0.460
HLVE = 5.461
HLVB = 3.561
HLVS = 0.393
ROLOE = 8.990
ROLOB = 3.722
ROLOS = 8.230
ROPE = 7.860
ROPB = 7.860
ROPS = 7.860
CLOE = 0.544526
CLOB = 0.5732231
CLOS = 0.60090
CPE = 0.12
CPB = 0.12
CPS = 0.12

DYNO1200
DYNO1210
DYNO1220
DYNO1230 , 87
DYNO1240 , 88
DYNO1250 , 89
DYNO1260 , 90
DYNO1270 , 91
DYNO1280 , 92
DYNO1290 , 93
DYNO1300 , 94
DYNO1310 , 95
DYNO1320 , 96
DYNO1330 , 97
DYNO1340 , 98
DYNO1350 , 99
DYNO1360 , 100
DYNO1370 , 101
DYNO1380 , 102
DYNO1390 , 103
DYNO1400 , 104

C
C

ORGANIC FLOW

WOL = 722.8
WOLVAR = 1.0

DYNO1410
DYNO1420
DYNO1430
DYNO1440 , 105
DYNO1450 , 106
DYNO1460
DYNO1470
DYNO1480

C
C
C
C

INTERMEDIATE VALUES

ORGANIC SIDE
CS1 = ALOS * RCLOS * CLOS
CS2 = CLOS / LSUR * WOL
CS3 = FLOS * PLOS
CB1 = ALOB * RCLOB * CLOB
CB2 = CLOB / LEVA * WOL
CB3 = HLOB * PLOB
CE1 = ALOE * RCLOE * CLOE
CE2 = CLOE / LECO * WOL
CE3 = HLOE * PLOE

DYNO1490
DYNO1500
DYNO1510 , 107
DYNO1520 , 108
DYNO1530 , 109
DYNO1540 , 110
DYNO1550 , 111
DYNO1560 , 112
DYNO1570 , 113
DYNO1580 , 114
DYNO1590 , 115

C

WALL
DS1 = APS * ROPS * CPS
DS2 = FLOS * PLOS
DS3 = HLVS * PLVS
DB1 = APB * ROPB * CPB
DB2 = FLVB * PLOB
DB3 = FLVB * PLVB

DYNO1600
DYNO1610 , 116
DYNO1620 , 117
DYNO1630 , 118
DYNO1640 , 119
DYNO1650 , 120
DYNO1660 , 121
DYNO1670 , 122

SAHYB2 DER 04/11/67
 EXTERNAL FORMULA NUMBER - SOURCE STATEMENT - INTERNAL FORMULA NUMBER(S)

	DE1=APE*ROPE*CPE	DYNO1680	,123
	DE2=FLOF*PLOF	DYNO1690	,124
	DE3=FLVE*PLVE	DYNO1700	
C		DYNO1710	
C	TOTAL THERMAL COEFFICIENTS	DYNO1720	
C		DYNO1730	
	SUPERHEATER	DYNO1740	,125
	DO 100 J=1,3	DYNO1750	,126
	C2(J)=CS2/CS1	DYNO1760	,127
	C3(J)=CS3/CS1	DYNO1770	,128
	D1(J)=DS2/DS1	DYNO1780	,129
	D2(J)=(-CS2-DS3)/DS1	DYNO1790	,130
	D3(J)=DS3/DS1	DYNO1800	,131
100	CONTINUE	DYNO1810	
C	BOILER	DYNO1820	,132 ,133
	DO 110 J=4,6	DYNO1830	,134
	C2(J)=CB2/CB1	DYNO1840	,135
	C3(J)=CB3/CB1	DYNO1850	,136
	D1(J)=DB2/DB1	DYNO1860	,137
	D2(J)=(-CB2-DB3)/DB1	DYNO1870	,138
	D3(J)=DB3/DB1	DYNO1880	,139
110	CONTINUE	DYNO1890	
C	ECONOMISER	DYNO1900	,140 ,141
	DO 120 J=7,8	DYNO1910	,142
	C2(J)=+CE2/CE1	DYNO1920	,143
	C3(J)=CE3/CE1	DYNO1930	,144
	D1(J)=DE2/DE1	DYNO1940	,145
	D2(J)=(-CE2-DE3)/DE1	DYNO1950	,146
	D3(J)=DE3/DE1	DYNO1960	,147
120	CONTINUE	DYNO1970	
C		DYNO1980	
C		DYNO1990	
C		DYNO2000	
C		DYNO2010	
C		DYNO2020	
C	***** EQUATIONS *****	DYNO2030	
200	CONTINUE	DYNO2040	,148 ,149
	CALL VARIAT	DYNO2050	,150
	CALL SECCND(T,X,DX,PAR)	DYNO2060	,151
C		DYNO2070	
C	DELAY LINES	DYNO2080	
	TIN=DELAY(9,TAU2/WOLVAR,ST2,X(12))	DYNO2090	
	TOUT=2.*X(3)-TIN	DYNO2100	,152
	TOL=DELAY(10,TAU1/WOLVAR,ST1,TOUT)	DYNO2110	,153
		DYNO2120	,154
C		DYNO2130	
C	REACTOR KINETICS	DYNO2140	
		DYNO2150	
	CT=CT0+AC*CC*(X(3)-DTCO)+AU*GC*(X(3)-DTCO)+AU*GU*(X(1)-DTUO-X(3)+D	DYNO2160	,155
	1TCO)+X(11)	DYNO2170	
	TRET=SIGMAP(VLA,X,4,9)	DYNO2180	,156
	PNTR=- (TRET*VL) / (CT*BB-1.)	DYNO2190	,157
C		DYNO2200	
C	REGULATOR EQUATIONS	DYNO2210	
	CALL REGUL(T,X,DX,PAR)	DYNO2220	,158
		DYNO2230	

C			DYN02240		
C		REACTOR THERMAL EQUATIONS	DYN02250		
C		DX(1)=A11*PNTR-A12*(X(1)-X(2))	DYN02260	,159	
		DX(2)=A21*(X(1)-X(2))-A22*(X(2)-X(3))*WOLVAR	DYN02270	,160	
		DX(3)=A31*WOLVAR*(X(2)-X(3))-A32*(X(3)-TIN)	DYN02280	,161	
			DYN02290		
C		DELAYED NEUTRONS	DYN02300		
C			DYN02310		
C		B(I)=BETA(I)/VL	DYN02320		
C		DO 220 I=4,9	DYN02330	,162	
	220	DX(I)=-X(I)*VLA(I)+PNTR*CT*B(I)	DYN02340	,163	
			DYN02350		
C		HEAT EXCHANGER ORGANIC SIDE	DYN02360		
C			DYN02370		
C		DX(12)=(-C3(1)-C2(1)*WOLVAR)*X(12)+C2(1)*TOL*WOLVAR+C3(1)*X(20)	DYN02380		
		DO 230 I=13,19	DYN02390	,164	,165
		J=I-1	DYN02400	,166	
		K=I+8	DYN02410	,167	
	230	DX(I)=(-C3(J)-C2(J)*WOLVAR)*X(I)+C2(J)*X(I-1)*WOLVAR+C3(J)*X(K)	DYN02420	,168	
			DYN02430	,169	
			DYN02440		
C		WALL EQUATION	DYN02450		
C			DYN02460		
		DO 240 I=20,27	DYN02470	,170	,171
		K=I-8	DYN02480	,172	
		J=I-19	DYN02490	,173	
	240	DX(I)=D1(J)*X(K)+D2(J)*X(I)+D3(J)*TSEC(J)	DYN02500	,174	
		RETURN	DYN02510	,175	,176
		END	DYN02520	,177	
			DYN02530	,178	

EXTERNAL FORMULA NUMBER - SOURCE STATEMENT - INTERNAL FORMULA NUMBER(S)

C	SUBROUTINE REGUL(T,X,DX,PAR)	DYN02550		
	REGULATOR	DYN02560		
	DIMENSION X(100),DX(100),PAR(100)	DYN02570		
	COMMON/VARVAR/TF,CTO,POWVAR,WOLVAR,PNVAR,DERROR,TAVZ	DYN02580		
	COMMON/SECVAR/TSEC(8),PNTR,ERROR,REG,TAV,CT,TOUT,	DYN02590		
	1TOL,TIN,TSAT,POWER	DYN02600		
	LOGICAL SWITCH	DYN02610		
	IF(SWITCH(3)) GO TO 100	DYN02620		
C		DYN02630		
C		DYN02640		
C	REGULATOR PARAMETERS	DYN02650	,1	,2 ,3
	DERROR=0.0	DYN02660	,4	
	PNVAR=1.0	DYN02670	,5	
	AINERT=2.0	DYN02680	,6	
	PNOM=4.0	DYN02690	,7	
	PNTR=PNOM	DYN02700	,8	
	TAVZ=318.00	DYN02710	,9	
	PRESN=62.0	DYN02711	,10	
	R1=1.0/PNCM	DYN02720	,11	
	R2=1.0/TAVZ	DYN02730	,12	
	R3=0.5/PRESN	DYN02731	,13	
	R4=1.0E-2	DYN02740	,14	
	R5=2.5E-2	DYN02750		
C	MECHANICAL LIMITS OF CONTROL RODS	DYN02760	,15	
	UPLI=200.0E-5	DYN02770	,16	
	DOWNLI=-200.0E-5	DYN02780	,17	
	SPDLI=15.0E-5	DYN02790	,18	
100	CONTINUE	DYN02800		
C	EQUATIONS	DYN02810		
	TAV=0.5*(TOL+X(19))	DYN02820	,19	
	ERROR=-R1*(PNTR-PNOM*PNVAR)-R2*(TAV-TAVZ)-R3*(X(28)-PRESN)+DERROR	DYN02830	,20	
	DX(10)=R4*ERROR	DYN02840	,21	
	REG=X(10)+R5*ERROR	DYN02850	,22	
	SPEED=AINERT*(REG-X(11))	DYN02860	,23	
	DSPEED=ABS(SPEED)-SPDLI	DYN02870	,24	
	COMP10=CCMPAR(DSPEED,10)	DYN02880	,25	
	IF(SPEED)110,120,120	DYN02890	,26	
110	SPEED=SPEED*(1.-COMP10)-SPDLI*COMP10	DYN02900	,27	
	GO TO 130	DYN02910	,28	
120	SPEED=SPEED*(1.-COMP10)+SPDLI*COMP10	DYN02920	,29	
130	DX(11)=SPEED	DYN02930	,30	
	COMP9=CCMPAR(X(11)-UPLI,9)	DYN02940	,31	
	COMP8=CCMPAR(DOWNLI-X(11),8)	DYN02950	,32	
	X(11)=X(11)*(1.-COMP9-COMP8)+UPLI*COMP9+DOWNLI*COMP8	DYN02960	,33	
	RETURN	DYN02970	,34	
	END	DYN02980	,35	
		DYN02990	,36	

```

C
C
SUBROUTINE SECOND(T,X,DX,PAR) DYN03010
    EQUATIONS SECONDARY SIDE DYN03020
    ***** DYN03030
COMMON/VARVAR/TF,CTO,POWVAR,WOLVAR,PNGAR,DEROR,TAVZ DYN03040
COMMON/SUPHT/I,H(4),WREQ,G2 DYN03050
COMMON/SECVAR/ISEC(3),PNTR,ERROR,REG,TAV,CT,TOUT, DYN03060
1TOL,TIN,TSAT,POWER DYN03070
COMMON/SECPAR/PLVE,PLVB,PLVS,HLVE,HLVB,HLVS,LECO,ALVE,ALVB,ALVS,ADDYN03080
1,AR,LSUR,LEVA,V,LD,LR,VLDO DYN03090
COMMON/RECRD/WF,WC,VS,VSPEC,ISAT,ILIQ,ROSAT DYN03100
DIMENSION X(100),DX(100),PAR(100) DYN03110
REAL I,ISAT,ILIQ,LECO,LR,LD,K2,LSUR,HLVS DYN03120
LOGICAL SWITCH DYN03130
IF(SWITCH(2)) GO TO 300 DYN03140
*****PARAMETERS***** DYN03150
DYN03160
DYN03170
DYN03180
DYN03190
MISCELLANEOUS PARAMETERS DYN03200
DYN03210
DYN03220
DYN03230
DYN03240
DYN03250
DYN03260
DYN03270
DYN03280
DYN03290
DYN03300
DYN03310
DYN03320
DYN03330
DYN03340
DYN03350
DYN03360
DYN03370
DYN03371
DYN03372
DYN03380
DYN03390
DYN03400
DYN03410
DYN03420
DYN03430
DYN03440
DYN03450
DYN03460
DYN03470
DYN03480
DYN03490
DYN03500
DYN03510
DYN03520
DYN03530
WCK=0.1 ,1
WC=0.0 ,2
WREQC=79.22 ,3
AVS=0.25874 ,4
BVS=-0.4209E-3 ,5
POWER=175.505EC6 ,6
POWVAR=1.0 ,7
RR=15. ,8
PZERO=X(32) ,9
VSO=AVS+BVS*PZERO ,10
K2=((RR*WREQC)**2)*(VLIQ+VSO/(RR+1.))/(VSO/(RR+1.)) ,11
ROLVE=750. ,12
CLVE=1.1 ,13
TF=190. ,14
CLVE=1.1 ,15
BIPRO=103. ,16
AI=461.34 ,17
BIL=1.194 ,18
BLAT=-1.51514 ,19
VLIQ=0.0013930 ,20
ROD=1.70.00136 ,21
E1=(PLVE*HLVE)/(ALVE*ROLVE*CLVE) ,22
E2=CLVE/(ALVE*ROLVE*CLVE*LECO) ,23
FF1=1./(AR*LR) ,24
F1=(PLVB*LR*HLVB)/(3.*AR*LR) ,25
F2=1./(AC*LD*ROD) ,26
F3=1./(V*BIPRO) ,27
F4=1./V ,28
DYN03460
DYN03470
DYN03480
DYN03490
DYN03500
DYN03510
DYN03520
DYN03530
PARAMETERS SUPERHEATER ,31
G2=PLVS*LSUR*HLVS ,32
TENTATIVE INITIAL ENTHALPIES ,33
H(1)=730. ,34
H(2)=713.
    
```

SAHYB2 SECOND 04/11/67
 EXTERNAL FORMULA NUMBER - SOURCE STATEMENT - INTERNAL FORMULA NUMBER(S)

C	H(3)=692.	DYN03540	
C	READ OUT SUBROUTINE	DYN03550	
C	CALL RECCRD(T,X,DX)	DYN03560	,35
C		DYN03570	
C	*****EQUATIONS*****	DYN03580	
C	300 CONTINUE	DYN03590	
C		DYN03600	,36
C	SECONDARY FLOW EQUATIONS	DYN03610	
C		DYN03620	
C		DYN03630	
C	DH=H(1) -CLVE*TF	DYN03640	,37
C	WREQ=POWER*POWVAR/(4187.*DH)	DYN03650	,38
C		DYN03660	
C		DYN03670	
C	BOILER AND UPPER DOME	DYN03680	
C		DYN03690	
C	TSAT=TLSAT(X(28))	DYN03700	,39
C	VS=VSVAP(X(28),TSAT)	DYN03710	,40
C	ISAT=EVSAT(TSAT)	DYN03720	,41
C	ILIQ=ELSAT(TSAT)	DYN03730	,42
C	VSPEC=VLIQ+X(30)*VS	DYN03740	,43
C	WR=SQRT(K2*(X(30)*VS/VSPEC))	DYN03750	,44
C	I=AI+BIPRO*(X(28)/X(29))	DYN03760	,45
C	CLAT=ISAT-ILIQ	DYN03770	,46
C	ROSAT=I./VS	DYN03780	,47
C		DYN03790	
C	SECONDARY TEMPERATURES	DYN03800	
C		DYN03810	
C	BOILER	DYN03820	
C	DO 310 IK=4,6	DYN03830	,48
C	310 TSEC(IK)=TSAT	DYN03840	,49
C		DYN03850	
C	ECONOMISER	DYN03860	
C	EE2=E2*WREQ	DYN03870	,50
C	EE1=1./(E1+EE2)	DYN03880	,51
C	TSEC(8)=(E1*X(27)+EE2*TF)*EE1	DYN03890	,52
C	TSEC7=(E1*X(26)+EE2*TSEC(8))*EE1	DYN03900	,53
C	COMP2=COMPAR(TSEC7-TSAT,2)	DYN03910	,54
C	TSEC(7)=TSEC7*(1.-COMP2)+TSAT*COMP2	DYN03920	,55
C		DYN03930	,56
C		DYN03940	
C	CONDENSATION RATE	DYN03950	,57
C	WCC=X(29)-ROSAT	DYN03960	,58
C	WC=WCK*WCC*(COMPAR(WCC,1))	DYN03970	
C		DYN03980	,59
C	SOMMA=F1*(X(23)+X(24)+X(25)-3.*TSAT)+(CLVE*WREQ*TSEC(7)+WR*X(31)-	DYN03990	
C	I(WR+WREQ)*(ILIQ+X(30)*CLAT))*FF1	DYN04000	
C		DYN04010	,60
C	PDER=(-AI*(X(30)*(WREQ+WR)-WREQ-WC)+ISAT*(X(30)*(WREQ+WR))-WREQ*I-	DYN04020	
C	IILIQ*WC)*F3	DYN04030	
C		DYN04040	
C	X(28)=P STEAM PRESSURE	DYN04050	,61
C	DX(28)=PDER	DYN04060	
C		DYN04070	
C	X(29)=RO BOILING MIX. DENSITY	DYN04080	,62
C	DX(29)=F4*(X(30)*(WREQ+WR))-WREQ-WC)	DYN04090	

		04/11/67	
SAHYB2 SECOND		EXTERNAL FORMULA NUMBER	INTERNAL FORMULA NUMBER(S)
		- SOURCE STATEMENT	-
C			DYN04100
C	X(30)=XX STEAM QUALITY		DYN04110 ,63
	DX(30)=(VSPEC/CLAT)*SOMMA-((BIL+BLAT*X(30))*PDER)/CLAT		DYN04120
C			DYN04130
C	X(31)=IDCW ENTHAL DOWNCOMMER		DYN04140 ,64
	DX(31)=F2*WR*(ILIQ-X(31))		DYN04150
C			DYN04160
C	ENTHALPY EQUATIONS SUPERHEATER		DYN04170
			DYN04180 ,65
	CALL SUPHTR(X)		DYN04190 ,66
	RETURN		DYN04200 ,67
	END		DYN04210 ,68

SAHYB2 SUPHTR

EXTERNAL FORMULA NUMBER

SOURCE STATEMENT

04/11/67
INTERNAL FORMULA NUMBER(S)

C	SUBROUTINE SUPHTR(X)	DYNO4230		
C	SUPERHEATER SECONDARY SIDE	DYNO4240		
C	H(J) ENTHALPY OF SUPERHEATED STEAM IN CELL J	DYNO4250		
C	DIMENSION GH(3), ABE(3), E(3), EOLD(3), STPP(3), X(10)	DYNO4260		
	REAL I	DYNO4270		
	LOGICAL GH	DYNO4280		
	COMMON/SECVAR/TSEC(3), PNTR, ERROR, REG, TAV, CT, TOUT,	DYNO4290		
	1TOL, TIN, TSAT, POWER	DYNO4300		
	COMMON/SUPHT/I, H(4), WREQ, G2	DYNO4310		
	DIMENSION VP(7)	DYNO4320		
C	DATA (VP(L), L=1,7)/40., 60., 80., 100., 130., 160., 200./	DYNO4330		
C	NZ NUMBER OF ZONES FINITE DIFFERENCES	DYNO4340		
C	TOLERANCE OF ONE PER CENT ON H(J)	DYNO4350		
C	DATA TOLER, NZ, NZP1/16., 3, 4/	DYNO4360		
	DO 5 J=1, 3	DYNO4370		
	GH(J)=.FALSE.	DYNO4380		
5	STPP(J)=16.	DYNO4390		
	H(4)=1	DYNO4400	, 1	
C	MAIN ITERATION LOOP	DYNO4410	, 2	
	DO 100 JJ=1, NZ	DYNO4420	, 3	, 4
	J=NZP1-JJ	DYNO4430		
	JK=J+19	DYNO4440		
10	CONTINUE	DYNO4450	, 5	
	EOLD(J)=E(J)	DYNO4460	, 6	
C	X(28) STEAM PRESSURE	DYNO4470	, 7	
C	TSEC(J)= FTWOV(1,7,H(J),X(28),VP)	DYNO4480	, 8	
C	ENTHALPY EQUILIBRIUM EQUATION	DYNO4490	, 9	
C	E(J)= (H(J+1)-H(J))+G2*(X(JK)-TSEC(J))/WREQ	DYNO4500		
	ABE(J)=ARS(E(J))	DYNO4510		
	IF(ABE(J).LT.TCLER) GO TO 100	DYNO4520	, 10	
C	IF(E(J).GT.0.) GO TO 20	DYNO4530		
	IF(EOLD(J).GT.0.) STPP(J)=STPP(J)*0.5	DYNO4540		
	H(J)=H(J)-STPP(J)	DYNO4550	, 11	
	GO TO 10	DYNO4560		
20	IF(EOLD(J).LE.0.) STPP(J)=STPP(J)*0.5	DYNO4570	, 12	
	H(J)=H(J)+STPP(J)	DYNO4580	, 13	
	GO TO 10	DYNO4590		
100	CONTINUE	DYNO4600	, 14	, 15 , 16
	RETURN	DYNO4610	, 17	, 18 , 19
	END	DYNO4620	, 20	, 21 , 22
		DYNO4630	, 23	
		DYNO4640	, 24	
		DYNO4650	, 25	, 26 , 27
		DYNO4660	, 28	
		DYNO4670	, 29	
		DYNO4680	, 30	, 31
		DYNO4690	, 32	
		DYNO4700	, 33	

SAHYB2 VARIAT 04/11/67
 EXTERNAL FORMULA NUMBER - SOURCE STATEMENT - INTERNAL FORMULA NUMBER(S)

C
C
C
C
C
C
C
C

SUBROUTINE VARIAT DYN04720
 COMMON/VARVAR/TF,CTO,POWVAR,WOLVAR,PNVAR,DERROR,TAVZ DYN04730
 INSERT HERE VARIATION LAWS FOR DYN04740
 TF FEEDWATER TEMPERATURE IN DEGREES DYN04750
 CTO REACTIVITY=1. AT EQUILIBRIUM DYN04760
 POWVAR SECONDARY POWER VARIATION=1. AT NOMINAL POWER DYN04770
 WOLVAR ORGANIC FLOW VARIATION=1. AT N.P. DYN04780
 PNVAR REACTOR POWER=1. AT N.P. DYN04790
 DERROR DISTURBANCE ON REGULATOR=0. AT EQUILIBRIUM DYN04800
 TAVZ REFERENCE ORGANIC MEDIUM TEMPERATURE IN DEGREES DYN04810
 DYN04820
 DYN04830
 DYN04840 ;1
 DYN04850 ;2

RETURN
 END

SAHYB2 RECORD 04/11/67
 EXTERNAL FORMULA NUMBER - SOURCE STATEMENT - INTERNAL FORMULA NUMBER(S)

C
C
C

SUBROUTINE RECORD(T,X,DX) DYN04870
 DIMENSION X(100),DX(100) DYN04880
 COMMON/VARVAR/TF,CTO,POWVAR,WOLVAR,PNVAR,DERROR,TAVZ DYN04890
 COMMON/SUPHT/I,H(4),WREQ,C2 DYN04900
 COMMON/SECVAR/TSEC(2),P,ITR,ERROR,REG,TAV,CT,TOUT, DYN04910
 1TOL,TIN,TSAT,POWER DYN04920
 COMMON/SECPAR/PLVE,PLVB,PLVS,HLVE,HLVB,HLVS,LECO,ALVE,ALVB,ALVS,AD DYN04930
 1,AR,LSUR,LEVA,V,LD,LR,VLDO DYN04940
 COMMON/RECRO/WR,WC,VS,VSPEC,ISAT,ILIQ,ROSAT DYN04950
 DYN04960
 DYN04970
 DYN04980
 DYN04990
 READ OUT STATEMENTS OF SAHYB ARE GROUPED HERE
 CALL WRITE(MIPNTR,PNTR,5HERROR,ERROR,3HREG,REG,3HTAV,TAV,2HCT,CT, DYN05000
 14HTOUT,TOUT,5HTOL,TOL,5HTIN,TIN,4HTSAT,TSAT,4HWREQ,WREQ,2HWR,WR, DYN05010
 22HWC,WC,5HTSEC1,TSEC(1),5HTSEC2,TSEC(2),5HTSEC3,TSEC(3),4HH(1), DYN05020
 3H(1),4HH(2),H(2),4HH(3),H(3),2HVS,VS,5HVSPEC,VSPEC,4HISAT,ISAT, DYN05030
 44HILIQ,ILIQ,5HROSAT,ROSAT,5HTSEC7,TSEC(7),5HTSEC8,TSEC(8)) ;1
 CALL OUTPUT(1,2,3,10,11,12,13,14,15,16,17,18,19,20,21,22,23,24, DYN05040
 125,26,27,28,29,30,31) DYN05050
 DYN05060 ;2
 DYN05070 ;3
 DYN05080 ;4

RETURN
 END

SAIYB2 VSVAP 04/11/67
 EXTERNAL FORMULA NUMBER - SOURCE STATEMENT - INTERNAL FORMULA NUMBER(S)

FUNCTION VSVAP(P,T)	DYN05100	
DATA(R,A,B,C,D,L,F,CP,DP,EP)/1.34992E-02,4.7331E-03,2.93945E-03,4.135507E-02,6.670106E-04,35.17360E-05,8.06857E-05,1.55108,1.26591,1.322735/	DYN05110	
SIGMA=P*4.4316E-03	DYN05130	
TAU=(T+27.315)*1.5448E-03	DYN05140	,1
TAU1=TAU**2.32	DYN05150	,2
SIGMA1=SIGMA*SIGMA/(TAU**14)	DYN05160	,3
VSVAP=R*TAU/SIGMA-A/TAU1+E*(CP-SIGMA)*TAU1-SIGMA1*(B-(DP*SIGMA-TAU	DYN05170	,4
1**3)*D*SIGMA+C/(TAU**18))-(1.-EP*SIGMA)*F*TAU	DYN05180	
RETURN	DYN05190	,5
END	DYN05200	,6
	DYN05210	,7

SAIYP2 TLSAT 04/11/67
 EXTERNAL FORMULA NUMBER - SOURCE STATEMENT - INTERNAL FORMULA NUMBER(S)

FUNCTION TLSAT(P)	DYN05230	
DOUBLE PRECISION A	DYN05240	
DIMENSION A(15)	DYN05250	
DATA (A(I),I=1,15)/-4.292460291D-2,-4.26856351D-7,1.534373134D-6,2.18207171172D-5,-1.874177519D-1,-3.739348425D-4,1.52837729D-3,2.1296822011D-2,2.127700463D-1,2.5575357647,2.785424215D+1,9.909271199D+1/	DYN05260	
PP=ALOC(P)	DYN05270	
S=A(1)*PP+A(2)	DYN05280	
DO 10 I=7,15	DYN05290	,1
S=S*PP+A(I)	DYN05300	,2
10 CONTINUE	DYN05310	,3
TLSAT=S	DYN05320	,4
RETURN	DYN05330	,5
END	DYN05340	,6
	DYN05350	,7
	DYN05360	,8
	DYN05370	,9

SAHYB2 EVSAT 04/11/67
 EXTERNAL FORMULA NUMBER - SOURCE STATEMENT - INTERNAL FORMULA NUMBER(S)

FUNCTION EVSAT(T)	DYNO5380	
DOUBLE PRECISION A	DYNO5390	
DIMENSION A(10)	DYNO5400	
DATA (A(I), I=1,7)/2,456728183D-1,-2.252469249,6.681528737,-1.02888	DYNO5410	
1362D+1,3.76167557D+0,4.335160398D+1,5.972570406D+2/	DYNO5420	
TT=T*0.51	DYNO5430	,1
S=A(1)*TT+A(2)	DYNO5440	,2
DO 10 I=3,7	DYNO5450	,3
S=S*TT+A(I)	DYNO5460	,4
10 CONTINUE	DYNO5470	,5 ,6
EVSAT=S	DYNO5480	,7
RETURN	DYNO5490	,8
END	DYNO5500	,9

SAHYB2 ELSAT 04/11/67
 EXTERNAL FORMULA NUMBER - SOURCE STATEMENT - INTERNAL FORMULA NUMBER(S)

FUNCTION ELSAT(T)	DYNO5520	
DOUBLE PRECISION A	DYNO5530	
DIMENSION A(15)	DYNO5540	
DATA (A(I), I=1,10)/6.607297978D-2,-9.465226031D-1,5.700027955,-1.8	DYNO5550	
16838884D+1,3.620722288D+1,-4.19863442D+1,2.885444361D+1,-1.06332556	DYNO5560	
21D+1,1.014852419D+2,-1.135796422D-2/	DYNO5570	
TT=T*0.51	DYNO5580	,1
S=A(1)*TT+A(2)	DYNO5590	,2
DO 10 I=3,10	DYNO5600	,3
S=S*TT+A(I)	DYNO5610	,4
10 CONTINUE	DYNO5620	,5 ,6
ELSAT=S	DYNO5630	,7
RETURN	DYNO5640	,8
END	DYNO5650	,9

APPENDIX III1) Example of input

The input should be done for each case following section 10.

This example should be considered as indicative; the initial conditions represent an equilibrium state which has been verified with the analogue computation.

The tables have been extracted from standard steam tables* and may be considered as a permanent part of DYNOR, unless the range of pressures or temperatures need to be extended.

2) Example of output

Equilibrium at 100% of nominal power and after 418 seconds of problem time; these figures are indicative, since they may be altered modifying the references' values to the regulator.

* Ernst SCHMIDT VDI:
VDI Wasserdampf tafeln, Ausgabe A (kcal-at),
R. Oldenbourg, Muenchen, 1963
See also appendix IV

DATA (Zones de 10 colonnes)

PROBLEM										DATE										PAGE 1										OF 2																																																	
1	2	3	4	5	6	7	8	9	10	11	12	13	14	15	16	17	18	19	20	21	22	23	24	25	26	27	28	29	30	31	32	33	34	35	36	37	38	39	40	41	42	43	44	45	46	47	48	49	50	51	52	53	54	55	56	57	58	59	60	61	62	63	64	65	66	67	68	69	70	71	72	73	74	75	76	77	78	79	80
1	IDENTIFICATION										STANDARD										DYNOR																																																										
2	NUMBER OF DIFFERENTIAL EQUATIONS																				37																																																										
3	N. OF PAR																				0																																																										
4	N. OF TABLES																				7																																																										
5	FINAL TIME (SECONDS)																				500.																																																										
6	(INITIAL) INTEGRATION STEP																				0.1																																																										
7	OUTPUT STEP																				5.																																																										
8	INTEGRATION OPTION (ADAMS-MOULTON)																				2																																																										
9	TU	TEMP. OF URANIUM										X1	682.661																																																																		
10	TG	TEMP. OF CLADDING										X2	384.253																																																																		
11	TC	TEMP. OF COOLANT										X3	324.572																																																																		
12	C1	DEL. NEUTR. GROUP 1										X4	5.22557+05																																																																		
13	C2											2	X5	3.43709+06																																																																	
14	C3											3	X6	4.58242+07																																																																	
15	C4											4	X7	6.64070+07																																																																	
16	C5											5	X8	2.92937+08																																																																	
17	C6											6	X9	9.82904+07																																																																	
18	INTE	INTEGRATED ERROR										X10	-3.0158-04																																																																		
19	ROCON	CONTROL REACTIVITY										X11	-3.0158-04																																																																		
20	TORG 1	ORGANIC TEMPERATURE										X12	373.622																																																																		
21	TORG 2											X13	368.697																																																																		
22	TORG 3											X14	361.454																																																																		
23	TORG 4											X15	322.776																																																																		
24	TORG 5											X16	300.703																																																																		
25	TORG 6											X17	288.106																																																																		

APPENDIX IV

Superheater steam tables:

Temperature versus enthalpy, for different values of pressure.

(Note that the first point of each table is the enthalpy of saturated water).

TABLE 1	40 ATM	N. OF POINTS
2.5819800E	02	2.4917200E 02
6.6946499E	02	2.4917200E 02
6.7020399E	02	2.5000000E 02
6.7909599E	02	2.6000000E 02
6.8713199F	02	2.7000000E 02
6.9457399E	02	2.8000000E 02
7.0158799E	02	2.9000000E 02
7.0828499E	02	3.0000000E 02
7.1474199E	02	3.1000000E 02
7.2101199E	02	3.2000000E 02
7.2713299E	02	3.3000000E 02
7.3313599E	02	3.4000000E 02
7.3904300E	02	3.5000000E 02
7.4487099E	02	3.6000000E 02
7.5063300E	02	3.7000000E 02
7.5633999E	02	3.8000000E 02
7.6200200E	02	3.9000000E 02
7.6762600F	02	4.0000000E 02

** NUMBER OF POINTS IN TABLE 1 = 18 **

TABLE 2	60 ATM	N. OF POINTS
2.8817400E	02	2.7428100E 02
6.6525199E	02	2.7428100E 02
6.7145599E	02	2.8000000E 02
6.8141499E	02	2.9000000E 02
6.9043199E	02	3.0000000E 02
6.9875000E	02	3.1000000E 02
7.0653799E	02	3.2000000E 02
7.1391700E	02	3.3000000E 02
7.2097600E	02	3.4000000E 02
7.2778000E	02	3.5000000E 02
7.3437999E	02	3.6000000E 02
7.4081299E	02	3.7000000E 02
7.4711099E	02	3.8000000E 02
7.5329500E	02	3.9000000E 02
7.5938599E	02	4.0000000E 02

** NUMBER OF POINTS IN TABLE 2 = 15 **

TABLE 3	80 ATM	N. OF POINTS	** NUMBER OF POINTS IN TABLE	3	=	13	**
3.1264499E	02	2.9361900E	02				
6.5899299E	02	2.9361900E	02				
6.6702999E	02	3.0000000E	02				
6.7642399E	02	3.1000000E	02				
6.8665899E	02	3.2000000E	02				
6.9800899E	02	3.3000000E	02				
7.0667799E	02	3.4000000E	02				
7.1481100E	02	3.5000000E	02				
7.2252199E	02	3.6000000E	02				
7.2989500E	02	3.7000000E	02				
7.3699399E	02	3.8000000E	02				
7.4386999E	02	3.9000000E	02				
7.5056199E	02	4.0000000E	02				

TABLE 4	100 ATM	N. OF POINTS	** NUMBER OF POINTS IN TABLE	4	=	12	**
3.3404900E	02	3.0953999E	02				
6.5174499E	02	3.0953999E	02				
6.5239899E	02	3.1000000E	02				
6.6629599E	02	3.2000000E	02				
6.7655499E	02	3.3000000E	02				
6.8456700E	02	3.4000000E	02				
6.9959099E	02	3.5000000E	02				
7.0685799E	02	3.6000000E	02				
7.1752099E	02	3.7000000E	02				
7.2570099E	02	3.8000000E	02				
7.3349000E	02	3.9000000E	02				
7.4096299E	02	4.0000000E	02				

TABLE 5 130 ATM	N. OF POINTS	** NUMBER OF POINTS IN TABLE 5	= 10 **
3.3630950E 00	3.2930700E 02		
6.4013199E 02	3.2930700E 02		
6.4100899E 02	3.3000000E 02		
6.5722400E 02	3.4000000E 02		
6.7143499E 02	3.5000000E 02		
6.8402549E 02	3.6000000E 02		
6.9551299E 02	3.7000000E 02		
7.0597099E 02	3.8000000E 02		
7.1565400E 02	3.9000000E 02		
7.2471499E 02	4.0000000E 02		

TABLE 6 160 ATM	N. OF POINTS	** NUMBER OF POINTS IN TABLE 6	= 8 **
3.9084200E 02	3.4572900E 02		
6.2445399E 02	3.4572500E 02		
6.3558800E 02	3.5000000E 02		
6.5312600E 02	3.6000000E 02		
6.6850600E 02	3.7000000E 02		
6.8218600E 02	3.8000000E 02		
6.9451900E 02	3.9000000E 02		
7.0577399E 02	4.0000000E 02		

TABLE 7 200 ATP

N. OF POINTS

** NUMBER OF POINTS IN TABLE 7 = 6 **

4.2922195E 02	3.6407000E 02
6.1366255E 02	3.6407000E 02
6.2346500E 02	3.7000000E 02
6.4313095E 02	3.8000000E 02
6.6034499E 02	3.9000000E 02
6.7560995E 02	4.0000000E 02

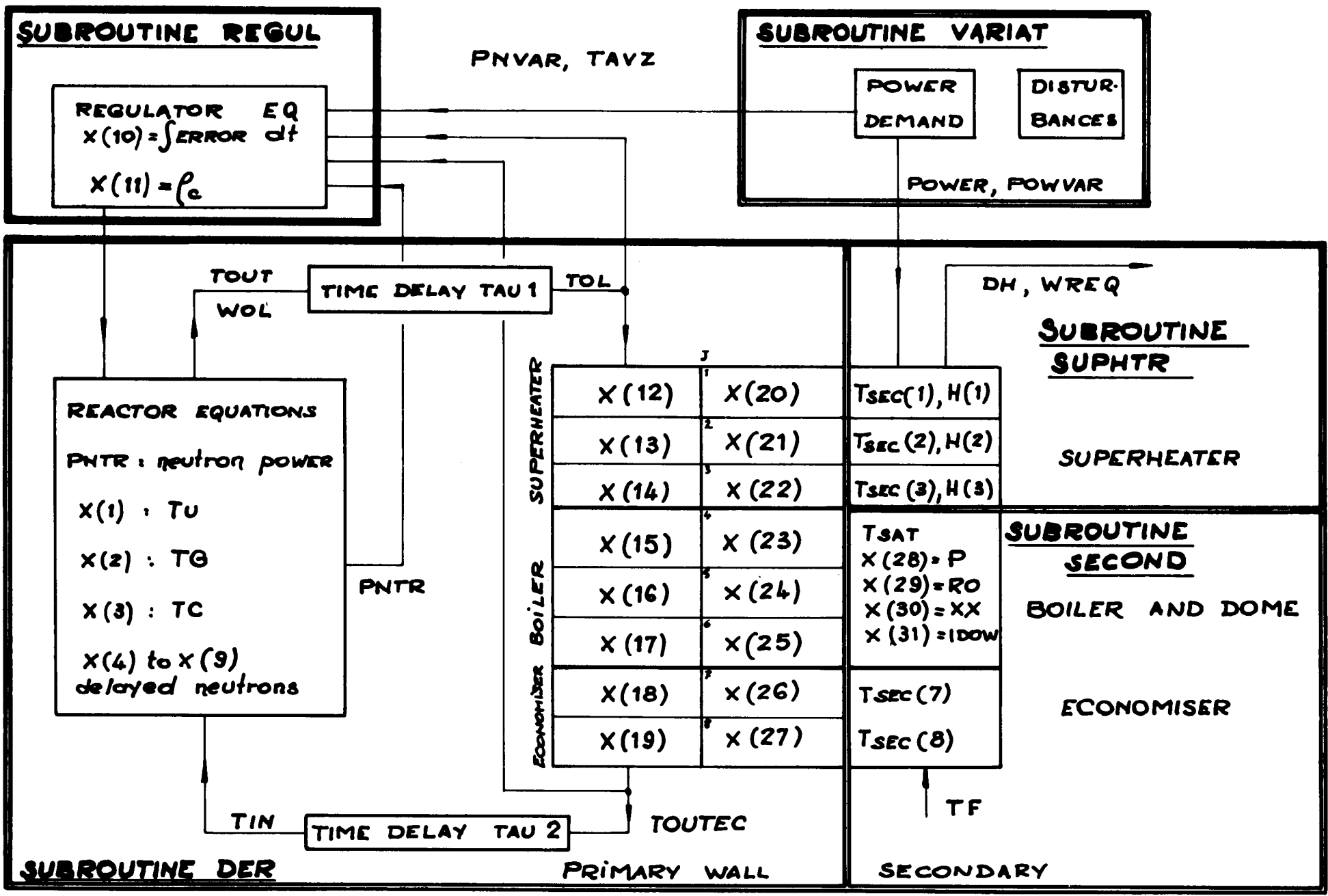


Fig. 1
 60.

REFERENCES

- (1) **Control of Nuclear Reactors and Power Plants**
M.A. Schultz
McGraw-Hill Book Company, Inc.

- (2) **SAHYB-2: A Program for the Solution of Differential**
Equations using an Analogue-Oriented Language
H. d'Hoop, R. Monterosso
EUR 3622e

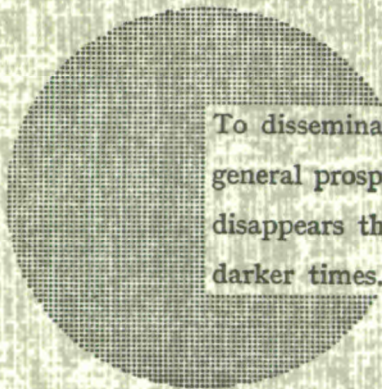
NOTICE TO THE READER

All Euratom reports are announced, as and when they are issued, in the monthly periodical **EURATOM INFORMATION**, edited by the Centre for Information and Documentation (CID). For subscription (1 year : US\$ 15, **£ 6.5**) or free specimen copies please write to :

Handelsblatt GmbH
"Euratom Information"
Postfach 1102
D-4 Düsseldorf (Germany)

or

**Office central de vente des publications
des Communautés européennes**
2, Place de Metz
Luxembourg



To disseminate knowledge is to disseminate prosperity — I mean general prosperity and not individual riches — and with prosperity disappears the greater part of the evil which is our heritage from darker times.

Alfred Nobel

SALES OFFICES

All Euratom reports are on sale at the offices listed below, at the prices given on the back of the front cover (when ordering, specify clearly the EUR number and the title of the report, which are shown on the front cover).

OFFICE CENTRAL DE VENTE DES PUBLICATIONS DES COMMUNAUTES EUROPEENNES

2, place de Metz, Luxembourg (Compte chèque postal N° 191-90)

BELGIQUE — BELGIË

MONITEUR BELGE
40-42, rue de Louvain - Bruxelles
BELGISCH STAATSBLAD
Leuvenseweg 40-42, - Brussel

LUXEMBOURG

OFFICE CENTRAL DE VENTE
DES PUBLICATIONS DES
COMMUNAUTES EUROPEENNES
9, rue Goethe - Luxembourg

DEUTSCHLAND

BUNDESANZEIGER
Postfach - Köln 1

NEDERLAND

STAATSDRUKKERIJ
Christoffel Plantijnstraat - Den Haag

FRANCE

SERVICE DE VENTE EN FRANCE
DES PUBLICATIONS DES
COMMUNAUTES EUROPEENNES
26, rue Desaix - Paris 15^e

ITALIA

LIBRERIA DELLO STATO
Piazza G. Verdi, 10 - Roma

UNITED KINGDOM

H. M. STATIONERY OFFICE
P. O. Box 569 - London S.E.1

EURATOM — C.I.D.
51-53, rue Belliard
Bruxelles (Belgique)

CDNA04254ENC